SCIENTIFIC COMMITTEE
NINETEENTH REGULAR SESSION

Koror, Palau

16–24 August 2023

Analysing potential inputs to the 2024 stock assessment of Western and Central Pacfic silky shark (*Carcharhinus falciformis*)

WCPFC-SC19-2023/SA-WP-10-Rev1
28 July 2023

Philipp Neubauer[1], **Kyuhan Kim**[1], **Kath Large**[1], **Stephen Brouwer**[2]

[1] **Dragonfly Data Science**

[2] **Saggitus Consulting**

Revision 1:

Fixed typo in caption of Table 8, changing label from from longline to purse-seine; fixed appendix numbering.

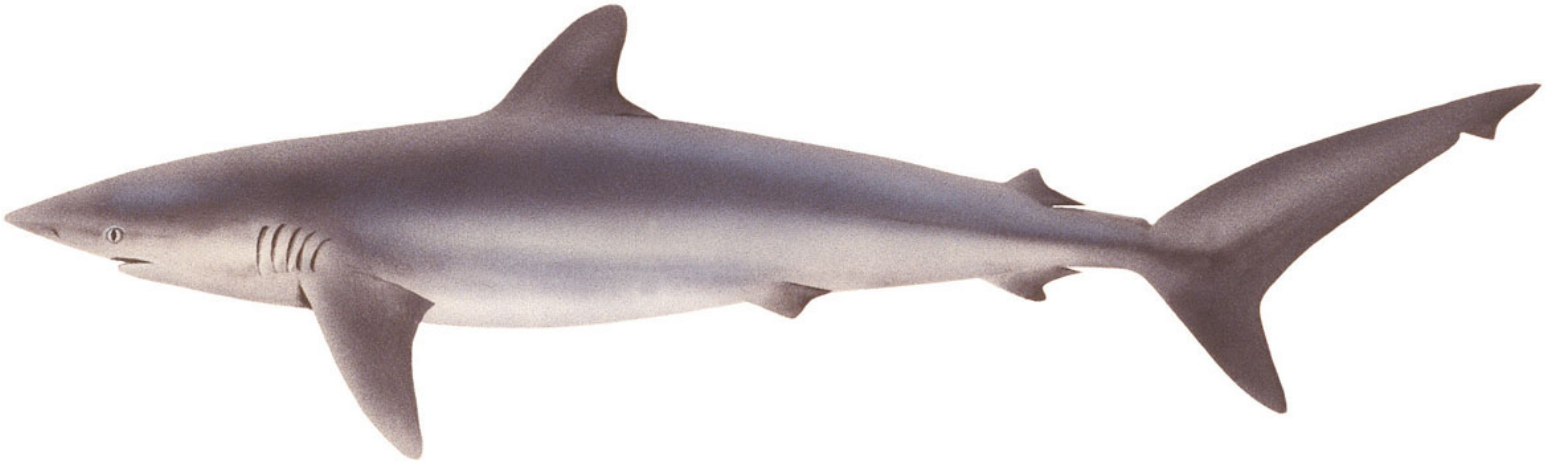

Analysing potential inputs to the 2024 stock assessment of Western and Central Pacfic silky shark (*Carcharhinus falciformis*)

Authors:
Philipp Neubauer
Kyuhan Kim
Kath Large
Stephen Brouwer

DRAGONFLY
Data Science

SAGGITUS

Cover Notes

To be cited as:

Neubauer, Philipp; Kim, Kyuhan; Large, Kath; Brouwer, Stephen (2023). Analysing potential inputs to the 2024 stock assessment of Western and Central Pacfic silky shark (*Carcharhinus falciformis*), 171 pages. WCPFC-SC19-2023/SA-WP-10-Rev1. Report to the WCPFC Scientific Committee. Nineteenth Regular Session, 16–24 August 2023.

CONTENTS

EXECUTIVE SUMMARY

Silky shark (*Carcharhinus falciformis*) are caught in longline and purse-seine fisheries in the western and central Pacific ocean (WCPO). Previous assessments had indicated that the stock was possibly overfished and that overfishing was occurring. However, these assessments also highlighted large uncertainties in inputs, with inconsistent longline indices, and inconsistent signals in other indices compounding uncertainties.

The present project endeavoured to thoroughly investigate potential methods for reconstructing overall catch, CPUE and length compositions for use in a potential assessment, which is scheduled for 2024. The present study represents year one of the two year project to assess silky shark.

We followed recent shark assessments and reconstructed catch of silky shark in the WCPO by extrapolating from a catch rate model for observer data. We used multi-model inference via Bayesian hierarchical stacking to derive a best estimate of catches in longline and purse-seine fisheries. To alleviate concerns that recent observed catch rates may be biased low due to non-retention measures for Silky sharks, we also compared our predictions with predictions from a model that ignored a year effect, which may be subject to reporting bias. Both predictions led to similar declines in catch since 2013, and our comparative approach led us to conclude that the majority of this decline was due to changes in total effort and effort distribution, rather than reporting changes.

CPUE trends in longline fisheries were highly variable, and as for previous assessments, were not consistent with other analyses. A more gradual approach to the analysis suggested highly variable trends in longline CPUE for silky shark among observer programs. As a result, any aggregate trend was estimated to be nearly flat. We therefore concluded that longline indices are unlikely to be useful for silky shark with the present datasets.

Purse seine CPUE, on the other hand, was highly consistent among observer programs across the WCPO, and showed good consistency between free-school and floating object-associated sets, both of which showed substantial increases in catch rates in recent years across the WCPO. Size composition analyses supported this trend, with scaled model-predicted length compositions showing the progression of a likely strong 2012 cohort progressing through the fishery until at least 2020.

The following recommendations are made:

- We conclude that there are likely sufficient data and a sufficiently consistent signal in the different datasets, especially from purse-seine, to conduct a stock assessment.
- Recent CPUE shows an increasing trend across all purse seine fisheries, which

mirrors declines in longline catch since 2013.

- We suggest that our analyses provide evidence that changes in reported interactions from longline vessels due to non-retention measures do not change over-all trends in interactions for silky shark, and do not change the conclusion that longline interactions with silky sharks have declined substantially from their peak in 2013.
- We suggest that a fully integrated assessment could be attempted, based on the consistency of datasets developed herein.
- As year effects are relatively minor in the longline fisheries, future catch reconstruction attempts could extrapolate interactions further back in time to avoid complications with assuming or estimating initial fishing mortalities in the assessments.
- Alternative assessment methods (for example spatial risk assessments) could be run in parallel with an integrated assessment, and provide an alternative approach that is independent of recent longline data, and allow for multi-model inference that can strengthen conclusions and potentially management advice from an integrated approach.

1. INTRODUCTION

The stock status of silky shark (*Carcharhinus falciformis*) in the Western and Central Pacific Ocean (WCPO) has been difficult to assess. Since the first stock assessment of silky sharks in WCPO (Rice and Harley 2012), assessments have shown large uncertainties about stock biomass and fishing mortality. The first stock assessment in 2012 was rejected due to inconsistencies between different data sources and model outcomes, leading to additional analyses that included alternative catch estimates (Rice 2012a) and CPUE indices being developed (Rice 2012b). The updated stock assessment in 2013 (Rice and Harley 2013) was accepted for the provision of management advice. That assessment estimated that overfishing was likely occurring and that the stock was in an over-fished state, but large uncertainties remained.

In 2018, an FAO ABNJ led project for a Pacific-wide assessment could not come up with a suitable model for Pacific-wide silky shark stocks (Clarke et al. 2018b). The inability to fit a suitable model at this scale was partly due to differences between CPUE trends in the WCPO and the Eastern Pacific Ocean (EPO) that could not be reconciled in the model, despite attempts to parametrise the models with oceanography-driven movement rates between EPO and WCPO. In particular, "estimating basin scale movement dynamics was not adequate to account for the different trends in the CPUE indices from the two regions." (Clarke et al. 2018b).

An addendum to the Pacific-wide study led to a WCPO assessment, predicated on the observation that abundance signals co-vary with the NINA4 index, which was taken to reflect changes in silky shark catchability with ENSO fluctuations in the WCPO (Clarke et al. 2018a). The importance of oceanographic drivers was also highlighted by Lennert-Cody et al. (2019), but the signal was found to be strongest for small silky sharks. The outcome of the 2018 stock assessment for WCPO silky shark were once again highly uncertain, although best estimates for biomass status suggested lower levels of depletion than the first WCPO assessment. Overfishing was still considered likely.

Overall, these studies highlight the considerable uncertainty that can be expected for any silky shark assessments. This uncertainty derives from a number of key difficulties with the interpretation of silky shark catch data, and their relation to stock structure and potential migrations, both of which are poorly understood, with contradictory signals from a range of datasets (Clarke et al. 2018b, see also Appendix A).

In this report, we analysed available catch, catch rate and length composition information in the context of developing time-series of catch, CPUE and length-composition that could be used for a WCPO silky shark assessment. The present study attempted to interpret trends in the context of assessment options for silky shark.

2. METHODS

2.1 Description of datasets

We used a range of data-sources held by the Pacific Community (SPC) who are the custodians of data supplied to the WCPFC by Members, Cooperating Non-Members and Participating Territories (CCMs). These datasets were extracted by SPC upon request, and analysed by the assessment team.

The following datasets were used for analysis:

- **L-BEST:** SPC's best (raised) estimates of longline effort (in hooks) for fleets in the WCPFC Convention Area, available at the 5°× month × year × flag × fleet resolution.
- **S-BEST:** SPC's best (raised) estimates of purse-seine effort (in sets) for fleets in the WCPFC Convention Area, available at the 1°× month × year × flag × set-type × fleet resolution.
- **Observer programmes for the WCPO longline fleet:** The observer dataset for the WCPFC longline fleet available to SPC was used for the analysis, including data from the SPC's Regional Observer Program and national observer programmes. Records collected by longline observers that are relevant to this assessment are key

fishing event attributes (including date and time, location), as well as information on gear and catch:

  - Gear/set characteristics (hooks between floats, total number of hooks fished);
  - species;
  - fate code of the catch (e.g., discarded or retained);
  - condition at capture and at release (if not retained); and
  - length and the sex of the individual.

- **Logsheet-reported [1] operational data for WCPO purse-seine and longline fleets:** Reported by day, flag, EEZ, latitude and longitude, set type, vessel, catch and effort. Silky shark were not reported consistently on log-sheets for either purse-seine or longline fisheries before the introduction of CMM2013-08.

Previous stock assessments for silky shark focused on observer data, since operational data was not deemed suitable for deriving indices of abundance or catch information. In contrast, recent stock assessments projects for blue shark and mako shark used a range of indices derived from logsheet-reported data, subset for vessels and flags that were consistently reporting (Neubauer et al. 2021, Large et al. 2022). However, the latter relied on consistent reporting from a small set of flags (mainly JP, EU, NZ and AU) in high latitudes. For silky shark and other tropical species (such as oceanic white-tip), which are caught across a number of EEZs and in the tropical high-seas, data from these flags with relatively consistent reporting likely represents too small a proportion of catch and effort to be useful for estimating abundance trends.

2.2 Estimating fishery interactions from observer data

We opted to follow recent silky shark assessments and estimate interactions from observer data. While this procedure is potentially biased by conservation measures in place since 2014 (CMM2013-08), there are few useful alternatives available. Trade-based catch reconstructions were used in the previous assessment for silky shark (Clarke et al. 2018b) as an alternative to potentially biased observer data (Rice 2012a), time-series based on fin-trade sampling are not without substantial problems (see Tremblay-Boyer et al. 2019, for a detailed discussion). Most difficult is the inability to scrutinise such estimates on the basis of data - they essentially represent assumptions about species compositions and fin-trade volumes that are extrapolated in time, and are unlikely to be correct in recent times given non-retention measures in place in the WCPFC and in many EEZs.

[1] Note: Not all logsheet and observer data are available for stock assessments of elasmobranchs. As a result, the SPC could not release logsheet or observer data from some WCPFC CCMs in some years for the silky shark stock assessment and related analyses.

Instead of using trade-based estimates, we aimed to try and develop a better understanding of recent catch-rates, especially in longline fleets where retention measures may lead to substantial number of sharks going unnoticed or unidentified by observers if they are cut free before being within a distance that would allow observers to identify the animals.

2.2.1 Estimation of catch rates from observed sets

Observer data from longline and purse-seine data were used to analyse trends in catch rates as well as to extrapolate observed catch rates to best estimates of over-all fishing effort in the WCPO in order to estimate over-all interaction rates. Catch-rate models were similar, but not identical, for the two tasks: catch rate model for prediction require the use of variables that are available for the over-all effort datasets; these are restricted to vessel flag, month, year, and estimated catch of main tuna and billfish target species. Observer data for CPUE can be analysed using observer-program and gear factors as standardising variables.

CPUE analyses also provide a way to inspect consistency of trends among gear types, and to understand the impact of non-retention measures on composition data and extrapolated catch estimates from longline data. Specifically, by analysing observer CPUE along a number of strata, we can gain an understanding of the likely change in reporting along these strata using a comparative approach. While this approach doesn't allow for an estimation of the absolute levels of reporting changes across the whole fleet (i.e., all fleets may be affected to some degree), we can get a relative estimate that can provide insights into potential solutions for reconstructing total interaction levels.

Catch rates were standardised using a progression of models aimed at exploring the importance of oceanographic and gear factors on CPUE. Models were similar between longline and purse-seine, with both models using a negative-binomial model with over-dispersion adjustment (Tremblay-Boyer & Neubauer 2019). The model used the number of hooks (or sets) as an offset. In the case of longline CPUE, we estimated smooth effects for the number of hooks (effectively allowing for non-linear catch rates with the number of hooks) and hooks between floats. For purse-seine, analyses were split between associated and un-associated sets given differences in length-composition for these gear-types.

For longline, we applied CPUE models to four distinct subsets for analysis.

1. We used all observer data available for the tropical WCPO. This dataset includes observation from target fisheries, but an observer-program-year interaction specified as a random effect allows for deviations from a global annual trend for each observer program. This dataset was used to test for over-all consistency

among observer programs, without an expectation of deriving a useful index.

2. A dataset of long-running observer programmes was prepared following Tremblay-Boyer and Neubauer (2019), using observer data from FMOB, HWOB, FJOB, PFOB, and NCOB.

3. A dataset following Clarke et al. (2018b), restricting the analysis to data between 29^o and 7^o South, and longitudes between 152^o and 200^o.

4. A dataset with only distant water fishing fleets, which accounted for the majority of recent observer data in the tropical WCPO.

Clarke et al. (2018a) suggested variations in catchability with ENSO (specifically, the NINA4 index; Figure 1) may be driving catchability in WCPFC longline fisheries, and a time-varying catchability formulation was adopted for the accepted model. We incorporated this aspect by including the NINA4 index in two ways. First, a main effect for the NINA4 index was applied as the mean over the preceding three years for indices of small and associated purse seine, or four years for all other (i.e., not small fish) longline indices, reflecting an approximate time-frame over which indices might integrate. Secondly, we added an interaction term with observer-program, to investigate if region specific trends in catchability (or local abundance) driven by NINA4 could alter expected the over-all index.

A series of models were run from a simple non-standardised model for annual catch rate, and sequentially adding effects to the model, with the full model taken as the standardisation model for each analysis.

The full longline CPUE model was given by:

```
obs_int | hooks ~ (1|yy) +
                  (1|program_code*yy) +
                 s(log(hooks)) +
                 s(log(HBF)) +
                  (1|vessel_id)) +
                  (1|mm) +
                 s(SST) +
                   NINA4_MA(3/4) +
                  (1+NINA4_MA(3/4)|program_code) +
                t2(lon5,lat5)
```

with all variables added sequentially according to the formula above. The same approach was taken for purse-seine by set type, omitting any hook related variables and vessel id (the latter was not available in the data extract). All models were fitted

with brms using full Bayesian inference from MCMC, with four chains run for 1000 iterations each, discarding 500 iterations as burn-in and retaining 2000 iterations for inference across the four chains.

2.2.2 Extrapolation of observed catch rates to WCPO-wide effort

Similar models were used for extrapolating from observed interactions to WCPO-wide effort. A difficult aspect of extrapolating observer catch-effort, beyond potential issues due to non-retention measures, is the non-representative distribution of observed effort. Relative to over-all effort, observer effort in both longline and purse-seine has only been relatively widespread in recent years (Tables 3–8).

The lack of representative effort makes it difficult to develop models on the basis of model selection, which will favour models that best predict the observed interactions, but may not perform optimally across effort that is poorly observed. To counter this potential bias in selected models, Large et al. (2022) used-cross validation weighted by the total effort. However, this method is computationally intensive, and evaluating cross-validation for a large number of strata (e.g., vessel flags), or a range of different strata (flags, latitude) for a number of candidate models is prohibitive.

To circumvent the high computational overhead of the previous method, and to allow more flexibility in the variables used to judge model performance, we cast the model weighting as a linear-modelling problem, estimating predictive capacity of individual models as a function of covariates, which can be used to predict model weights for prediction datasets that are not well represented in the training set. Specifically, we use Bayesian hierarchical stacking, a model-based estimation of stacking weights (Yao et al. 2022). The procedure uses the expected log-posterior predictive density estimate per model and data point (Yao et al. 2018), and then uses a logistic-linear model to estimate the effect of covariates on the predictive ability of individual models. The corresponding stacking model was written in Stan (Appendix B), using flag, year, latitude and set-type (for purse-seine) as covariates, and producing corresponding predictions over the full effort data for longline and purse-seine datasets.

Previous catch reconstruction models for sharks in the tropical WCPO separated short-lived target shark fisheries in the western tropical Pacific from non-target fisheries (Tremblay-Boyer & Neubauer 2019). The main difference in approaches for these fisheries was that fishery-year effects were assumed constant or target fisheries, effectively assuming that fisheries in the area continued to catch sharks at high (target) catch rates. Such a treatment may no longer be appropriate since there is no indication of continued high shark catches from these fisheries, and we therefore included these fisheries in our over-all model, using model formulations with flag-year interactions and spatial/spatio-temporal terms, as well as model selection to fit the model.

Candidate models included variations on a base model. The base model for longline observer effort included year, month, SST, chlorophyll-a, distance to coast and the amount of swordfish catch. Alternative models added non-linear effects for hooks, flag, NINA4 indices and various spatio-temporal terms. The corresponding model for purse-seine excluded swordfish catch but added set-type-year interactions.

Table 1: Table of models used for multi-model predictions of longline interactions with silky shark in the tropical WCPO . All models were run with and without over-dispersion adjustment for the negative binomial variance (see Tremblay-Boyer and Neubauer (2019)).

Model	Model terms
base	(1|yy) + (1|mm) + s(SST) + s(chla) + s(swo-n) + s(dist2coast)
base.flag	base + (1|flag-id)
base.hooks	base + s(log(hooks))
base.flag.hooks	base + s(log(hooks)) + (1|flag-id)
base.space	base + t2(lon5,lat5)
base.space.hooks	base + t2(lon5,lat5) + s(log(hooks))
base.space.hooks.flag	base + t2(lon5,lat5) + s(log(hooks)) + (1|flag-id)
base.space.flagyy	base + t2(lon5,lat5) + (1|flag-id) + (1|flag-id:yy)
base.space.hooks.flagyy	base + t2(lon5,lat5) + s(log(hooks)) + (1|flag-id) + (1|flag-id:yy)
base.spacetime	base + t2(lon5,lat5,mm)
base.spacetime.hooks	base + t2(lon5,lat5,mm) + s(log(hooks))
base.spacetime.hooks.flag	base + t2(lon5,lat5,mm) + s(log(hooks)) + (1|flag-id)
base.spacetime.flagyy	base + t2(lon5,lat5,mm) + (1|flag-id) + (1|flag-id:yy)
base.spacetime.hooks.flagyy	base + t2(lon5,lat5,mm) + s(log(hooks)) + (1|flag-id) + (1|flag-id:yy)
base.spacetime.yy	base + t2(lon5,lat5,yy)
base.spacetimehooks.yy	base + t2(lon5,lat5,yy) + s(log(hooks))
base.hooks.spacetime.yy.flag	base + t2(lon5,lat5,yy) + s(log(hooks)) + (1|flag-id)
base.spacetime.nina	base + t2(NINA4,lon5,lat5)
base.spacetimehooks.nina	base + t2(NINA4,lon5,lat5) + s(log(hooks))
base.hooks.spacetime.nina.flag	base + t2(NINA4,lon5,lat5) + s(log(hooks)) + (1|flag-id)

Table 2: Table of models used for multi-model predictions of purse-seine interactions with silky shark in the tropical WCPO . All models were run with and without over-dispersion adjustment for the negative binomial variance (see Tremblay-Boyer and Neubauer (2019)).

Model	Model terms
base	(1+set-type|yy) + (1|mm) + s(SST) + s(chla) + s(dist2coast)
base.flag	base + (1|flag-id)
base.space	base + t2(lon5, lat5)
base.space.flag	base + t2(lon5, lat5) + (1|flag-id)
base.space.flagyy	base + t2(lon5, lat5) + (1|flag-id) + (1|flag-id:yy)
base.spacetime	base + t2(lon5, lat5, mm)
base.spacetime.flag	base + t2(lon5, lat5, mm) + (1|flag-id)
base.spacetime.flagyy	base + t2(lon5, lat5, mm) + (1|flag-id) + (1|flag-id:yy)
base.spacetime.nina	base + s(NINA4)
base.spacetime.nina.flag	base + t2(NINA4,flag-id)
base.spacetime.nina.flagyy	base + s(NINA4) + (1|flag-id) + (1|flag-id:yy)
base.spacetime.nina	base + t2(NINA4, lon5, lat5)
base.spacetime.nina.flag	base + t2(NINA4, lon5, lat5) + (1|flag-id)
base.spacetime.nina.flagyy	base + t2(NINA4, lon5, lat5) + (1|flag-id) + (1|flag-id:yy)

2.3 Model-based scaling of length composition data

Length composition data for sharks from both purse-seine and longline data have not been collected in a representative manner across the fleets over time and space (Figures 2, 3). This poses a problem in that the lack of representative sampling across key sources of variability can lead to biased estimates of catch compositions. Biased compositions can, in turn, lead to false signals if composition data is not reflective of biological processes represented in the assessment model (Minte-Vera et al. 2017), and even down-weighting composition data may not be sufficient to eliminate such signals (Wang & Maunder 2017). It is therefore important to get an unbiased representation of composition data that corrects for biased sampling and appropriately scales composition data.

The present study used a standardisation model for composition data. The model is similar to the one developed in Neubauer and Kim (in press). The procedure adjusts the length-frequency samples based on spatial and temporal variability, similar to CPUE standardisation. However, unlike CPUE, rather than removing variation across strata, it predicts length-compositions across catch (or CPUE for index fisheries). This procedure has the advantage that reasonably smooth length-frequency distributions (i.e., filtering out variance from highly multi-modal length-frequency distributions that result from low sample numbers) for sparsely sampled strata can be extracted, even if individual samples in those strata are unlikely to provide a reliable estimate of the actual length frequencies. Random effects formulations ensure the sharing of information across strata.

The formulation is an extension of the multinomial GLM, which was developed for estimating length frequencies of New Zealand rock lobster removals (D. Webber, unpublished analysis). The extension here was achieved by factorising the multinomial distribution into independent Poisson distributions for total measurements (N_s) in sample s, and a second Poisson distribution with mean $\lambda_{i,s}$ over draws $n_{i,s}$ for the number of fish in length category i in sample s. Length proportions π can then be recovered by setting $\pi_i = \lambda_i / \sum_j (\lambda_j)$. This setting allows the formulation as a straightforward Poisson GLM, using the total counts N_s in sample s as an offset term.

We implemented this model using vessel flag, area (defined as 10^ox10^o bins) and year, as well as set-type for purse seine data. For each term, an interaction with year effects allows prediction of area-flag-year (and set-type) specific length compositions from available data, with predictions reflecting the amount of information and variability within strata. There was little evidence for sex-bias in any of the data (Figure 4), and we therefore did not include sex in the analysis.

Analyses were run independently for longline and purse seine observer data, and restricted to the tropical WCPO (-20^o–20^o Latitude) The model was implemented in brms and run via:

```
bf(n ~ (1|bin) +
       (1|bin:yy) +
       (1|bin:area) +
       (1|bin:area:yy) +
       (1|bin:flag_id) +
       (1|bin:flag_id:yy)  +
```

```
offset(log(N))).
```

The model can be used to obtain predictions for corresponding strata in catch or CPUE data (or predictions), and scaled using relative catch in each stratum when aggregating to larger scales. For example, predictions and scaling can be achieved at an area-flag-year stratum for longline data, with scaled estimates the combined to an annual predicted composition.

3. RESULTS

3.1 Models of catch rates based on observer data

3.1.1 Longline observer indices

Different subsets of longline CPUE observer data led to slightly different, but overall flat observer indices (Figure 5). Only the distant water-index showed a consistent decrease post-2014. The flat index in all other subsets was driven by a lack of consistency, and generally noisy nature of trends across regional observer indices, even for the series of established long running observer programs (Figure 6). We considered these inconsistencies as indicators that no consistent longline index can be constructed across the overall region. Complete diagnostics for the indices developed for longline are given in Appendix C.

3.1.2 Purse-seine observer indices

In contrast to longline indices, purse seine CPUE was highly consistent between set types (Figure .7), with very minimal standardisation effects (Figures 8, 9) and high consistency among regional observer programs within set-types (Figures 10, 11).

The overall CPUE index for both associated and free-school sets declined between the early 2000s and around 2010. The free-school index subsequently increased from 2010 to 2020, with CPUE doubling over that decade. The associated-set index also increased over the same period, but the increase was not as pronounced and occurred slightly later. The associated-set index also showed a strong increase in catch rates in the late 1990s, although this increase was only supported by data from two observer programs which cover that period (US: TTOB, PNA: FAOB; Figure 11).

Both indices were corrected for climatic conditions expressed by the NINA4 index (Figures 12, 13). The main standardisation was by the main effect for the index, rather than through differential effects on indices for individual observer programs (via the interaction term with observer programs; Figures 10, 11), leading to a downwards correction of recent increases, without however removing the recent increasing trend in both indices.

3.2 Predicting interactions across the WCPO

3.2.1 Longline interactions with silky shark across the WCPO

Across candidate models, the highest weights were associated with two models (Figure 14 a,b), with the main model that accounted for the majority of weight for tropical effort (-20–20 degrees latitude) being a model with spatio-temporal terms for spatial fields by month, and flag-year interactions (Figure 14c). Overall, there was relatively little change in predicted model weights from the training set to the prediction dataset (Figure 14d). None of the models with high weights included NINA4 based formulations. Model diagnostics suggested good fits to data across available strata (Appendix D).

Predictions on the basis of total hooks per stratum (Figures 15, 16), led to predictions of high and stable total interactions in the western tropical Pacific in the late 1990s and early 2000s (Figure 17), where CPUE was predicted to be highest (Figure 16). The predictions were not driven by the inclusion of shark-target fisheries, but was also seen for other vessel flags fishing in the region, mainly for TW flagged vessels. Given the high total effort by the latter in the western Pacific in the 1990s and early 2000s, a large proportion of total interactions were attributed to TW flagged vessels (Figure 18). Shark target fisheries in PNG accounted for a relatively large number of captures over a period of 5 years prior to 2014 (Figure 18), but the cessation of this fishery in 2014 led to a substantial decline in reported interactions.

Total predicted interactions declined precipitously from a high-point in 2013 to the present day (Figure 17). Much of this decline was attributed to the decline in predicted interactions by distant-water fishing nation vessels (TW, JP, KR, CN) and PNG target fisheries (Figure 18). To understand to what extent this trends was due to changes in spatial fishing effort as opposed to non-reporting of interactions after the CMM2013-08, we inspected predictions from a model without flag-year interaction effect but with a spatial effect. By comparing predicted catch and year trends in such a model, we can partial out effects of variables other then flag-specific year trends on trends in predicted interactions. This inspection revealed a very similar trend to the multi-model predictions (Figure 19), with lower catch leading up to 2013, but similar declines in predicted interactions since. The estimated year effect for this model showed a variable trend over the prediction period (Figure 19).

3.2.2 Purse-seine interactions with silky shark across the WCPO

In contrast to longline models, one of the two purse-seine models with high weight included a term for NINA4 by latitude and longitude (Figure 20 a,b). This model appeared to perform better for southern hemisphere effort (Figure 20c). Again, model weights changed little from the input to the prediction datasets (Figure 20c).

Predicted interactions in purse-seine fisheries strongly mirrored the highly spatially concentrated nature of the fishing effort (Figure 21), with high predicted interactions in the western equatorial Pacific. Due to high observer coverage in purse-seine fisheries, predicted interaction rates had low uncertainty (Figure 21), showed a decline in object-associated set interactions from a high in 2005 to a low around 2008 (Figure 22), and recent increases mirroring increasing catch-rates. Similar recent increases were found in free-school sets, but due to lower overall catch-rates (Figure 21), predicted interactions

were lower than for object-associated sets (Figure 22). Most interactions were attributed to vessel-flag states with high effort the western equatorial Pacific (Solomon Islands, Papua New Guinea), but also United States flagged vessels (Figure 23).

3.3 Standardised length frequency compositions

3.3.1 Longline length composition

Length-compositions were highly variable among years within areas and vessel-flags (Figure 24), with most variation in composition models explained by corresponding interaction terms with the year variable. The model was able to fit data at across all strata (Figures 25, 26, 27,28).

There was little consistency in marginal effects between years, but some years (e.g., 2015, 2016, 2019) showed consistently higher than average numbers of small silky sharks, whereas other years showed higher-than-average abundance of large sharks (1997, 2011) (Figure 29). Vessel-state effects showed smaller than average (<100 cm) sharks being caught by US flagged vessels, with slightly larger (∼100 cm) sharks being consistently caught by PG and KR flagged vessels (Figure 30). Other vessel-flags did not show consistent deviations from average compositions. Fisheries in the southern equatorial (-10 – 0 degrees) caught mostly smaller fisher between 150 to 180 degrees longitude, there was a trend towards larger sharks towards the central Pacific (Figure 32).

In association with stratified catches, the scaled length frequencies suggested a dominance of small fish (∼100 cm) in fisheries (TW and PG) which accounted for most of the interactions over time (Figures 33, 34). Other fisheries at slightly higher latitudes (e.g., FJ, NC, PF, and US) showed distinct secondary modes of larger individuals (∼150 cm) that was not present at lower latitudes. Scaled compositions by year showed a decline of the predicted proportion of large individuals when interactions peaked around 2013 (Figure 35). There was a secondary peak in large individuals that re-appeared around 2016 with and remained present in the data in recent years.

3.3.2 Purse-seine length composition

Purse seine length compositions were dominated by differences between set-type (Figure 36), with object associated sets catching predominantly small sharks (Figure 37). Model fits were good across all strata (Figures 38, 39, 40,41). Overall year-effects were inconsistent in early years, but 2012 and 2013 showed high proportions of small (young of year) fish, which consequently transitioned into larger size classes until 2020 (Figure 42). Other estimated effects were less consistent (Figure 43, 44).

While many flags showed a large peak of small sharks caught in purse seine (Figure 46,47), with a small secondary peak with large fish. Scaled annual length compositions reflected the estimated conditional effects, with a signal suggesting a trend of reductions in large silky sharks by year up to 2012 followed by the presence of a large and growing cohort between 2012 an 2022 (Figure 48).

4. DISCUSSION

Previous stock assessments for silky shark highlighted large inconsistencies between input datasets for successive assessments (Clarke et al. 2018b), especially in long-line indices that had been used as primary indices of abundance up to that point. We found long-line CPUE to be highly variable, both within series for individual observer programmes and among series from different regional programs. Individual series were often very noisy, leading to overall flat estimated indices across subsets of observer programs. Our analysis attempted to be more granular, allowing for trends within regional observer programs, and used a range of diagnostics to develop a better understanding of drivers of long-line CPUE. However, few consistencies emerged from that analysis, and we were not able to reproduce indices that resembled previous indices for long-line fisheries of silky shark. The high variability in indices may be driven by targeting practices and gear configuration factors that are difficult to account for given inconsistent reporting of gear attributes in long-line observer data across a large number of observer programs.

Although we found little consistency in long-line catch rates, purse seine catch rates were consistent across all observer programs, and across set-types. Purse-seine CPUE is often difficult to interpret, and has previously been questioned as an index of abundance for silky shark (Clarke et al. 2018b), the high level of consistency in a bycatch species could point to this series being a useful indicator of abundance of silky sharks. In addition, standardised scaled length compositions by year showed a similarly consistent signal for purse seine, with recent recruitment evident and growing through the fishery between 2012 and 2020. This increase was also mirrored in long-line compositions, although it was less obvious. Some long-line observer indices supported this recent increase in CPUE (e.g., Figure 6).

The recent increase in CPUE in purse seine mirrors declines in predicted long-line interactions with silky shark in the WCPO. Clarke et al. (2018b) strongly criticized the use of observer CPUE to estimate total interactions in the long-line fishery since CMM2013-08, suggesting that observers may not always see sharks when they are cut free, and are therefore likely to under-report silky shark. While this concern is important, we found relatively little difference in model predictions between models using flag-year interactions and those using random draws from estimated year level random effects, and no indication that declines in CPUE are chiefly responsible for driving the decline in predicted interactions. The predictions are rather due to declines in the numbers of hooks set as well as spatial distribution of long-line effort. Nevertheless, CPUE may still under-estimate the true interaction rate as the recent increase in purse-seine CPUE is not apparent in long-line CPUE (but long-line compositions do show hints of this trend).

Uncertainty in long-line interactions is almost certainly higher than is currently represented in predicted captures, and should be accounted for in any subsequent analysis. We suggest that predictions based on the random effect distributions for years could be used for all years post-2013, thereby leading to an alternative catch time-series that would only account for targeting and spatial changes. Such an analysis is shown in Figure 19 and supports recent declines even in the absence of year effects in reporting rates.

While stock structure and movement of silky sharks in the WCPO remain highly uncertain, the consistency in purse-seine trends across large areas suggests that the

populations in the region behave synchronously, and could be assessed as a single population. In addition, the consistency in trends could allow fitting of integrated assessments. Such models would need to account for uncertainties about recent longline catch, but would provide a basis to integrate available information to derive stock status estimation. Alternative assessment methods based on risk assessment methodologies (Neubauer et al. 2019, Griffiths et al. 2019) would not explicitly account for the recent trends observed through the use of the time-series. But by applying such a method on two periods - e.g., a high catch period (2010-2012), and recent years, it may be possible to contrast how spatial effort distribution links to fishing mortality of silky sharks in each period. Such distribution changes may have led to lower estimated fishing mortality in recent years, which may explain recent increased CPUE without needing to rely on observer data.

If an integrated assessment were attempted, our modelling suggests that year effects are relatively minor in the longline fisheries, and interaction rates could be extrapolated back further in time to avoid complications with assuming or estimating initial fishing mortalities in a stock assessment. Our attempt to derive predictions by integrating over year effects suggests that long-term trends are largely driven by the amount and location of fishing effort, such that extrapolated interaction rates may be reasonable.

In conclusion, we provide evidence for recent increases in CPUE, combined with supporting signals in length compositions, that suggest a potential recovery of silky shark in WCPO fisheries. While shark stock assessments are difficult due to patchy input data, we suggest that the present analysis provides a relatively consistent picture that provides a good basis to attempt a stock assessment in 2024. We further suggest that such an assessment could be paired with a risk assessment to perform multi-model inference and reduce the reliance on a single combination of datasets.

The following recommendations are made:

- We conclude that there are likely sufficient data and a sufficiently consistent signal in the different datasets, especially from purse-seine, to conduct a stock assessment.
- Recent CPUE shows an increasing trend across all purse seine fisheries, which mirrors declines in longline catch since 2013.
- We suggest that our analyses provide evidence that changes in reported interactions from longline vessels due to non-retention measures do not change over-all trends in interactions for silky shark, and do not change the conclusion that longline interactions with silky sharks have declined substantially from their peak in 2013.
- We suggest that a fully integrated assessment could be attempted, based on the consistency of datasets developed herein.
- As year effects are relatively minor in the longline fisheries, future catch reconstruction attempts could extrapolate interactions further back in time to avoid complications with assuming or estimating initial fishing mortalities in the assessments.
- Alternative assessment methods (for example spatial risk assessments) could be run in parallel with an integrated assessment, and provide an alternative approach

that is independent of recent longline data, and allow for multi-model inference that can strengthen conclusions and potentially management advice from an integrated approach.

ACKNOWLEDGEMENTS

The authors would like to thank SPC, particularly Peter Williams and Emmanuel Schneiter for providing the WCPFC Members data for these analyses. We would also like to thank Paul Hamer and the stock assessment team at SPC for constructive discussions throughout this work and for comments on earlier drafts of this report, and the SPC Pre-Assessment Workshop Members for their helpful feedback on the catch reconstruction and CPUE proposals. The authors would also like to thank the SPC for providing the funding for this work.

5. REFERENCES

Clarke, S.; Langley, A.; Lennert-Cody, C.; Aures-de-Silva, A., & Maunder, M. (2018a). *Addendum to Pacific-wide silky shark (Carcharhinus falciformis) stock status assessment* (tech. rep. No. SC14-SA-WP-08a). WCPFC.

Clarke, S.; Langley, A.; Lennert-Cody, C.; Aures-de-Silva, A., & Maunder, M. (2018b). *Pacific-wide silky shark (Carcharhinus falciformis) stock status assessment* (tech. rep. No. SC14-SA-WP-08). WCPFC.

Grant, M. I.; Smart, J. J.; Rigby, C. L.; White, W.; Chin, A.; Baje, L., & Simpfendorfer, C. A. (2019). Intraspecific demography of the silky shark (*Carcharhinus falciformis*): implications for fisheries management. *ICES Journal of Marine Science*, *77*(1), 241–255. doi:10.1093/icesjms/fsz196

Grant, M. I.; Smart, J. J.; White, W. T.; Chin, A.; Baje, L., & Simpfendorfer, C. A. (2018). Life history characteristics of the silky shark (*Carcharhinus falciformis*) from the central west Pacific. *Marine and Freshwater Research*, *69*(4). doi:10.1071/MF17163

Griffiths, S. P.; Kesner-Reyes, K.; Garilao, C.; Duffy, L. M., & Román, M. H. (2019). Ecological assessment of the sustainable impacts of fisheries (easi-fish): A flexible vulnerability assessment approach to quantify the cumulative impacts of fishing in data-limited settings. *Marine Ecology Progress Series*, *625*, 89–113.

Hoyos-Padilla, E. M.; Ceballos-Vazquez, B. P., & Galvan-Magana, F. (2012). Reproductive biology of the silky shark (*Carcharhinus falciformis*) (Chondrichthyes: Carcharhinidae) off the west coast of Baja California Sur, Mexico. *Journal of Applied Ichthyology*, *18*, 15–24.

Joung, S. J.; Chen, C. T.; Lee, H. H., & Liu, K. M. (2008). Age, growth, and reproduction of silky sharks, *Carcharhinus falciformis*, in northeastern Taiwan waters. *Fisheries Research*, *90*, 78–85. doi:10.1016/j.fishres.2007.09.025

Large, K.; Neubauer, P.; Brouwer, S., & Kai, M. (2022). *Input data for the 2022 South Pacific Shortfin Mako Shark stock assessment* (tech. rep. No. WCPFC-SC18-2022/SA-IP-13). WCPFC.

Lennert-Cody, C. E.; Clarke, S. C.; Aires-da-Silva, A.; Maunder, M. N.; Franks, P. J. S.; Román, M.; Miller, A. J., & Minami, M. (2019, January). The importance of environment and life stage on interpretation of silky shark relative abundance indices for the equatorial pacific ocean. *Fisheries Oceanography*, *28*(1), 43–53.

Minte-Vera, C. V.; Maunder, M. N.; Aires-da-Silva, A. M.; Satoh, K., & Uosaki, K. (2017, August). Get the biology right, or use size-composition data at your own risk. *Fisheries Research*, *192*, 114–125. doi:10.1016/j.fishres.2017.01.014

Neubauer, P.; Large, K.; Kai, M.; Tasi, W., & Liu, K. (2021). *Input data for the 2021 South Pacific blue shark (Prionace glauca) stock assessment* (tech. rep. No. WCPFC-SC17-2021/SA-IP-18). WCPFC.

Neubauer, P.; Richards, Y., & Tremblay-Boyer, L. (2019). *Alternative assessment methods for oceanic white-tip shark* (tech. rep. No. WCPFC-SC15-2019/SA-IP-13). WCPFC.

Neubauer, P. & Kim, K. (in press). Stock assessment and management procedure evaluation for pāua (*Haliotis iris*) in PAU 5D. *New Zealand Fisheries Assessment Report*, *2023/XX*.

Oshitani, S.; Nakano, H., & Tanaka, S. (2003). Age and growth of the silky shark Carcharhinus falciformis from the Pacific Ocean. *Fisheries Science*, *69*, 456–464.

Peatman, T.; Bell, L.; Allain, V.; Caillot, S.; Williams, P.; Tuiloma, I.; Panizza, A.; Tremblay-Boyer, L.; Fukofuka, S., & Smith, N. (2018). *Summary of longline fishery bycatch at a regional scale, 2003-2017* (tech. rep. No. WCPFC-SC14-2018/ST-WP-03). WCPFC.

Rice, J. (2012a). *Alternate catch estimates for silky and oceanic whitetip sharks in Western and Central Pacific Ocean* (tech. rep. No. SC8-SA-IP-12). WCPFC.

Rice, J. (2012b). *Catch per unit effort of oceanic whitetip sharks in the Western and Central Pacific Ocean* (tech. rep. No. SC8-SA-IP-11). WCPFC.

Rice, J. & Harley, S. (2012). *Stock assessment of silky sharks in the Western and Central Pacific Ocean* (tech. rep. No. SC8-SA-WP-07). WCPFC.

Rice, J. & Harley, S. (2013). *Updated stock assessment of silky sharks in the Western and Central Pacific Ocean* (tech. rep. No. SC9-SA-WP-03). WCPFC.

Sanchez-de Ita, A.; Qiunonez-Velazquez, C.; Galvan-Magana, F.; Bocanegra-Castillo, N., & Felix-Uraga, R. (2011). Age and growth of the silky shark (*Carcharhinus falciformis*) from the west coast of Baja California Sur, Mexico. *Journal of Applied Ichthyology*, *27*, 20–24.

Tremblay-Boyer, L.; Carvalho, F.; Neubauer, P., & Pilling, G. (2019). *Stock assessment for oceanic whitetip shark in the Western and Central Pacic Ocean* (tech. rep. No. WCPFC-SC15-2019/SA-WP-06). WCPFC.

Tremblay-Boyer, L. & Neubauer, P. (2019). *Historical catch reconstruction and CPUE standardization for the stock assessment of oceanic whitetip shark in the Western and Central Pacic Ocean* (tech. rep. No. WCPFC-SC15-2019/SA-IP-17). WCPFC.

Wang, S.-P. & Maunder, M. N. (2017, August). Is down-weighting composition data adequate for dealing with model misspecification, or do we need to fix the model? *Fisheries Research*, *192*, 41–51. doi:10.1016/j.fishres.2016.12.005

Yao, Y.; Pirš, G.; Vehtari, A., & Gelman, A. (2022, December 1). Bayesian hierarchical stacking: Some models are (somewhere) useful. *Bayesian Analysis*, *17*(4).

Yao, Y.; Vehtari, A.; Simpson, D.; Gelman, A., et al. (2018). Using stacking to average bayesian predictive distributions (with discussion). *Bayesian Analysis*, *13*(3), 917–1007. Publisher: International Society for Bayesian Analysis.

TABLES

5.1 Observer data availability

5.1.1 Longline observer data

Table 3: Number of observer - reported silky shark interactions by flag in the data extract from the SPC observer database for longline fishing events.

Year	AU	BZ	CK	CN	FJ	FM	JP	KI	KR	MH	NC	NZ	PF	PG	PW	SB	TO	TV	TW	US	VN	VU	WS
1995	9	0	0	152	11	3	38	0	0	0	0	0	0	0	0	0	0	0	390	26	0	0	0
1996	13	0	0	141	8	0	8	0	0	0	78	0	0	10	0	14	0	0	40	47	0	0	0
1997	10	0	0	159	30	5	56	0	0	0	0	0	23	0	0	117	0	0	132	27	0	0	0
1998	0	0	0	102	0	2	28	0	5	0	17	0	0	0	0	345	1	0	1962	54	0	0	0
1999	0	0	0	168	38	11	33	0	1498	0	8	0	0	675	0	156	3	0	1054	93	0	0	0
2000	0	0	0	160	0	20	30	0	0	0	0	0	0	1217	3	44	7	0	365	238	0	0	2
2001	0	0	0	262	46	8	27	0	0	0	2	0	0	1641	0	24	0	0	1542	606	0	0	9
2002	3	0	0	0	5	7	7	0	12	0	7	0	2	5565	0	168	0	0	1341	817	0	0	0
2003	0	0	0	18	44	4	11	0	0	0	12	0	2	1932	0	166	0	0	32	138	0	0	0
2004	5	0	0	366	53	137	7	0	0	0	17	1	53	3372	0	57	50	0	2022	264	0	0	0
2005	19	0	0	195	176	111	47	0	16	0	7	2	26	8324	0	0	2	0	0	58	0	0	0
2006	9	0	0	731	199	119	14	0	243	0	0	0	18	8887	0	0	75	0	315	518	0	0	0
2007	6	0	0	1435	130	228	13	0	32	0	0	1	35	3264	0	0	34	0	75	234	0	0	0
2008	15	0	4	287	118	116	0	6	0	39	3	0	2	1626	0	0	11	0	500	126	0	0	0
2009	2	0	13	94	170	0	3	0	0	2	35	0	8	0	0	0	19	0	177	282	0	39	0
2010	9	0	2	5	60	0	0	0	0	0	29	0	24	4158	0	0	0	0	200	253	0	170	0
2011	11	0	13	14	103	0	0	0	83	0	38	0	3	4194	0	3	0	0	5220	289	0	427	0
2012	15	0	0	239	9	11	0	0	282	0	8	0	5	22651	0	592	1	0	3629	225	0	0	0
2013	27	0	90	171	113	19	0	5	446	0	5	0	6	11491	0	65	0	0	3693	322	0	476	0
2014	11	0	65	138	206	278	18	0	607	0	5	0	19	8755	0	86	2	0	3542	223	0	68	0
2015	10	0	67	11	392	70	367	39	1045	0	6	0	40	128	0	41	1	0	1289	230	0	421	0
2016	0	0	14	756	553	790	666	49	316	90	63	0	166	134	0	0	10	42	1480	352	0	269	0
2017	0	0	80	1077	324	1	523	40	675	33	74	0	157	0	9	0	7	1	1933	152	0	0	102
2018	0	0	29	244	548	57	707	23	652	69	77	0	55	44	0	100	8	5	1810	166	0	170	0
2019	0	0	61	126	700	44	705	190	917	21	33	0	56	0	0	367	18	3	1256	245	0	29	27
2020	0	0	0	134	624	37	13	53	508	6	53	0	73	0	0	0	34	0	460	108	0	0	0
2021	0	0	0	140	338	24	1	2	174	85	10	0	65	0	0	0	65	0	1334	174	0	0	0

Table 4: Proportion of observer effort by flag in the data extract from the SPC observer database for longline fishing events.

Year	Obs. sets	AU	JP	KR	NC	NZ	CN	PF	TW	FJ	FM	US	CK	TO	PG	SB	WS	PW	KI	MH	VU	VN	TV	BZ
1990	305	0.14	0.86	0.00	0.00	0.00	0.00	0.00	0.00	0.00	0.00	0.00	0.00	0.00	0.00	0.00	0.00	0.00	0.00	0.00	0.00	0.00	0.00	0.00
1991	790	0.38	0.62	0.01	0.00	0.00	0.00	0.00	0.00	0.00	0.00	0.00	0.00	0.00	0.00	0.00	0.00	0.00	0.00	0.00	0.00	0.00	0.00	0.00
1992	920	0.36	0.61	0.01	0.00	0.02	0.00	0.00	0.00	0.00	0.00	0.00	0.00	0.00	0.00	0.00	0.00	0.00	0.00	0.00	0.00	0.00	0.00	0.00
1993	1235	0.45	0.50	0.00	0.00	0.00	0.01	0.00	0.03	0.00	0.00	0.00	0.00	0.00	0.00	0.00	0.00	0.00	0.00	0.00	0.00	0.00	0.00	0.00
1994	1173	0.26	0.45	0.00	0.00	0.01	0.02	0.00	0.08	0.00	0.00	0.17	0.00	0.00	0.00	0.00	0.00	0.00	0.00	0.00	0.00	0.00	0.00	0.00
1995	1063	0.19	0.35	0.00	0.00	0.07	0.09	0.00	0.06	0.03	0.00	0.18	0.01	0.02	0.00	0.00	0.00	0.00	0.00	0.00	0.00	0.00	0.00	0.00
1996	1101	0.14	0.25	0.00	0.05	0.13	0.07	0.00	0.05	0.01	0.01	0.26	0.01	0.00	0.01	0.01	0.00	0.00	0.00	0.00	0.00	0.00	0.00	0.00
1997	1497	0.10	0.18	0.00	0.00	0.26	0.07	0.04	0.05	0.02	0.02	0.21	0.00	0.00	0.00	0.05	0.00	0.00	0.00	0.00	0.00	0.00	0.00	0.00
1998	1408	0.00	0.08	0.05	0.02	0.28	0.06	0.00	0.16	0.00	0.02	0.23	0.00	0.05	0.00	0.04	0.00	0.00	0.00	0.00	0.00	0.00	0.00	0.00
1999	1059	0.00	0.05	0.05	0.02	0.32	0.08	0.00	0.10	0.05	0.02	0.16	0.00	0.02	0.04	0.08	0.00	0.00	0.00	0.00	0.00	0.00	0.00	0.00
2000	1417	0.00	0.04	0.00	0.00	0.20	0.05	0.00	0.06	0.00	0.03	0.47	0.00	0.02	0.05	0.06	0.01	0.01	0.00	0.00	0.00	0.00	0.00	0.00
2001	2219	0.02	0.01	0.00	0.01	0.21	0.05	0.00	0.04	0.01	0.01	0.51	0.00	0.00	0.09	0.03	0.01	0.00	0.00	0.00	0.00	0.00	0.00	0.00
2002	4018	0.10	0.02	0.04	0.01	0.08	0.00	0.02	0.03	0.01	0.01	0.51	0.00	0.00	0.05	0.12	0.00	0.00	0.00	0.00	0.00	0.00	0.00	0.00
2003	3368	0.12	0.01	0.00	0.03	0.14	0.01	0.06	0.01	0.05	0.00	0.42	0.00	0.00	0.04	0.10	0.00	0.00	0.00	0.00	0.00	0.00	0.00	0.00
2004	4540	0.10	0.01	0.00	0.02	0.10	0.04	0.04	0.03	0.03	0.01	0.50	0.00	0.02	0.05	0.04	0.00	0.00	0.00	0.00	0.00	0.00	0.00	0.00
2005	5036	0.10	0.03	0.02	0.01	0.07	0.04	0.05	0.00	0.09	0.01	0.51	0.00	0.00	0.07	0.00	0.00	0.00	0.00	0.00	0.00	0.00	0.00	0.00
2006	5810	0.09	0.01	0.03	0.01	0.05	0.12	0.05	0.01	0.06	0.02	0.48	0.00	0.02	0.05	0.00	0.00	0.00	0.00	0.00	0.00	0.00	0.00	0.00
2007	5111	0.07	0.01	0.02	0.01	0.08	0.11	0.03	0.01	0.06	0.01	0.56	0.00	0.01	0.02	0.00	0.00	0.00	0.00	0.00	0.00	0.00	0.00	0.00
2008	4740	0.11	0.00	0.00	0.02	0.05	0.03	0.04	0.03	0.07	0.01	0.56	0.01	0.02	0.04	0.00	0.00	0.00	0.00	0.00	0.00	0.00	0.00	0.00
2009	5055	0.08	0.00	0.00	0.04	0.08	0.04	0.09	0.03	0.04	0.00	0.56	0.01	0.01	0.00	0.00	0.00	0.00	0.00	0.00	0.01	0.00	0.00	0.00
2010	4501	0.05	0.00	0.00	0.05	0.06	0.02	0.10	0.04	0.04	0.00	0.59	0.01	0.00	0.01	0.00	0.00	0.00	0.00	0.00	0.03	0.00	0.00	0.00
2011	5654	0.05	0.00	0.02	0.03	0.04	0.01	0.06	0.22	0.05	0.00	0.42	0.01	0.00	0.02	0.01	0.00	0.00	0.00	0.00	0.04	0.02	0.00	0.00
2012	7971	0.03	0.00	0.05	0.02	0.03	0.09	0.05	0.27	0.02	0.00	0.32	0.00	0.00	0.08	0.05	0.00	0.00	0.00	0.00	0.00	0.00	0.00	0.00
2013	11939	0.02	0.00	0.06	0.01	0.02	0.09	0.04	0.33	0.06	0.01	0.21	0.01	0.00	0.02	0.01	0.00	0.00	0.00	0.00	0.10	0.00	0.00	0.00
2014	10788	0.01	0.01	0.03	0.01	0.03	0.07	0.04	0.33	0.15	0.03	0.23	0.01	0.00	0.02	0.02	0.00	0.00	0.00	0.00	0.01	0.00	0.00	0.00
2015	10723	0.01	0.17	0.04	0.01	0.03	0.00	0.03	0.29	0.16	0.02	0.17	0.01	0.00	0.01	0.01	0.00	0.00	0.01	0.00	0.02	0.00	0.00	0.00
2016	13268	0.00	0.13	0.02	0.01	0.02	0.07	0.02	0.28	0.17	0.03	0.18	0.01	0.00	0.01	0.00	0.00	0.00	0.01	0.02	0.01	0.00	0.01	0.00
2017	16189	0.00	0.09	0.04	0.01	0.02	0.13	0.03	0.35	0.11	0.00	0.15	0.03	0.00	0.00	0.00	0.00	0.00	0.01	0.02	0.00	0.00	0.00	0.00
2018	18394	0.00	0.08	0.04	0.01	0.02	0.09	0.01	0.34	0.15	0.01	0.14	0.02	0.00	0.00	0.02	0.00	0.00	0.00	0.02	0.03	0.00	0.00	0.00
2019	20175	0.00	0.11	0.06	0.01	0.01	0.13	0.02	0.29	0.13	0.02	0.14	0.01	0.00	0.00	0.03	0.01	0.00	0.01	0.01	0.02	0.00	0.00	0.00
2020	14794	0.00	0.01	0.05	0.01	0.01	0.21	0.03	0.37	0.13	0.02	0.14	0.00	0.00	0.00	0.00	0.00	0.00	0.01	0.00	0.00	0.00	0.00	0.00
2021	12812	0.00	0.00	0.03	0.02	0.01	0.15	0.04	0.41	0.09	0.00	0.21	0.00	0.01	0.00	0.00	0.00	0.00	0.01	0.01	0.00	0.00	0.00	0.00

Table 5: Proportion (in number of hooks) of longline effort coverage based on observer effort by flag in the data extract from the SPC observer database for longline fishing events.

Year	Hooks (millions)	AU	CK	CN	FJ	FM	JP	NZ	TW	US	NC	PG	TO	PF	KR	WS	PW	KI	MH	VU	SB	TV
1995	36.18	0.06	0.01	0.00	0.01	0.00	0.01	0.03	0.00	0.01	0.00	0.00	0.00	0.00	0.00	0.00	0.00	0.00	0.00	0.00	0.00	0.00
1996	30.26	0.09	0.07	0.00	0.00	0.01	0.00	0.05	0.00	0.02	0.04	0.02	0.05	0.00	0.00	0.00	0.00	0.00	0.00	0.00	0.00	0.00
1997	30.82	0.05	0.00	0.01	0.01	0.03	0.00	0.24	0.00	0.02	0.00	0.00	0.00	0.02	0.00	0.00	0.00	0.00	0.00	0.00	0.00	0.00
1998	42.31	0.00	0.00	0.00	0.00	0.01	0.00	0.16	0.00	0.02	0.01	0.00	0.04	0.00	0.00	0.00	0.00	0.00	0.00	0.00	0.00	0.00
1999	49.13	0.00	0.00	0.00	0.01	0.01	0.00	0.10	0.00	0.01	0.01	0.01	0.01	0.00	0.00	0.00	0.00	0.00	0.00	0.00	0.00	0.00
2000	35.94	0.00	0.00	0.00	0.00	0.01	0.00	0.07	0.00	0.06	0.00	0.01	0.01	0.00	0.00	0.03	0.04	0.00	0.00	0.00	0.00	0.00
2001	46.80	0.00	0.00	0.01	0.00	0.01	0.00	0.08	0.00	0.08	0.01	0.00	0.00	0.00	0.00	0.00	0.00	0.00	0.00	0.00	0.00	0.00
2002	63.71	0.00	0.01	0.00	0.00	0.01	0.00	0.05	0.00	0.10	0.02	0.03	0.00	0.01	0.00	0.00	0.00	0.00	0.00	0.00	0.00	0.00
2003	54.90	0.00	0.00	0.00	0.01	0.01	0.00	0.11	0.00	0.07	0.03	0.02	0.00	0.03	0.00	0.00	0.00	0.00	0.00	0.00	0.00	0.00
2004	55.69	0.00	0.00	0.00	0.01	0.02	0.00	0.12	0.00	0.11	0.03	0.00	0.07	0.02	0.00	0.00	0.00	0.00	0.00	0.00	0.00	0.00
2005	39.64	0.00	0.00	0.01	0.03	0.05	0.00	0.15	0.00	0.10	0.01	0.05	0.01	0.03	0.00	0.00	0.00	0.00	0.00	0.00	0.00	0.00
2006	59.38	0.00	0.01	0.00	0.02	0.12	0.00	0.13	0.00	0.10	0.02	0.05	0.08	0.03	0.01	0.00	0.00	0.00	0.00	0.00	0.00	0.00
2007	65.86	0.00	0.00	0.01	0.02	0.01	0.00	0.21	0.00	0.09	0.02	0.01	0.03	0.02	0.00	0.00	0.00	0.00	0.00	0.00	0.00	0.00
2008	52.34	0.00	0.01	0.00	0.02	0.02	0.00	0.11	0.00	0.10	0.03	0.06	0.09	0.00	0.00	0.00	0.00	0.09	0.02	0.00	0.00	0.00
2009	66.51	0.00	0.01	0.00	0.01	0.00	0.00	0.22	0.00	0.11	0.08	0.00	0.07	0.06	0.00	0.00	0.00	0.00	0.00	0.00	0.00	0.00
2010	55.54	0.00	0.00	0.00	0.01	0.00	0.00	0.13	0.00	0.13	0.09	0.01	0.02	0.00	0.00	0.00	0.00	0.00	0.00	0.00	0.00	0.00
2011	73.00	0.00	0.02	0.00	0.00	0.00	0.00	0.08	0.00	0.11	0.07	0.02	0.00	0.00	0.00	0.00	0.00	0.00	0.00	0.02	0.00	0.00
2012	78.03	0.00	0.00	0.01	0.00	0.00	0.00	0.12	0.00	0.11	0.00	0.00	0.01	0.05	0.00	0.00	0.00	0.00	0.00	0.00	0.28	0.00
2013	71.98	0.00	0.05	0.02	0.00	0.02	0.00	0.14	0.00	0.13	0.00	0.06	0.00	0.00	0.00	0.01	0.00	0.03	0.00	0.00	0.23	0.00
2014	72.91	0.00	0.08	0.00	0.00	0.00	0.00	0.14	0.00	0.11	0.00	0.04	0.02	0.04	0.00	0.00	0.00	0.00	0.00	0.01	0.00	0.00
2015	75.98	0.00	0.00	0.00	0.00	0.04	0.08	0.15	0.00	0.09	0.00	0.05	0.00	0.03	0.00	0.00	0.00	0.00	0.00	0.01	0.00	0.00
2016	66.41	0.00	0.04	0.02	0.00	0.05	0.08	0.12	0.00	0.10	0.00	0.07	0.03	0.00	0.01	0.00	0.00	0.00	0.00	0.00	0.00	0.15
2017	70.30	0.00	0.11	0.04	0.00	0.00	0.07	0.15	0.00	0.10	0.00	0.00	0.04	0.00	0.04	0.00	0.00	0.04	0.04	0.01	0.00	0.06
2018	69.96	0.00	0.09	0.03	0.00	0.02	0.07	0.11	0.07	0.11	0.00	0.01	0.02	0.03	0.03	0.00	0.00	0.02	0.07	0.04	0.03	0.07
2019	77.14	0.00	0.07	0.05	0.12	0.03	0.11	0.08	0.00	0.10	0.00	0.00	0.04	0.04	0.04	0.02	0.00	0.06	0.04	0.03	0.05	0.03
2020	62.87	0.00	0.00	0.05	0.11	0.03	0.01	0.08	0.06	0.08	0.07	0.00	0.11	0.04	0.02	0.00	0.00	0.02	0.01	0.00	0.00	0.00
2021	56.49	0.00	0.02	0.03	0.09	0.01	0.00	0.11	0.07	0.09	0.07	0.00	0.18	0.00	0.01	0.00	0.00	0.04	0.04	0.00	0.00	0.00

5.1.2 Purse-seine observer data

Table 6: Number of observer-reported silky shark interactions by flag in the data extract from the SPC observer database for purse-seine fishing events.

Year	CK	CN	EC	ES	FM	ID	JP	KI	KR	MH	NR	NZ	PG	PH	SB	SV	TV	TW	US	VU
1998	0.00	0.00	0.00	0.00	0.00	0.00	0.00	0.00	0.00	0.00	0.00	0.00	0.00	0.00	0.00	0.00	0.00	0.00	346.00	0.00
1999	0.00	0.00	0.00	0.00	0.00	0.00	0.00	0.00	0.00	0.00	0.00	0.00	0.00	0.00	57.00	0.00	0.00	0.00	883.00	0.00
2000	0.00	0.00	0.00	0.00	0.00	0.00	0.00	0.00	0.00	0.00	0.00	0.00	73.00	0.00	7.00	0.00	0.00	0.00	949.00	0.00
2001	0.00	0.00	0.00	0.00	60.00	0.00	0.00	0.00	0.00	51.00	0.00	0.00	93.00	0.00	0.00	0.00	0.00	0.00	697.00	0.00
2002	0.00	0.00	0.00	0.00	92.00	0.00	0.00	41.00	0.00	17.00	0.00	0.00	15.00	0.00	210.00	0.00	0.00	0.00	513.00	0.00
2003	0.00	0.00	0.00	0.00	339.00	0.00	0.00	78.00	0.00	312.00	0.00	0.00	40.00	0.00	219.00	0.00	0.00	0.00	939.00	511.00
2004	0.00	0.00	0.00	0.00	680.00	0.00	0.00	58.00	0.00	343.00	0.00	0.00	166.00	0.00	0.00	0.00	0.00	0.00	1564.00	1033.00
2005	0.00	0.00	0.00	0.00	359.00	0.00	0.00	0.00	0.00	288.00	0.00	0.00	235.00	567.00	247.00	0.00	0.00	0.00	1221.00	432.00
2006	0.00	0.00	0.00	0.00	124.00	0.00	0.00	0.00	0.00	280.00	0.00	0.00	265.00	0.00	0.00	0.00	0.00	0.00	242.00	1360.00
2007	0.00	0.00	0.00	0.00	165.00	0.00	0.00	61.00	0.00	96.00	0.00	0.00	275.00	0.00	0.00	0.00	0.00	0.00	703.00	1095.00
2008	0.00	0.00	0.00	0.00	225.00	0.00	0.00	71.00	0.00	109.00	0.00	0.00	38.00	0.00	256.00	0.00	0.00	0.00	1218.00	175.00
2009	0.00	27.00	0.00	2.00	251.00	0.00	767.00	159.00	126.00	244.00	0.00	51.00	247.00	313.00	0.00	166.00	1.00	108.00	1930.00	413.00
2010	0.00	495.00	548.00	912.00	518.00	0.00	1830.00	319.00	2243.00	501.00	0.00	299.00	990.00	52.00	57.00	305.00	90.00	1775.00	6374.00	830.00
2011	0.00	1220.00	1135.00	203.00	776.00	45.00	3105.00	310.00	2647.00	1780.00	0.00	261.00	640.00	188.00	220.00	445.00	52.00	3469.00	6722.00	538.00
2012	0.00	764.00	203.00	668.00	794.00	0.00	3287.00	480.00	1294.00	958.00	0.00	119.00	1089.00	120.00	9.00	30.00	10.00	2625.00	3684.00	1502.00
2013	0.00	1507.00	989.00	1436.00	64.00	0.00	4197.00	725.00	2304.00	1322.00	0.00	114.00	1298.00	245.00	0.00	215.00	10.00	4129.00	6018.00	1784.00
2014	0.00	1343.00	2414.00	2003.00	1141.00	0.00	4154.00	1736.00	1313.00	2877.00	0.00	202.00	2272.00	483.00	0.00	856.00	24.00	4488.00	6766.00	1393.00
2015	0.00	297.00	574.00	1236.00	1757.00	0.00	1717.00	1849.00	1848.00	1729.00	0.00	28.00	4035.00	574.00	95.00	501.00	45.00	3564.00	6333.00	314.00
2016	0.00	175.00	155.00	355.00	3316.00	0.00	5697.00	3631.00	3037.00	2357.00	0.00	78.00	6771.00	1979.00	1003.00	351.00	112.00	4668.00	8659.00	70.00
2017	0.00	47.00	973.00	1400.00	5560.00	0.00	6984.00	3391.00	3550.00	3548.00	0.00	161.00	12495.00	64.00	712.00	401.00	103.00	5919.00	10128.00	113.00
2018	0.00	1193.00	1387.00	1629.00	4308.00	0.00	5147.00	4897.00	4057.00	2845.00	81.00	57.00	10422.00	297.00	900.00	196.00	130.00	8381.00	9857.00	206.00
2019	54.00	49.00	2460.00	2310.00	6188.00	0.00	7737.00	6319.00	5217.00	4498.00	1135.00	0.00	13725.00	118.00	1464.00	756.00	66.00	17570.00	10069.00	814.00
2020	0.00	0.00	2025.00	732.00	4147.00	0.00	1345.00	3570.00	3047.00	1168.00	2889.00	0.00	1481.00	215.00	414.00	256.00	115.00	5255.00	4645.00	1056.00

Table 7: Proportion of total observer effort by flag in the data extract from the SPC observer database for purse - seine fishing events.

Year	Obs. sets	US	FM	KI	SB	PG	MH	VU	PH	CN	ES	JP	KR	NZ	SV	TV	TW	EC	ID	NR	CK
1995	747	1.00	0.00	0.00	0.00	0.00	0.00	0.00	0.00	0.00	0.00	0.00	0.00	0.00	0.00	0.00	0.00	0.00	0.00	0.00	0.00
1996	1273	1.00	0.00	0.00	0.00	0.00	0.00	0.00	0.00	0.00	0.00	0.00	0.00	0.00	0.00	0.00	0.00	0.00	0.00	0.00	0.00
1997	923	1.00	0.00	0.00	0.00	0.00	0.00	0.00	0.00	0.00	0.00	0.00	0.00	0.00	0.00	0.00	0.00	0.00	0.00	0.00	0.00
1998	904	0.91	0.06	0.03	0.00	0.00	0.00	0.00	0.00	0.00	0.00	0.00	0.00	0.00	0.00	0.00	0.00	0.00	0.00	0.00	0.00
1999	634	0.94	0.02	0.01	0.03	0.00	0.00	0.00	0.00	0.00	0.00	0.00	0.00	0.00	0.00	0.00	0.00	0.00	0.00	0.00	0.00
2000	789	0.91	0.00	0.01	0.03	0.05	0.00	0.00	0.00	0.00	0.00	0.00	0.00	0.00	0.00	0.00	0.00	0.00	0.00	0.00	0.00
2001	976	0.91	0.03	0.00	0.00	0.04	0.03	0.00	0.00	0.00	0.00	0.00	0.00	0.00	0.00	0.00	0.00	0.00	0.00	0.00	0.00
2002	1086	0.74	0.08	0.03	0.04	0.07	0.03	0.01	0.00	0.00	0.00	0.00	0.00	0.00	0.00	0.00	0.00	0.00	0.00	0.00	0.00
2003	1178	0.44	0.10	0.03	0.02	0.05	0.11	0.24	0.00	0.00	0.00	0.00	0.00	0.00	0.00	0.00	0.00	0.00	0.00	0.00	0.00
2004	1839	0.38	0.09	0.01	0.00	0.08	0.12	0.31	0.00	0.00	0.00	0.00	0.00	0.00	0.00	0.00	0.00	0.00	0.00	0.00	0.00
2005	1394	0.32	0.10	0.00	0.04	0.14	0.16	0.20	0.04	0.00	0.00	0.00	0.00	0.00	0.00	0.00	0.00	0.00	0.00	0.00	0.00
2006	1578	0.20	0.03	0.02	0.02	0.18	0.10	0.45	0.00	0.00	0.00	0.00	0.00	0.00	0.00	0.00	0.00	0.00	0.00	0.00	0.00
2007	1646	0.21	0.04	0.01	0.00	0.14	0.10	0.49	0.00	0.00	0.00	0.00	0.00	0.00	0.00	0.00	0.00	0.00	0.00	0.00	0.00
2008	1776	0.57	0.08	0.01	0.02	0.05	0.10	0.18	0.00	0.00	0.00	0.00	0.00	0.00	0.00	0.00	0.00	0.00	0.00	0.00	0.00
2009	5577	0.37	0.02	0.02	0.00	0.08	0.07	0.12	0.06	0.02	0.00	0.07	0.08	0.01	0.01	0.00	0.06	0.00	0.00	0.00	0.00
2010	18437	0.28	0.02	0.02	0.00	0.07	0.04	0.08	0.00	0.05	0.01	0.11	0.15	0.01	0.01	0.01	0.12	0.02	0.00	0.00	0.00
2011	19155	0.25	0.03	0.03	0.01	0.07	0.05	0.07	0.01	0.05	0.01	0.14	0.14	0.01	0.01	0.01	0.12	0.02	0.00	0.00	0.00
2012	22615	0.27	0.02	0.04	0.00	0.07	0.05	0.07	0.02	0.04	0.01	0.13	0.11	0.01	0.00	0.01	0.13	0.01	0.00	0.00	0.00
2013	26613	0.21	0.00	0.03	0.00	0.05	0.06	0.07	0.06	0.06	0.02	0.12	0.13	0.01	0.01	0.01	0.14	0.02	0.00	0.00	0.00
2014	28016	0.23	0.02	0.06	0.00	0.07	0.07	0.03	0.11	0.04	0.01	0.09	0.11	0.01	0.01	0.00	0.13	0.01	0.00	0.00	0.00
2015	27278	0.19	0.05	0.10	0.00	0.13	0.08	0.01	0.11	0.01	0.01	0.06	0.13	0.00	0.00	0.00	0.11	0.00	0.00	0.00	0.00
2016	25449	0.14	0.06	0.10	0.02	0.13	0.05	0.00	0.13	0.01	0.01	0.09	0.12	0.01	0.00	0.00	0.12	0.00	0.00	0.00	0.00
2017	27693	0.14	0.08	0.08	0.02	0.17	0.05	0.01	0.09	0.00	0.01	0.09	0.13	0.00	0.00	0.00	0.11	0.01	0.00	0.00	0.00
2018	31854	0.14	0.07	0.10	0.01	0.13	0.05	0.01	0.09	0.01	0.01	0.09	0.13	0.00	0.00	0.01	0.13	0.01	0.00	0.00	0.00
2019	32601	0.13	0.09	0.10	0.02	0.10	0.06	0.02	0.08	0.00	0.01	0.08	0.14	0.00	0.00	0.00	0.14	0.01	0.00	0.02	0.00
2020	12413	0.09	0.10	0.10	0.01	0.05	0.03	0.04	0.21	0.00	0.00	0.06	0.14	0.00	0.00	0.01	0.08	0.02	0.00	0.06	0.00

Table 8: Proportion (in number of sets) of purse-seine effort coverage based on observer effort by flag in the data extract from the SPC observer database for purse-seine events.

Year	Sets (1000s)	US	FM	KI	SB	PG	MH	VU	PH	CN	ES	JP	KR	NZ	SV	TV	TW	EC	ID	NR	CK	AU	FR
1995	32.07	0.12	0.00	0.00	0.00	0.00	0.00	0.00	0.00	0.00	0.00	0.00	0.00	0.00	0.00	0.00	0.00	0.00	0.00	0.00	0.00	0.00	0.00
1996	33.19	0.22	0.00	0.00	0.00	0.00	0.00	0.00	0.00	0.00	0.00	0.00	0.00	0.00	0.00	0.00	0.00	0.00	0.00	0.00	0.00	0.00	0.00
1997	34.10	0.18	0.00	0.00	0.00	0.00	0.00	0.00	0.00	0.00	0.00	0.00	0.00	0.00	0.00	0.00	0.00	0.00	0.00	0.00	0.00	0.00	0.00
1998	35.88	0.18	0.13	0.12	0.00	0.00	0.00	0.00	0.00	0.00	0.00	0.00	0.00	0.00	0.00	0.00	0.00	0.00	0.00	0.00	0.00	0.00	0.00
1999	31.62	0.18	0.04	0.05	0.02	0.00	0.00	0.00	0.00	0.00	0.00	0.00	0.00	0.00	0.00	0.00	0.00	0.00	0.00	0.00	0.00	0.00	0.00
2000	35.05	0.20	0.00	0.05	0.09	0.02	0.00	0.00	0.00	0.00	0.00	0.00	0.00	0.00	0.00	0.00	0.00	0.00	0.00	0.00	0.00	0.00	0.00
2001	33.98	0.23	0.04	0.00	0.00	0.01	0.04	0.00	0.00	0.00	0.00	0.00	0.00	0.00	0.00	0.00	0.00	0.00	0.00	0.00	0.00	0.00	0.00
2002	37.58	0.17	0.14	0.18	0.16	0.02	0.05	0.05	0.00	0.00	0.00	0.00	0.00	0.00	0.00	0.00	0.00	0.00	0.00	0.00	0.00	0.00	0.00
2003	39.27	0.17	0.12	0.25	0.07	0.01	0.15	0.86	0.00	0.00	0.00	0.00	0.00	0.00	0.00	0.00	0.00	0.00	0.00	0.00	0.00	0.00	0.00
2004	40.86	0.27	0.17	0.13	0.00	0.03	0.20	0.58	0.00	0.00	0.00	0.00	0.00	0.00	0.00	0.00	0.00	0.00	0.00	0.00	0.00	0.00	0.00
2005	45.77	0.19	0.15	0.00	0.10	0.03	0.23	0.20	0.01	0.00	0.00	0.00	0.00	0.00	0.00	0.00	0.00	0.00	0.00	0.00	0.00	0.00	0.00
2006	42.61	0.17	0.12	0.27	0.05	0.04	0.18	0.75	0.00	0.00	0.00	0.00	0.00	0.00	0.00	0.00	0.00	0.00	0.00	0.00	0.00	0.00	0.00
2007	47.05	0.18	0.16	0.13	0.00	0.03	0.19	0.50	0.00	0.00	0.00	0.00	0.00	0.00	0.00	0.00	0.00	0.00	0.00	0.00	0.00	0.00	0.00
2008	53.35	0.16	0.24	0.11	0.07	0.01	0.24	0.30	0.00	0.00	0.00	0.00	0.00	0.00	0.00	0.00	0.00	0.00	0.00	0.00	0.00	0.00	0.00
2009	53.00	0.25	0.16	0.19	0.02	0.06	0.43	0.70	0.03	0.04	0.01	0.06	0.07	0.08	0.34	0.16	0.06	0.00	0.00	0.00	0.00	0.00	0.00
2010	56.36	0.63	0.40	0.57	0.04	0.17	0.45	1.00	0.00	0.37	0.59	0.23	0.39	0.16	1.00	0.58	0.28	1.00	0.00	0.00	0.00	0.00	0.00
2011	59.75	0.78	0.54	0.44	0.12	0.16	0.46	1.00	0.02	0.28	0.25	0.18	0.41	0.22	0.76	0.40	0.32	0.94	0.00	0.00	0.00	0.00	0.00
2012	63.82	0.70	0.37	0.46	0.07	0.18	0.61	1.00	0.07	0.47	0.51	0.23	0.36	0.36	0.16	0.47	0.40	0.55	0.00	0.00	0.00	0.00	0.00
2013	62.62	0.72	0.10	0.43	0.00	0.16	0.76	1.00	0.23	0.49	1.00	0.27	0.52	0.24	0.63	0.39	0.46	1.00	0.00	0.00	0.00	0.00	0.00
2014	63.63	0.68	0.55	0.62	0.00	0.22	0.85	1.00	0.35	0.44	0.86	0.24	0.47	0.33	0.86	0.51	0.45	0.97	0.00	0.00	0.00	0.00	0.00
2015	50.98	0.70	0.84	0.81	0.03	0.53	0.80	1.00	0.47	0.27	0.48	0.24	0.59	0.11	0.65	0.45	0.49	0.87	0.00	0.00	0.00	0.00	0.00
2016	49.44	0.71	0.77	0.67	0.22	0.36	0.75	1.00	0.58	0.41	1.00	0.33	0.54	0.30	0.77	0.78	0.53	0.71	0.00	0.00	0.00	0.00	0.00
2017	54.61	0.83	0.75	0.56	0.29	0.38	0.83	0.74	0.50	0.13	1.00	0.33	0.57	0.37	1.00	0.70	0.47	0.69	0.00	0.00	0.00	0.00	0.00
2018	53.12	0.84	0.67	0.72	0.26	0.36	0.81	0.76	0.92	0.63	1.00	0.44	0.63	0.35	0.73	0.70	0.64	1.00	0.00	0.63	0.00	0.00	0.00
2019	56.64	0.86	0.64	0.61	0.33	0.40	0.70	0.67	0.59	0.95	1.00	0.37	0.60	0.00	1.00	0.73	0.63	1.00	0.00	0.72	1.00	0.00	0.00
2020	53.26	0.36	0.25	0.30	0.10	0.09	0.20	0.39	0.41	0.00	0.26	0.10	0.27	0.00	0.46	0.37	0.19	1.00	0.00	0.28	0.43	0.00	0.00

5.2 Logsheet data availability

Table 9: Number of reported silky shark captures by flag in the data extract from the SPC logsheet database for longline fishing events.

Year	AS	AU	BZ	CK	CN	ES	FJ	FM	GU	ID	JP	KI	KR	MH	NC	NU	NZ	PF	PG	PH	PT	PW	SB	SN	TO	TV	TW	US	VN	VU	WS
1998	0	0	0	0	0	0	0	0	0	0	0	0	0	0	0	0	0	0	0	0	0	0	0	0	0	0	0	0	0	0	240
1999	0	0	0	0	0	0	0	0	0	0	0	0	0	0	0	0	0	0	0	0	0	0	0	0	0	0	0	0	0	0	1
2001	0	3	0	0	0	0	0	0	0	0	0	0	0	0	0	0	0	0	0	0	0	0	0	0	0	0	0	0	0	0	0
2002	0	13	0	0	0	0	0	0	0	0	0	0	0	0	0	0	0	0	0	0	0	0	0	0	0	0	0	3	0	0	0
2003	0	34	0	0	0	0	0	0	0	0	0	0	0	0	0	0	0	0	0	0	0	0	0	0	0	0	0	2	0	0	0
2004	0	23	0	0	0	0	0	0	0	0	0	0	0	0	0	0	0	0	0	0	0	0	0	0	0	0	0	0	0	0	0
2005	0	67	0	0	0	72	0	0	0	0	0	0	0	0	0	0	0	0	0	0	0	0	0	0	0	0	0	0	0	0	0
2006	0	121	0	0	0	134	0	0	0	0	0	0	0	0	0	0	0	0	0	0	0	0	0	0	0	0	0	0	0	0	0
2007	0	144	0	0	0	45	0	0	0	0	0	0	0	0	0	0	0	0	0	0	0	0	0	0	0	0	0	358	0	0	0
2008	0	34	0	0	0	192	0	0	0	0	0	0	0	0	0	0	0	0	0	0	0	0	0	0	0	0	0	82	0	0	0
2009	0	27	0	0	0	66	0	0	0	0	0	0	0	0	0	0	0	0	0	0	0	0	0	0	0	0	1638	252	0	0	0
2010	0	29	0	0	0	34	0	0	0	0	0	0	0	0	2	0	0	0	0	0	0	0	0	0	0	0	15207	488	0	0	1
2011	0	29	0	0	0	12	7	0	0	0	0	0	0	0	2	0	0	0	0	0	0	0	0	0	0	0	209	541	0	37	14
2012	0	8	0	141	149	21	224	0	0	0	0	0	0	0	4	0	0	0	0	0	0	0	0	0	0	0	57	414	0	195	42
2013	0	133	0	134	118	205	773	0	0	0	4	0	0	0	0	0	0	0	4147	2	0	0	0	0	0	0	452	662	0	4201	105
2014	0	265	0	531	1282	0	229	423	0	0	1592	0	2251	0	0	0	0	49	21074	0	0	0	2	0	13	0	2834	838	0	56	2
2015	0	514	0	385	715	0	132	1359	0	0	0	0	942	1	152	0	0	406	0	0	0	0	123	0	8	0	600	1014	0	0	27
2016	0	136	0	178	328	0	144	849	0	0	0	298	1989	84	403	0	0	2021	0	0	0	0	10	0	39	0	153	786	0	28	54
2017	0	395	0	24	884	0	257	1388	0	0	0	69	728	741	612	0	0	1740	0	0	0	31	0	0	11	99	0	647	0	69	0
2018	0	130	0	130	1203	0	2317	2323	0	0	0	20	15	1350	640	0	0	2123	1211	0	0	1823	123	0	0	244	3	678	0	297	6
2019	0	57	0	252	257	0	4539	2320	0	0	0	0	1103	1495	481	0	0	1292	145	0	0	17760	126	0	4	0	0	1073	0	79	132
2020	0	248	0	68	1898	0	4406	4623	0	0	0	55	106	3459	549	0	0	1363	0	0	0	0	832	0	0	0	772	808	0	74	1
2021	0	60	0	0	797	0	3598	4549	0	0	0	44	141	1884	371	0	0	3435	0	0	0	0	1685	0	8	0	53	926	0	0	0
2022	0	0	0	46	1937	0	1745	2172	0	0	0	6	467	2624	545	0	0	1635	0	0	0	15	162	0	0	0	245	546	0	0	27

Table 10: Reported silky shark captures (in mt) by flag in the data extract from the SPC logsheet database for purse-seine fishing events.

Year	CK	CN	EC	ES	FM	FR	ID	JP	KI	KR	MH	NR	NZ	PA	PG	PH	SB	SV	TV	TW	US	VN	VU
1997	0.00	0.00	0.00	0.00	0.00	0.00	0.00	0.00	0.00	0.00	0.00	0.00	0.00	0.00	0.28	0.00	0.00	0.00	0.00	0.00	0.00	0.00	0.00
1998	0.00	0.00	0.00	0.00	0.00	0.00	0.00	0.00	0.00	0.00	0.00	0.00	0.00	0.00	0.32	0.00	0.00	0.00	0.00	0.00	0.00	0.00	0.00
2002	0.00	0.00	0.00	0.00	0.00	0.00	0.00	0.00	0.00	0.00	0.00	0.00	0.00	0.00	0.72	0.00	0.00	0.00	0.00	0.00	0.00	0.00	0.00
2003	0.00	0.00	0.00	0.00	0.00	0.00	0.00	0.00	0.00	0.00	0.00	0.00	0.00	0.00	1.70	0.00	0.00	0.00	0.00	0.00	0.00	0.00	0.00
2004	0.00	0.00	0.00	0.00	0.00	0.00	0.00	0.00	0.00	0.00	0.00	0.00	0.00	0.00	0.60	0.20	0.00	0.00	0.00	0.31	0.00	0.00	1.95
2005	0.00	0.00	0.00	0.00	0.00	0.00	0.00	0.00	0.00	0.00	0.00	0.00	0.00	0.00	8.04	0.78	0.00	0.00	0.00	0.71	0.00	0.00	0.20
2006	0.00	0.00	0.00	0.00	0.00	0.00	0.00	0.00	0.00	0.00	0.00	0.00	0.00	0.00	1.56	0.56	0.00	0.00	0.00	0.47	0.45	0.00	20.29
2007	0.00	0.00	0.00	0.00	0.00	0.00	0.00	0.00	0.00	0.20	0.00	0.00	0.00	0.00	13.35	3.17	0.00	0.00	0.00	0.97	0.71	0.00	0.02
2008	0.00	0.00	0.00	0.00	0.00	0.00	0.00	0.00	0.00	0.06	0.00	0.00	0.00	0.00	10.38	9.68	0.00	0.00	0.00	0.36	1.72	0.00	0.08
2009	0.00	0.68	0.00	0.00	0.00	0.00	0.00	0.11	0.00	8.27	0.25	0.00	0.20	0.00	4.83	0.78	0.00	0.00	0.00	0.42	0.41	0.00	0.78
2010	0.00	1.43	0.00	0.00	0.00	0.00	0.00	4.37	0.00	1.29	0.02	0.00	0.00	0.00	3.28	3.70	0.00	0.00	0.00	2.85	35.77	0.00	1.82
2011	0.00	1.44	0.00	0.00	4.74	0.00	0.00	16.12	0.00	7.16	2.12	0.00	0.80	0.00	6.07	7.06	0.00	0.00	2.14	57.91	89.30	0.00	17.65
2012	0.00	0.32	0.61	0.00	0.00	0.00	0.00	5.41	0.01	2.84	5.54	0.00	0.03	0.00	8.85	4.12	0.00	0.00	0.32	3.96	60.56	0.00	9.32
2013	0.00	1.96	0.00	0.00	1.17	0.00	0.00	0.71	0.00	12.21	0.32	0.00	0.14	0.00	6.03	2.36	0.00	0.00	0.14	8.74	36.97	0.00	18.06
2014	0.00	9.29	11.82	2.95	3.72	0.00	0.00	12.73	1.30	1.04	4.58	0.00	0.05	0.00	22.76	16.84	2.99	0.04	0.03	16.47	54.98	0.00	2.15
2015	0.00	5.54	0.35	0.39	15.10	0.00	0.00	69.14	10.72	49.47	3.92	0.00	0.85	0.00	69.83	30.23	1.53	3.22	0.03	41.77	47.01	0.00	0.00
2016	0.00	0.00	0.00	0.00	60.60	0.00	0.00	59.57	17.32	39.81	16.10	0.00	0.66	0.00	63.25	11.20	20.08	0.00	0.00	40.80	54.65	0.00	0.00
2017	0.00	0.80	0.00	0.00	24.44	0.00	0.00	26.32	20.31	40.18	10.40	0.00	0.00	0.00	61.80	3.32	10.66	0.03	0.00	35.88	48.15	0.00	0.15
2018	0.00	8.50	0.00	0.00	18.95	0.00	0.00	13.92	24.72	9.80	2.02	0.18	0.00	0.00	26.25	0.18	7.08	0.16	3.40	17.12	14.37	0.00	0.37
2019	0.00	0.20	0.00	0.00	34.22	0.00	0.00	37.20	70.57	4.78	4.55	2.74	0.10	0.00	20.76	0.00	8.09	1.56	0.00	48.95	22.69	0.00	0.84
2020	0.00	0.00	0.00	0.00	15.53	0.00	0.00	14.71	15.80	10.81	3.79	19.19	0.00	0.00	34.99	0.08	7.16	3.62	0.14	19.20	29.01	0.00	3.02
2021	0.00	0.00	0.00	0.00	8.97	0.00	0.00	4.19	8.58	2.22	7.98	9.39	0.00	0.00	9.38	0.00	3.06	3.98	2.84	17.85	34.82	0.00	2.31
2022	0.30	0.00	0.35	0.00	0.61	0.00	0.00	4.33	3.22	4.01	0.83	2.50	0.00	0.00	0.79	0.00	2.72	3.56	0.95	15.61	6.11	0.00	7.13

FIGURES

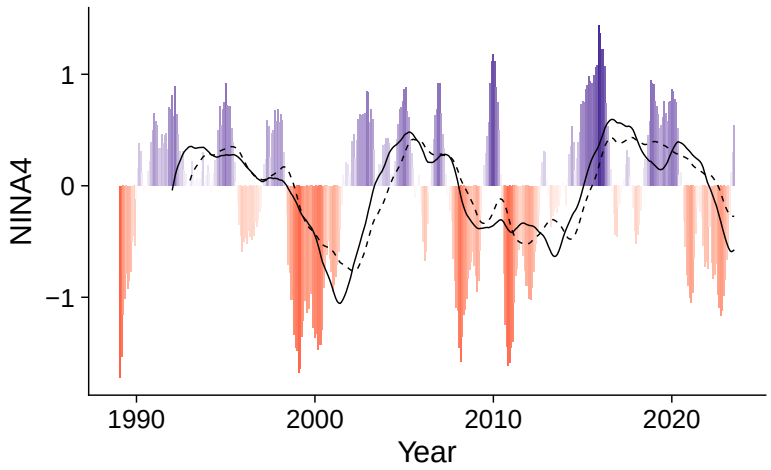

Figure 1: NINA4 index by year-month and associated 36 month (solid line) and 48 month (dashed line) lagged moving average timeseries, used for fisheries catching predominantly small and a mix of small and large sharks, respectively.

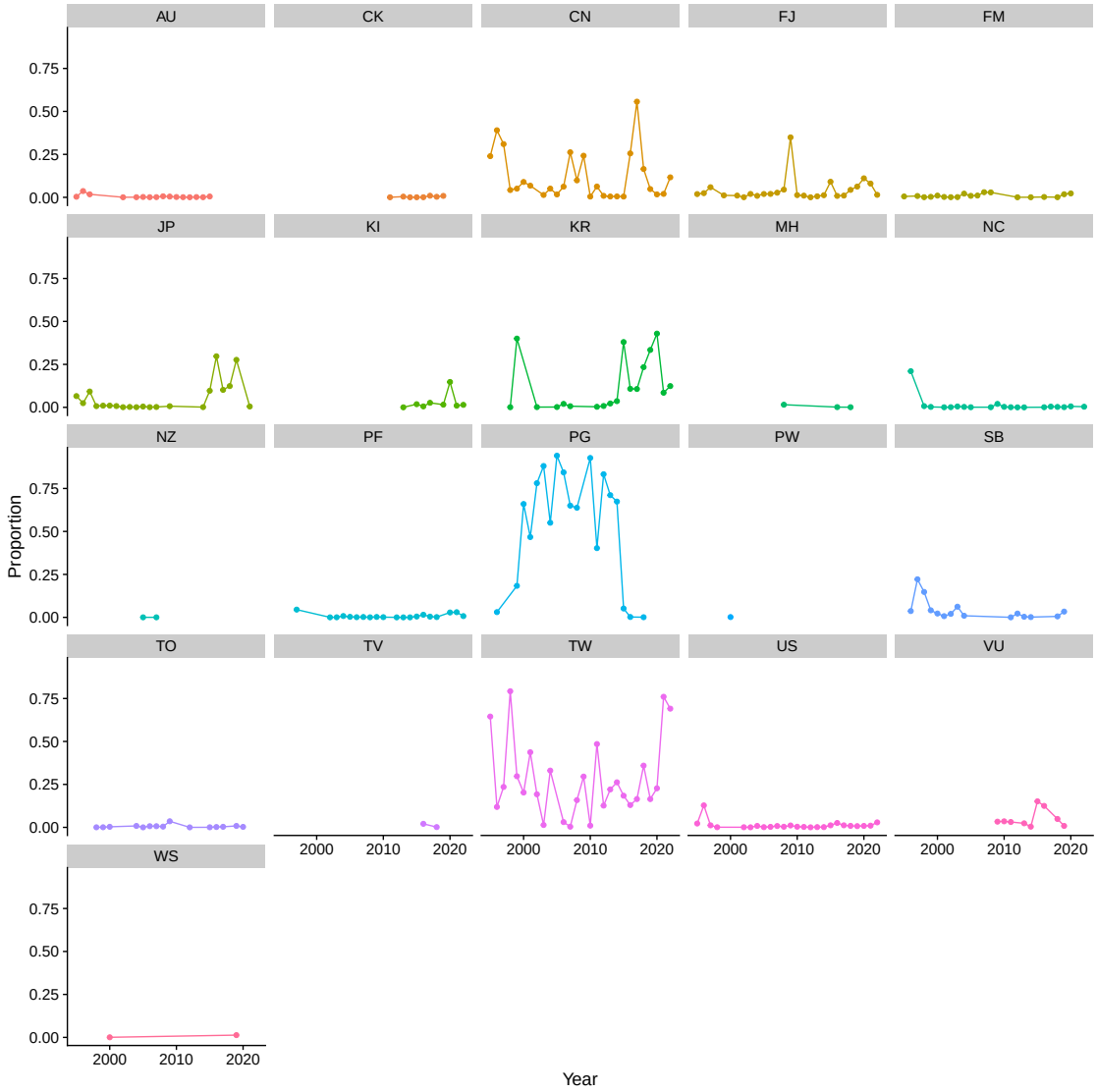

Figure 2: Proportion of length samples by vessel flag and year for observed longline sets.

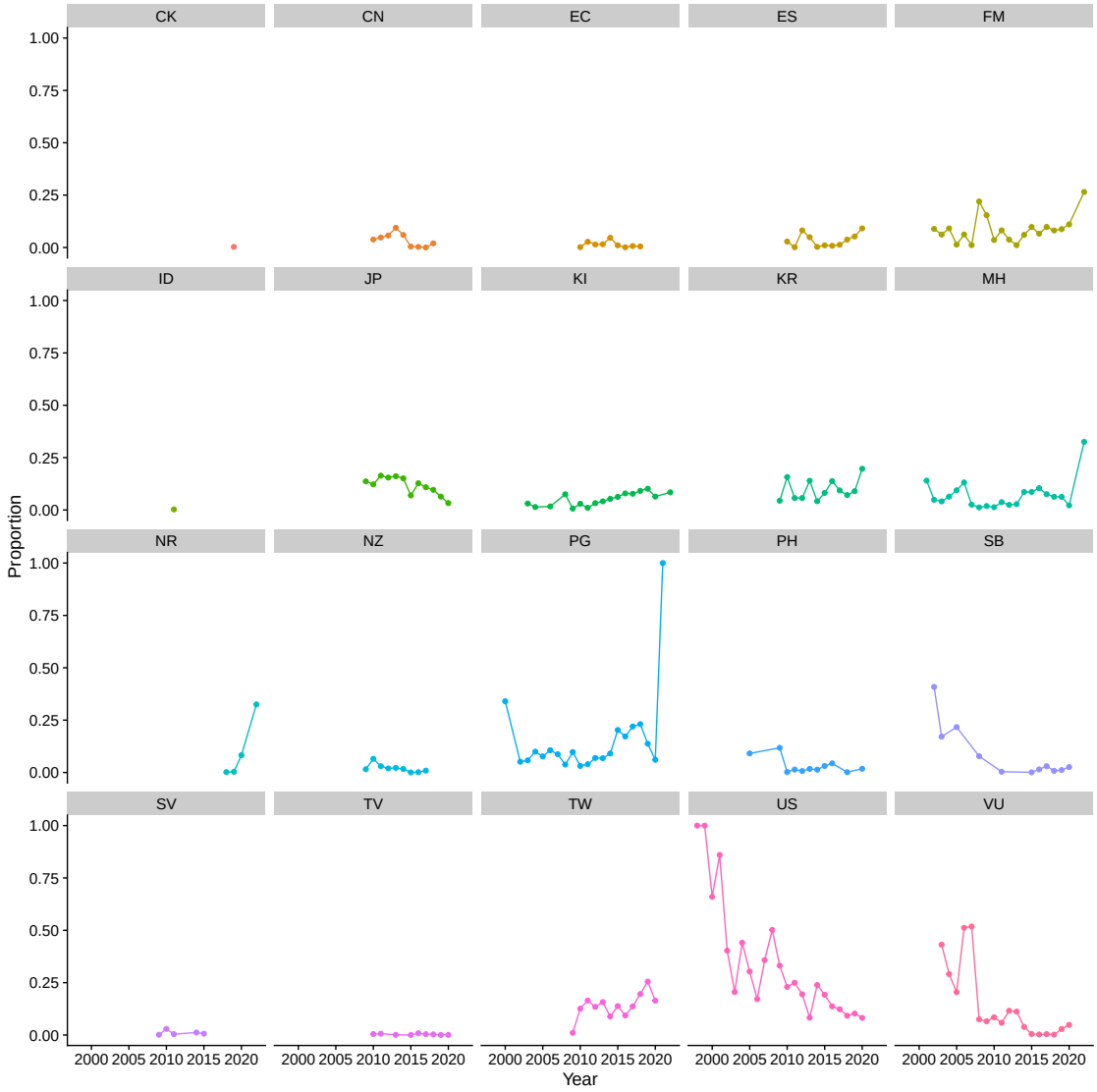

Figure 3: Proportion of length samples by vessel flag and year for observed purse-seine sets.

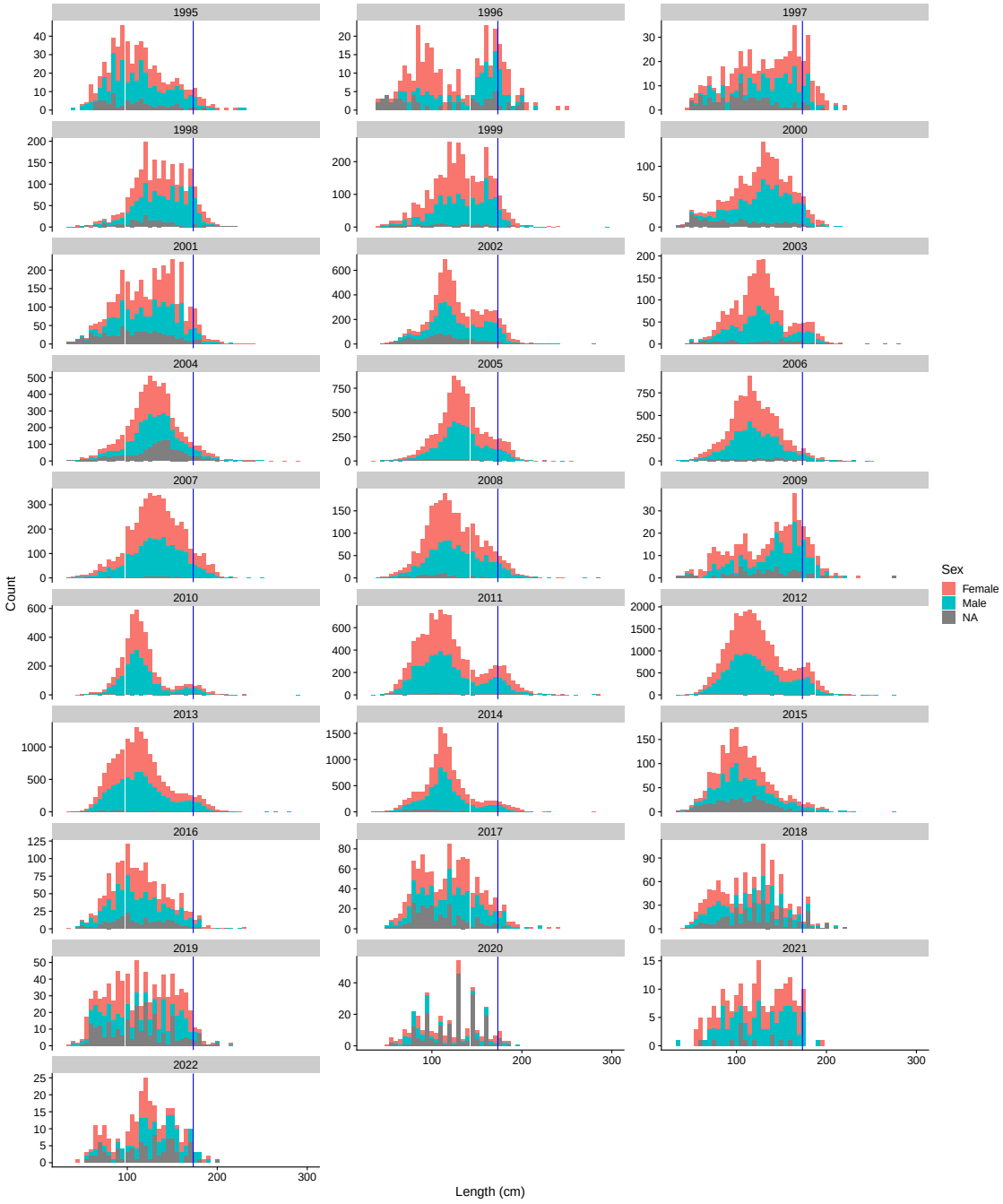

Figure 4: Length frequencies by sex and year for silky shark measured on observed longline sets. The length at maturity for females is indicated with a vertical line.

5.3 CPUE figures

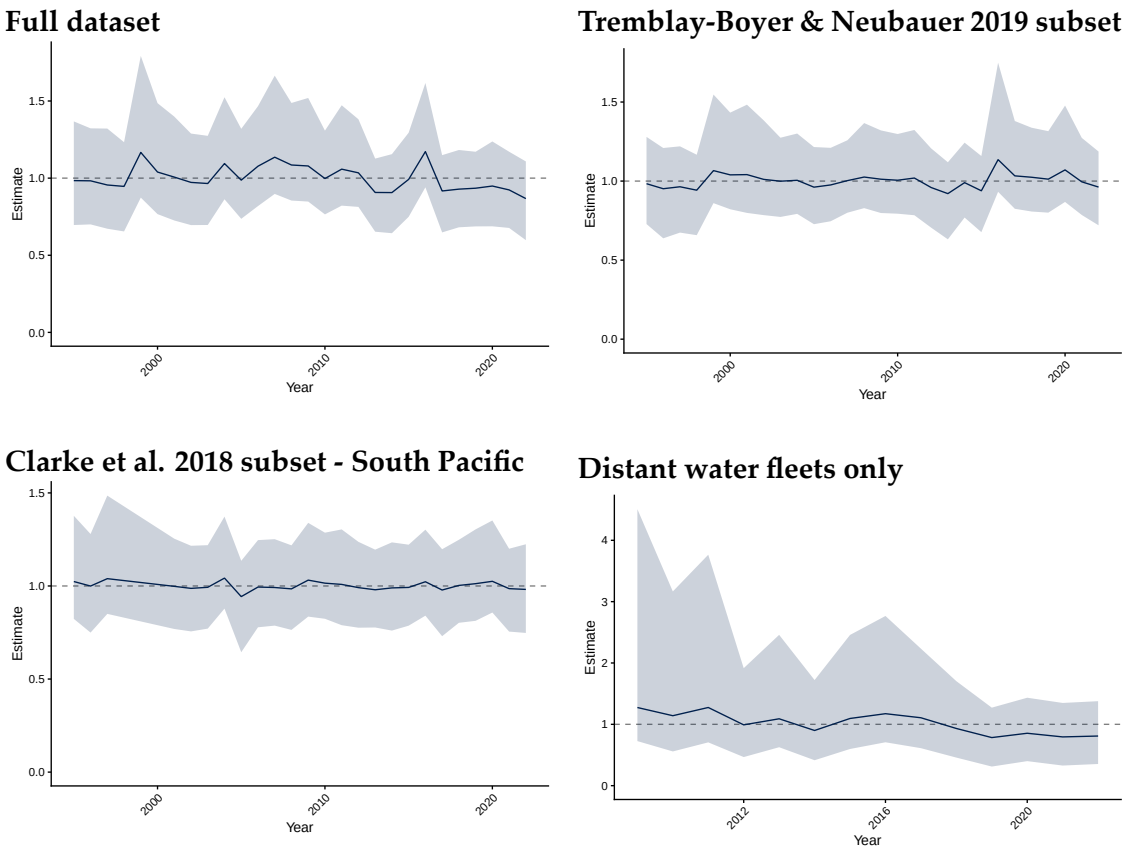

Figure 5: Longline CPUE across four distinct data-sets. Shown is the posterior median and 95% credible interval for the year effect, standardised for regional trends and operational and environmental variables.

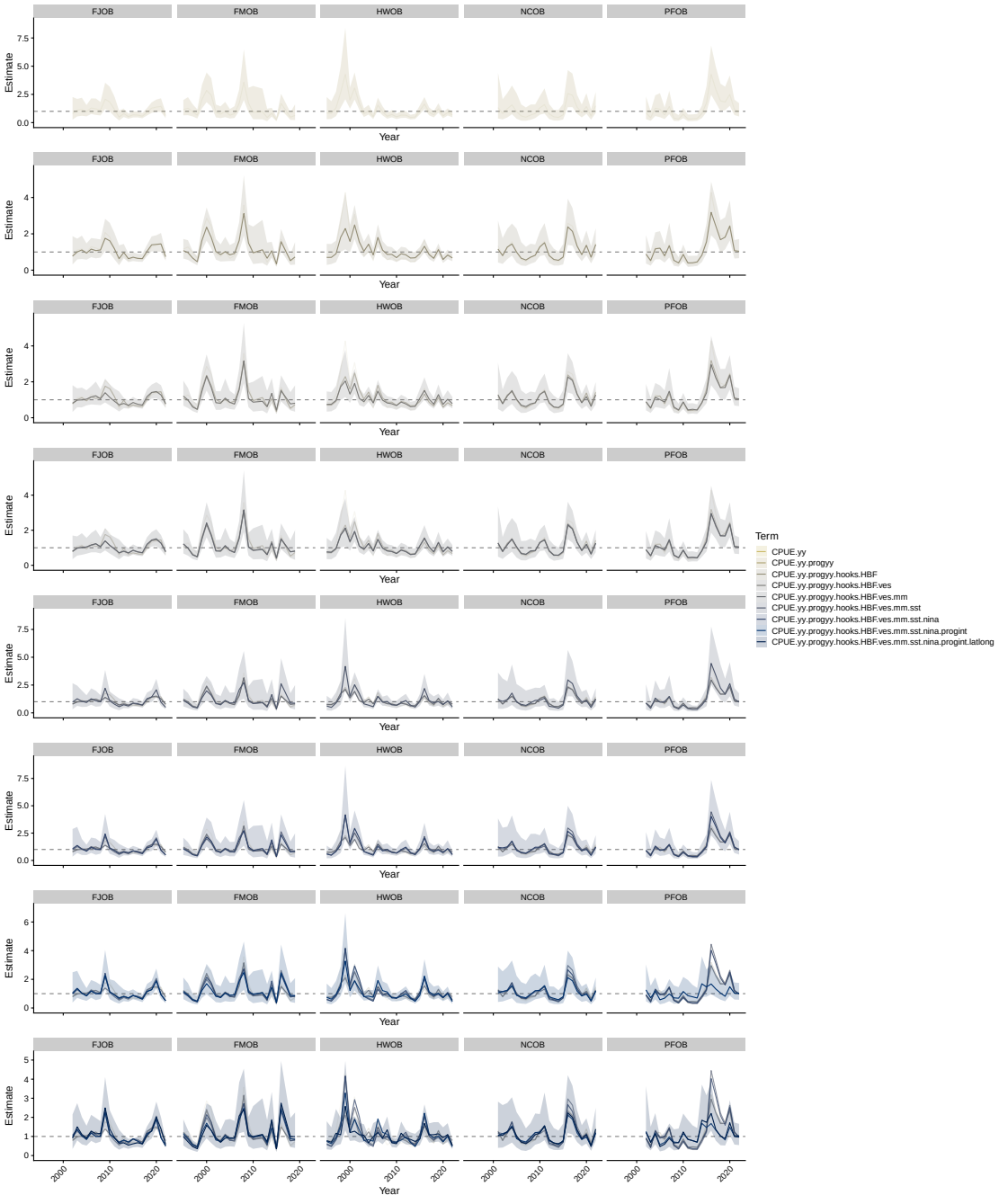

Figure 6: Longline CPUE standardisation effects by observer-program for standardisaton based on long-running observer programs only. Each row of plots corresponds to the addition of a variable, starting with a model that includes observer-program-year interactions. In each row, the posterior median and credible interval is shown for the updated model, posterior medians for the year effect from sub-models are shown for comparison.

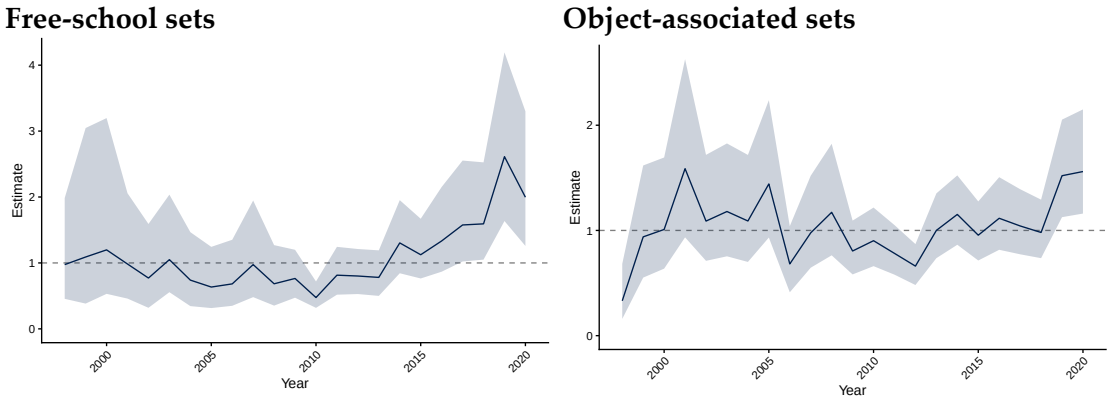

Figure 7: Purse-seine CPUE index by set-type. Shown is the posterior median and 95% credible interval for the year effect, standardised for regional trends and environmental variables.

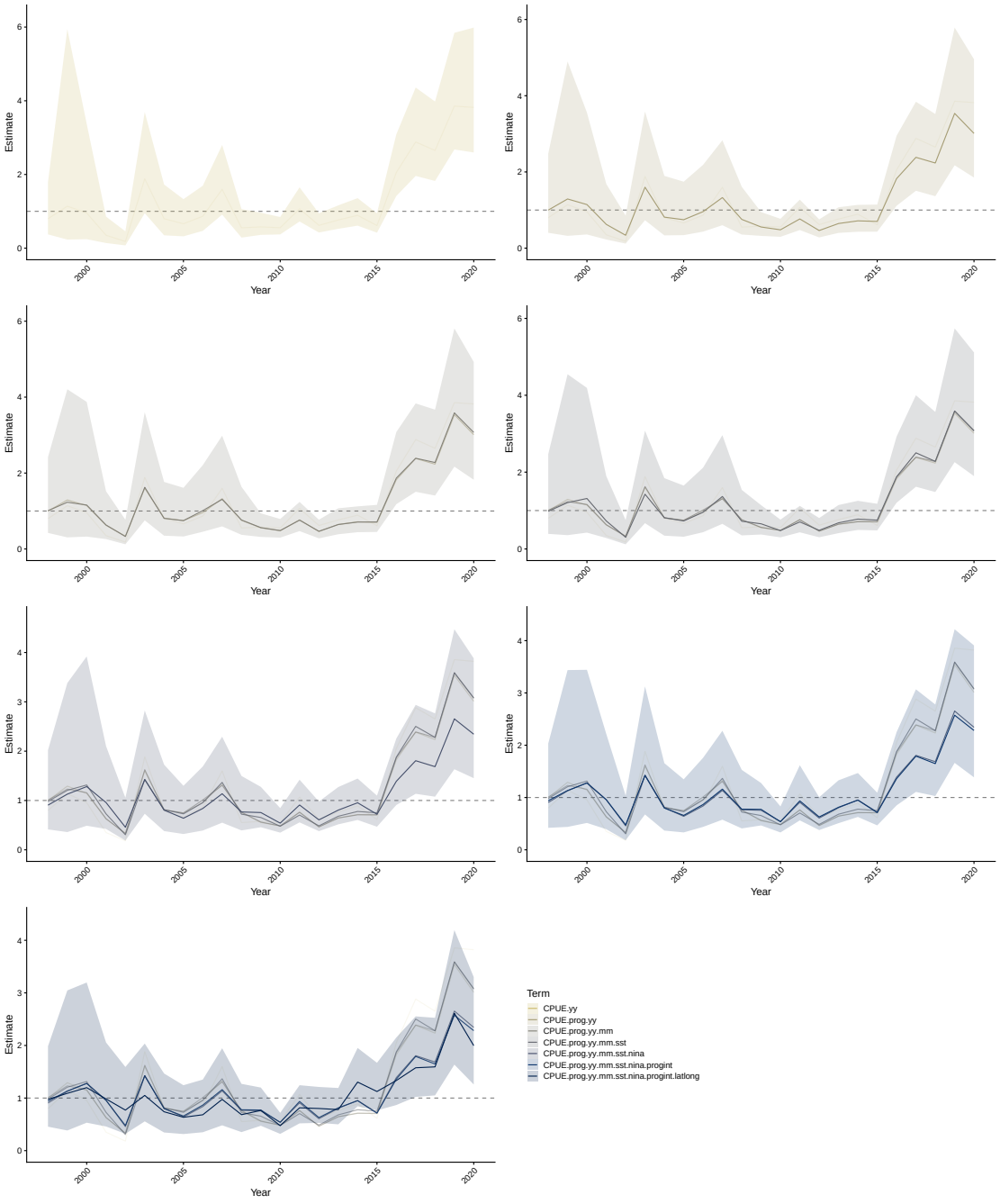

Figure 8: CPUE standardisation effects for free-school purse-seine sets. Each row of plots corresponds to the addition of a variable. In each row, the posterior median and credible interval is shown for the updated model, posterior medians for the year effect from sub-models are shown for comparison.

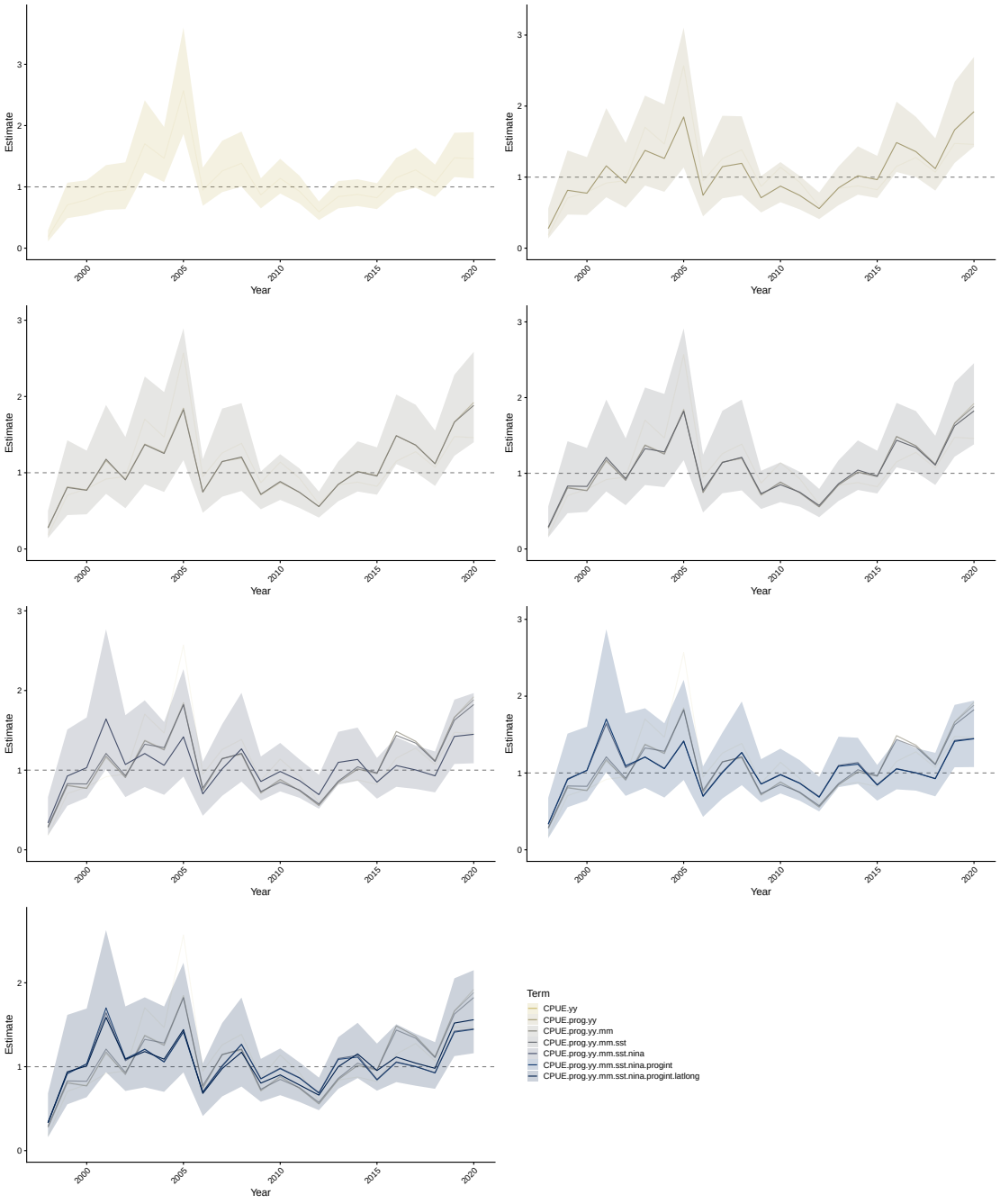

Figure 9: CPUE standardisation effects for object-associated purse-seine sets. Each row of plots corresponds to the addition of a variable. In each row, the posterior median and credible interval is shown for the updated model, posterior medians for the year effect from sub-models are shown for comparison.

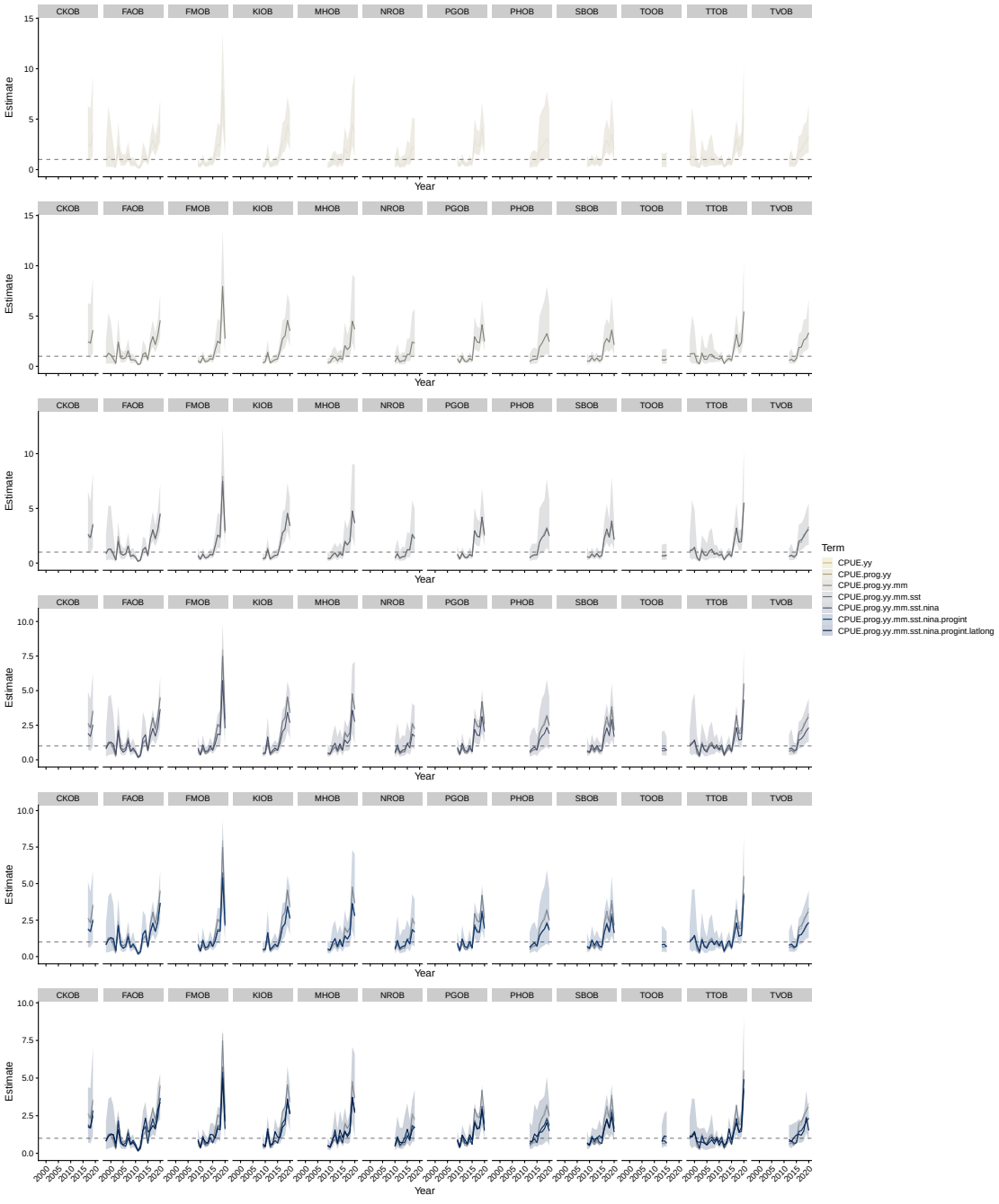

Figure 10: CPUE standardisation effects for free-school purse-seine sets by observer-program. Each row of plots corresponds to the addition of a variable, starting with a model that includes observer-program-year interactions. In each row, the posterior median and credible interval is shown for the updated model, posterior medians for the year effect from sub-models are shown for comparison.

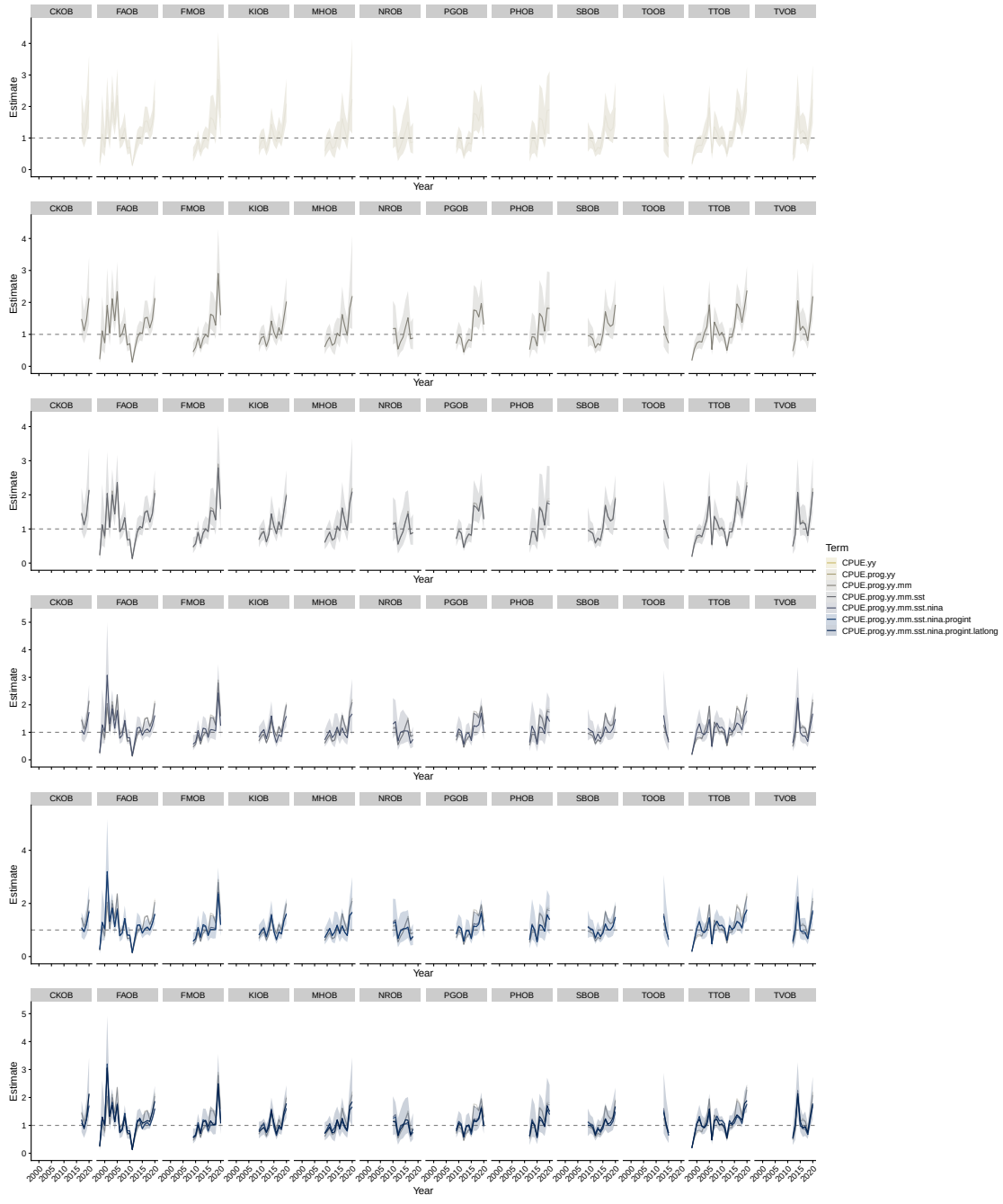

Figure 11: CPUE standardisation effects for object-associated purse-seine sets by observer-program. Each row of plots corresponds to the addition of a variable, starting with a model that includes observer-program-year interactions. In each row, the posterior median and credible interval is shown for the updated model, posterior medians for the year effect from sub-models are shown for comparison.

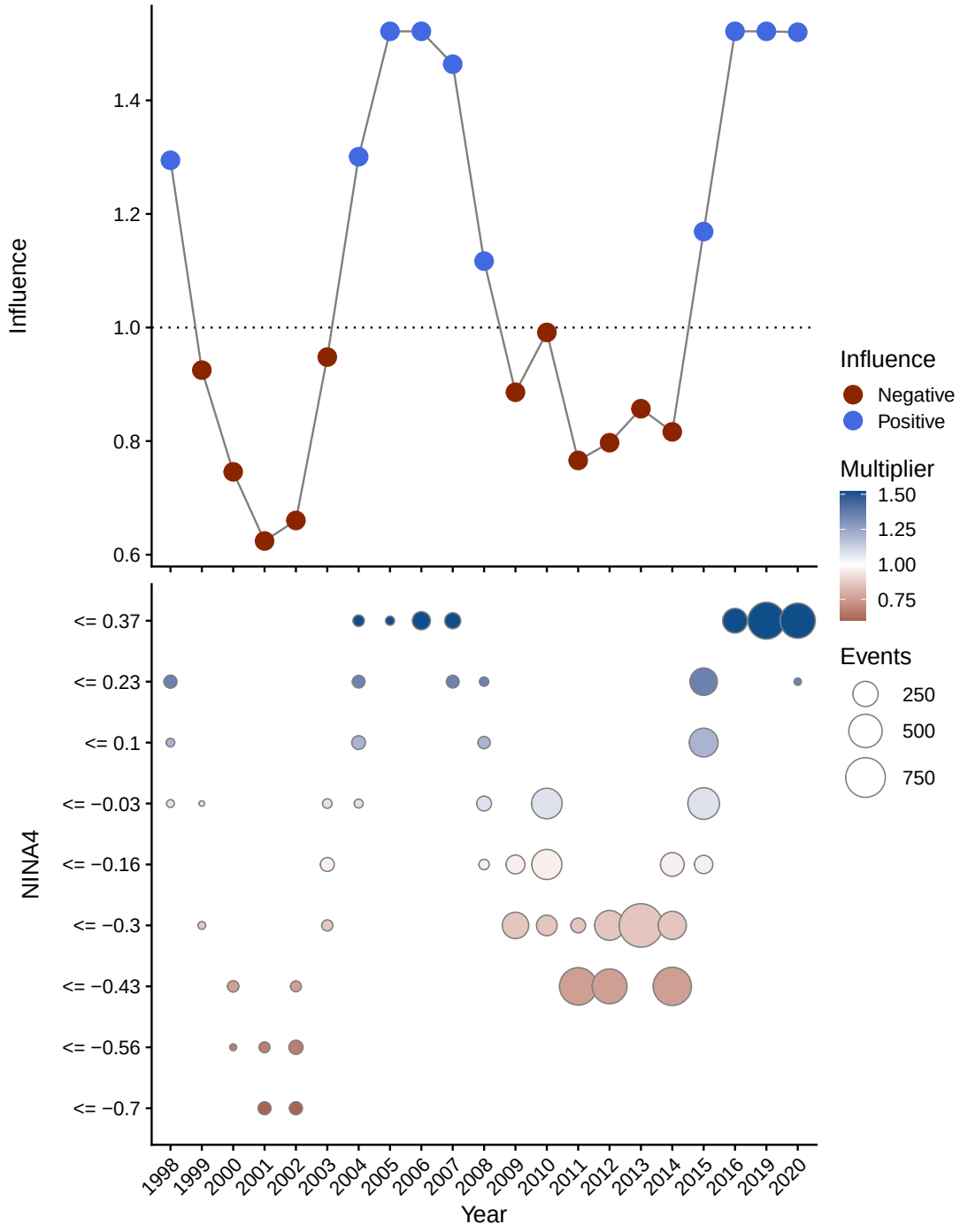

Figure 12: Influence of NINA4 index on catch-rates in observed free-school purse seine sets, with positive influence showing years where the over-all catch-rate in the model was standardised downward by the corresponding amount to account for influences of environmental conditions. Influence is shown in colour as a multiplier on average catch rates, with circle size corresponding to the amount of effort entering the model. Note that data for the 2022 year is preliminary.

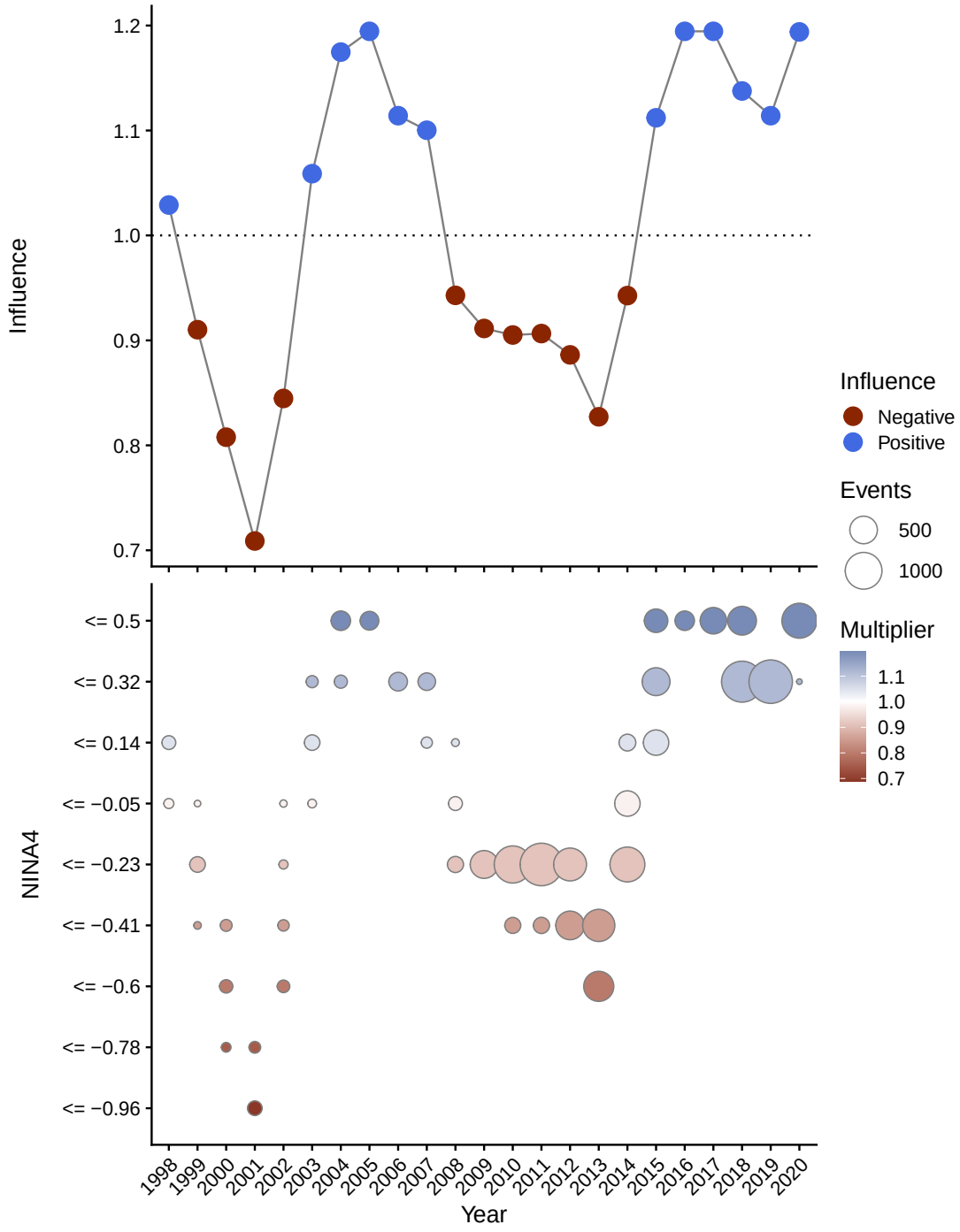

Figure 13: Influence of NINA4 index on catch-rates in observed object-associated purse seine sets, with positive influence showing years where the over-all catch-rate in the model was standardised downward by the corresponding amount to account for influences of environmental conditions. Influence is shown in colour as a multiplier on average catch rates, with circle size corresponding to the amount of effort entering the model. Note that data for the 2022 year is preliminary.

5.4 Predicting interactions across the WCPO

5.4.1 Longline interactions across the WCPO

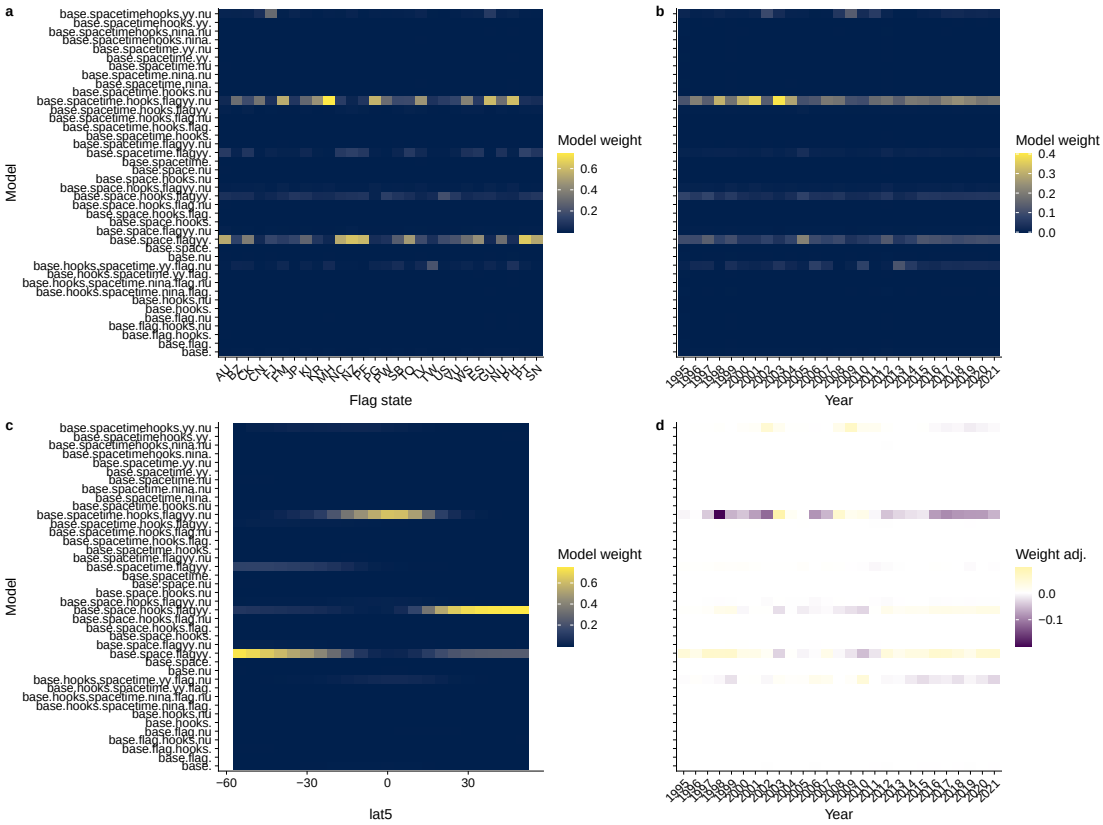

Figure 14: Model weight (geometric mean by stratum) for longline models by (a) vessel flag state, (b) year, and (c) latitude. The stacking-model weight adjustments between the training and prediction datasets by year are shown in (d).

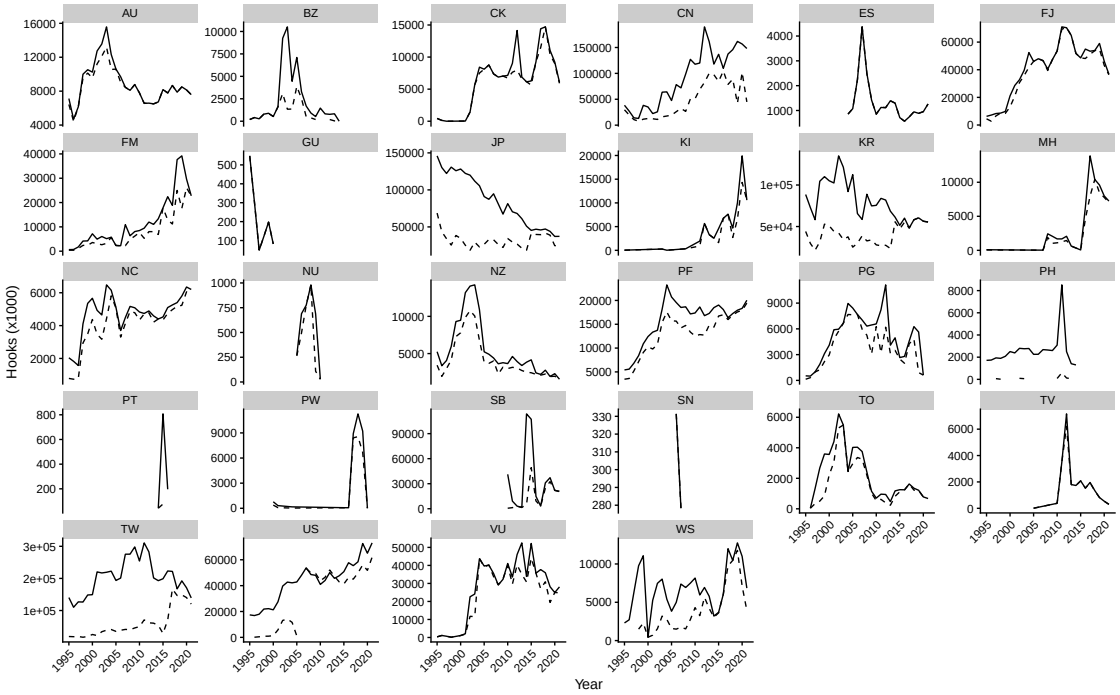

Figure 15: Estimated total hooks by fleet in L-BEST used for predictions of over-all catches of silky shark, with reported hooks in the operational log-sheet data shown for comparison (dashed lines).

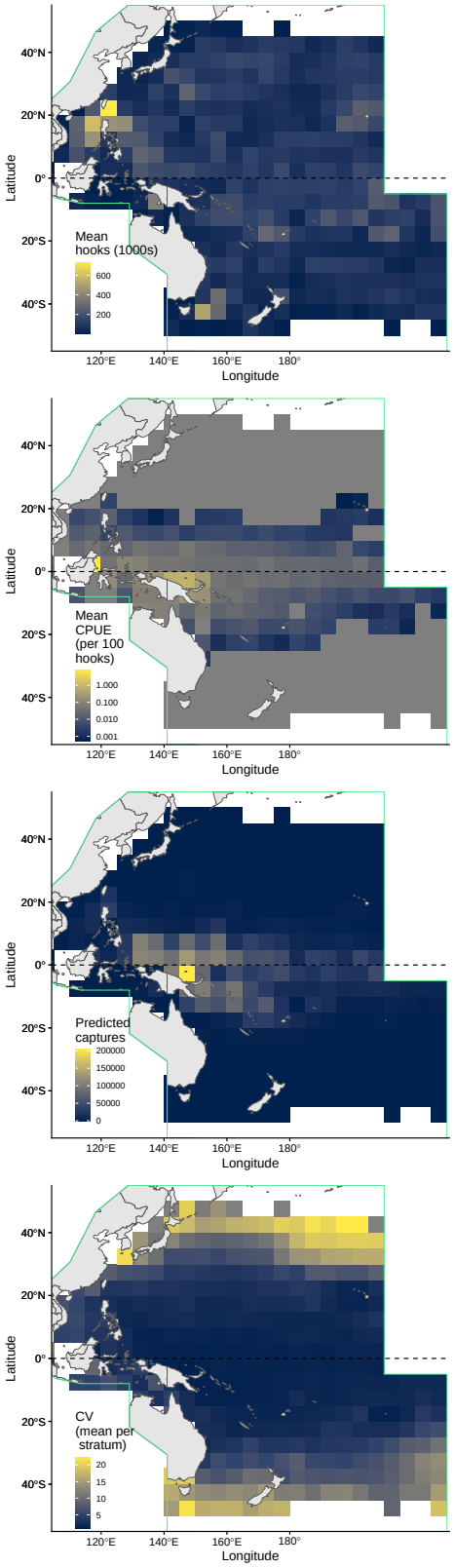

Figure 16: Mean number of hooks per spatial stratum (top), predicted CPUE surface (second from top) total interactions of silky shark per year-month-fleet stratum (third plot) from the observer catch rate GLMM, mean CV (bottom) of predicted numbers of silky shark per spatial stratum.

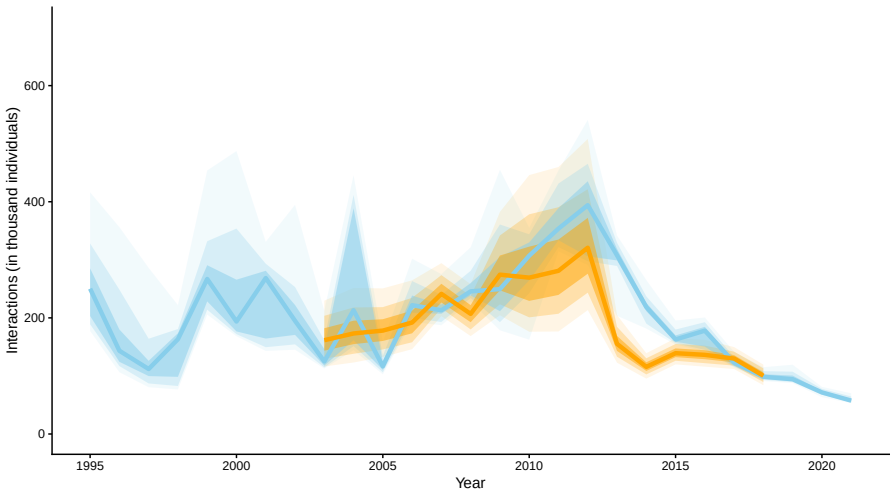

Figure 17: Predicted total silky shark interactions from the combined weighted catch reconstruction model; posterior median (blue line); 80% confidence (darkest blue), 90% confidence (mid blue) and 95% confidence (light blue). Predictions from Peatman et al. (2018) are shown in orange for comparison.

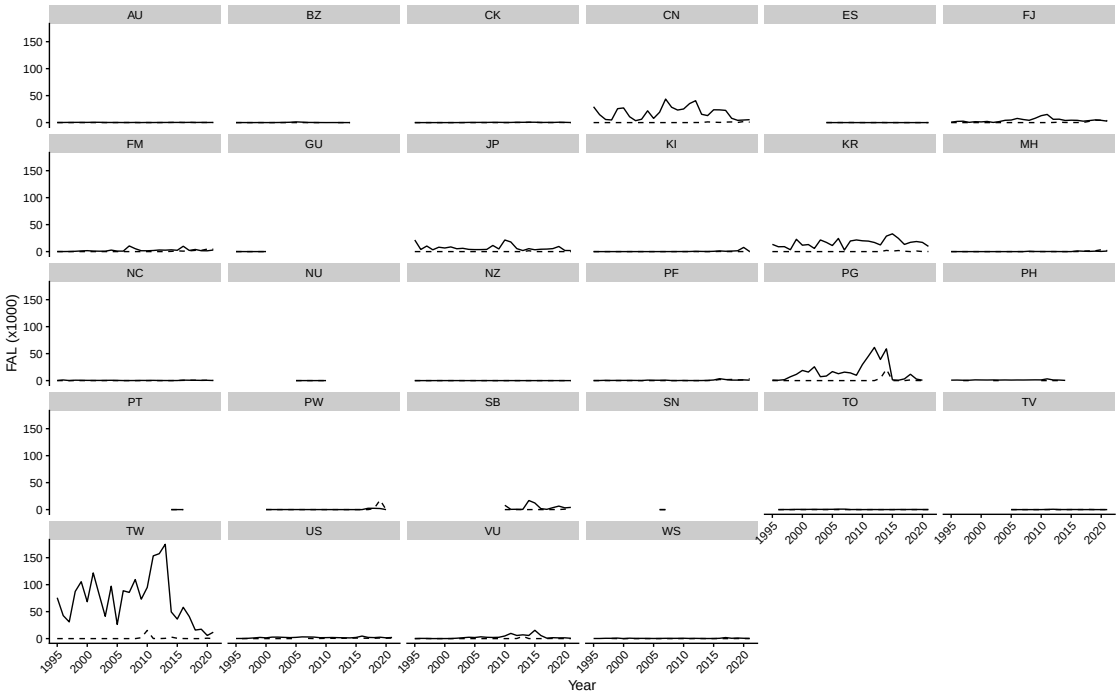

Figure 18: Predicted total silky shark interactions by fleet using the observer catch-rate GLMM in conjunction with L-BEST effort. Reported numbers of silky shark from the operational log-sheet data shown for comparison (dashed lines).

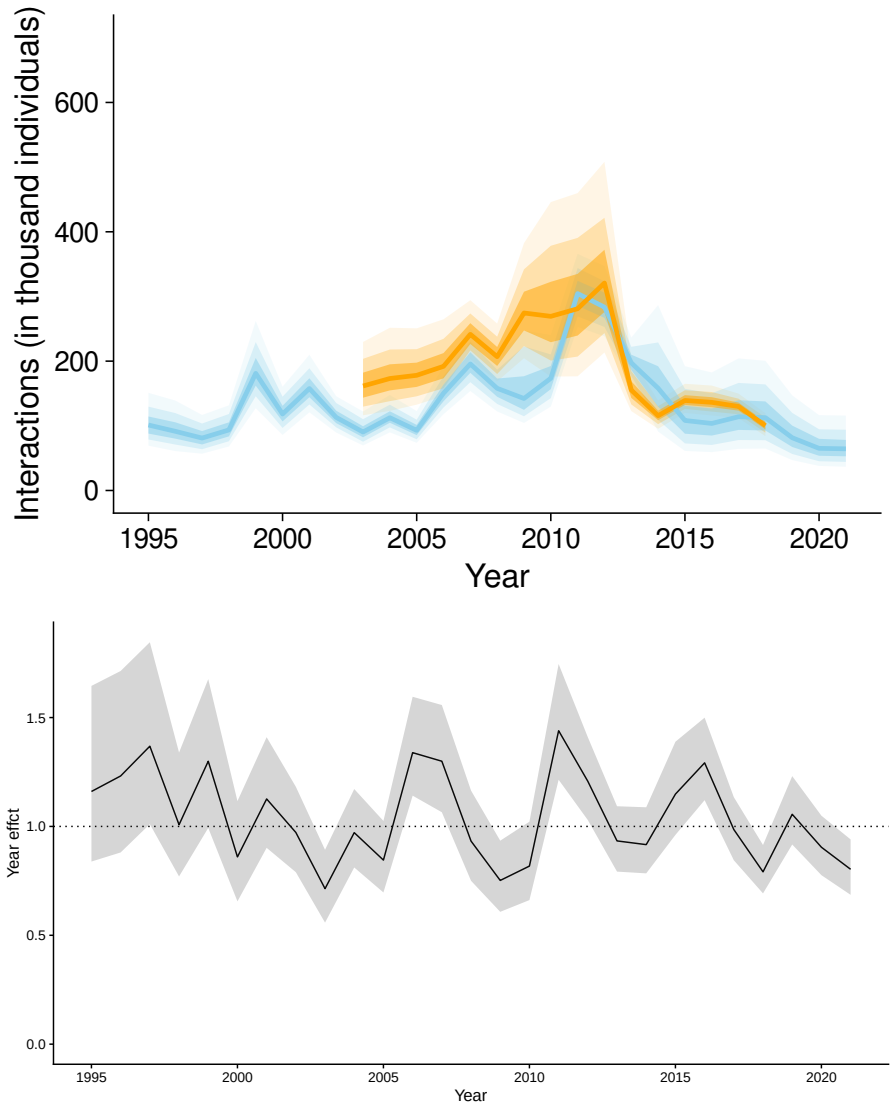

Figure 19: Predicted total silky shark interactions from a single best reconstruction model without flag-year interactions and drawing from random effects across years for year after 2013; posterior median (blue line); 80% confidence (dark blue), 90% confidence (mid blue) and 95% confidence (light blue). Predictions for the over-all year effect of that model are given. Estimates from Peatman et al. (2018) are shown in orange for comparison.

5.4.2 Purse-seine interactions across the WCPO

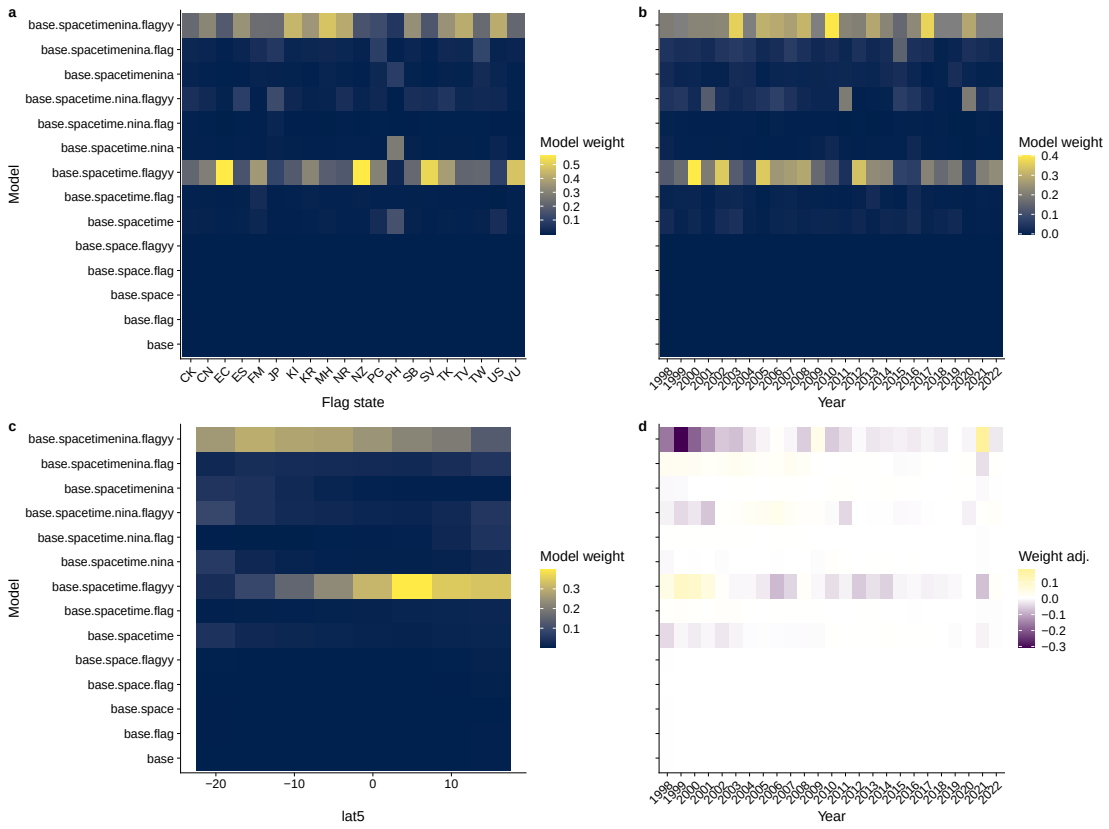

Figure 20: Model weight (geometric mean by stratum) for purse seine by (a) vessel flag state, (b) year, and (c) latitude. The stacking-model weight adjustments between the training and prediction datasets by year are shown in (d).

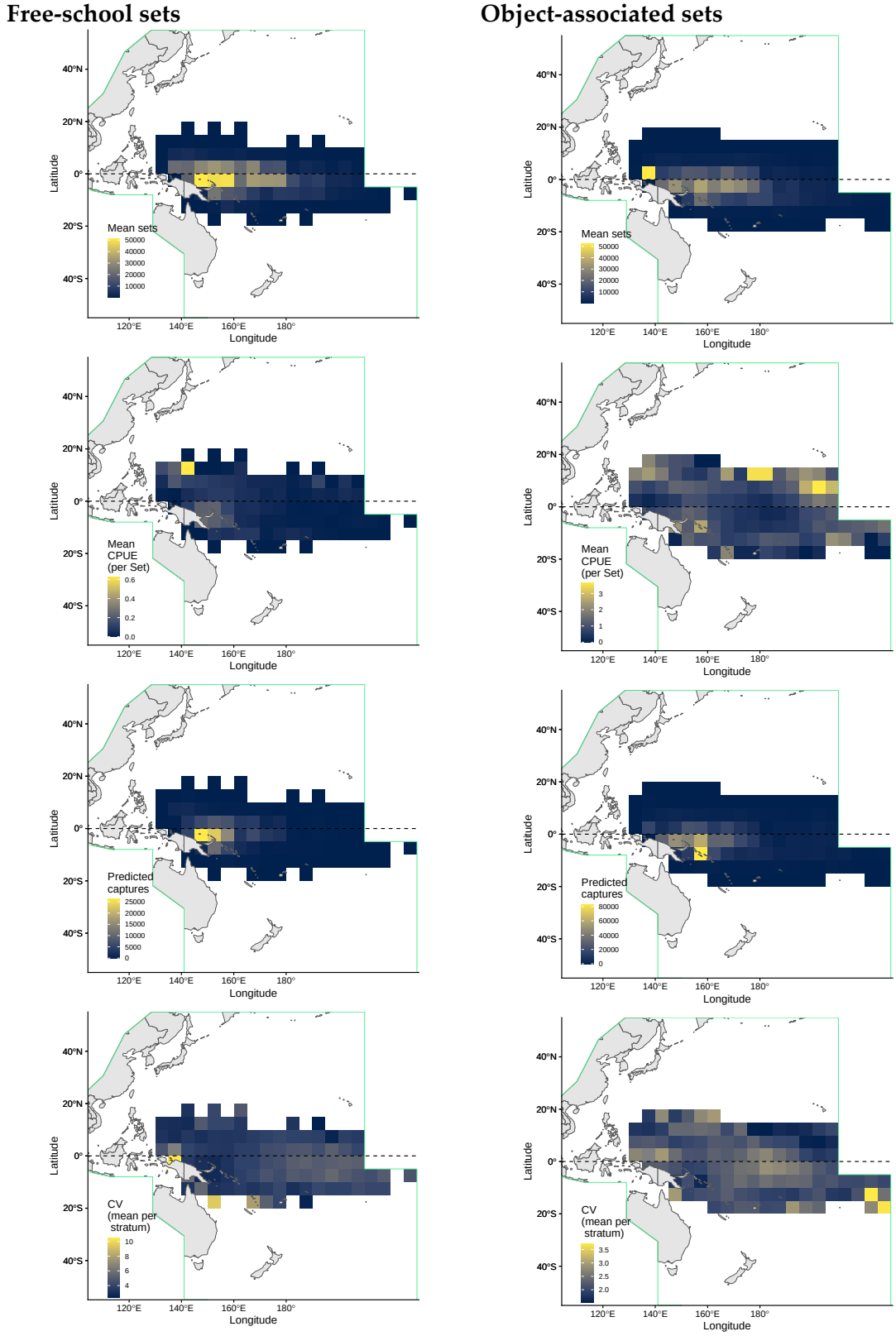

Figure 21: Predicted number of sets (top row), CPUE surface (second row) and predicted numbers of silky shark per spatial stratum (third row) given L-BEST effort hook numbers from the observer catch rate GLMM, (bottom row) mean CV of predicted numbers of silky shark per spatial stratum and set type.

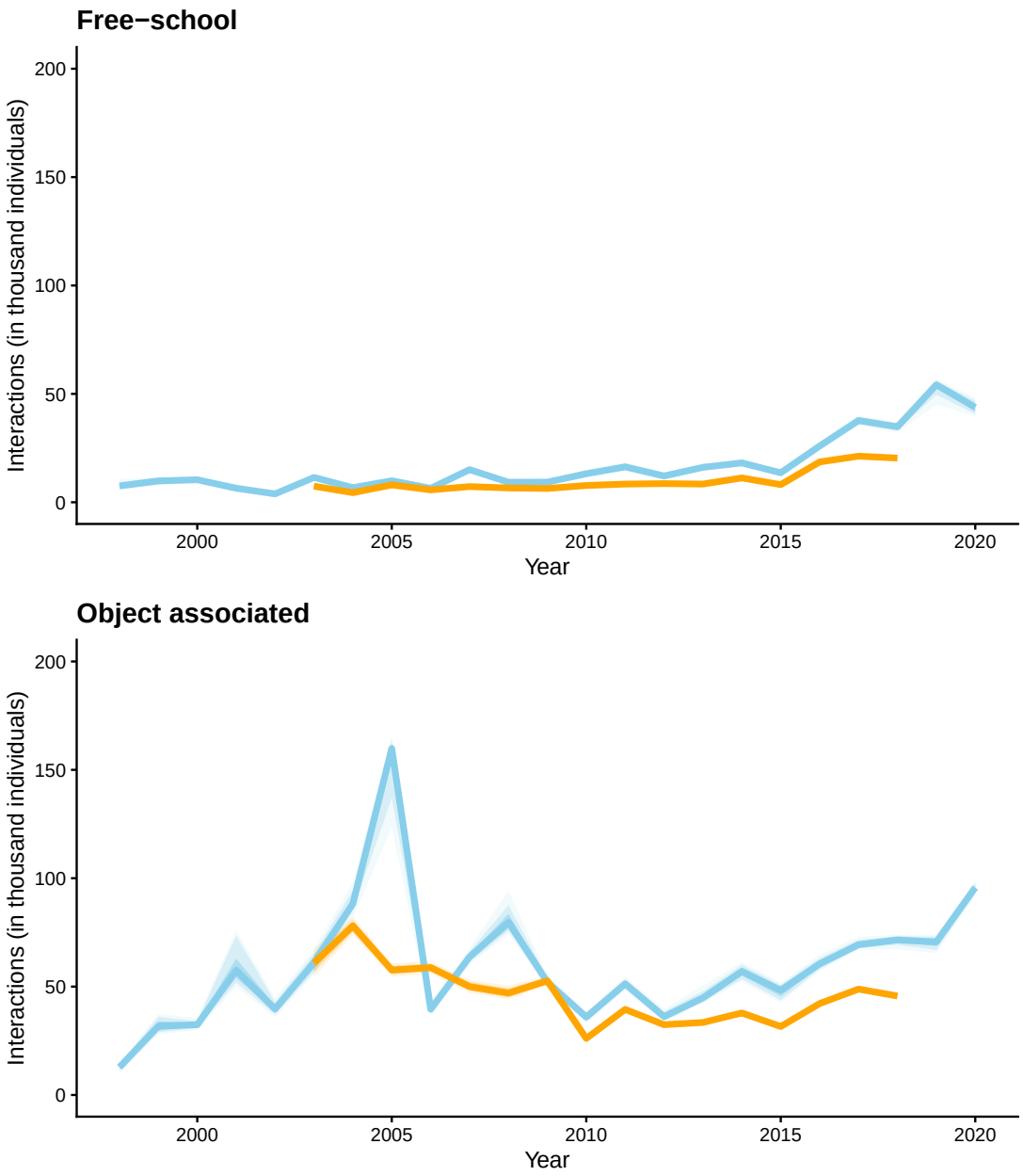

Figure 22: Predicted total silky shark interactions from the combined weighted reconstruction model; posterior median (blue line); 80% confidence (dark blue), 90% confidence (mid blue) and 95% confidence (light blue). Predictions from Peatman et al. (2018) are shown in orange for comparison.

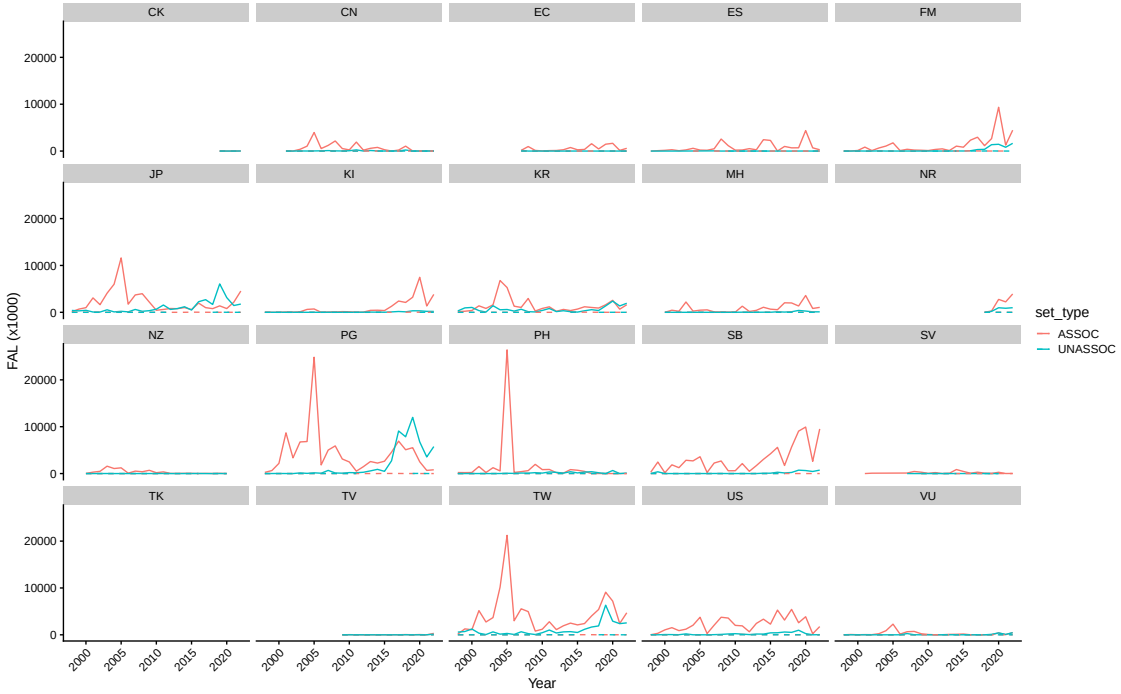

Figure 23: Predicted total silky shark interactions by fleet using the observer catch-rate GLMM in conjunction with S-BEST effort. Reported numbers of silky shark from the operational log-sheet data shown for comparison (dashed lines).

5.5 Lenght composition standardisation figures

5.5.1 Longline length composition

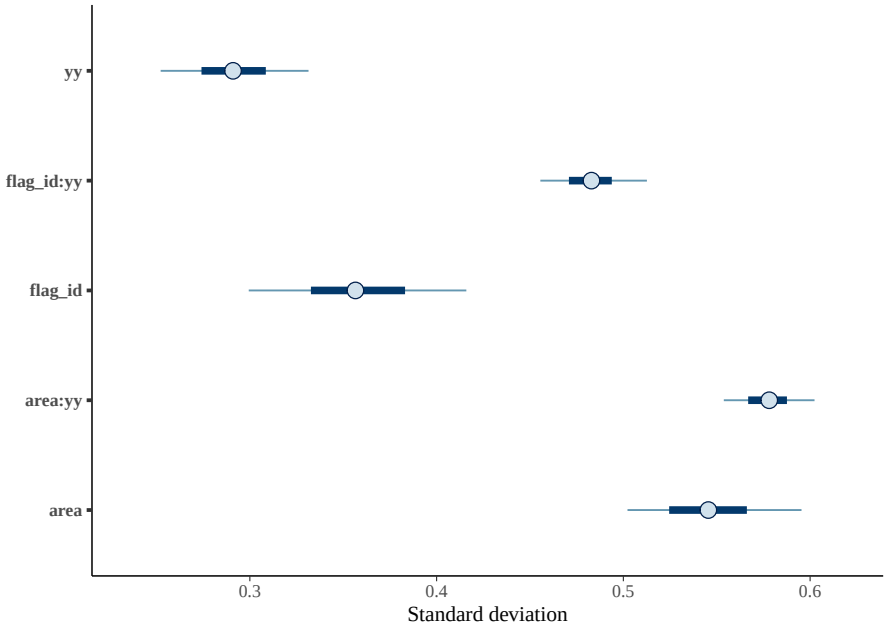

Figure 24: Length-composition standardisation model estimates (posterior median and 95% confidence interval) for standard deviation parameters associated with standardising effects.

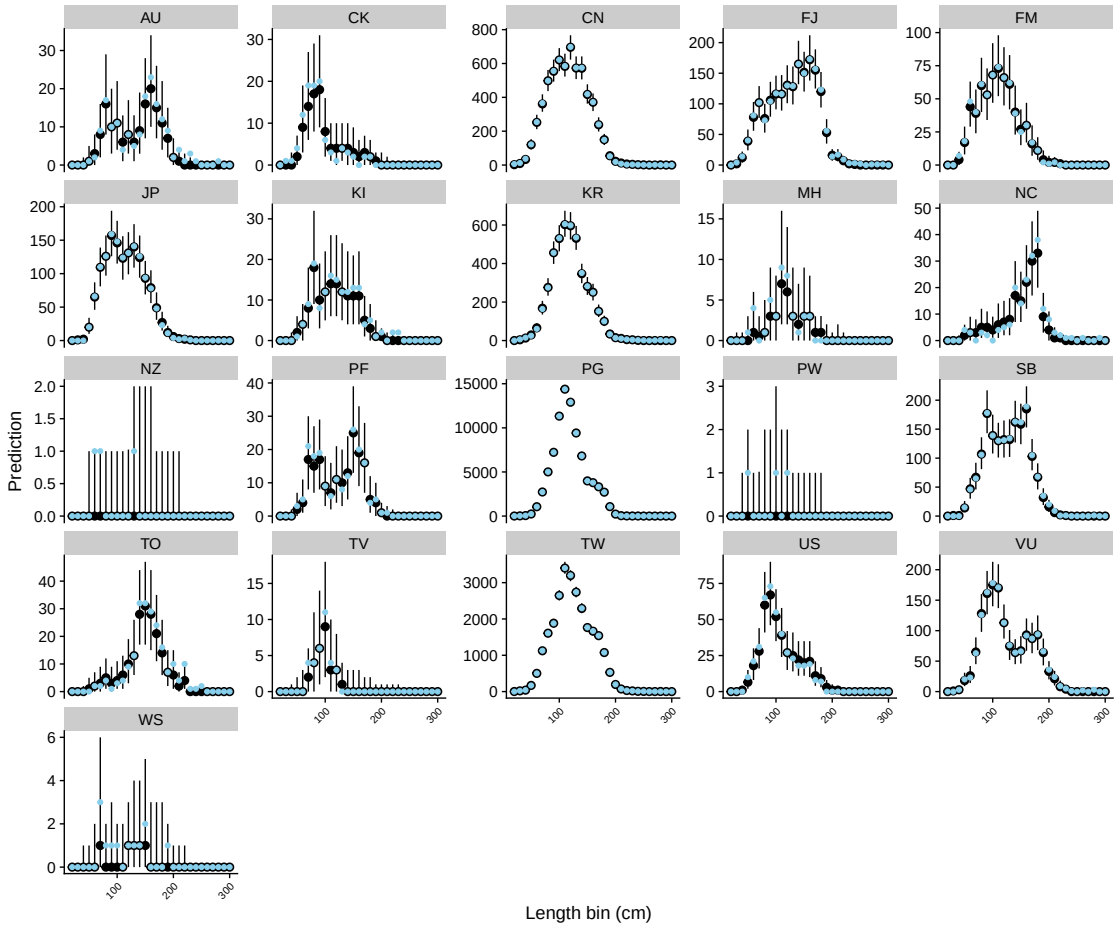

Figure 25: Length - composition standardisation model fit (black posterior median and 95% prediction interval) to the observed numbers in each 10 cm length bin (blue) by vessel flag in the WCPO longline fishery catching silky shark.

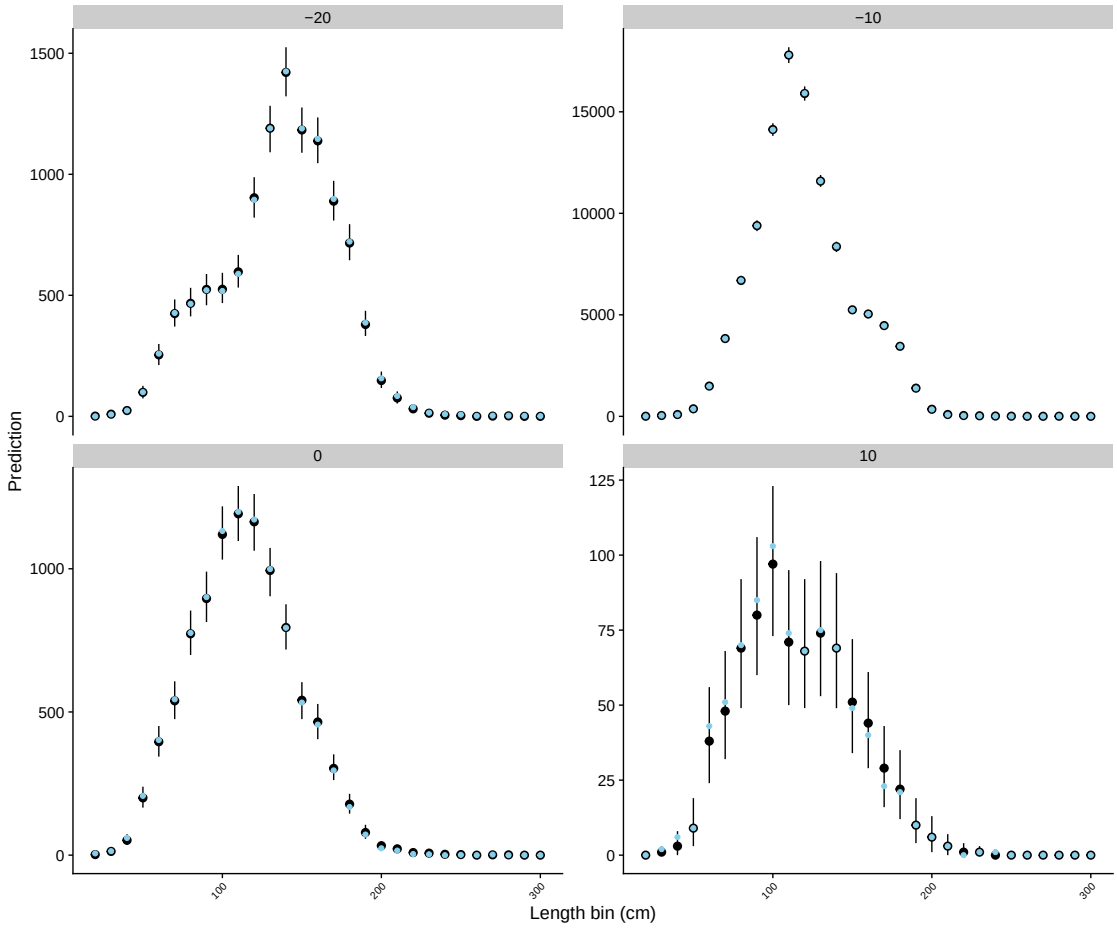

Figure 26: Length - composition standardisation model fit (black posterior median and 95% prediction interval) to the observed numbers in each 10 cm length bin (blue) by latitude in the WCPO longline fishery catching silky shark.

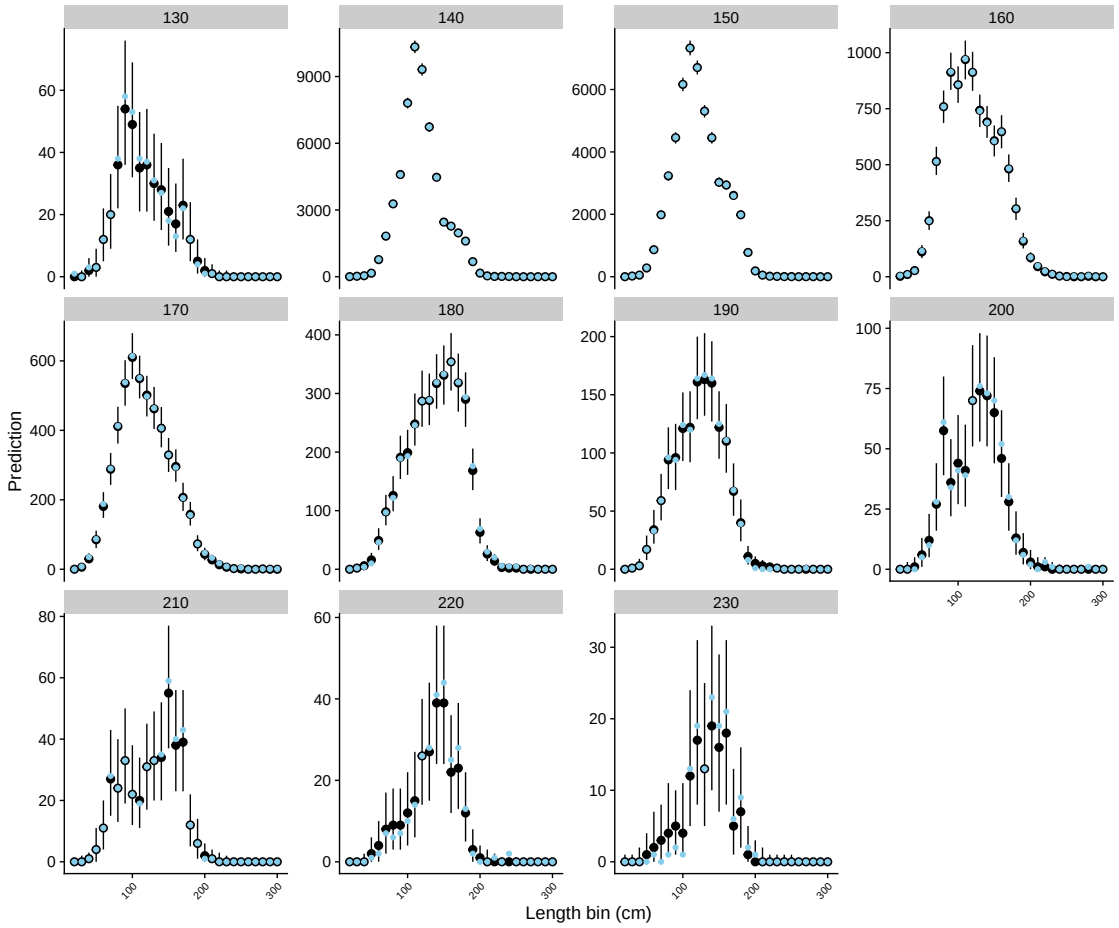

Figure 27: Length - composition standardisation model fit (black posterior median and 95% prediction interval) to the observed numbers in each 10 cm length bin (blue) by longitude in the WCPO longline fishery catching silky shark.

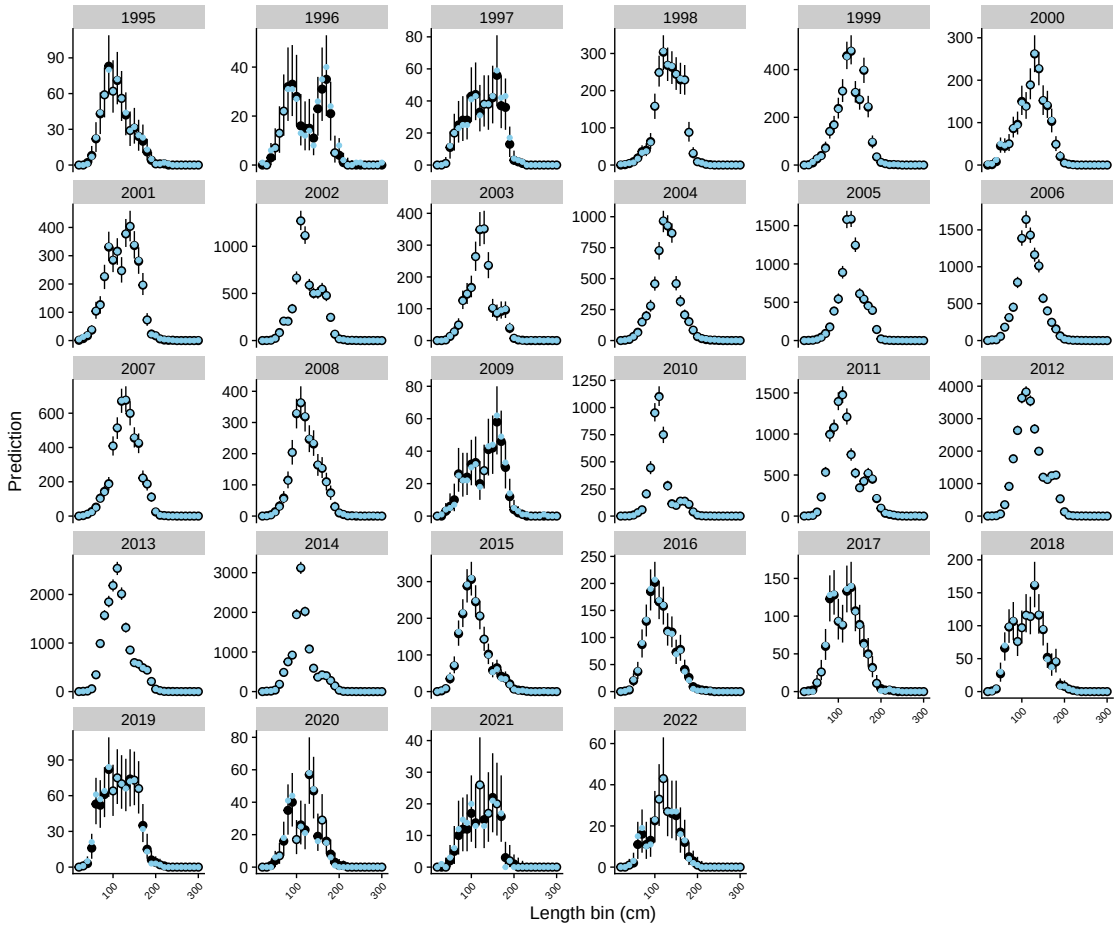

Figure 28: Length - composition standardisation model fit (black posterior median and 95% prediction interval) to the observed numbers in each 10 cm length bin (blue) by year in the WCPO longline fishery catching silky shark.

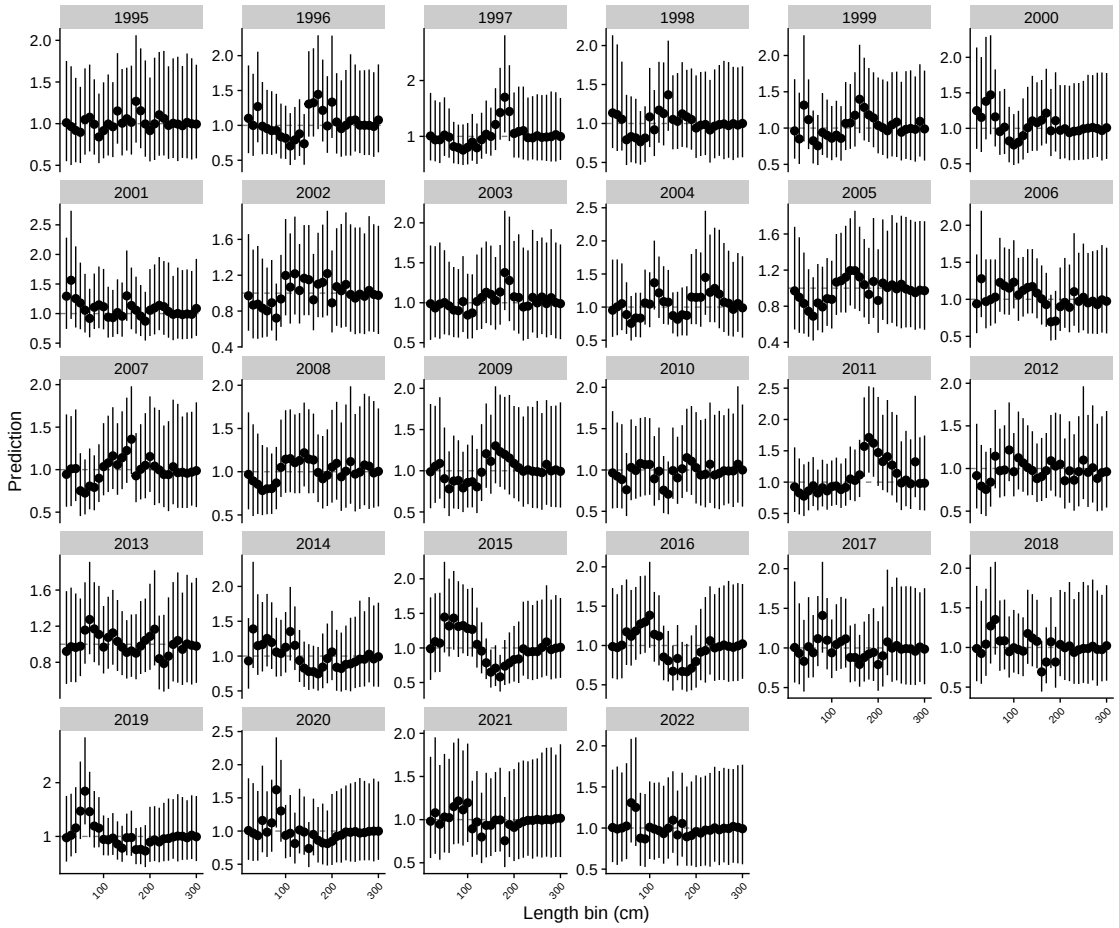

Figure 29: Year effect by 10 cm length bin, relative to the over-all mean length composition in the WCPO longline fishery catching silky shark, estimated by the length-composition standardisation model (black posterior median and 95% prediction interval).

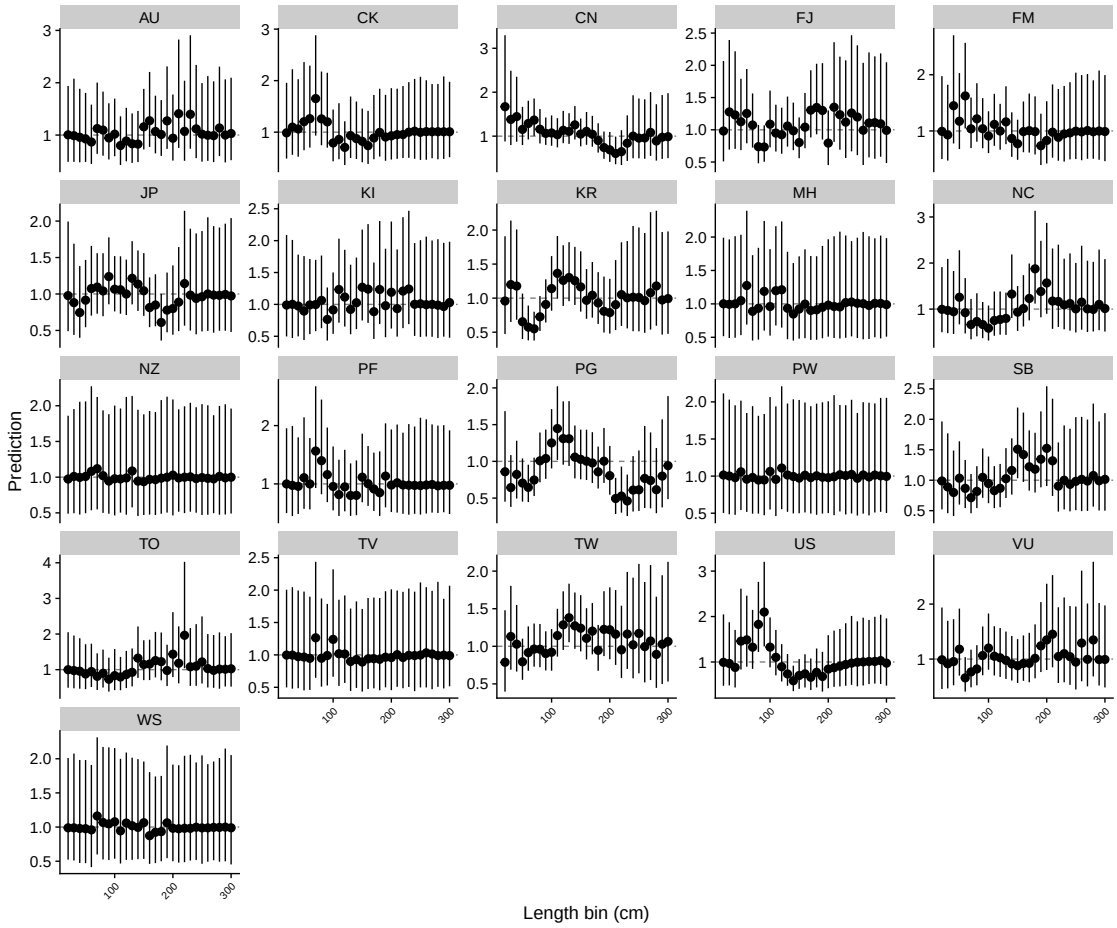

Figure 30: Vessel flag effect by 10 cm length bin, relative to the over-all mean length composition in the WCPO longline fishery catching silky shark, estimated by the length-composition standardisation model (black posterior median and 95% prediction interval).

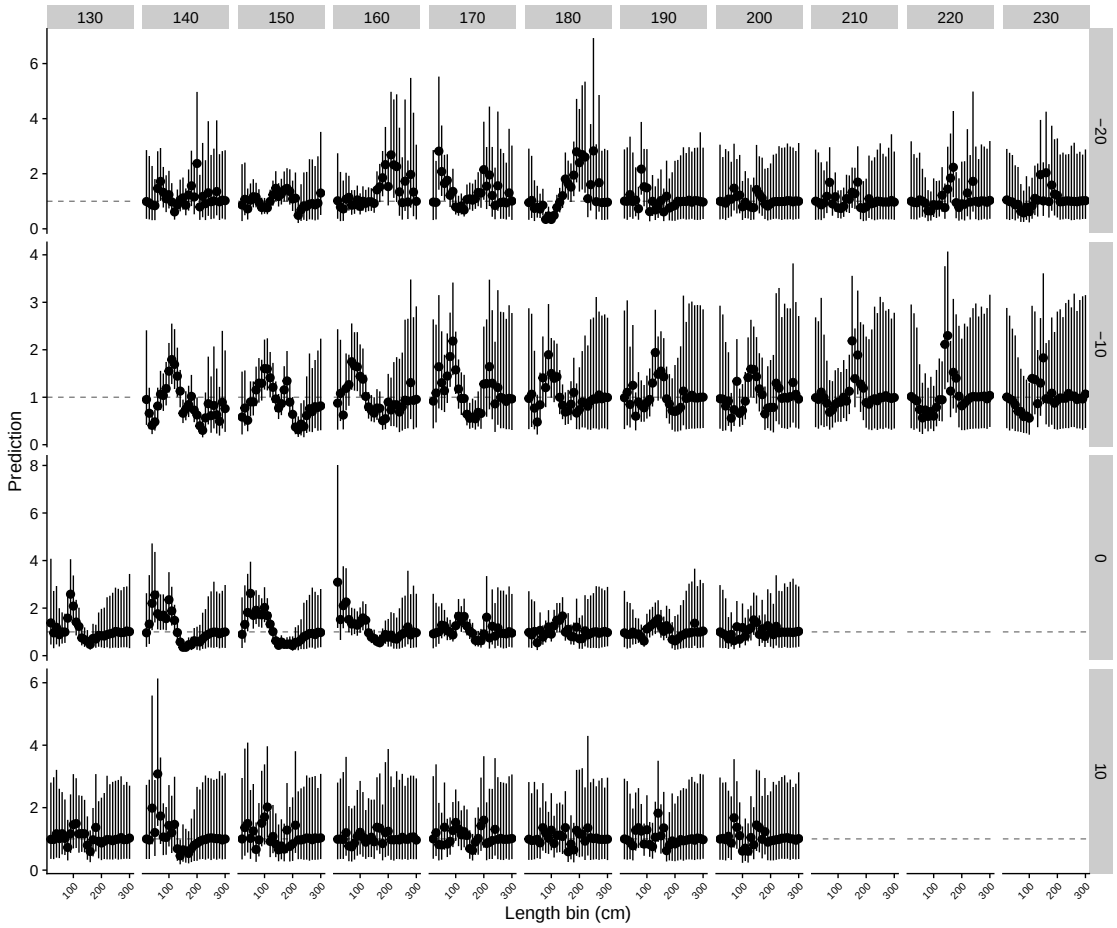

Figure 31: Area (10 degree grid) effect by 10 cm length bin in the WCPO longline fishery catching silky shark, relative to the over-all mean length composition, estimated by the length-composition standardisation model (black posterior median and 95% prediction interval).

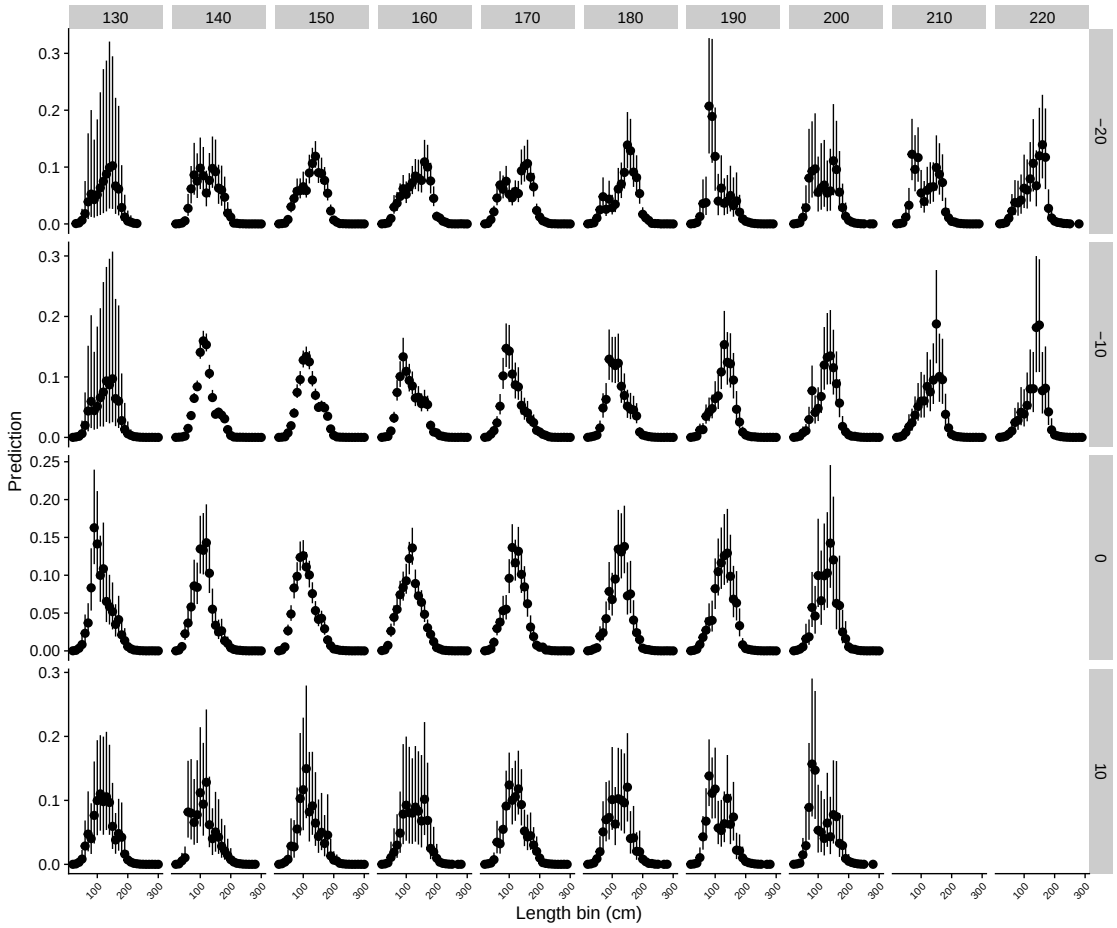

Figure 32: Predicted scaled length frequency by 10 cm length bin and 10 degree latitude-longitude bins, scaled by the predicted number of interactions at the level of model strata in the WCPO longline fishery catching silky shark, estimated by the length-composition standardisation model (black posterior median and 95% prediction interval).

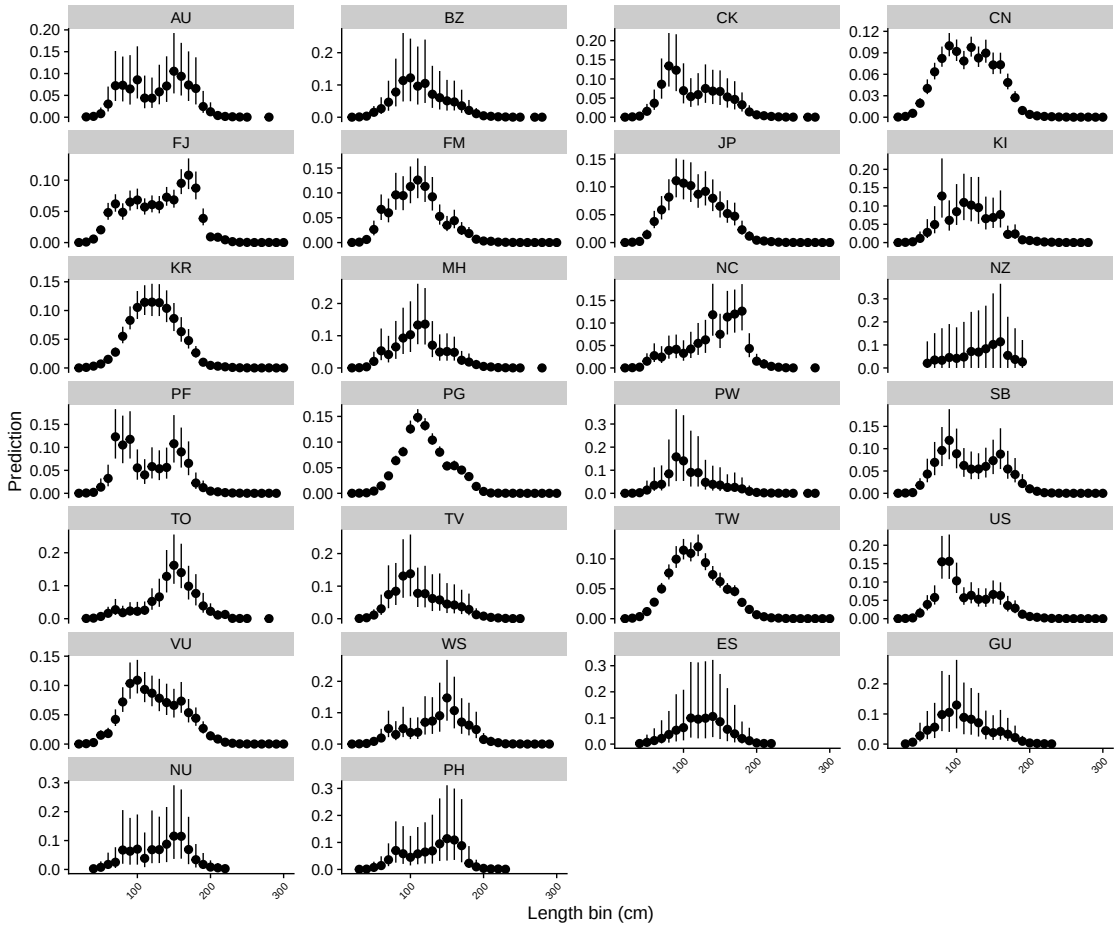

Figure 33: Predicted scaled length frequency by 10 cm length bin and vessel flag, scaled by the predicted number of interactions at the level of model strata in the WCPO longline fishery catching silky shark, estimated by the length-composition standardisation model (black posterior median and 95% prediction interval).

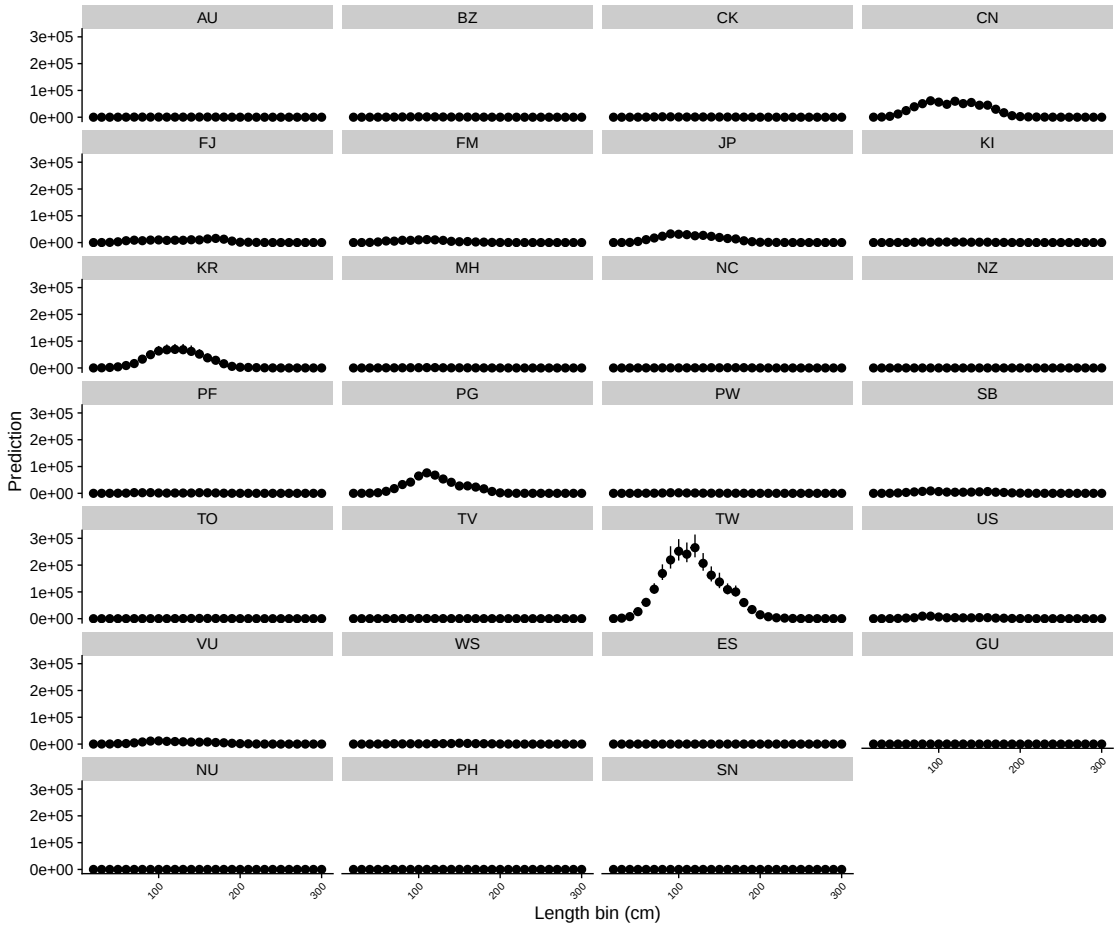

Figure 34: Predicted scaled catch at length by 10 cm length bin and vessel flag, scaled by the predicted number of interactions at the level of model strata in the WCPO longline fishery catching silky shark, estimated by the length-composition standardisation model (black posterior median and 95% prediction interval).

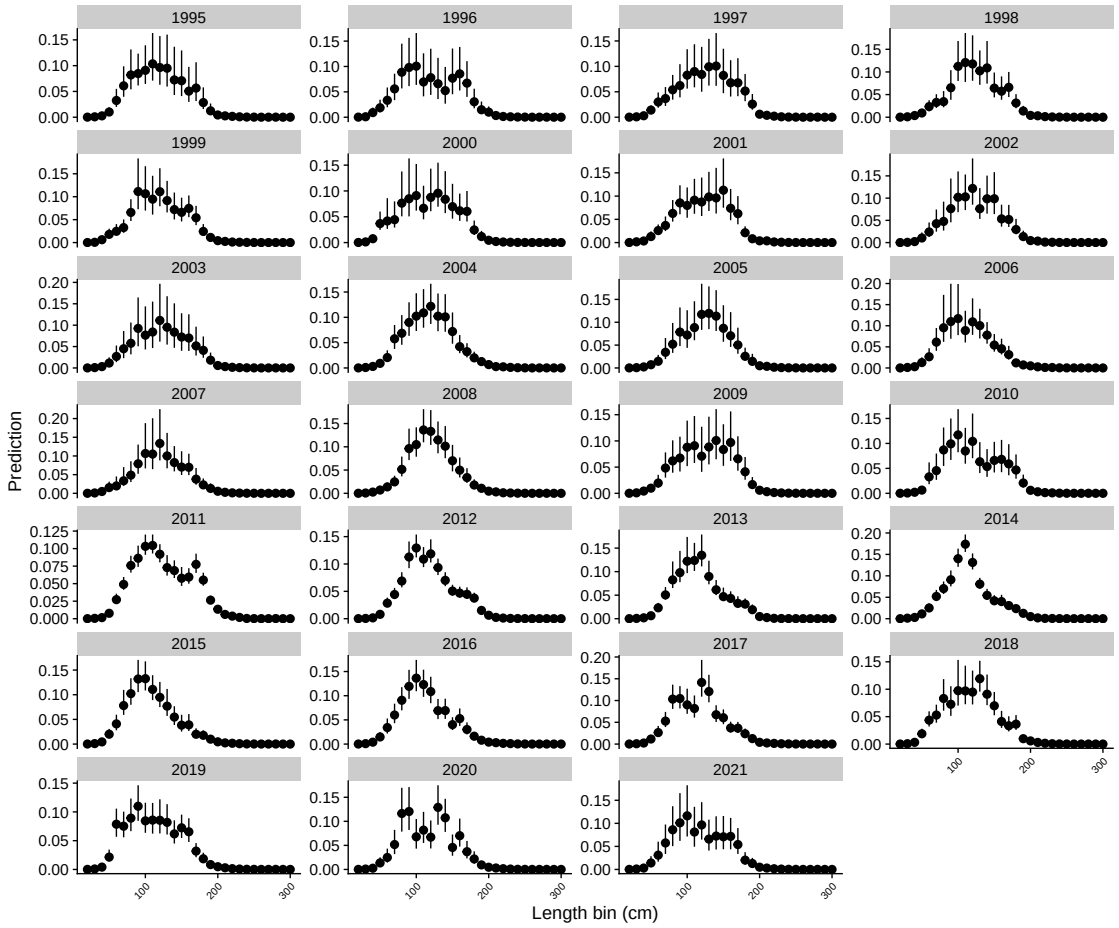

Figure 35: Predicted scaled length frequency by 10 cm length bin and year, scaled by the predicted number of interactions at the level of model strata in the WCPO longline fishery catching silky shark, estimated by the length-composition standardisation model (black posterior median and 95% prediction interval).

5.5.2 Purse-seine length composition

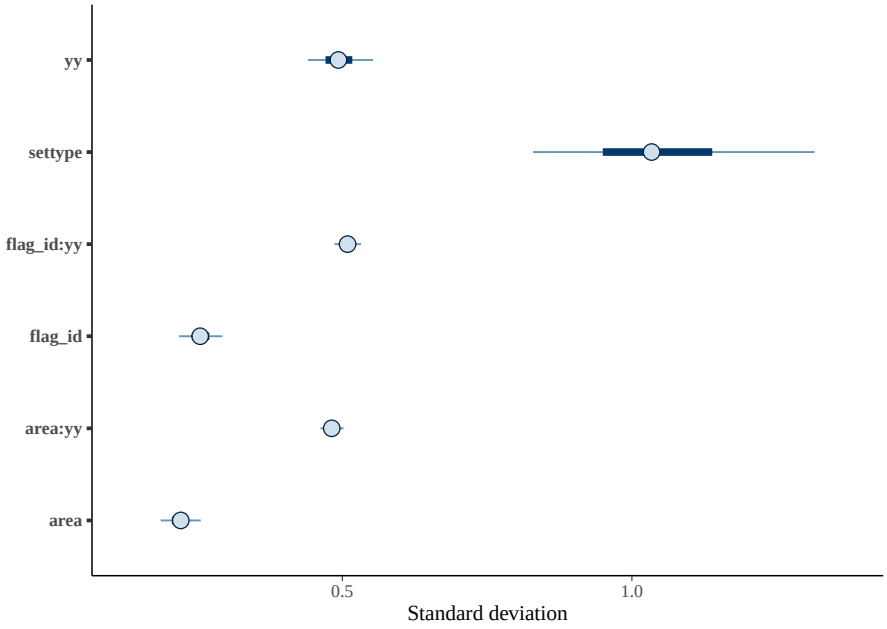

Figure 36: Length-composition standardisation model estimates (posterior median and 95% confidence interval) for standard deviation parameters associated with standardising effects.

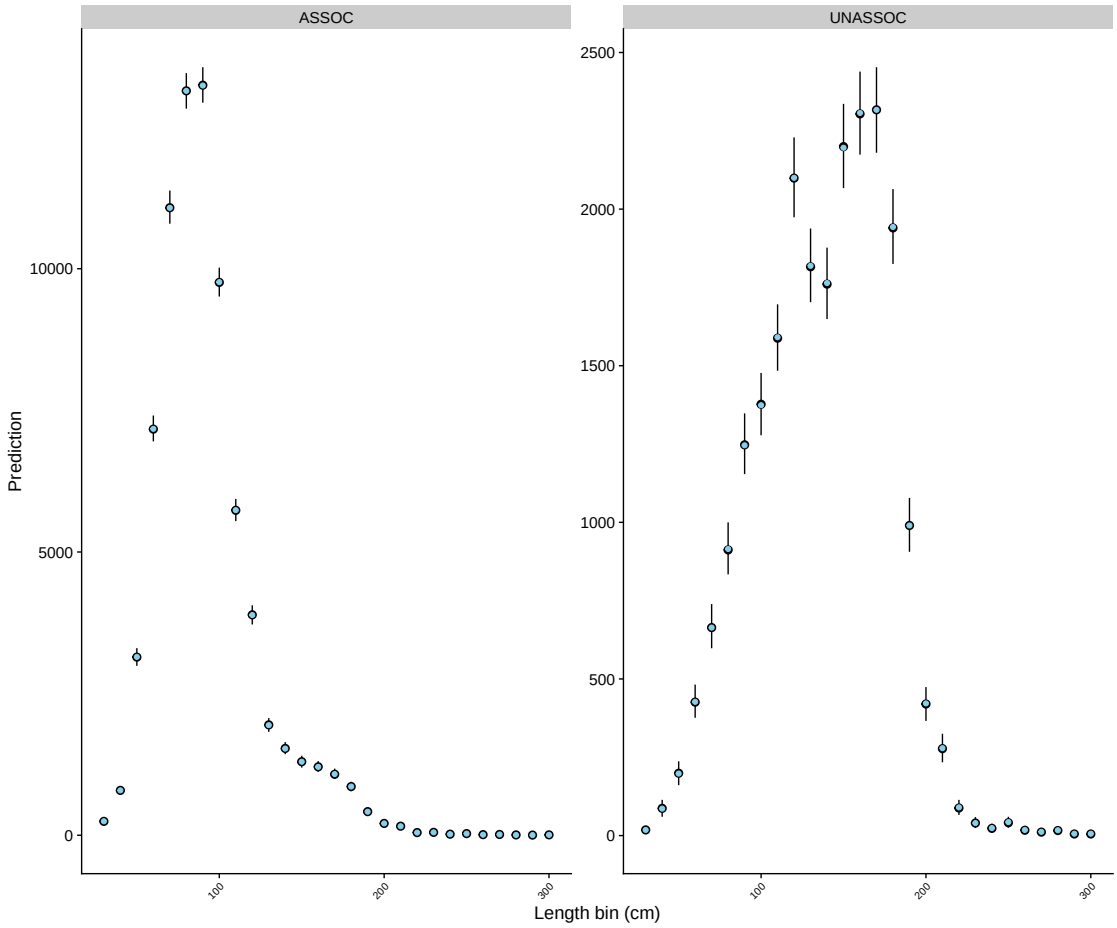

Figure 37: Length-composition standardisation model fit (black posterior median and 95% prediction interval) to the observed numbers in each 10 cm length bin (blue) by purse-seine set type (ASSOC: object-associated sets; UNASSOC: free-school (un-associated) sets) in the WCPO purse-seine fishery catching silky shark.

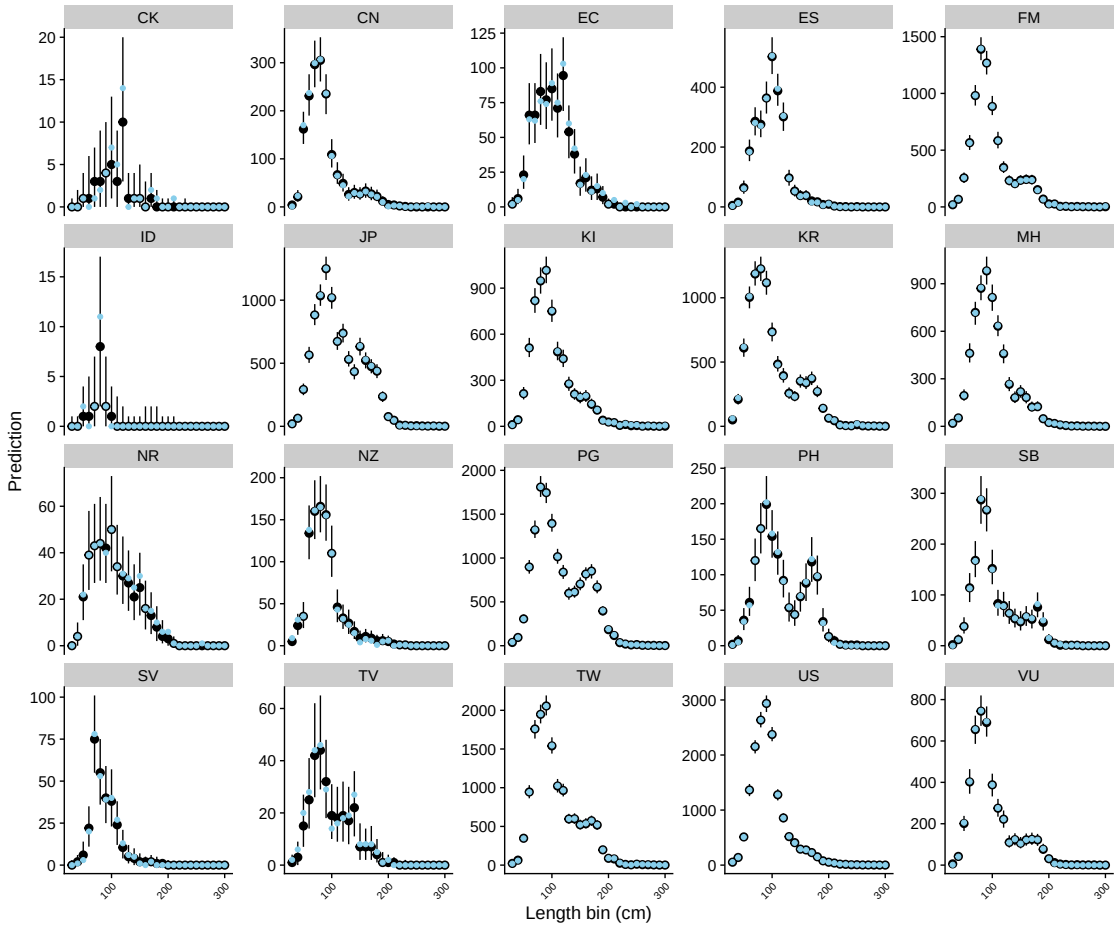

Figure 38: Length - composition standardisation model fit (black posterior median and 95% prediction interval) to the observed numbers in each 10 cm length bin (blue) by vessel flag in the WCPO purse - seine fishery catching silky shark.

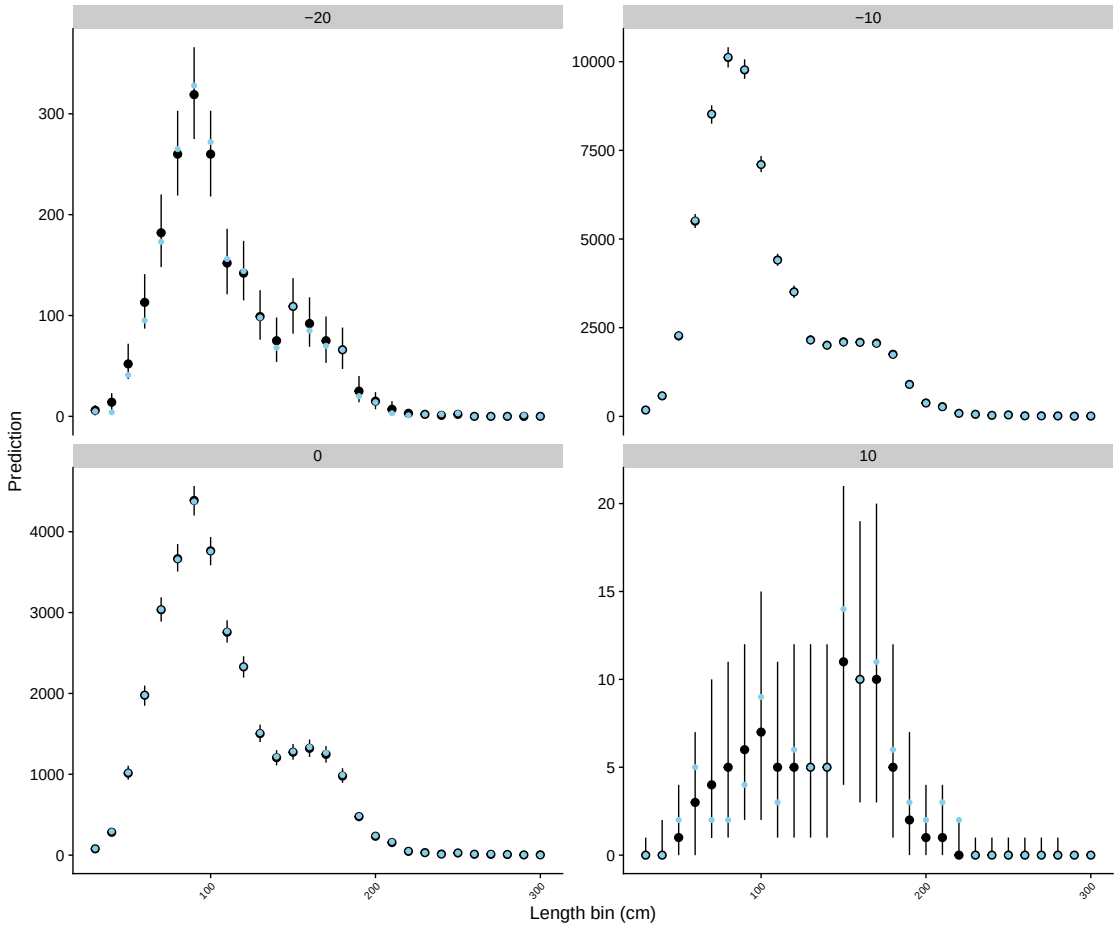

Figure 39: Length-composition standardisation model fit (black posterior median and 95% prediction interval) to the observed numbers in each 10 cm length bin (blue) by latitude in the WCPO purse-seine fishery catching silky shark.

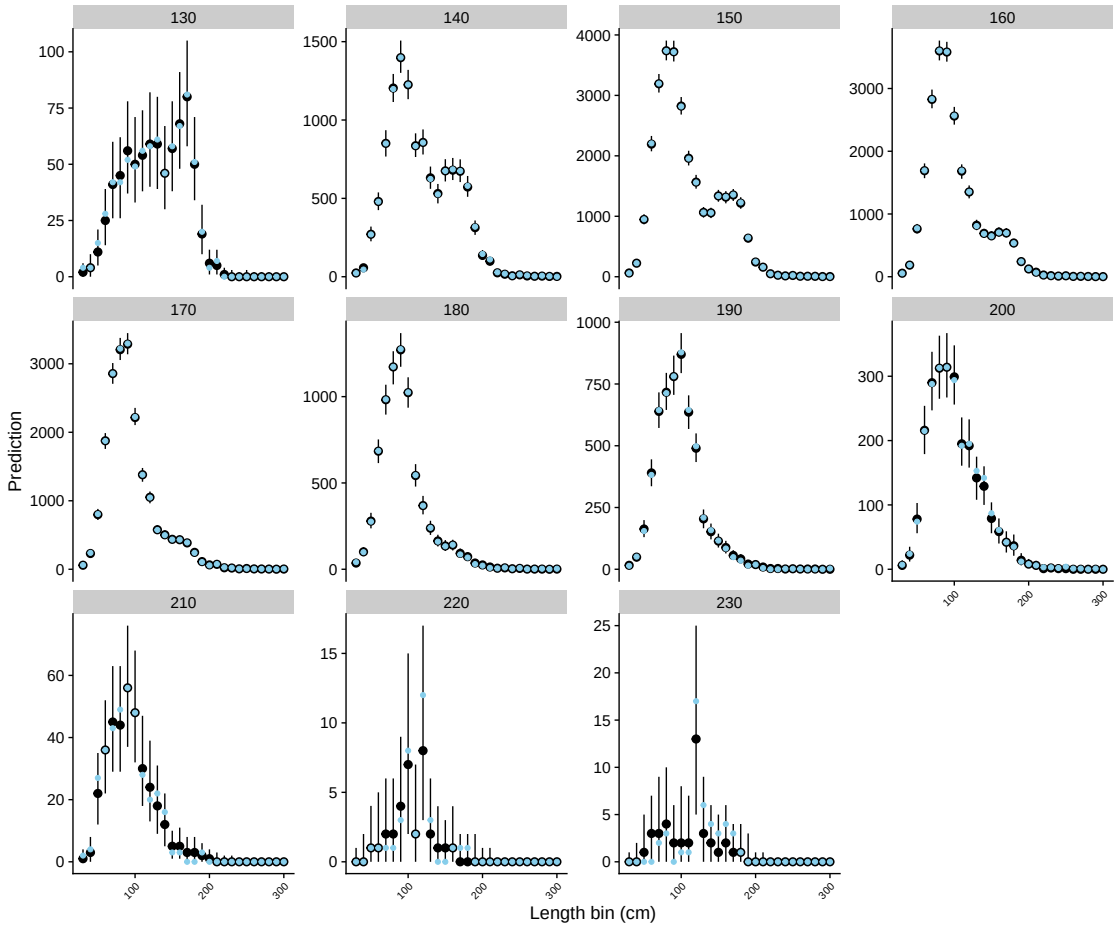

Figure 40: Length-composition standardisation model fit (black posterior median and 95% prediction interval) to the observed numbers in each 10 cm length bin (blue) by longitude in the WCPO purse-seine fishery catching silky shark.

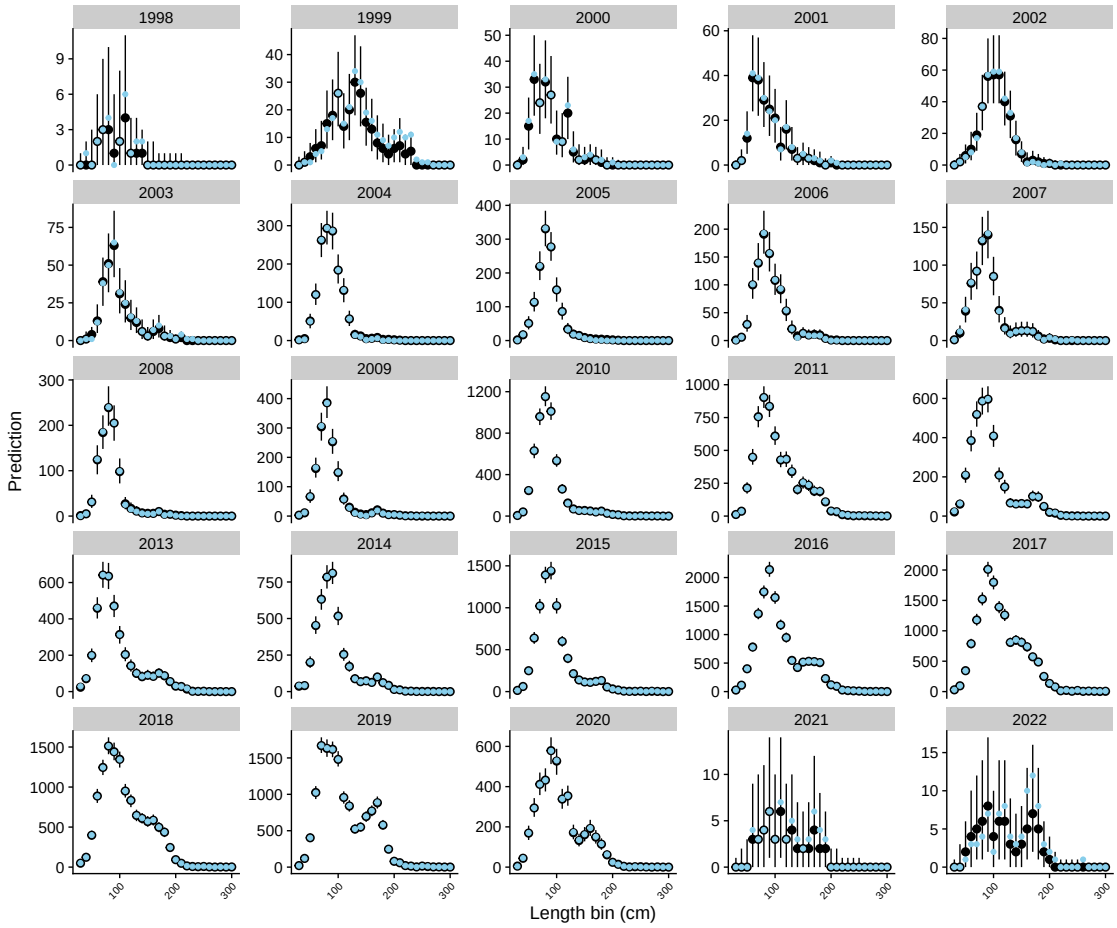

Figure 41: Length-composition standardisation model fit (black posterior median and 95% prediction interval) to the observed numbers in each 10 cm length bin (blue) by year in the WCPO purse-seine fishery catching silky shark.

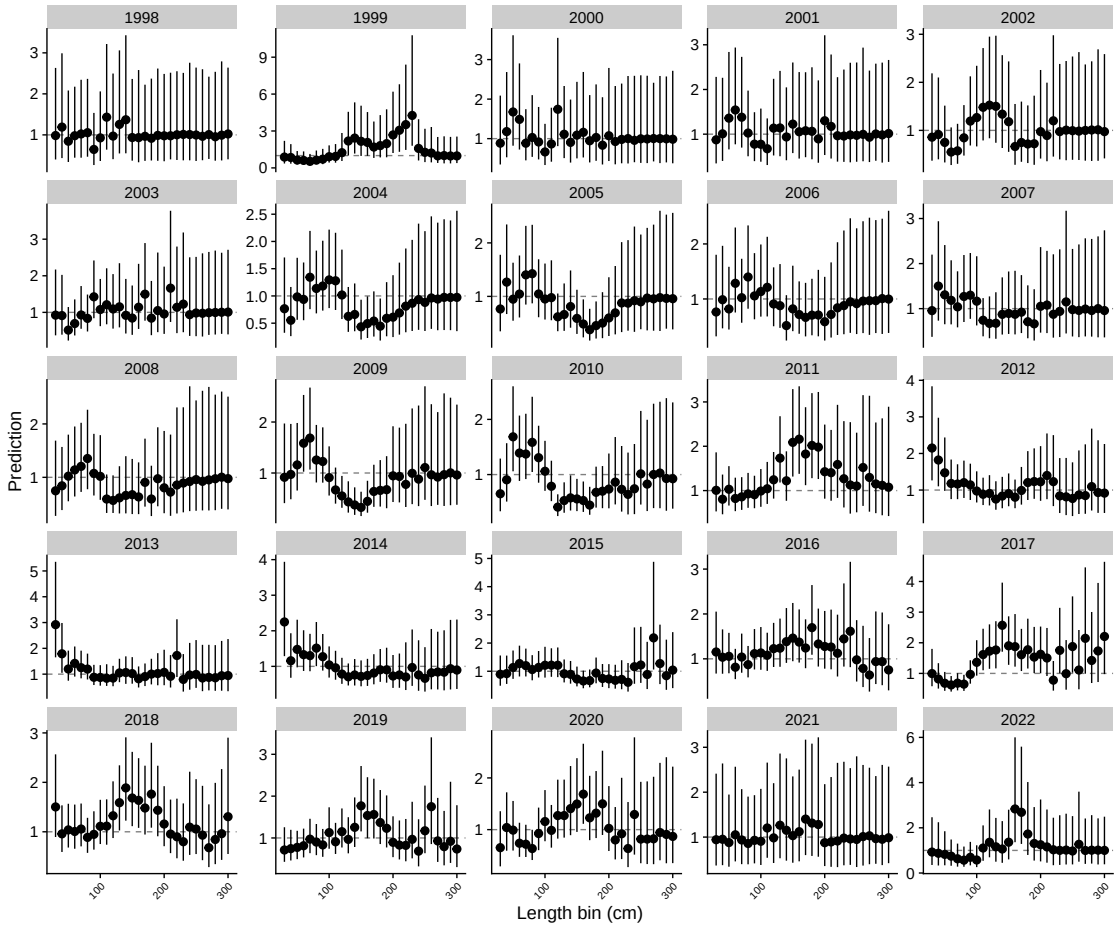

Figure 42: Year effect by 10 cm length bin, relative to the over-all mean length composition in the WCPO purse-seine fishery catching silky shark, estimated by the length-composition standardisation model (black posterior median and 95% prediction interval).

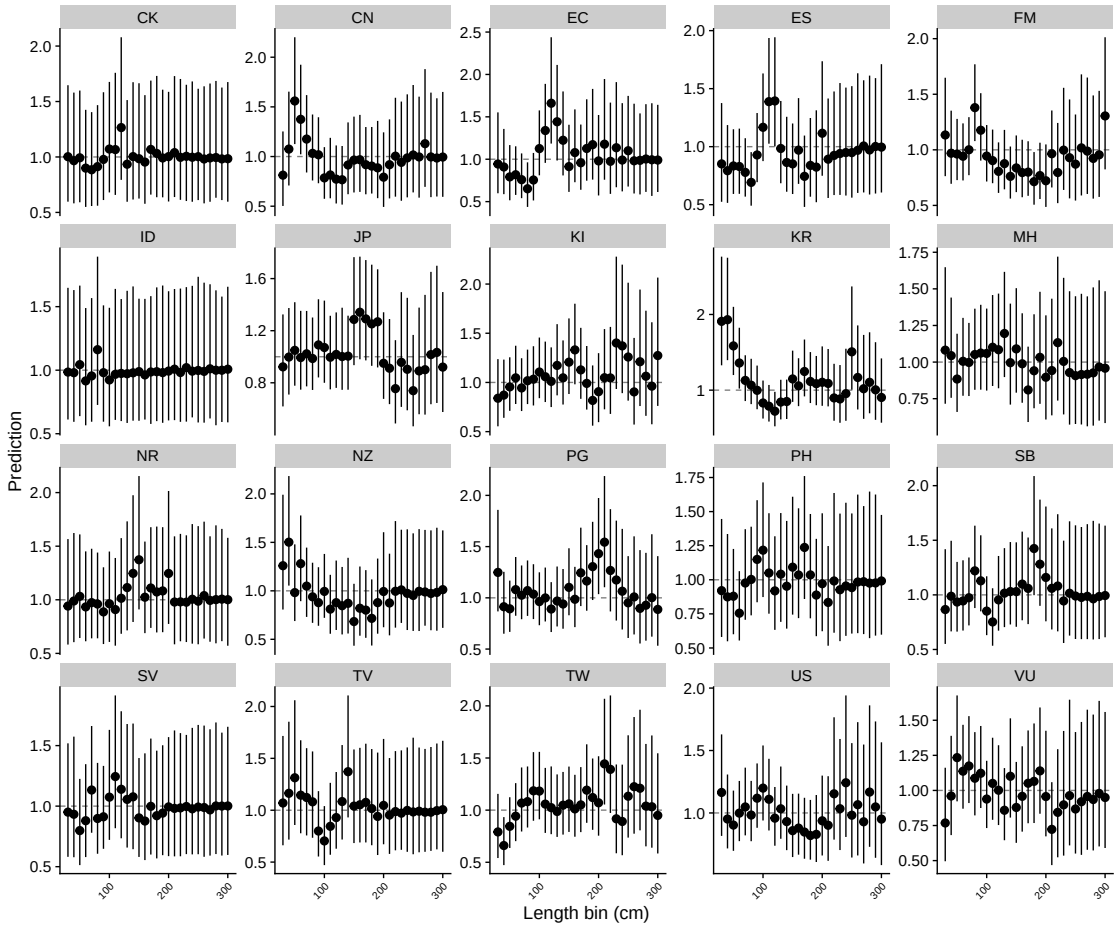

Figure 43: Vessel flag effect by 10 cm length bin, relative to the over-all mean length composition in the WCPO purse-seine fishery catching silky shark, estimated by the length-composition standardisation model (black posterior median and 95% prediction interval).

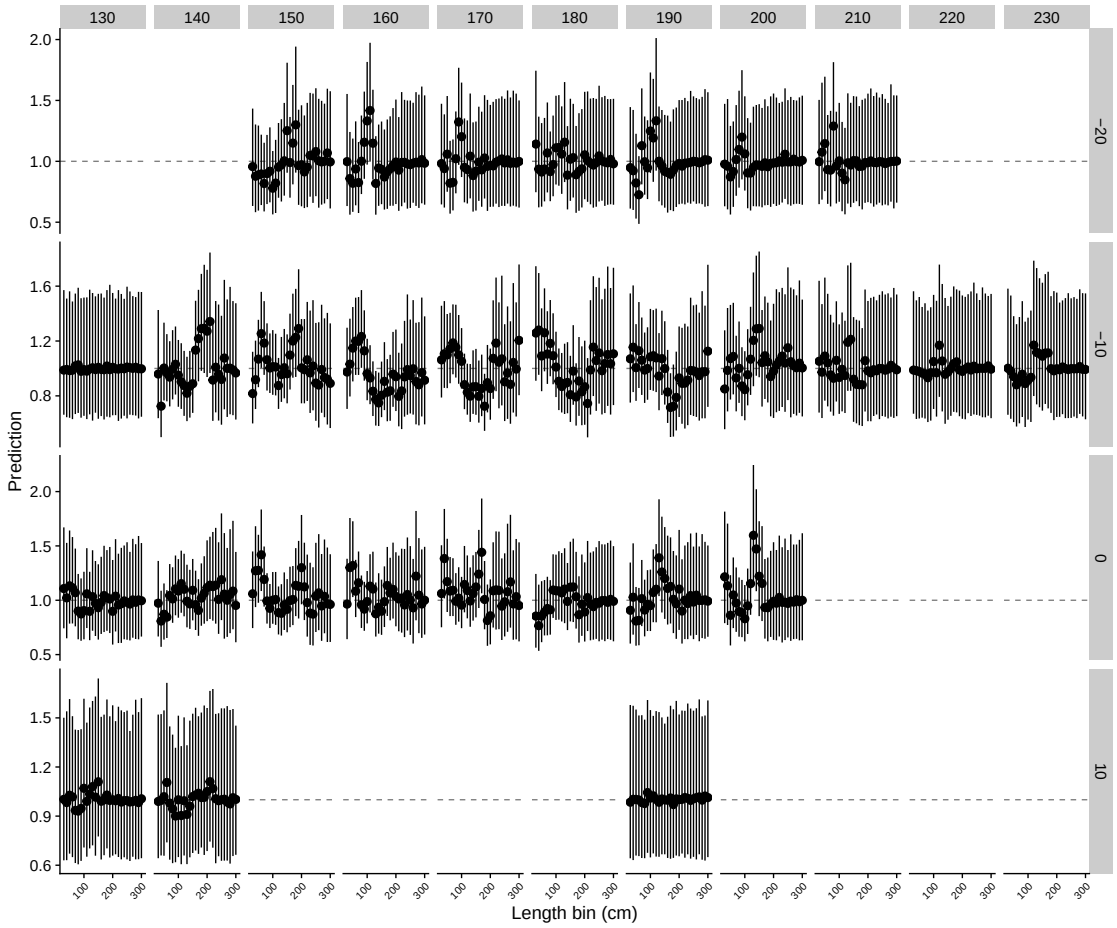

Figure 44: Area (10 degree grid) effect by 10 cm length bin in the WCPO purse-seine fishery catching silky shark, relative to the over-all mean length composition, estimated by the length-composition standardisation model (black posterior median and 95% prediction interval).

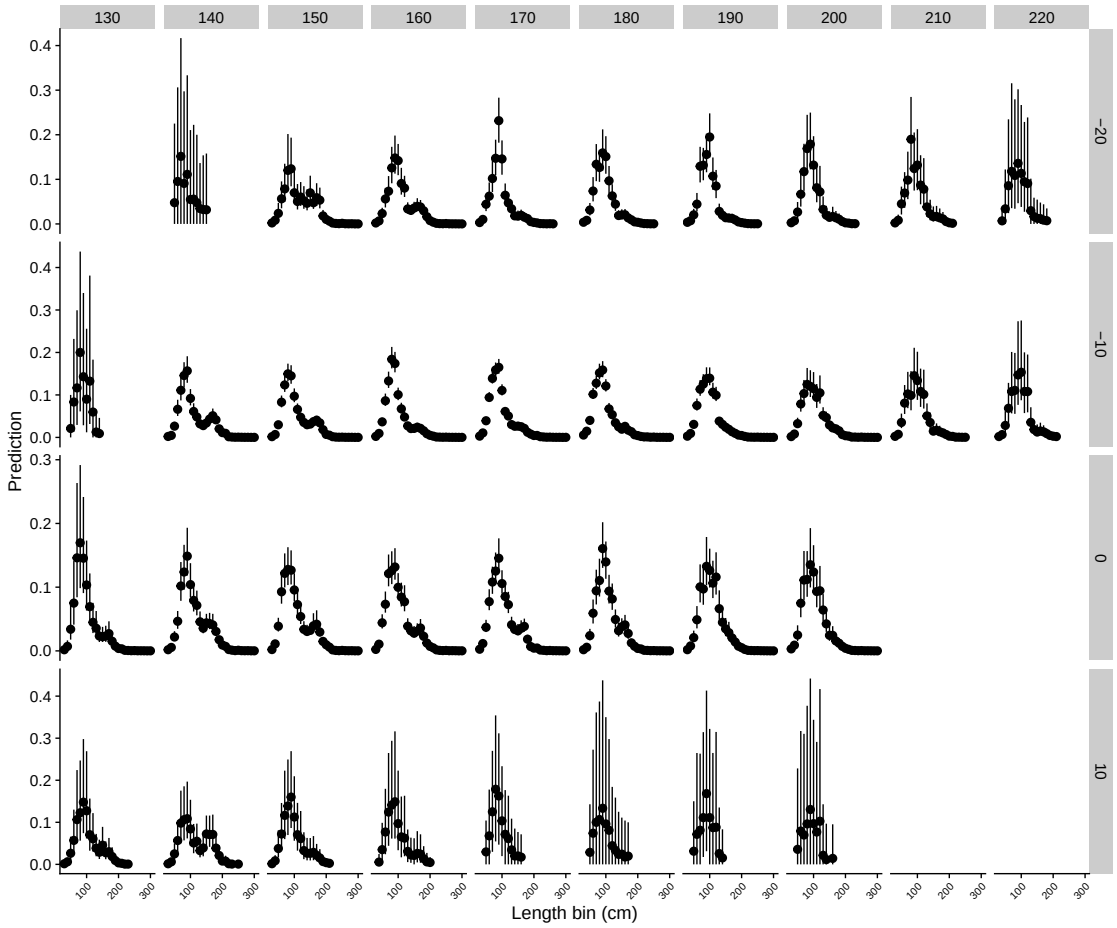

Figure 45: Predicted scaled length frequency by 10 cm length bin and 10 degree latitude-longitude bins, scaled by the predicted number of interactions at the level of model strata in the WCPO purse-seine fishery catching silky shark, estimated by the length-composition standardisation model (black posterior median and 95% prediction interval).

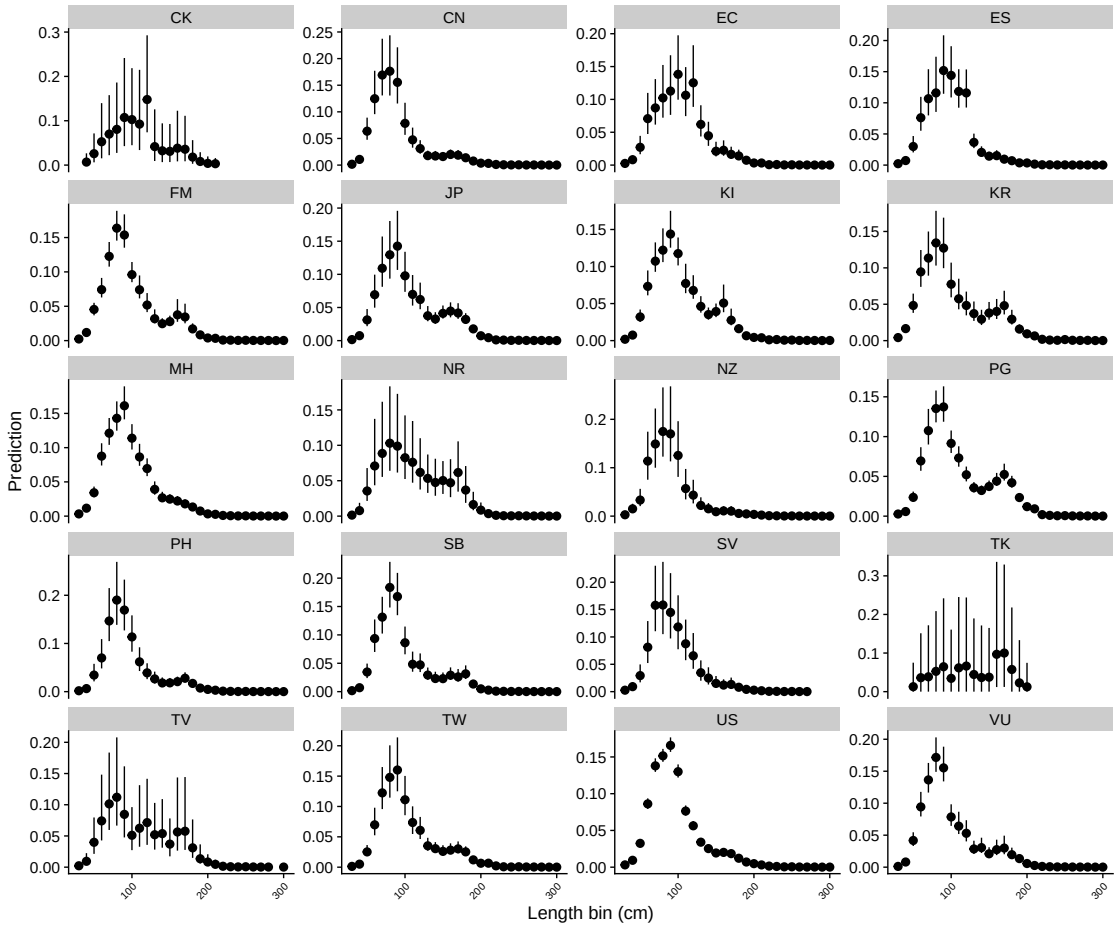

Figure 46: Predicted scaled length frequency by 10 cm length bin and vessel flag, scaled by the predicted number of interactions at the level of model strata in the WCPO purse-seine fishery catching silky shark, estimated by the length-composition standardisation model (black posterior median and 95% prediction interval).

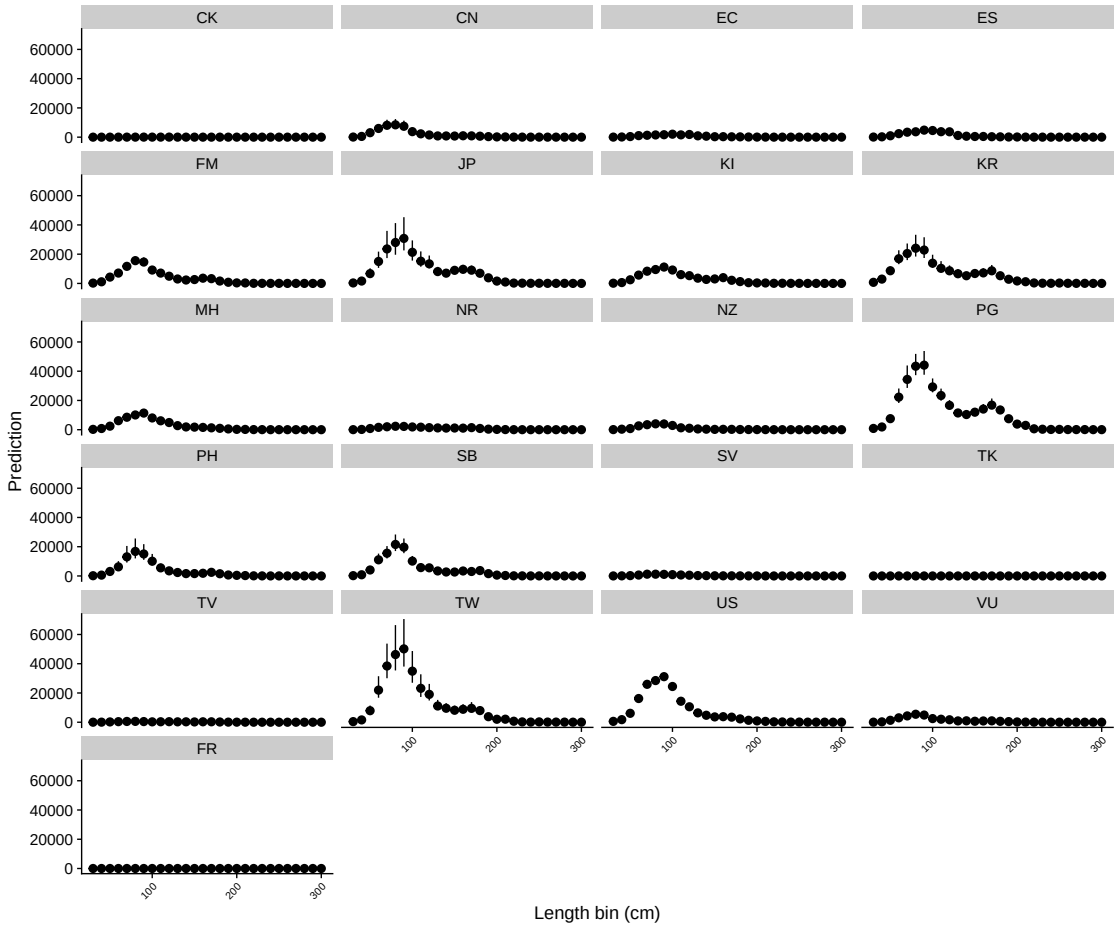

Figure 47: Predicted scaled catch at length by 10 cm length bin and vessel flag, scaled by the predicted number of interactions at the level of model strata in the WCPO purse-seine fishery catching silky shark, estimated by the length-composition standardisation model (black posterior median and 95% prediction interval).

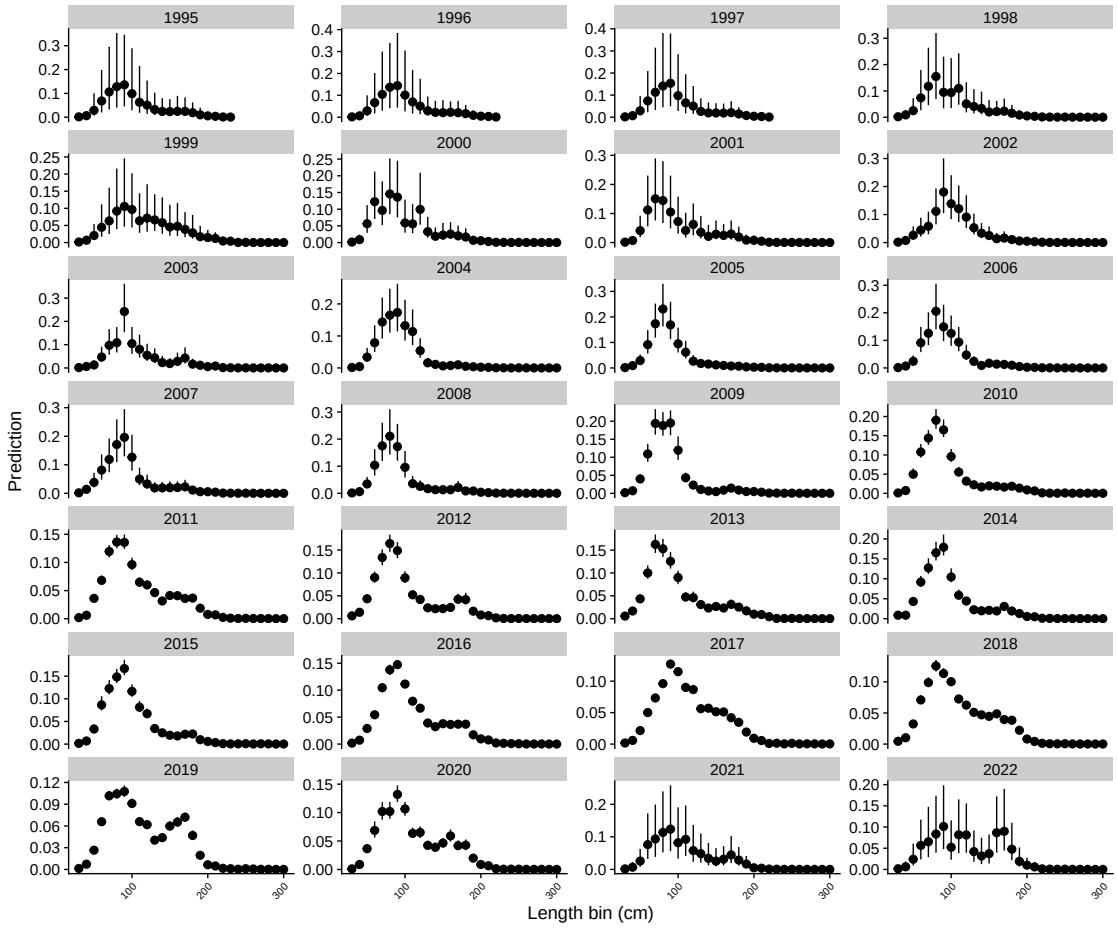

Figure 48: Predicted scaled length frequency by 10 cm length bin and year, scaled by the predicted number of interactions at the level of model strata in the WCPO purse-seine fishery catching silky shark, estimated by the length-composition standardisation model (black posterior median and 95% prediction interval).

APPENDIX A BIOLOGICAL CONTEXT

Estimates of biological parameters are available for silky shark from different regions, with several studies from the Western and Central Pacific. For the Central Pacific region Oshitani et al. 2003 estimated maximum age at 18 years, maturity-at-length as 204 cm TL for females and >186 cm for males, maturity-at-age as 6–7 years for females and 5–6 years for males, and litter size of 1–16 pups based on 153 observed females. Mean growth function parameter estimates were 66.8 cm TL for size at birth (L_0) and 288 cm TL for asymptotic length (L_∞).

For the Central West Pacific region, Grant et al. 2018 estimated maximum age at 42 years, A50 (age where 50% of the individuals sampled attained maturity) at 14 years for females and 12 years for males, L50 (length where 50% of the individuals sampled attained maturity) at 204 cm TL for females and 183 cm TL for males, and litter size of 3–13 pups based on 28 observed females. Mean growth function parameter estimates for this region were 82.7 cm TL for size at birth (L_0) and 268 cm TL for asymptotic length (L_∞).

For Northeastern Taiwan, Joung et al. 2008 estimated maximum age at 33 years, A50 at 9–10 years for females and 9 years for males, L50 at 210–220 cm TL for females and 213 cm TL for males, and litter size of 8–10 pups based on 4 observed females. Mean growth function parameter estimates for this region were 68.3 cm TL for size at birth (L_0) and 332 cm TL for asymptotic length (L_∞).

From the Eastern Pacific Sanchez-de Ita et al. 2011 and Hoyos-Padilla et al. 2012 estimated maximum age at 18 years, maturity-at-length as 180–182 cm TL for both females and males, maturity-at-age as 8 years for both sexes, and litter size of 2–9 pups based on 20 observed females. Mean growth function parameter estimates were 81.9 cm TL for size at birth (L_0) and 240 cm TL for asymptotic length (L_∞).

Grant et al. 2019 provide a summary of age-invariant estimates (using four different methods) of natural mortality by region, ranging from 0.16 to 0.25 y^{-1} for the Central Pacific, from 0.11 to 0.21 y^{-1} for the Central West Pacific, from 0.16 to 0.23 y^{-1} for the East Pacific, and from 0.16 to 0.23 y^{-1} for the Gulf of Mexico.

In their life history comparative study of silky shark Grant et al. 2019 concluded that different methodological approaches to sampling a population may result in different life history parameter estimates among studies, and that the life history variation reported for *C. falciformis* has serious implications for regional fisheries management as age- or life-stage-dependent management is most effective for long-lived elasmobranch species. The authors recommend that all regional life history parameter data, and potential for inaccuracies in such data, should be carefully considered in present and future stock status and fisheries management assessments of silky sharks.

APPENDIX B HIERARCHICAL STACKING MODEL

The present Stan model is based on formulations developed in Yao et al. 2022, extended to allow for predictions of model weights beyond the training dataset using the "generated quantities" block in Stan. Necessary inputs are described in the data section of the model.

```
data {
int < lower =1 > N; // number of observations
int N_pred; // number of predictions
int < lower =1 > d; // number of input variables
int < lower =1 > d_discrete ; // number of discrete dummy inputs
int < lower =1 > d_pred ; // number of discrete dummy inputs - prediction
int < lower =2 > K; // number of models
// when K =2 , replace softmax by inverse - logit for higher efficiency
matrix [N ,d] X; // predictors
matrix [N_pred ,d_pred+d-d_discrete] X_pred; // predictors for full prediction dataset
// including continuous and discrete in dummy variables , no constant
matrix [N ,K] lpd_point ; // the input pointwise predictive density
real < lower =0 > tau_mu ;
real < lower =0 > tau_discrete ; // global regularization for discrete x
real < lower =0 > tau_con ; // overall regularization for continuous x
}

transformed data {
matrix [N ,K] exp_lpd_point = exp ( lpd_point );
}

parameters {
vector [K -1] mu ;
real mu_0 ;
vector < lower =0 >[K -1] sigma ;
vector < lower =0 >[K -1] sigma_con ;
vector [d - d_discrete ] beta_con [K -1];
vector [ d_discrete ] tau [K -1]; // using non - centered parameterization
}

transformed parameters {
vector [d] beta [K -1];
simplex [K] w[N ];
matrix [N ,K] f;

for (k in 1:( K -1) ) beta [k] = append_row ( mu_0 * tau_mu + mu [k]* tau_mu +
sigma [k ]* tau [k], sigma_con [k ]* beta_con [k ]) ;

for (k in 1:( K -1) ) f[,k] = X * beta [k ];
f[,K] = rep_vector (0 , N);

for (n in 1: N) w[n] = softmax ( to_vector (f[n , 1: K ]) );
```

```
}

model{
for (k in 1:( K -1) ){
tau [k] ~ std_normal () ;
beta_con [k] ~ std_normal () ;
}
mu ~ std_normal () ;
mu_0 ~ std_normal () ;
sigma ~ normal (0 , tau_discrete );
sigma_con ~ normal (0 , tau_con );
for (i in 1: N) target += log ( exp_lpd_point [i ,] * w[i ]) ; // log likelihood
}
generated quantities {
vector [N] log_lik ;
simplex [K] w_pred[N_pred];

for (i in 1: N) log_lik [i] = log ( exp_lpd_point [i ,] * w[i ]);
if(N_pred>0){
matrix [N_pred ,K] f_pred;
vector [d_pred] beta_pred [K -1];
vector [d_pred] tau_pred [K -1]; // using non - centered parameterization


for (k in 1:( K -1) ) {

tau_pred[k,1:d_discrete] = tau[k] ;

if(d_pred>d_discrete) {
for (ds in (d_discrete+1):d_pred) tau_pred [k,ds] = normal_rng(0,1);
}

beta_pred [k] = append_row ( mu_0 * tau_mu + mu [k ]* tau_mu +
sigma [k ]* tau_pred [k], sigma_con [k ]* beta_con [k ]) ;
f_pred[,k] = X_pred * beta_pred[k ];
}
f_pred[,K] = rep_vector (0 , N_pred);

for (n in 1: N_pred) w_pred[n] = softmax ( to_vector (f_pred[n , 1: K ]) );
}
}
```

APPENDIX C CPUE DIAGNOSTICS - SUPPLEMENTARY FIGURES

C.1 CPUE diagnostics for all longline

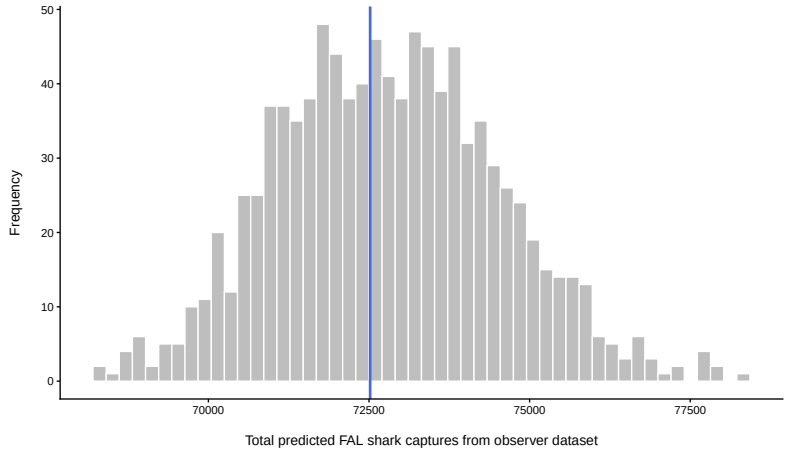

Figure C-1: Observed interactions (vertical line) and model predictions from the model used to derive CPUE from observed for all longline sets.

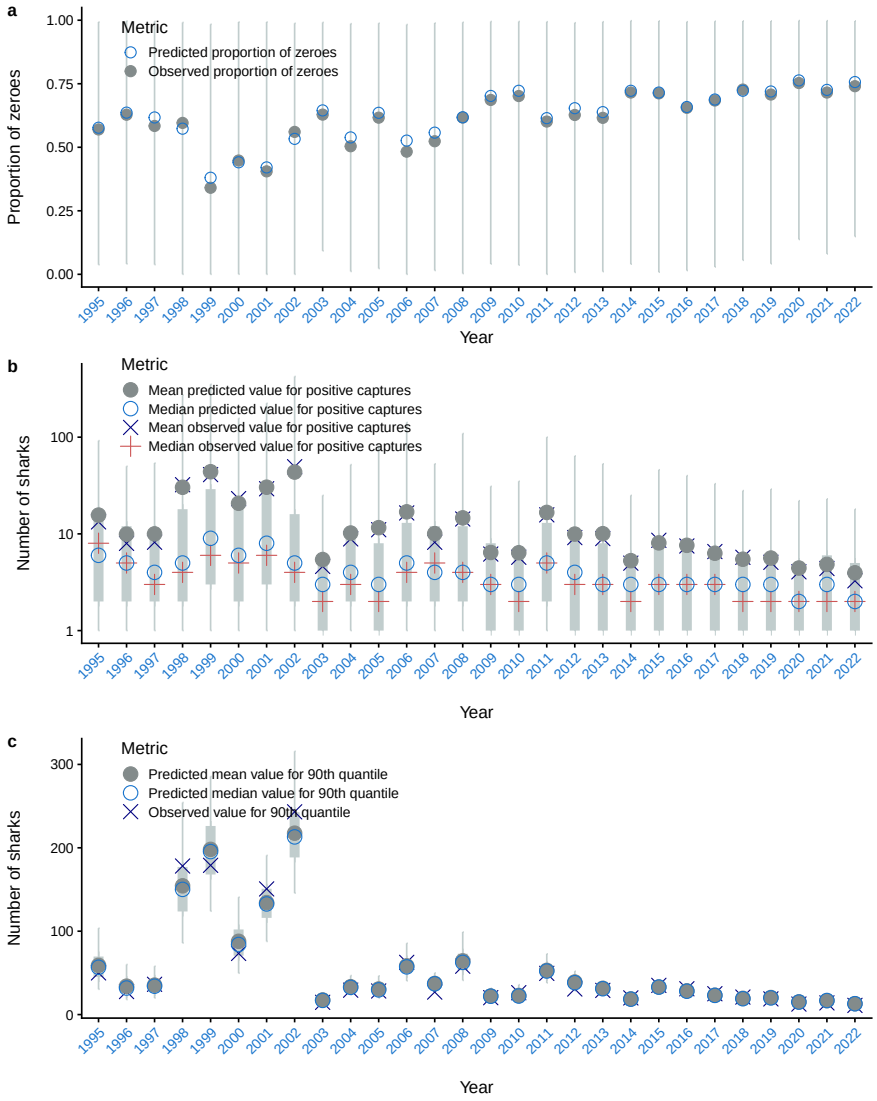

Figure C-2: Posterior predictive model diagnostics by model year for all longline sets, with (a) observed and predicted proportion of zero captures, (b) observed and predicted positive captures and (c) dispersion statistics (90% percentile) of observed data and predictions.

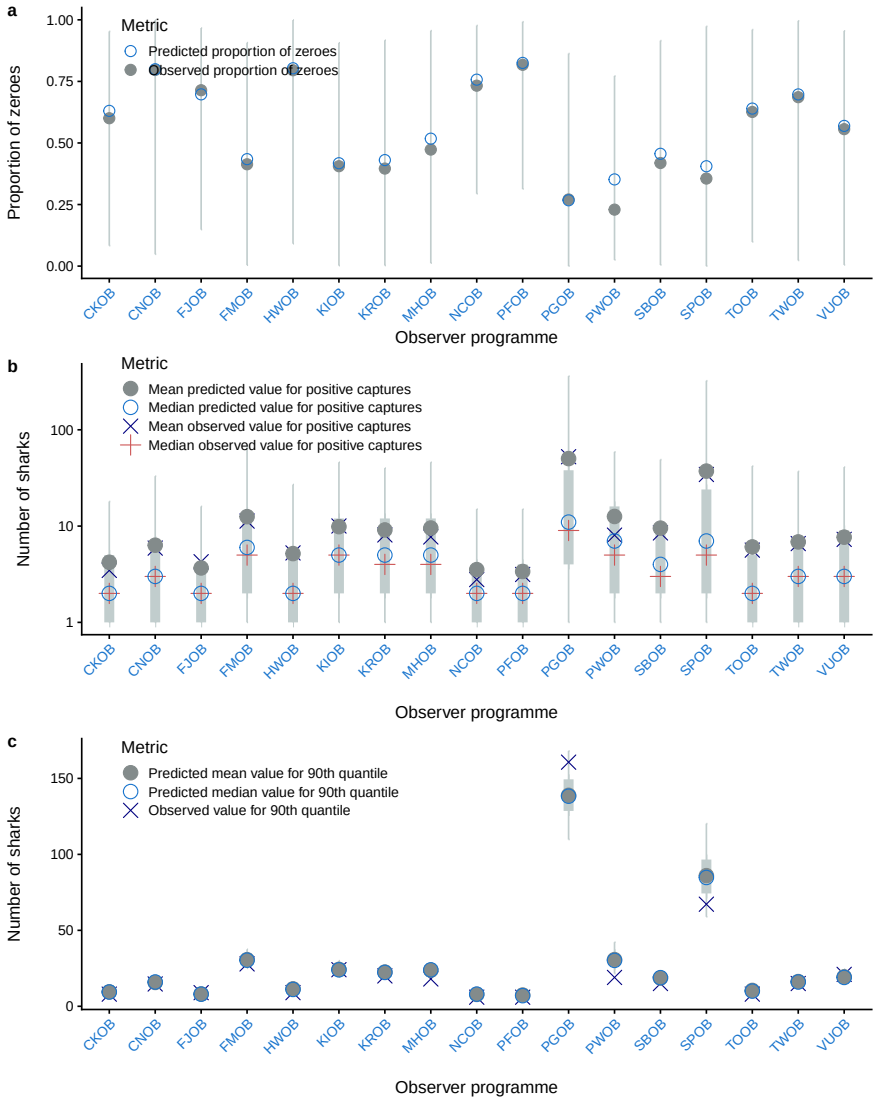

Figure C-3: Posterior predictive model diagnostics by observer program for all longline sets, with (a) observed and predicted proportion of zero captures, (b) observed and predicted positive captures and (c) dispersion statistics (90% percentile) of observed data and predictions.

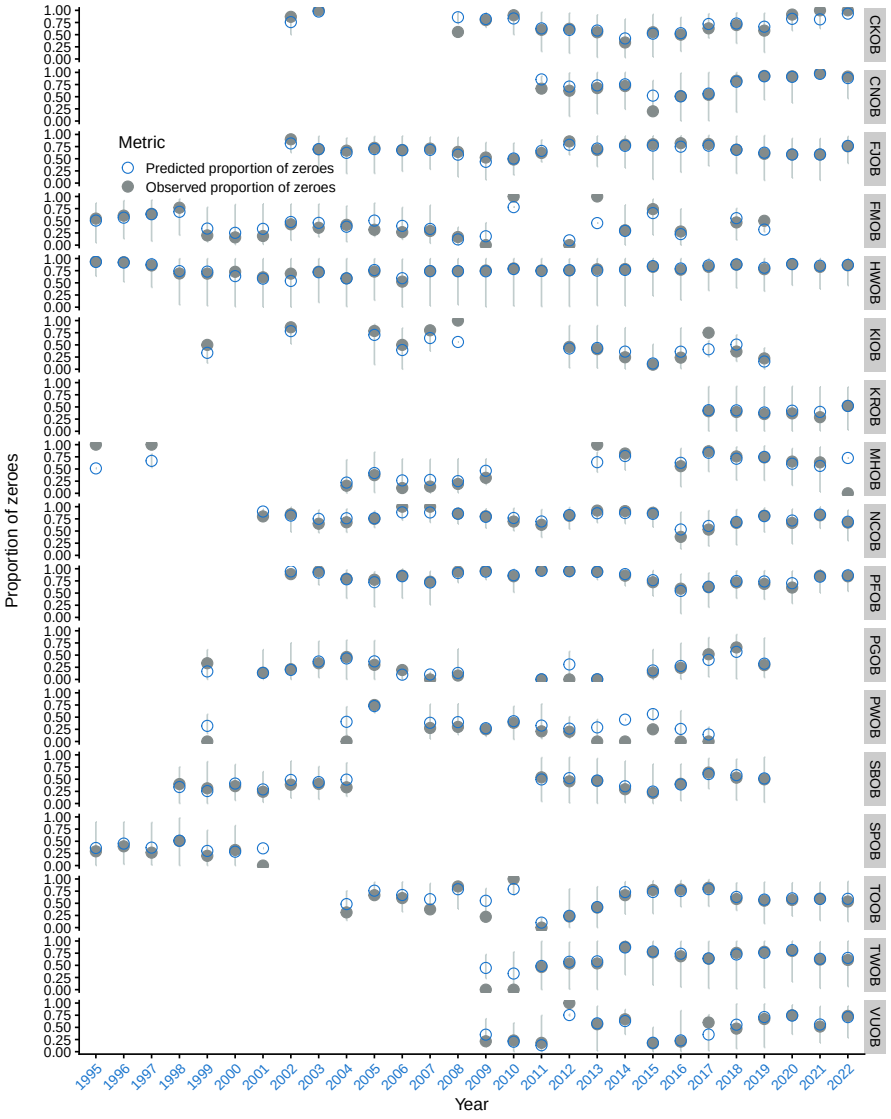

Figure C-4: Posterior predictive model diagnostics for observed and predicted proportion of zero captures by observer program and year for all longline sets.

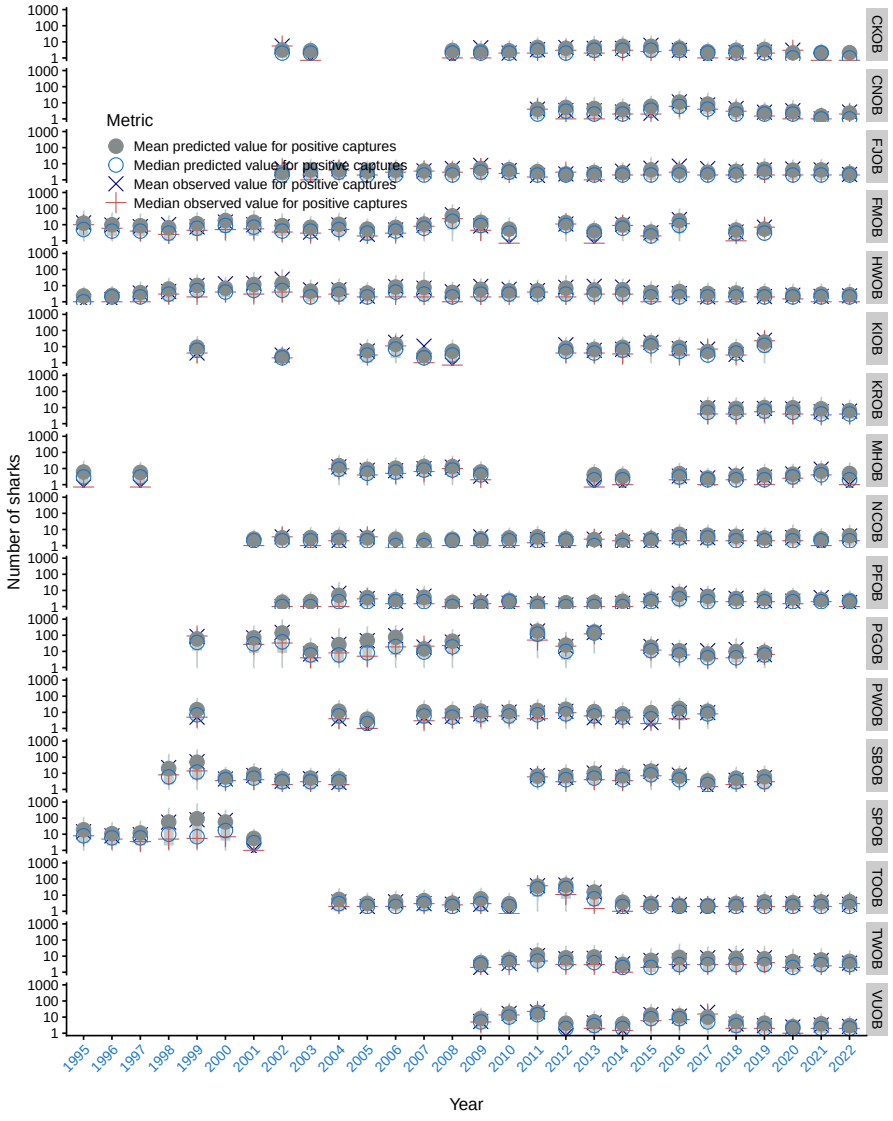

Figure C-5: Posterior predictive model diagnostics for bserved and predicted positive captures by observer program and year for all longline sets.

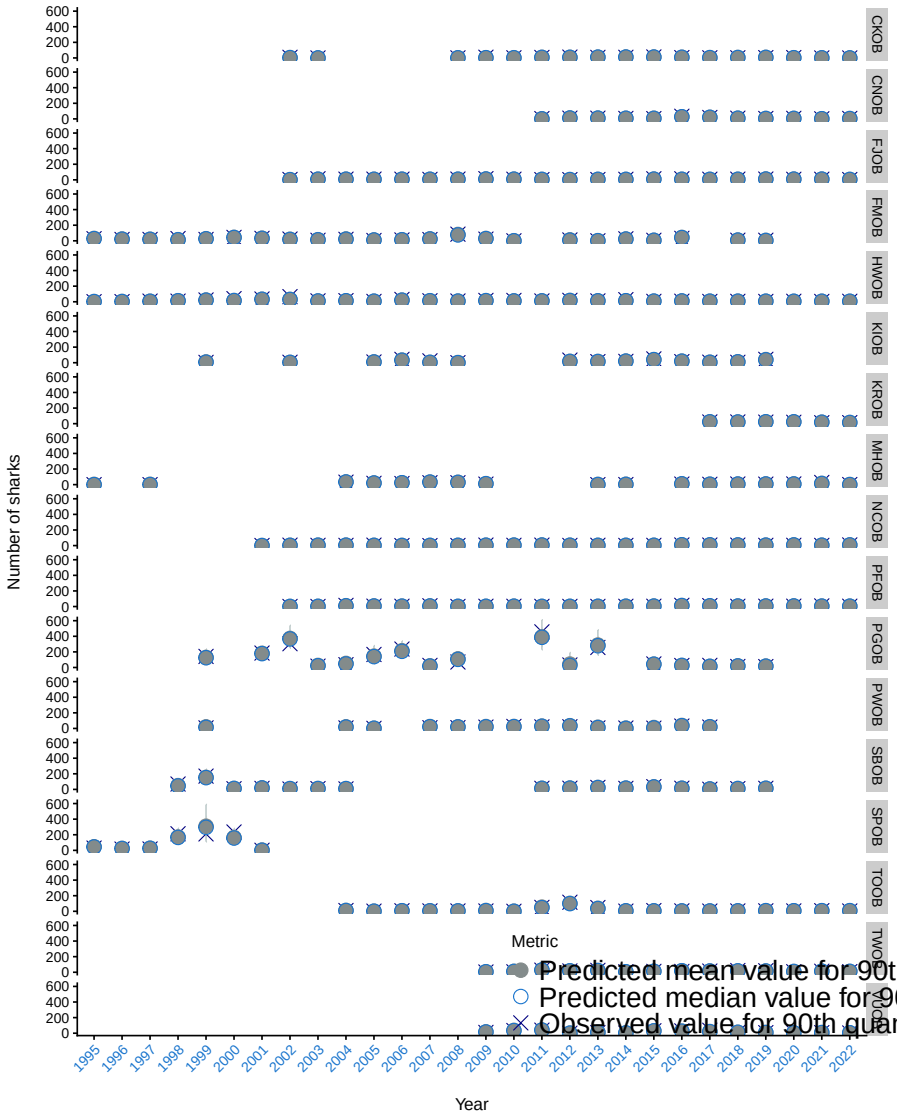

Figure C-6: Posterior predictive model diagnostics for dispersion statistics (90% percentile) of observed data and predictions by observer program and year for all longline sets.

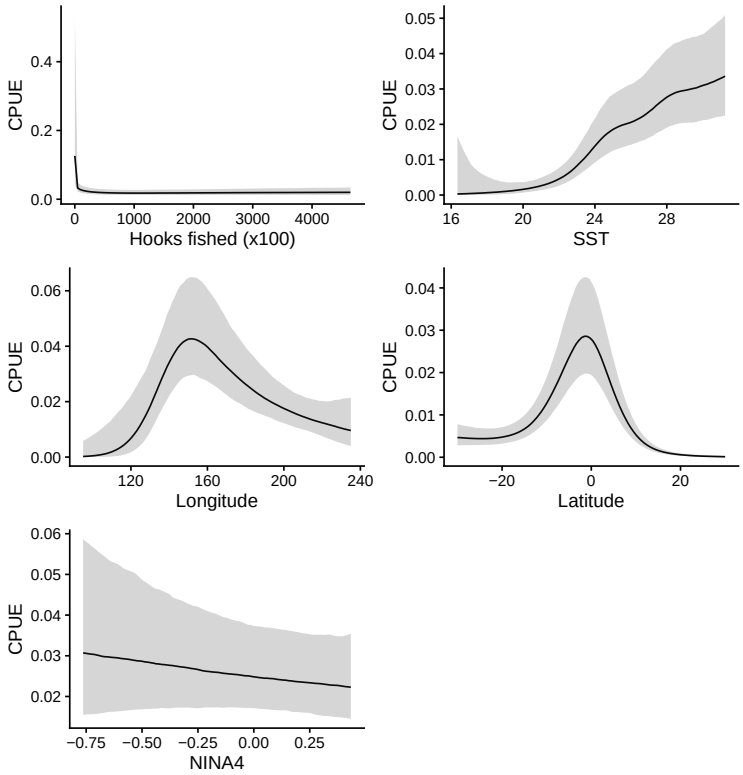

Figure C-7: Conditional effects estimated in the model used to derive CPUE from observed for all longline sets.

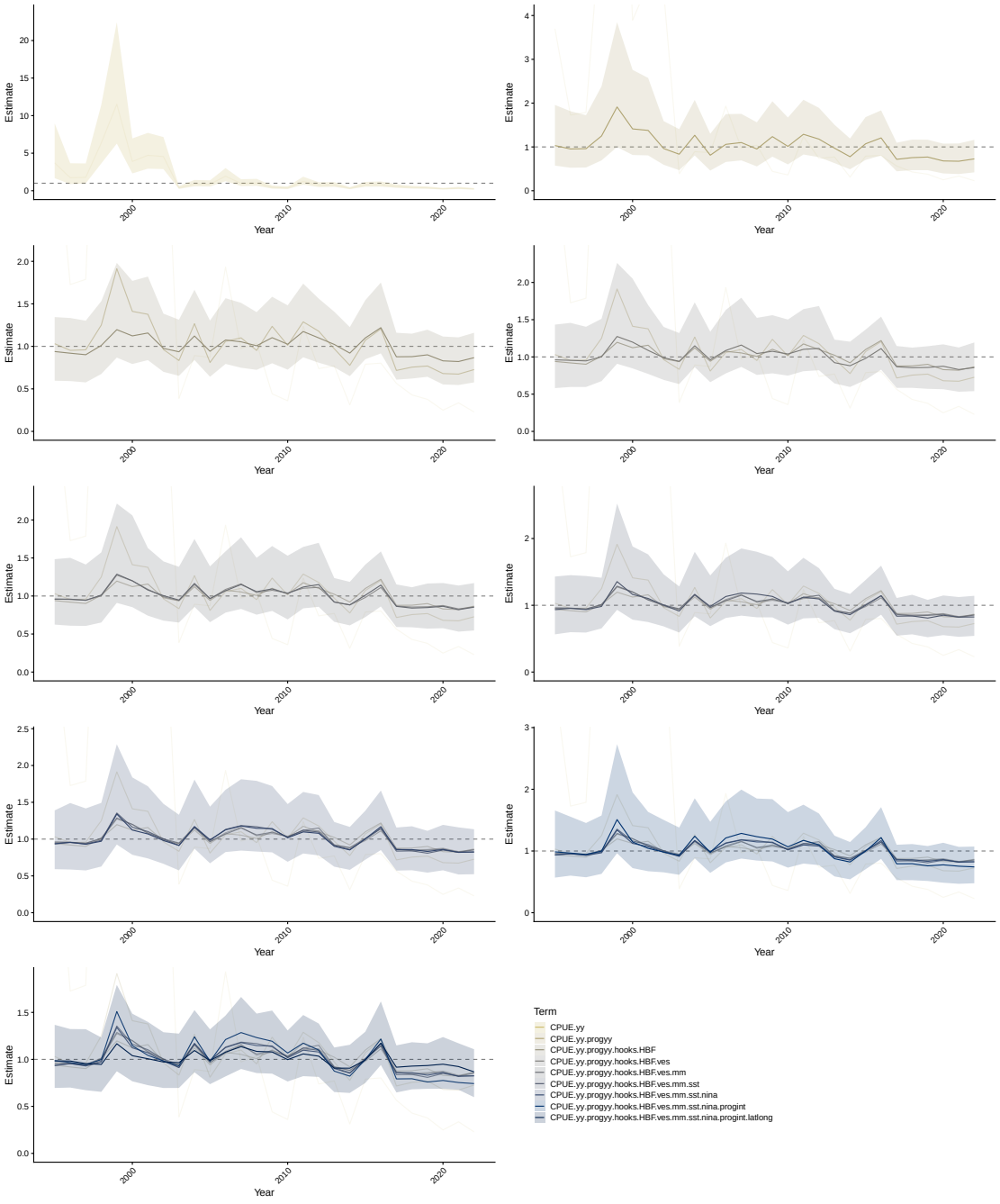

Figure C-8: CPUE standardisation effects for all longline sets. Each row of plots corresponds to the addition of a variable, starting with a model that includes observer - program - year interactions. In each row, the posterior median and credible interval is shown for the updated model, posterior medians for the year effect from sub - models are shown for comparison.

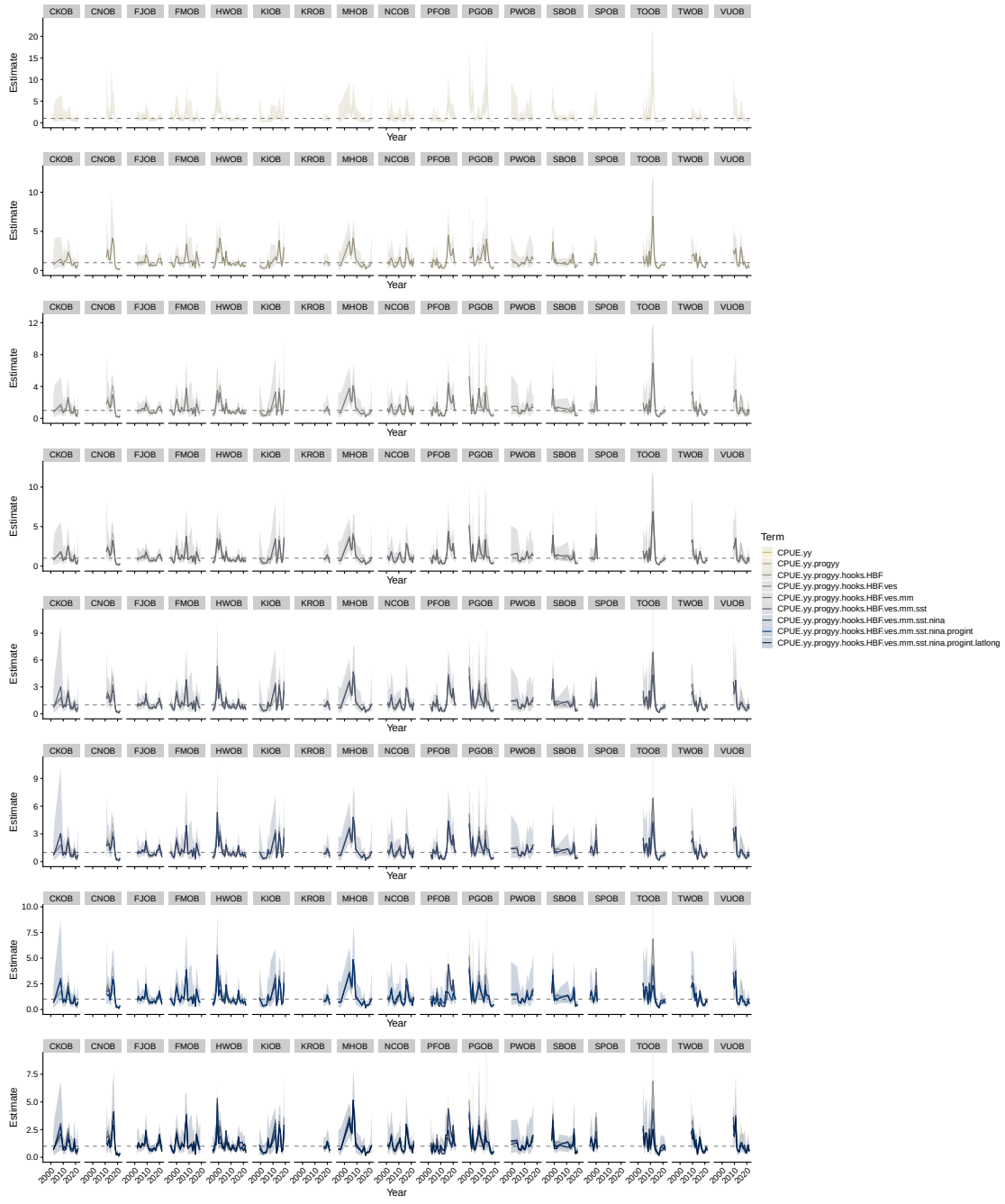

Figure C-9: CPUE standardisation effects for all longline by observer-program. Each row of plots corresponds to the addition of a variable, starting with a model that includes observer-program-year interactions. In each row, the posterior median and credible interval is shown for the updated model, posterior medians for the year effect from sub-models are shown for comparison.

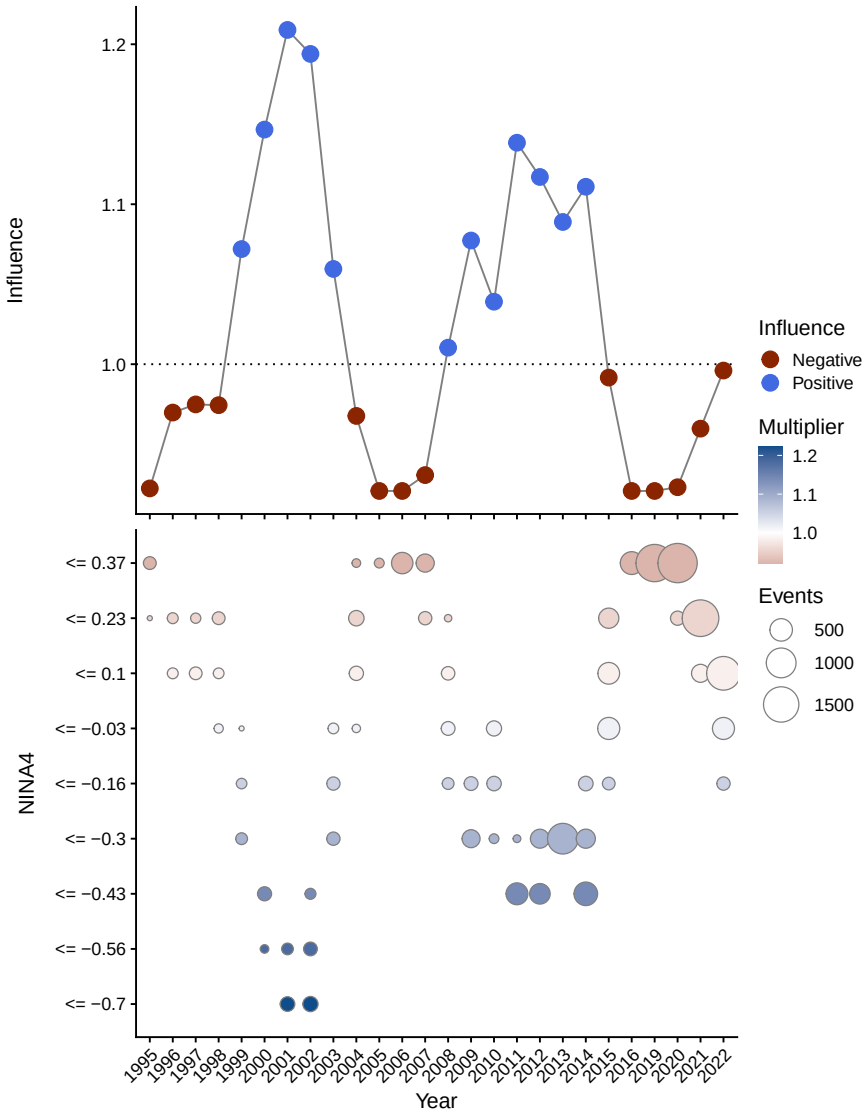

Figure C-10: Influence of the NINA4 index on catch-rates for all longline sets, with positive influence showing years where the over-all catch-rate in the model was standardised downward by the corresponding amount to account for influences the NINA4 index. Influence is shown in colour as a multiplier on average catch rates, with circle size corresponding to the amount of effort entering the model. Note that data for the 2022 year is preliminary.

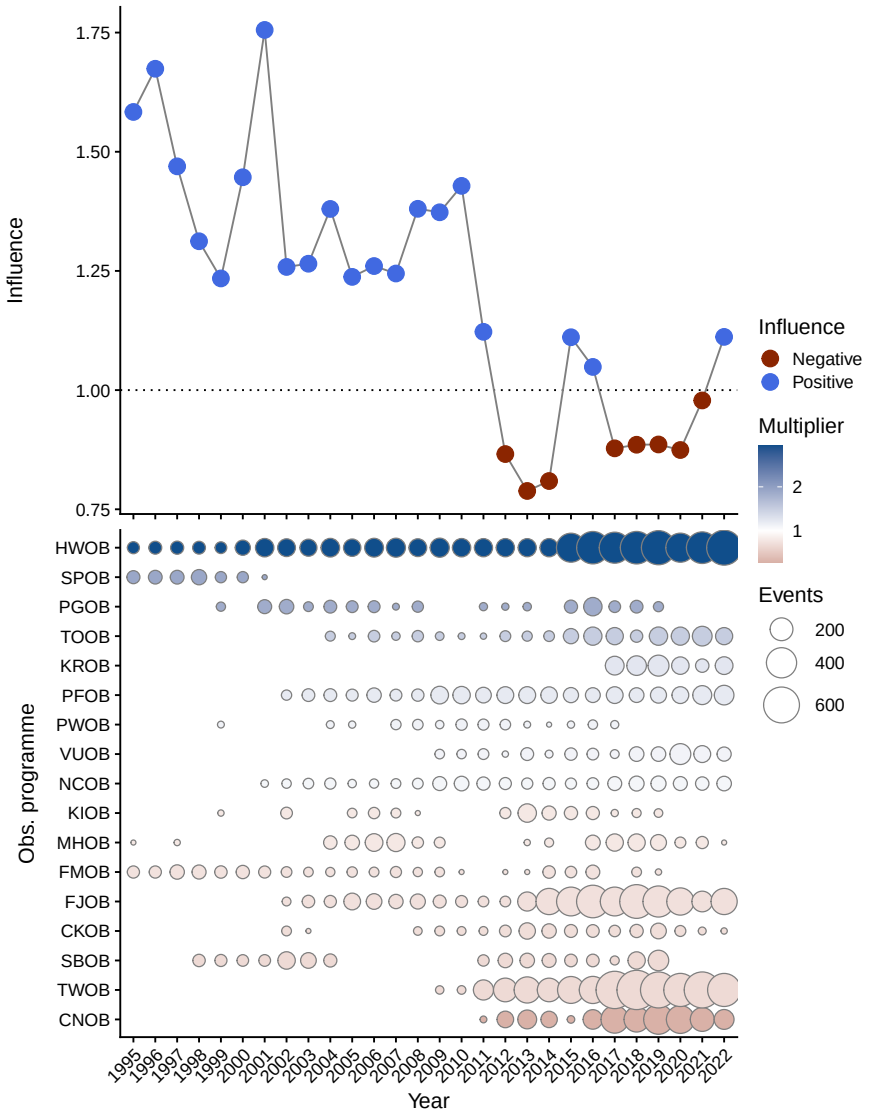

Figure C-11: Influence of observer program on catch-rates for all longline sets, with positive influence showing years where the over-all catch-rate in the model was standardised downward by the corresponding amount to account for influences of observer program. Influence is shown in colour as a multiplier on average catch rates, with circle size corresponding to the amount of effort entering the model. Note that data for the 2022 year is preliminary.

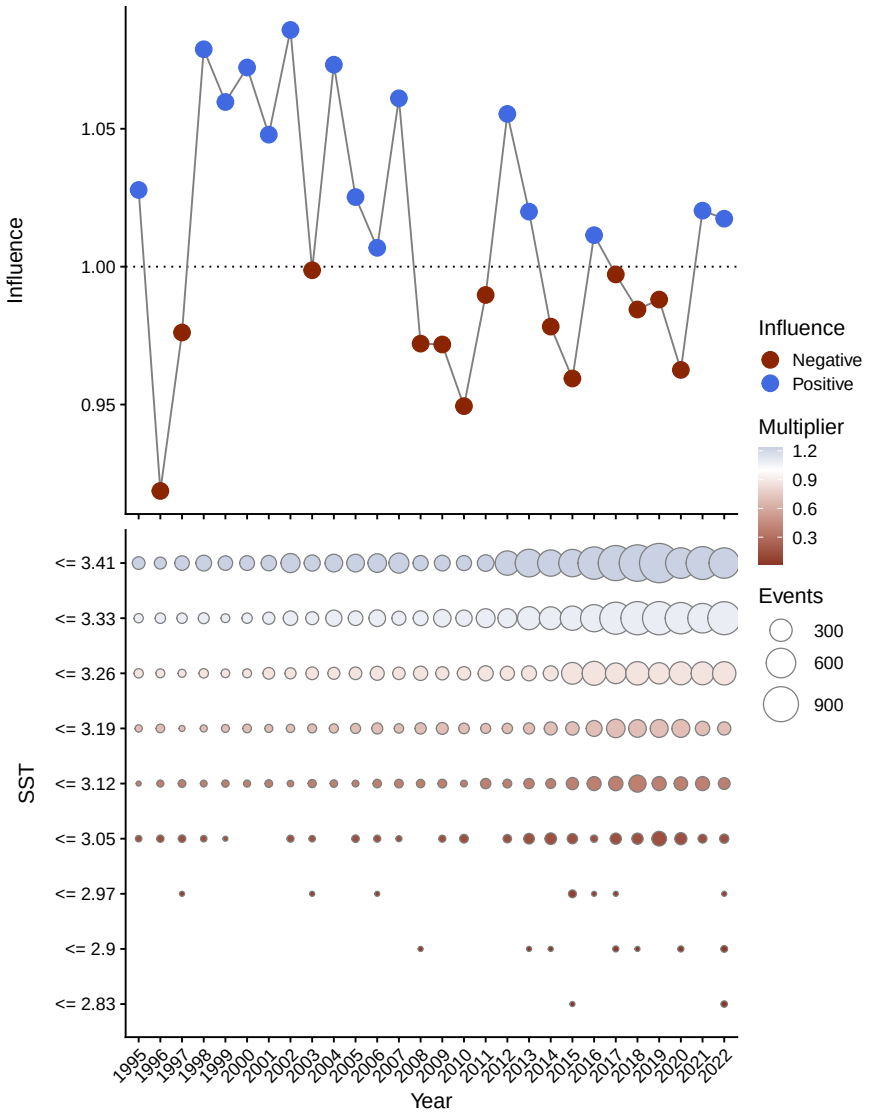

Figure C-12: Influence of sea-surface-temperature (SST) on catch-rates for all longline sets, with positive influence showing years where the over-all catch-rate in the model was standardised downward by the corresponding amount to account for influences of SST. Influence is shown in colour as a multiplier on average catch rates, with circle size corresponding to the amount of effort entering the model. Note that data for the 2022 year is preliminary.

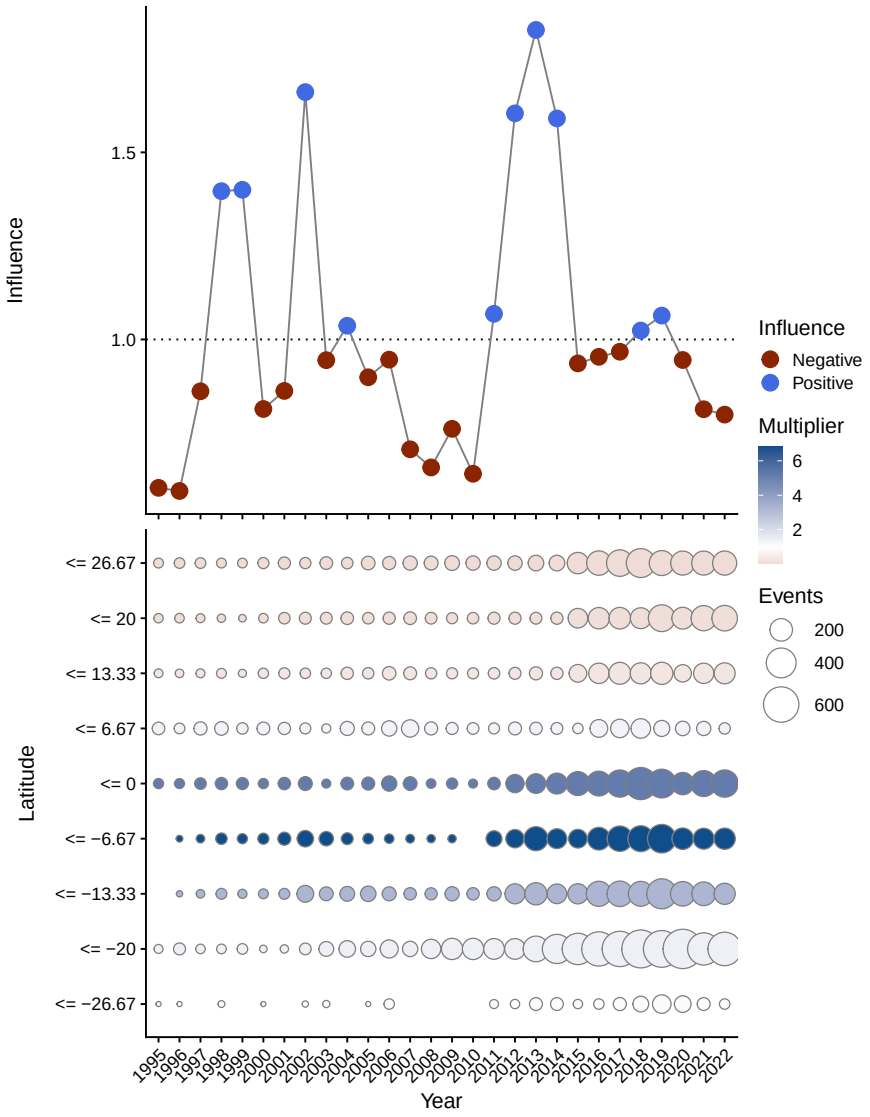

Figure C-13: Influence of latitude on catch-rates for all longline sets, with positive influence showing years where the over-all catch-rate in the model was standardised downward by the corresponding amount to account for influences of latitude. Influence is shown in colour as a multiplier on average catch rates, with circle size corresponding to the amount of effort entering the model. Note that data for the 2022 year is preliminary.

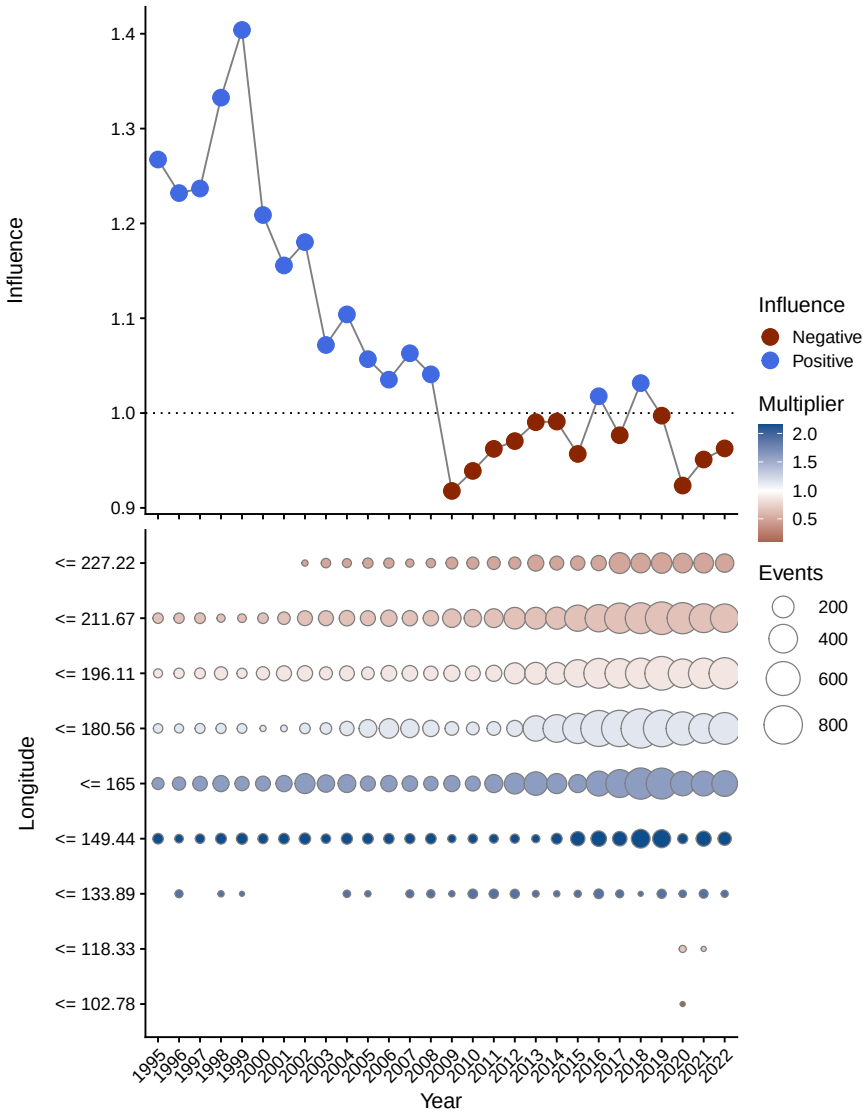

Figure C-14: Influence of longitude on catch-rates for all longline sets, with positive influence showing years where the over-all catch-rate in the model was standardised downward by the corresponding amount to account for influences of longitude. Influence is shown in colour as a multiplier on average catch rates, with circle size corresponding to the amount of effort entering the model. Note that data for the 2022 year is preliminary.

C.2 CPUE diagnostics for South Pacific longline (Clarke et al. 2018 subset)

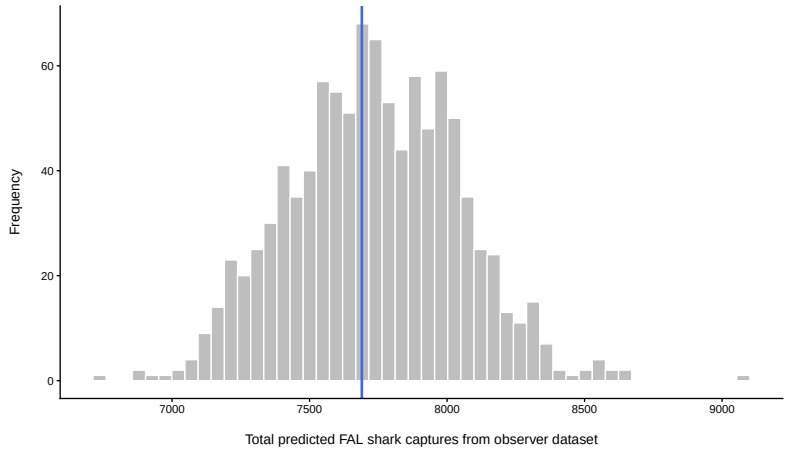

Figure C-15: Observed interactions (vertical line) and model predictions from the model used to derive CPUE from observed for South Pacific longline (Clarke et al. 2018 subset) sets.

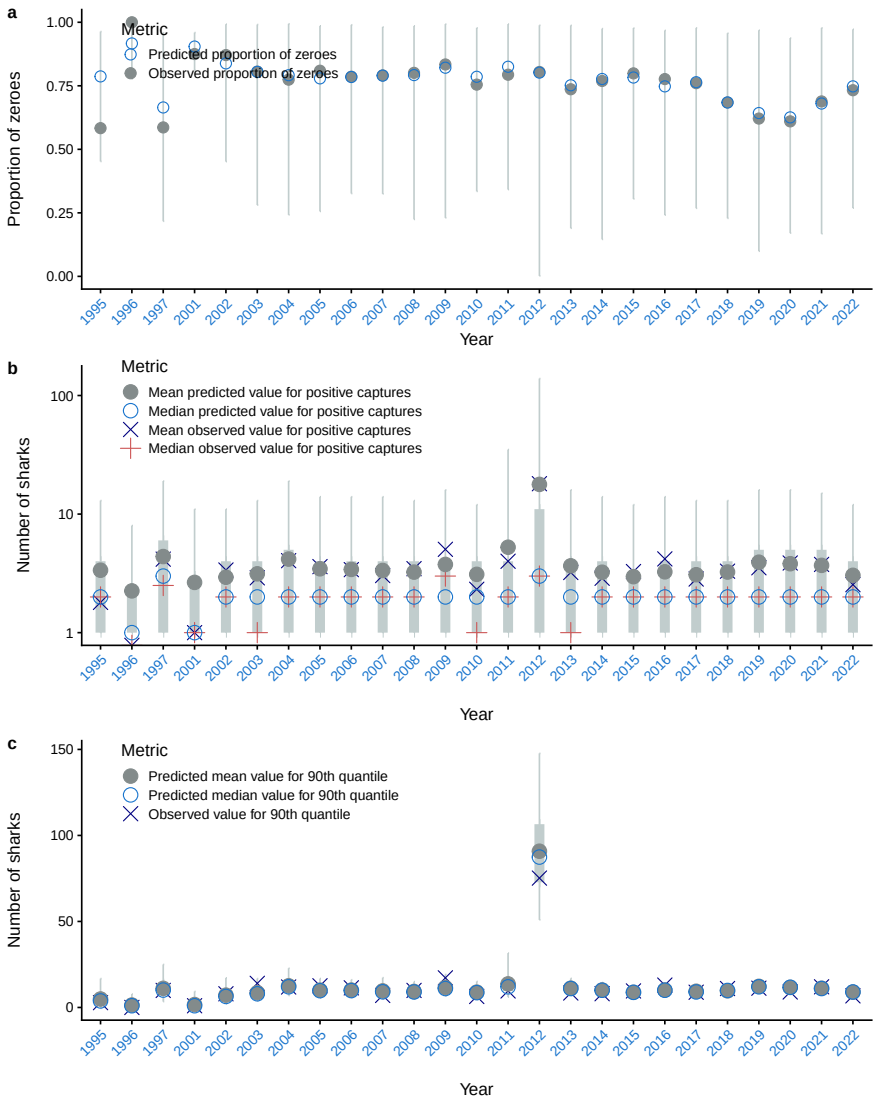

Figure C-16: Posterior predictive model diagnostics by model year for South Pacific longline (Clarke et al. 2018 subset) sets, with (a) observed and predicted proportion of zero captures, (b) observed and predicted positive captures and (c) dispersion statistics (90% percentile) of observed data and predictions.

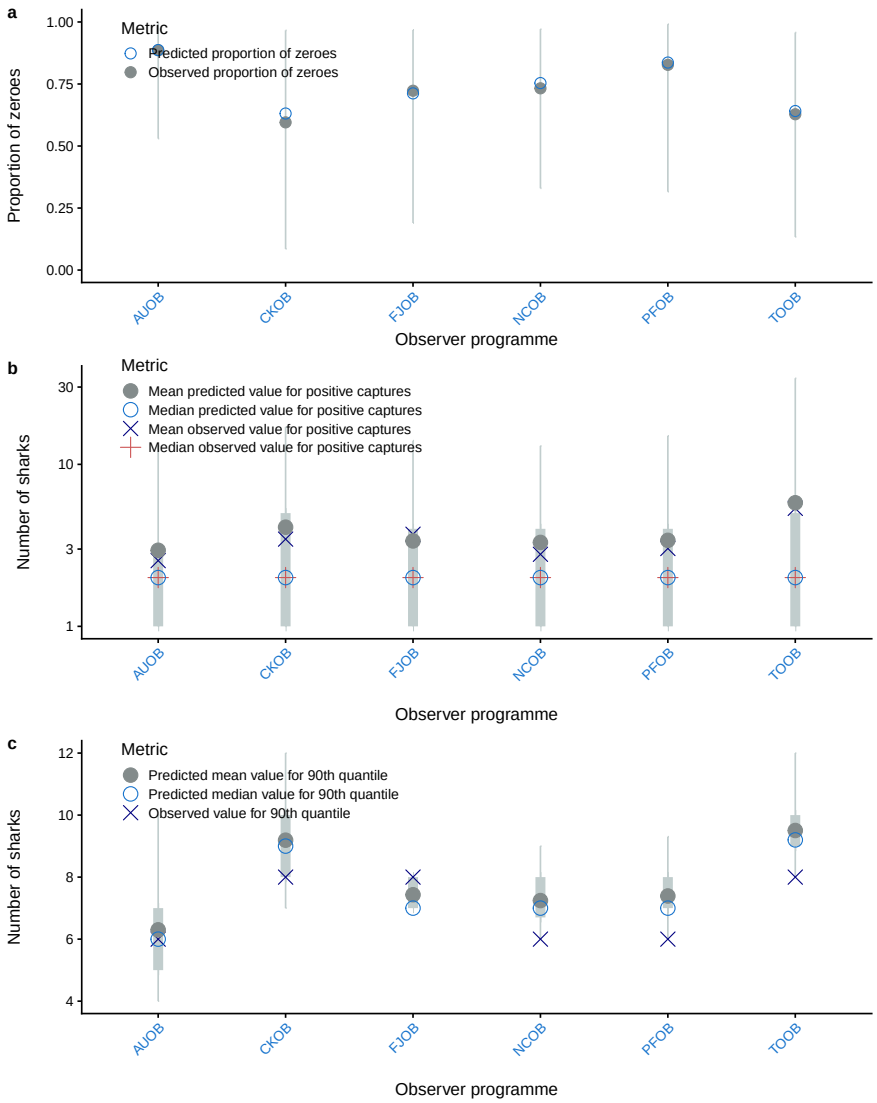

Figure C-17: Posterior predictive model diagnostics by observer program for South Pacific longline (Clarke et al. 2018 subset) sets, with (a) observed and predicted proportion of zero captures, (b) observed and predicted positive captures and (c) dispersion statistics (90% percentile) of observed data and predictions.

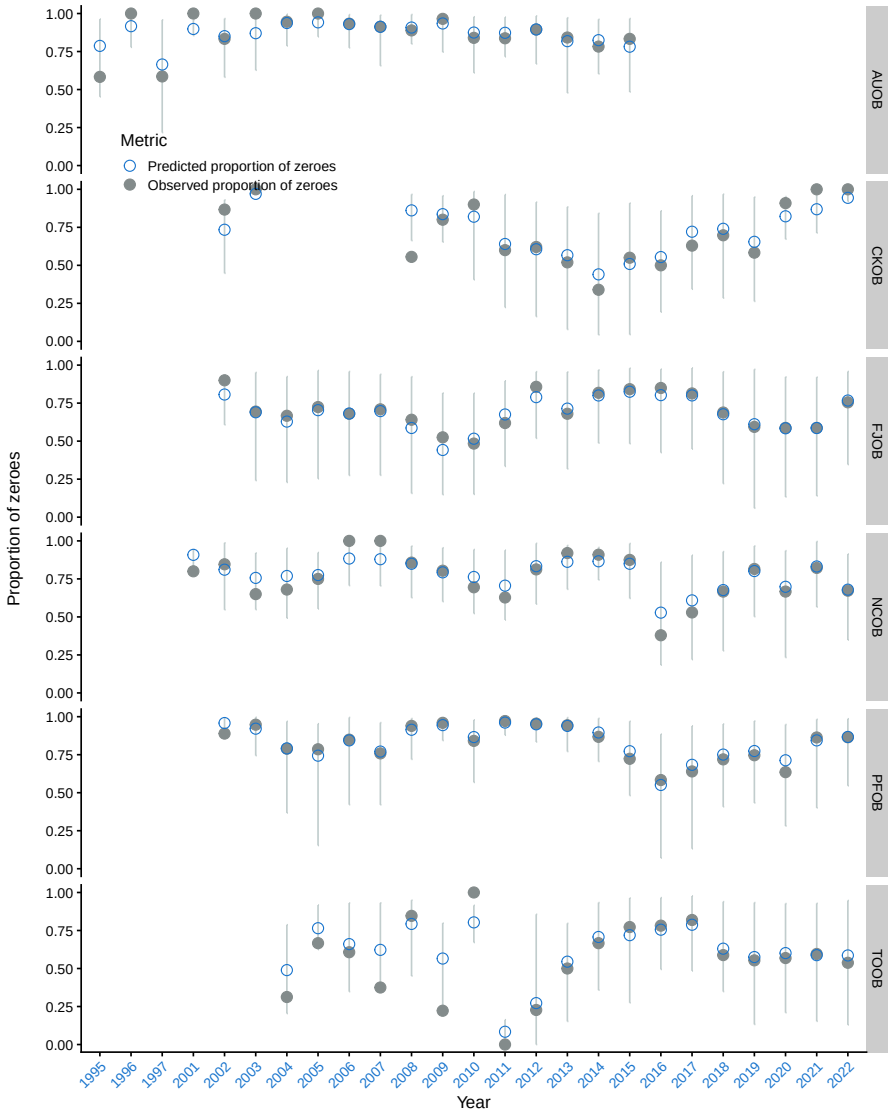

Figure C-18: Posterior predictive model diagnostics for observed and predicted proportion of zero captures by observer program and year for South Pacific longline (Clarke et al. 2018 subset) sets.

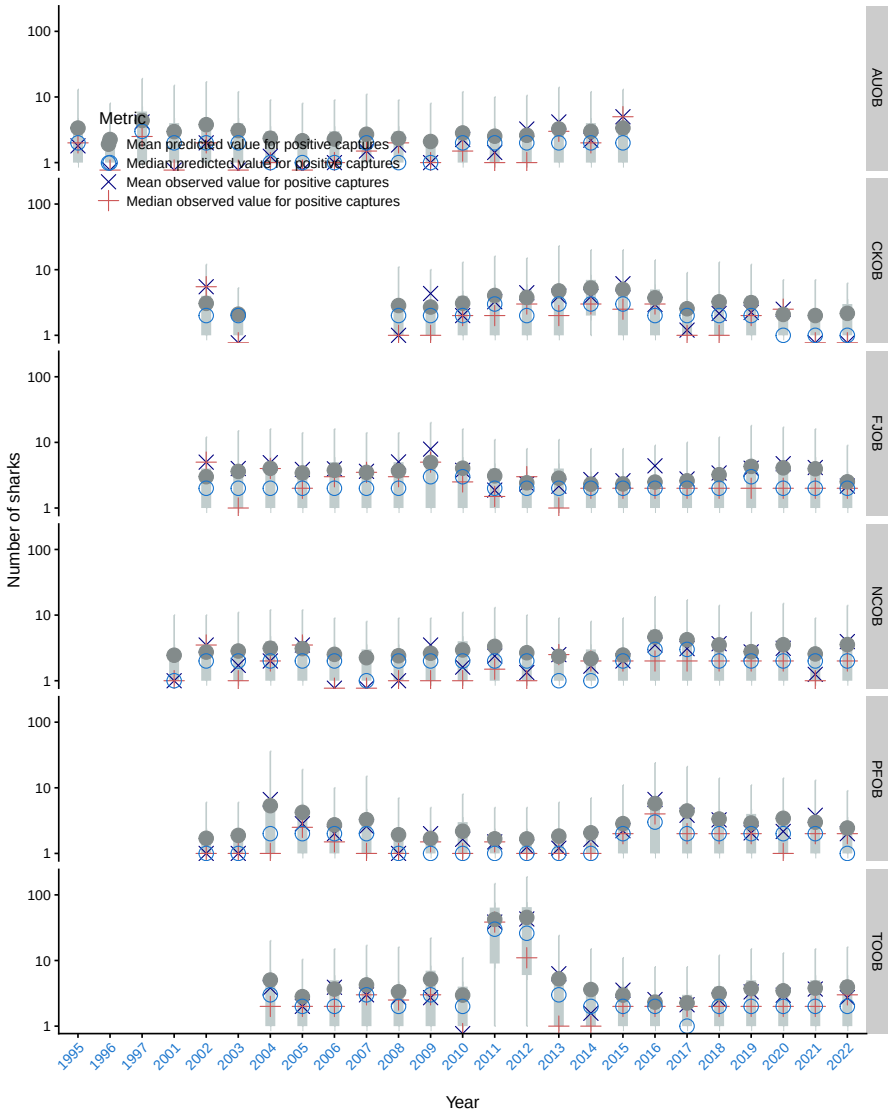

Figure C-19: Posterior predictive model diagnostics for bserved and predicted positive captures by observer program and year for South Pacific longline (Clarke et al. 2018 subset) sets.

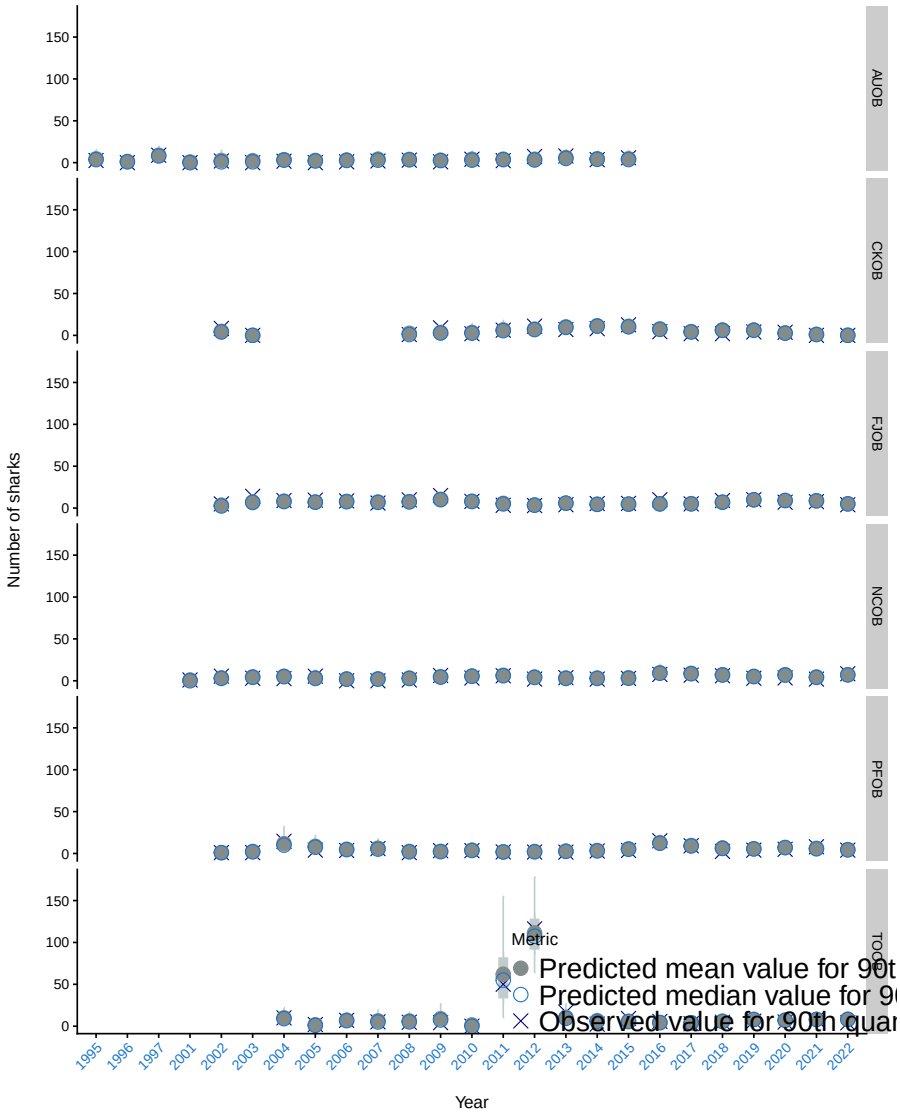

Figure C-20: Posterior predictive model diagnostics for dispersion statistics (90% percentile) of observed data and predictions by observer program and year for South Pacific longline (Clarke et al. 2018 subset) sets.

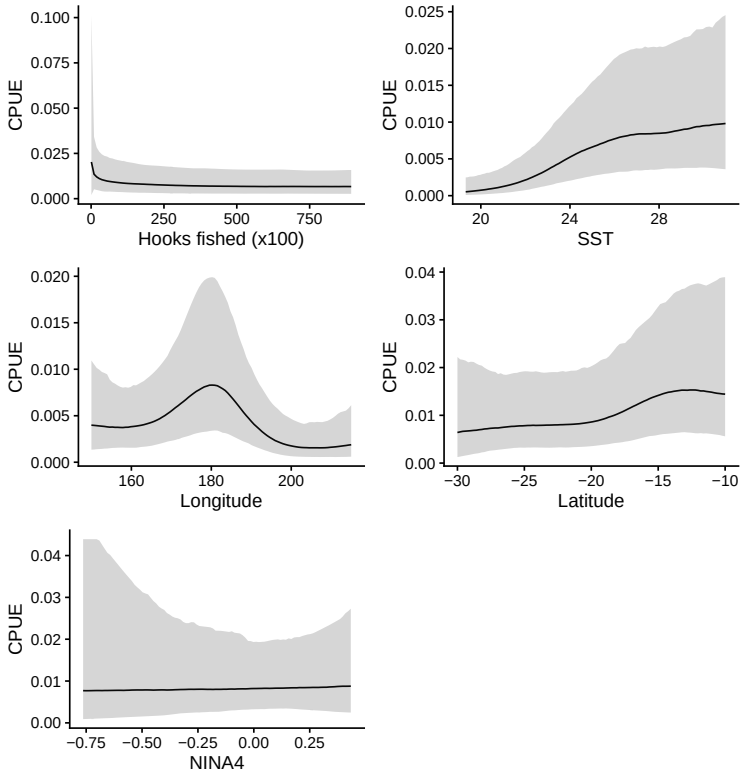

Figure C-21: Conditional effects estimated in the model used to derive CPUE from observed for South Pacific longline (Clarke et al. 2018 subset) sets.

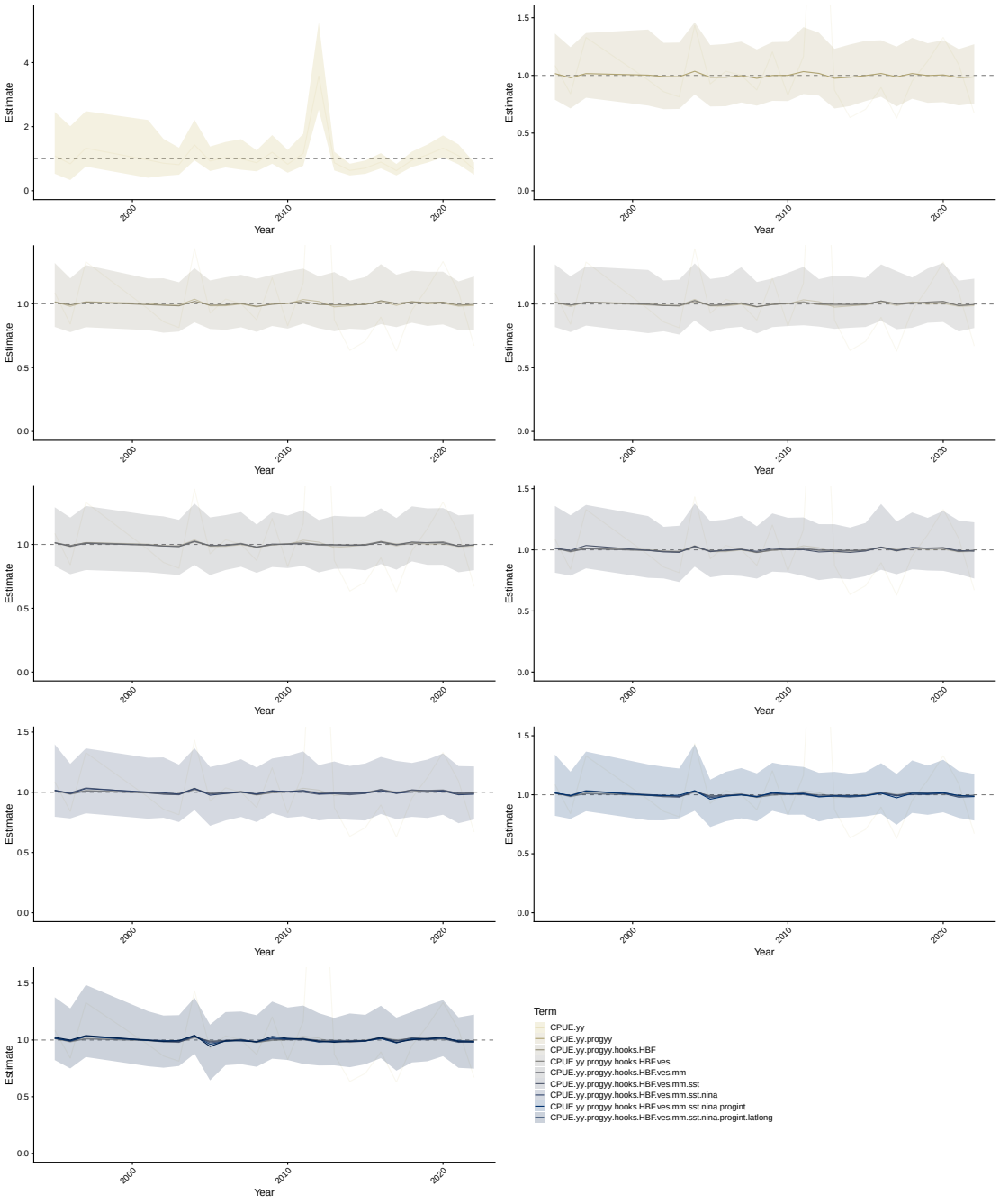

Figure C-22: CPUE standardisation effects for South Pacific longline (Clarke et al. 2018 subset) sets. Each row of plots corresponds to the addition of a variable, starting with a model that includes observer-program-year interactions. In each row, the posterior median and credible interval is shown for the updated model, posterior medians for the year effect from sub-models are shown for comparison.

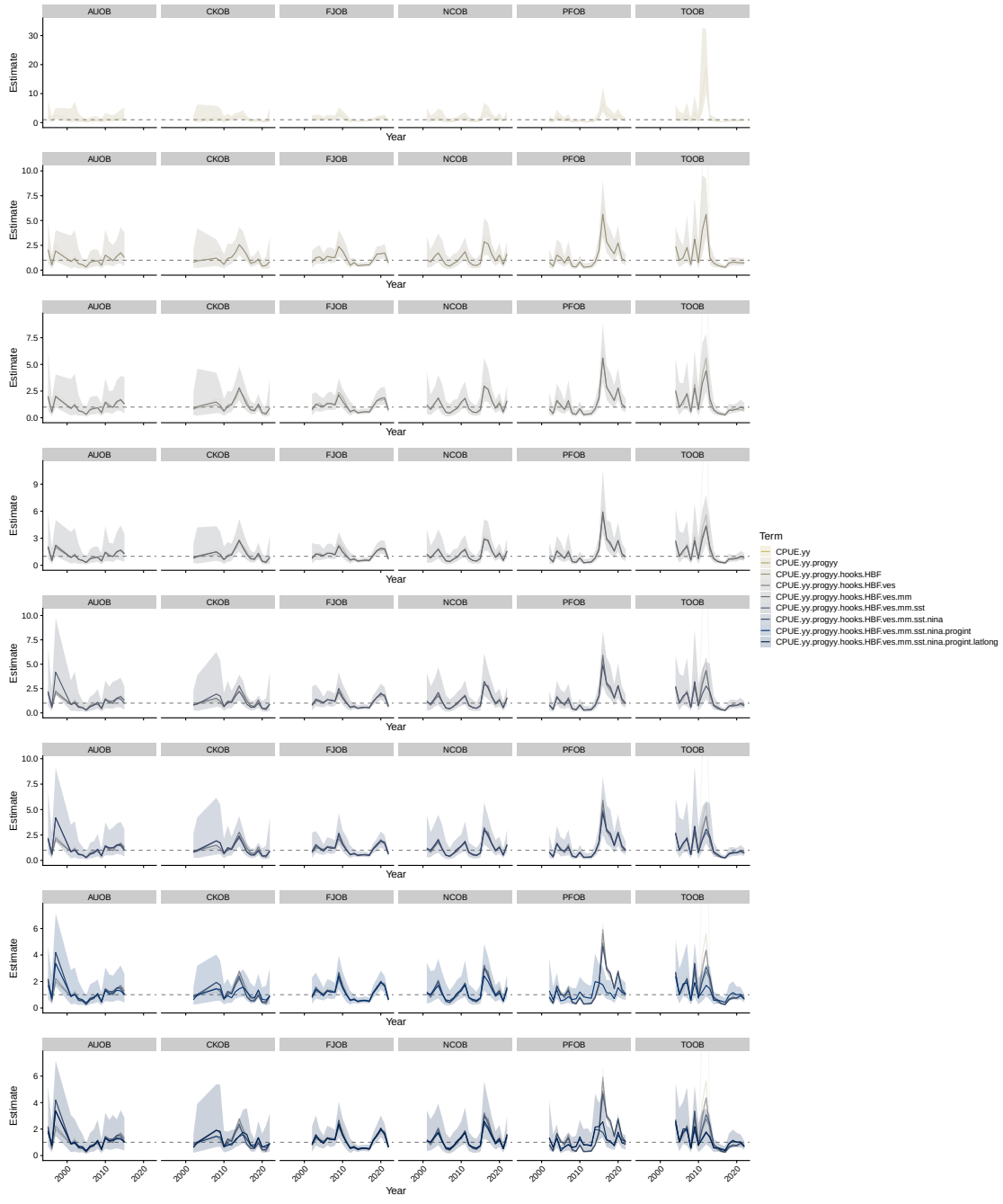

Figure C-23: CPUE standardisation effects for South Pacific longline (Clarke et al. 2018 subset) by observer-program. Each row of plots corresponds to the addition of a variable, starting with a model that includes observer-program-year interactions. In each row, the posterior median and credible interval is shown for the updated model, posterior medians for the year effect from sub-models are shown for comparison.

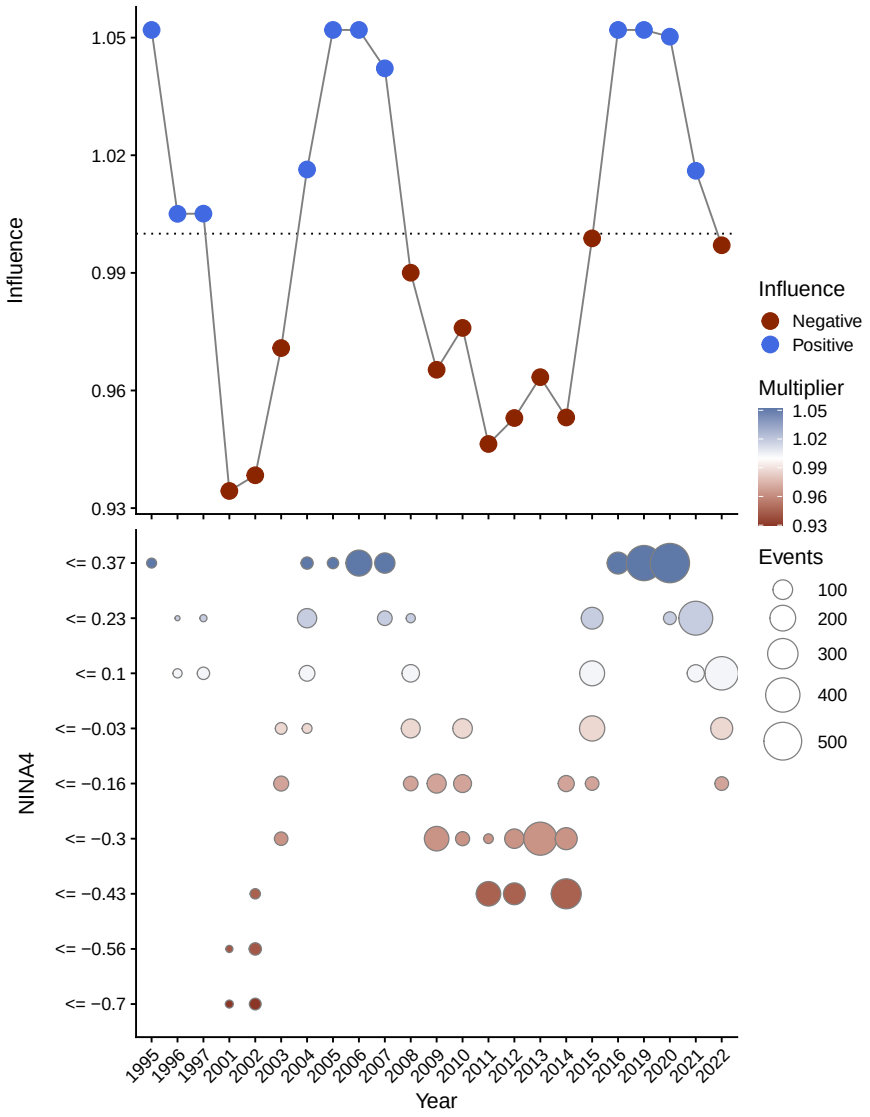

Figure C-24: Influence of the NINA4 index on catch-rates for South Pacific longline (Clarke et al. 2018 subset) sets, with positive influence showing years where the over-all catch-rate in the model was standardised downward by the corresponding amount to account for influences the NINA4 index. Influence is shown in colour as a multiplier on average catch rates, with circle size corresponding to the amount of effort entering the model. Note that data for the 2022 year is preliminary.

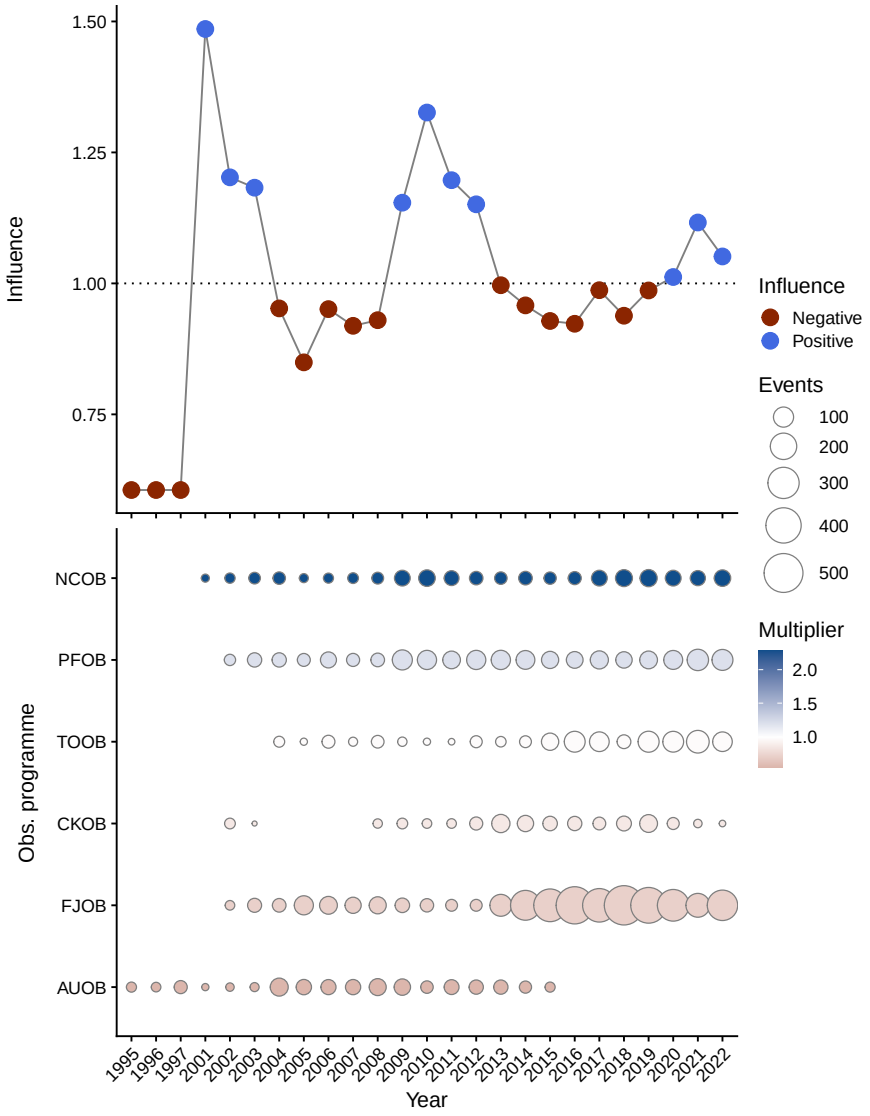

Figure C-25: Influence of observer program on catch-rates for South Pacific longline (Clarke et al. 2018 subset) sets, with positive influence showing years where the over-all catch-rate in the model was standardised downward by the corresponding amount to account for influences of observer program. Influence is shown in colour as a multiplier on average catch rates, with circle size corresponding to the amount of effort entering the model. Note that data for the 2022 year is preliminary.

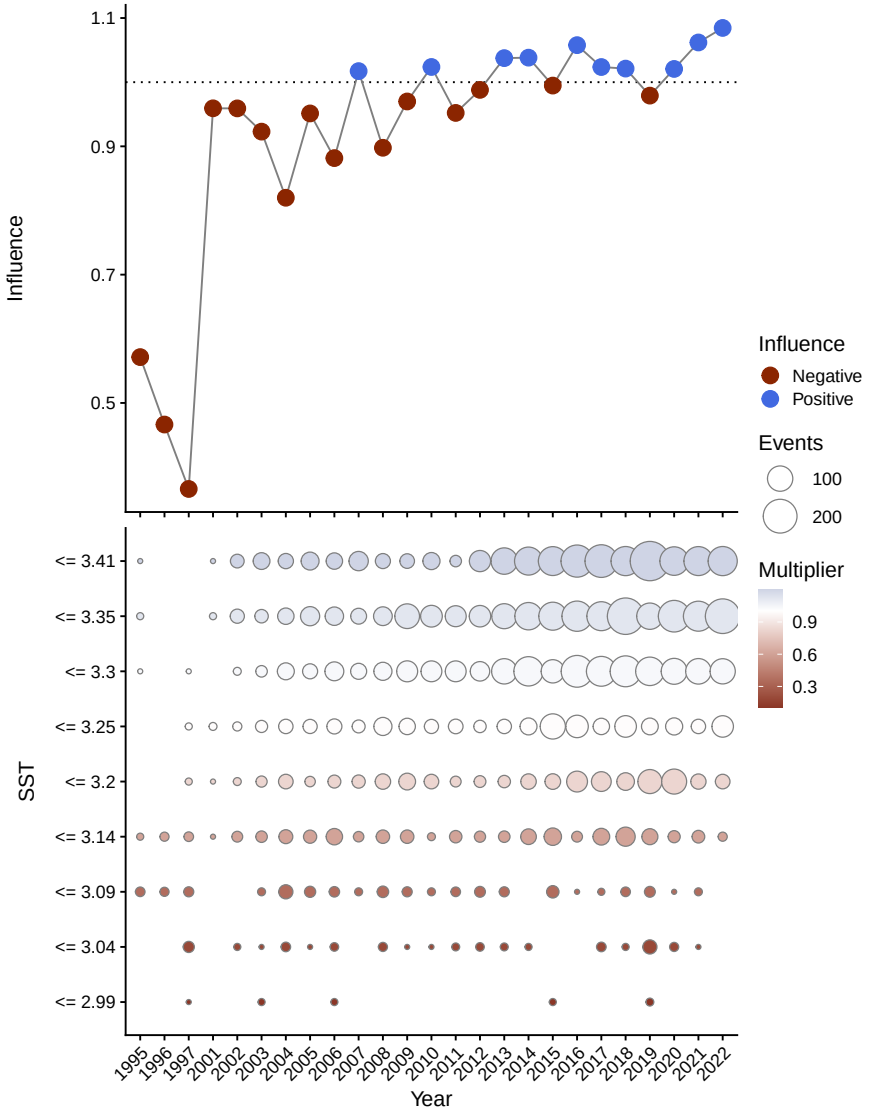

Figure C-26: Influence of sea-surface-temperature (SST) on catch-rates for South Pacific longline (Clarke et al. 2018 subset) sets, with positive influence showing years where the over-all catch-rate in the model was standardised downward by the corresponding amount to account for influences of SST. Influence is shown in colour as a multiplier on average catch rates, with circle size corresponding to the amount of effort entering the model. Note that data for the 2022 year is preliminary.

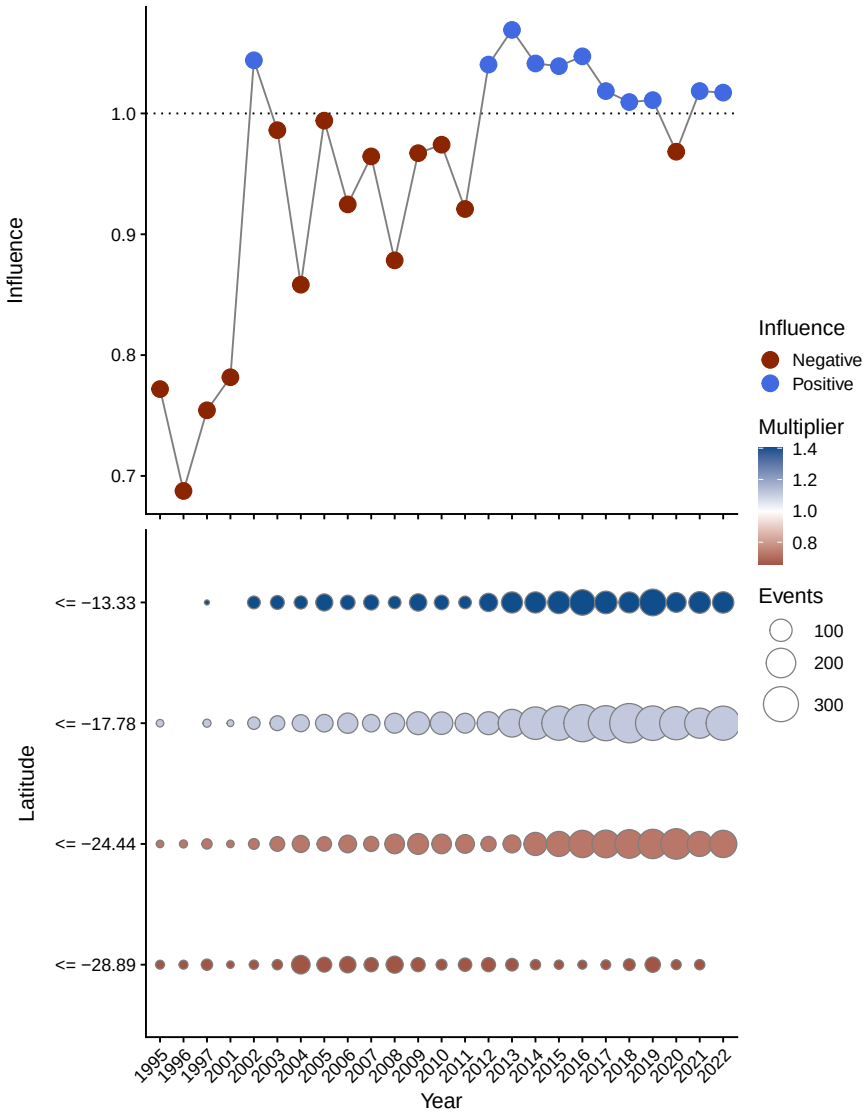

Figure C-27: Influence of latitude on catch-rates for South Pacific longline (Clarke et al. 2018 subset) sets, with positive influence showing years where the over-all catch-rate in the model was standardised downward by the corresponding amount to account for influences of latitude. Influence is shown in colour as a multiplier on average catch rates, with circle size corresponding to the amount of effort entering the model. Note that data for the 2022 year is preliminary.

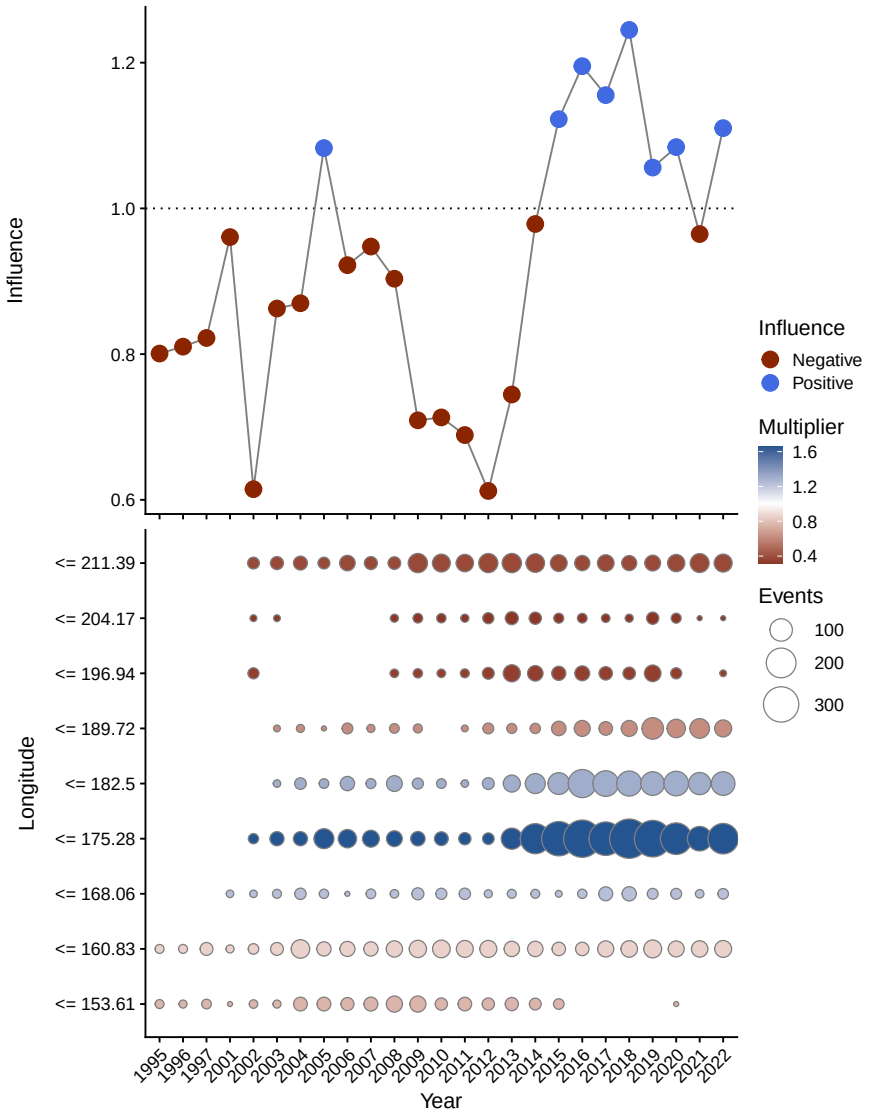

Figure C-28: Influence of longitude on catch-rates for South Pacific longline (Clarke et al. 2018 subset) sets, with positive influence showing years where the over-all catch-rate in the model was standardised downward by the corresponding amount to account for influences of longitude. Influence is shown in colour as a multiplier on average catch rates, with circle size corresponding to the amount of effort entering the model. Note that data for the 2022 year is preliminary.

C.3 CPUE diagnostics for long-running observer program longline (Tremblay-Boyer & Neubauer 2019)

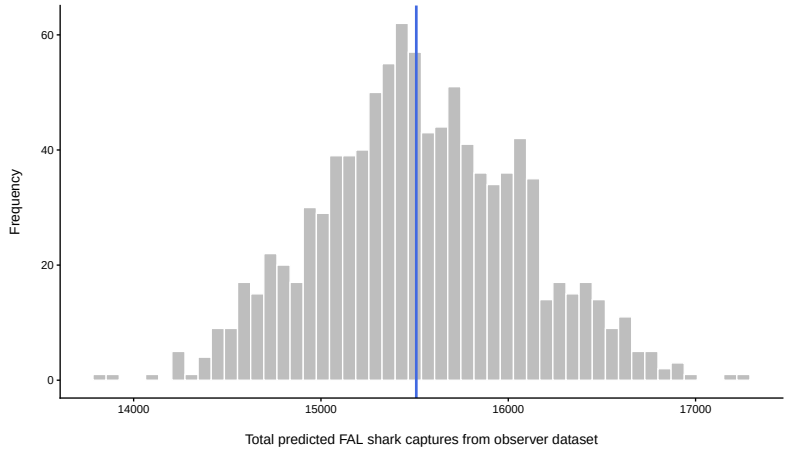

Figure C-29: Observed interactions (vertical line) and model predictions from the model used to derive CPUE from observed for long-running observer program longline (Tremblay-Boyer & Neubauer 2019) sets.

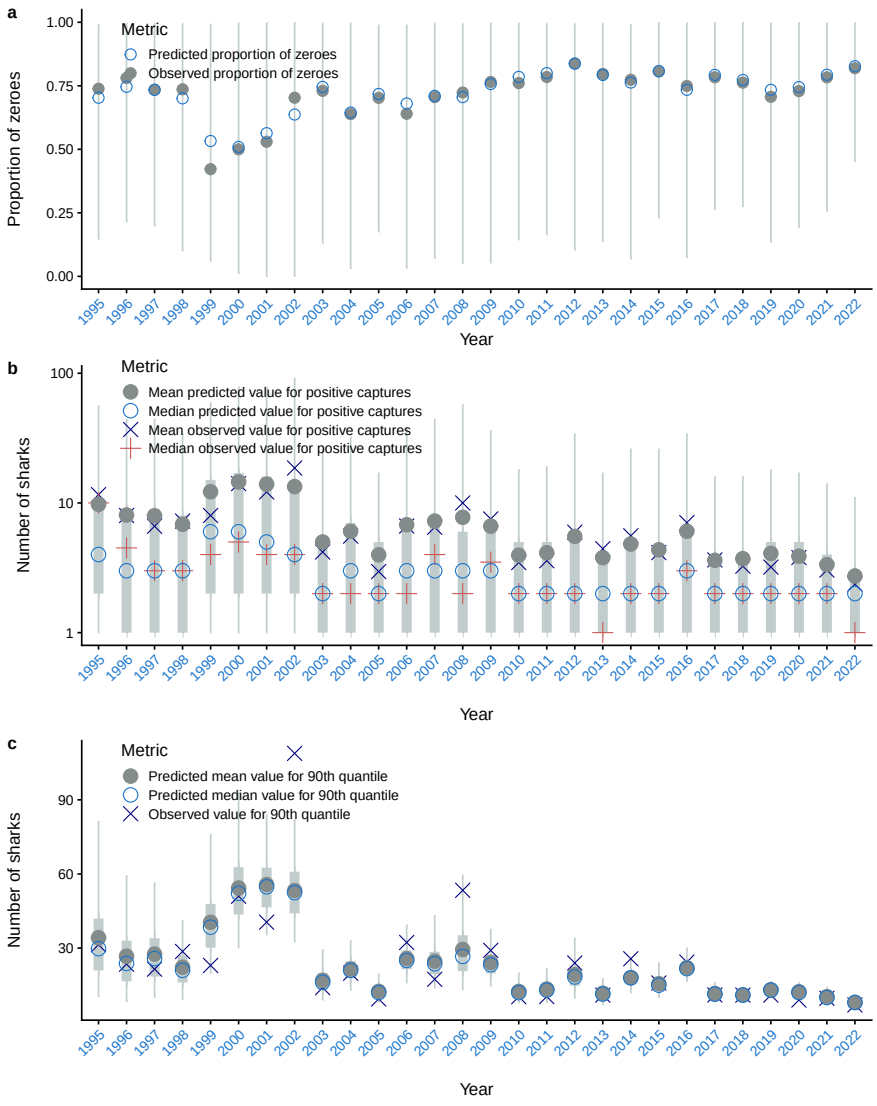

Figure C-30: Posterior predictive model diagnostics by model year for long-running observer program longline (Tremblay-Boyer & Neubauer 2019) sets, with (a) observed and predicted proportion of zero captures, (b) observed and predicted positive captures and (c) dispersion statistics (90% percentile) of observed data and predictions.

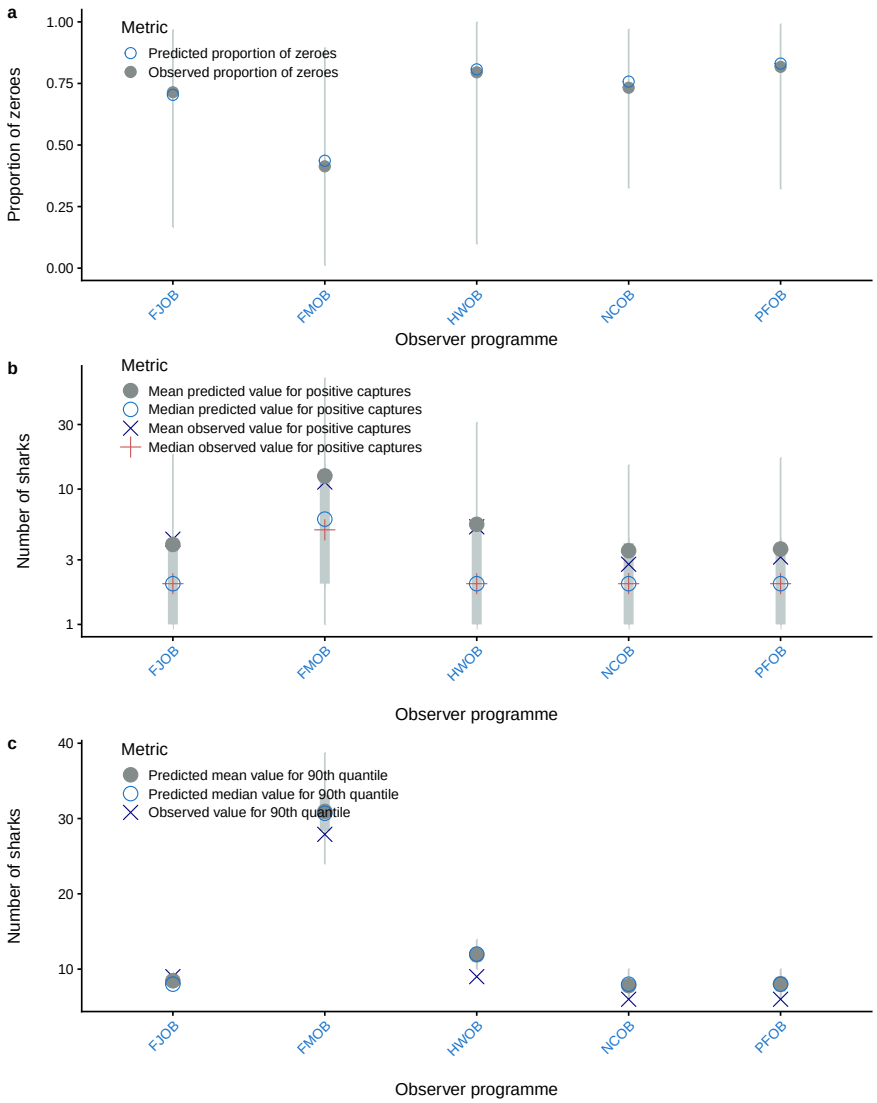

Figure C-31: Posterior predictive model diagnostics by observer program for long-running observer program longline (Tremblay-Boyer & Neubauer 2019) sets, with (a) observed and predicted proportion of zero captures, (b) observed and predicted positive captures and (c) dispersion statistics (90% percentile) of observed data and predictions.

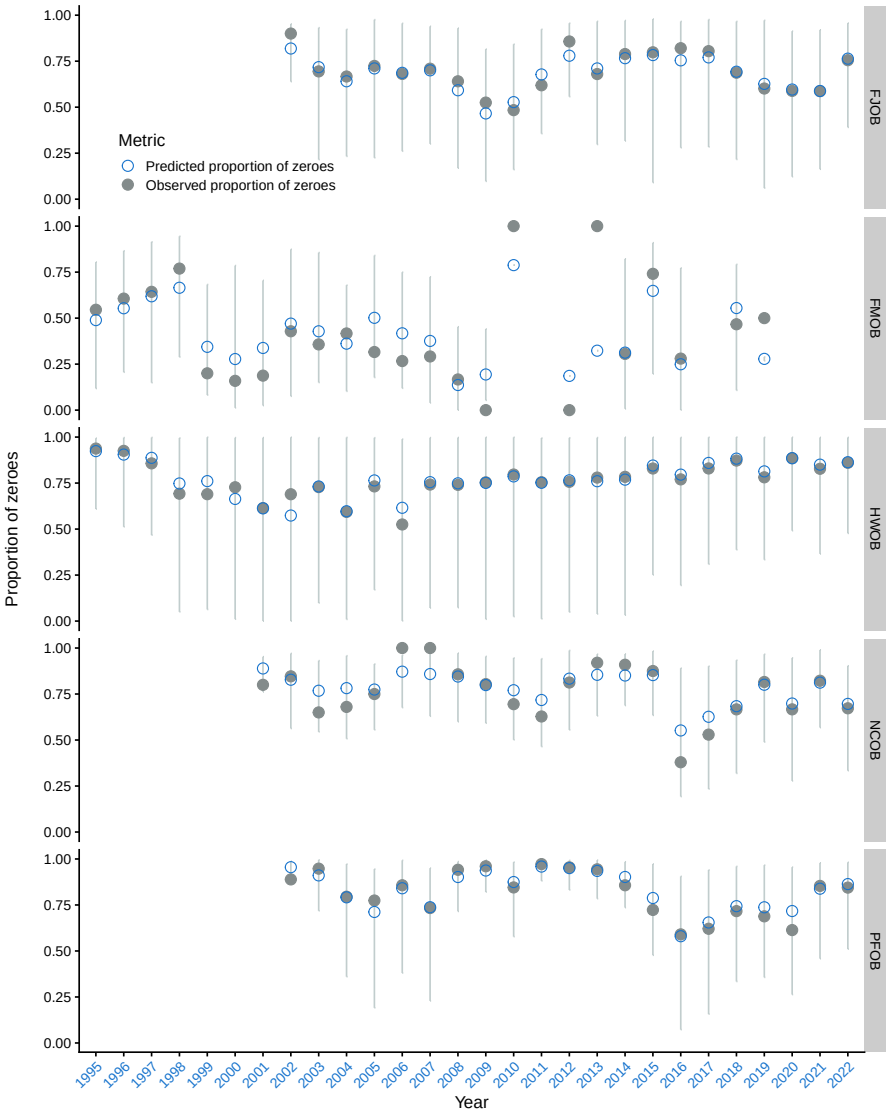

Figure C-32: Posterior predictive model diagnostics for observed and predicted proportion of zero captures by observer program and year for long-running observer program longline (Tremblay-Boyer & Neubauer 2019) sets.

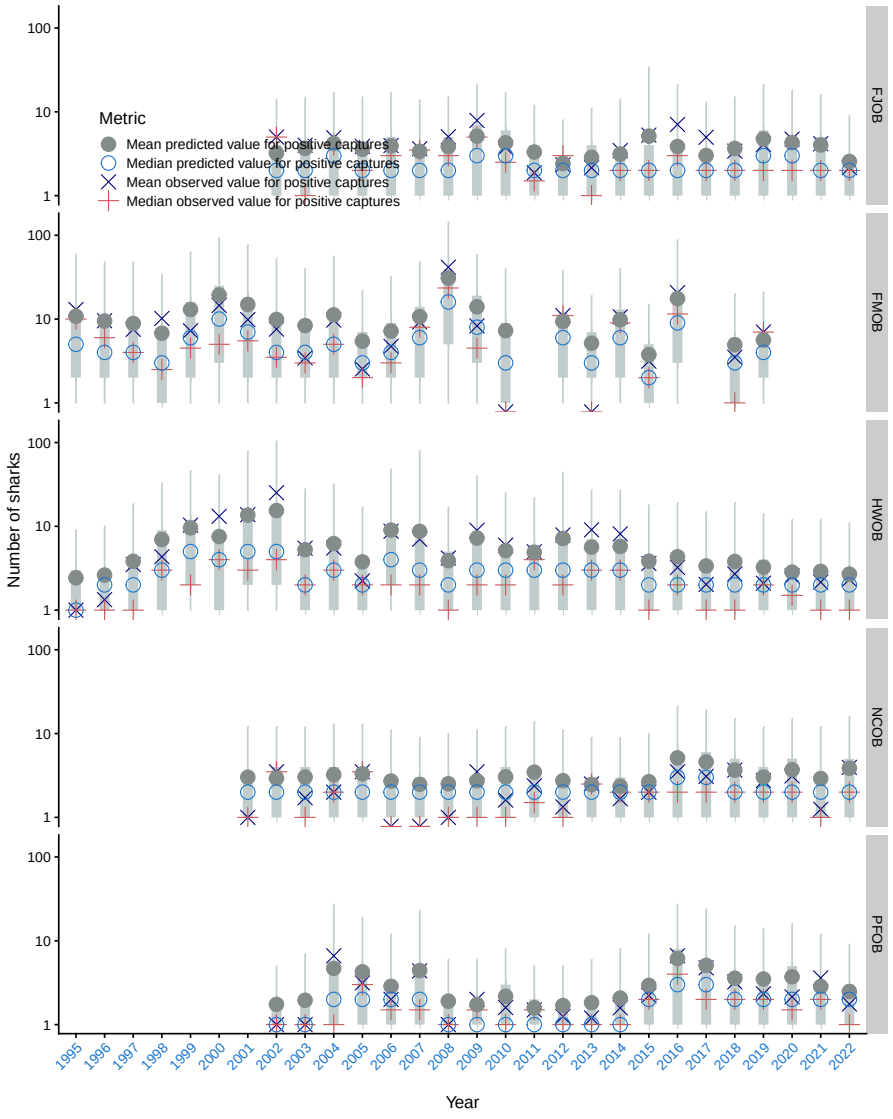

Figure C-33: Posterior predictive model diagnostics for bserved and predicted positive captures by observer program and year for long-running observer program longline (Tremblay-Boyer & Neubauer 2019) sets.

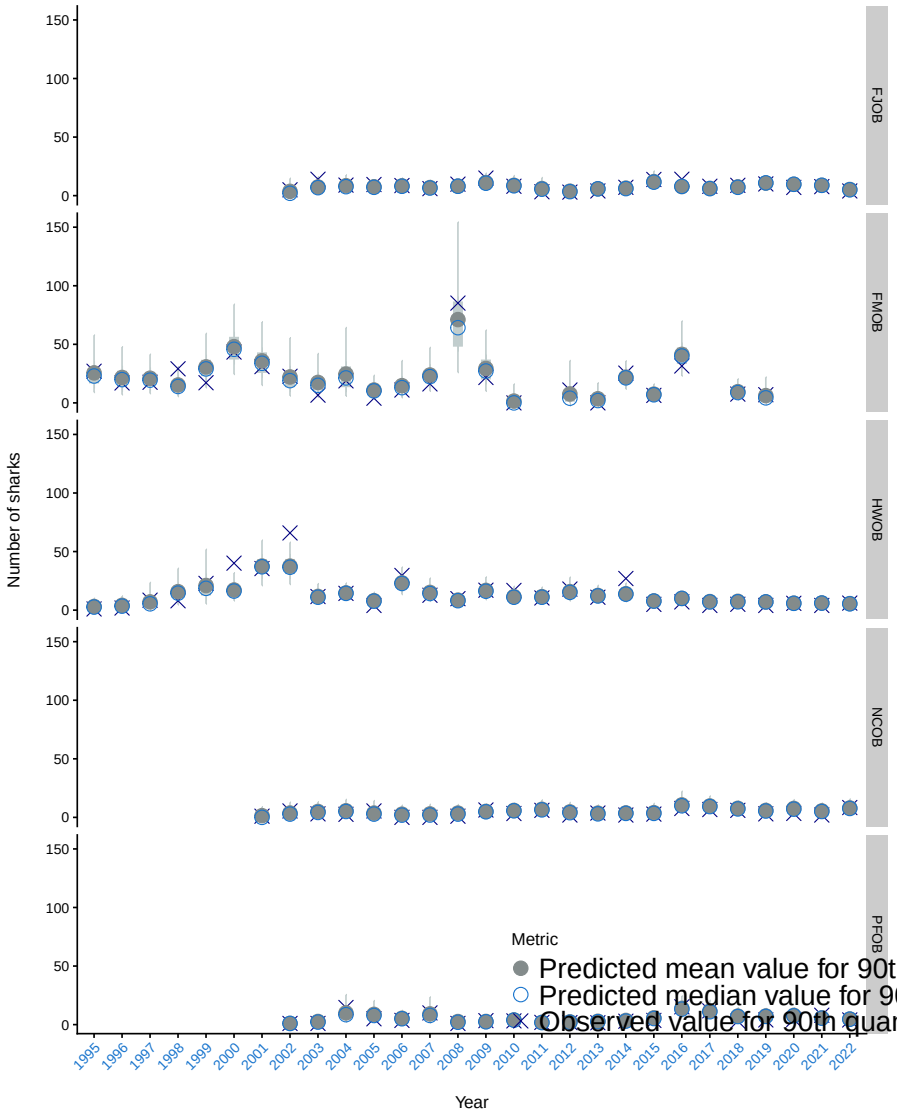

Figure C-34: Posterior predictive model diagnostics for dispersion statistics (90% percentile) of observed data and predictions by observer program and year for long-running observer program longline (Tremblay-Boyer & Neubauer 2019) sets.

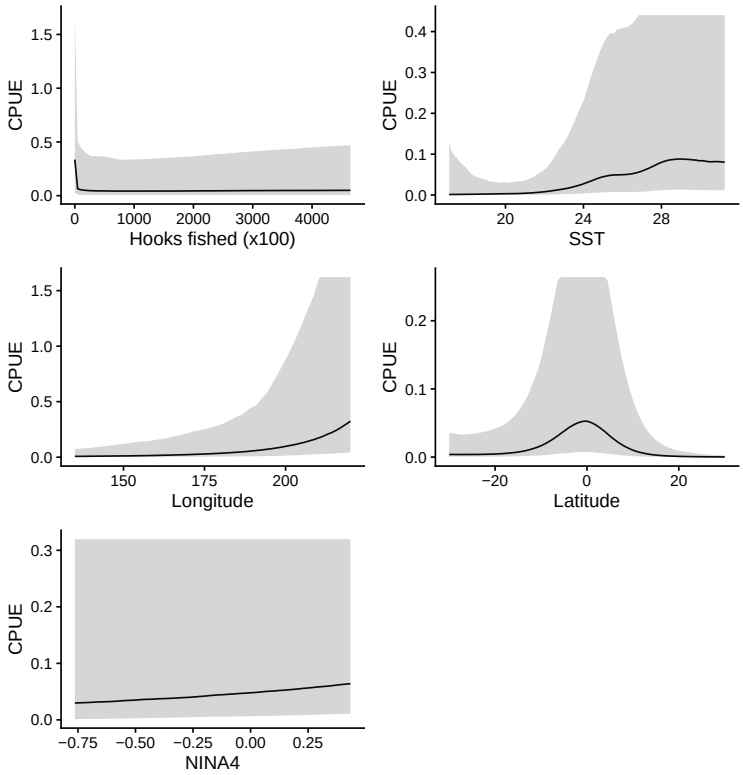

Figure C-35: Conditional effects estimated in the model used to derive CPUE from observed for long-running observer program longline (Tremblay-Boyer & Neubauer 2019) sets.

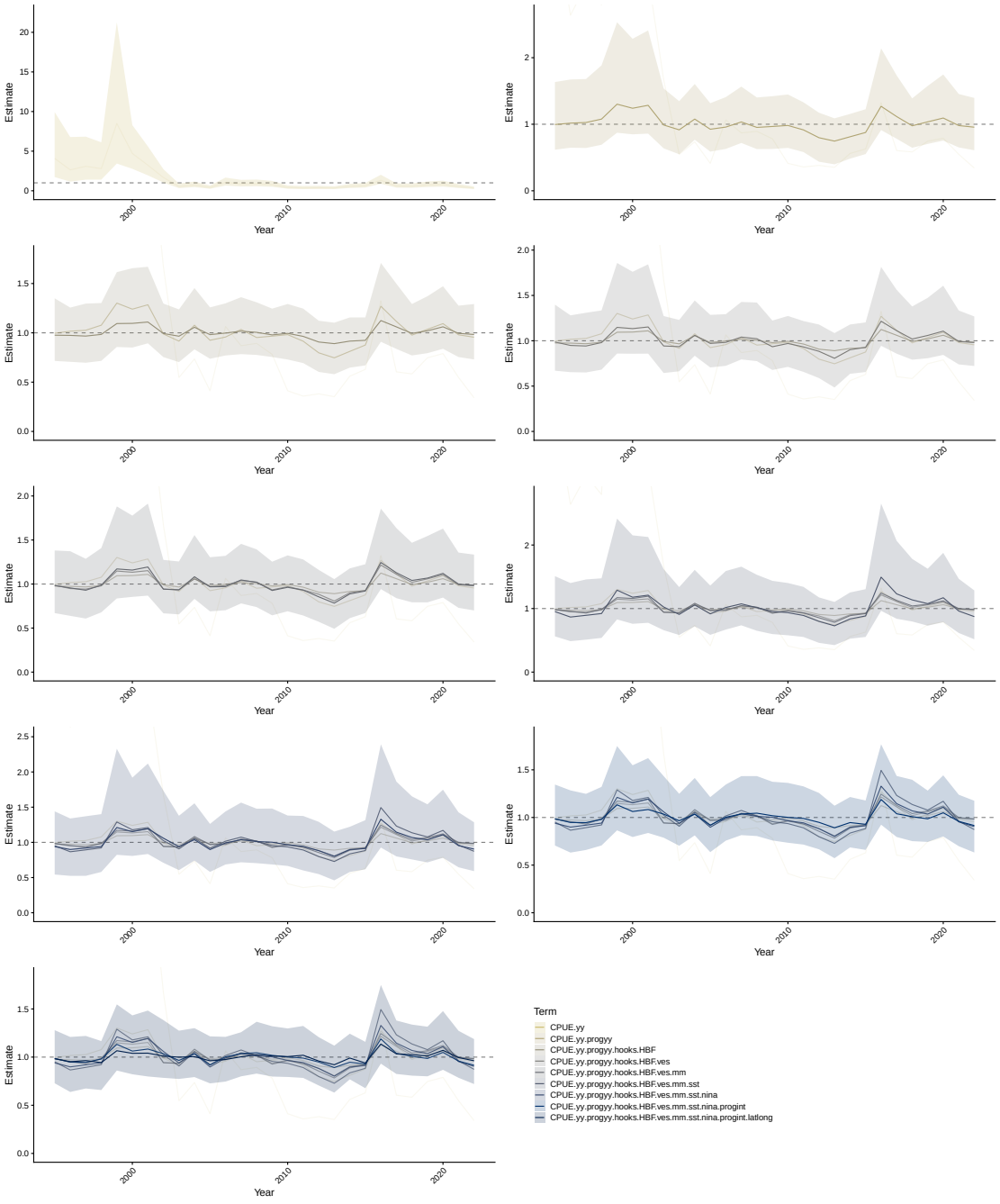

Figure C-36: CPUE standardisation effects for long-running observer program longline (Tremblay-Boyer & Neubauer 2019) sets. Each row of plots corresponds to the addition of a variable, starting with a model that includes observer-program-year interactions. In each row, the posterior median and credible interval is shown for the updated model, posterior medians for the year effect from sub-models are shown for comparison.

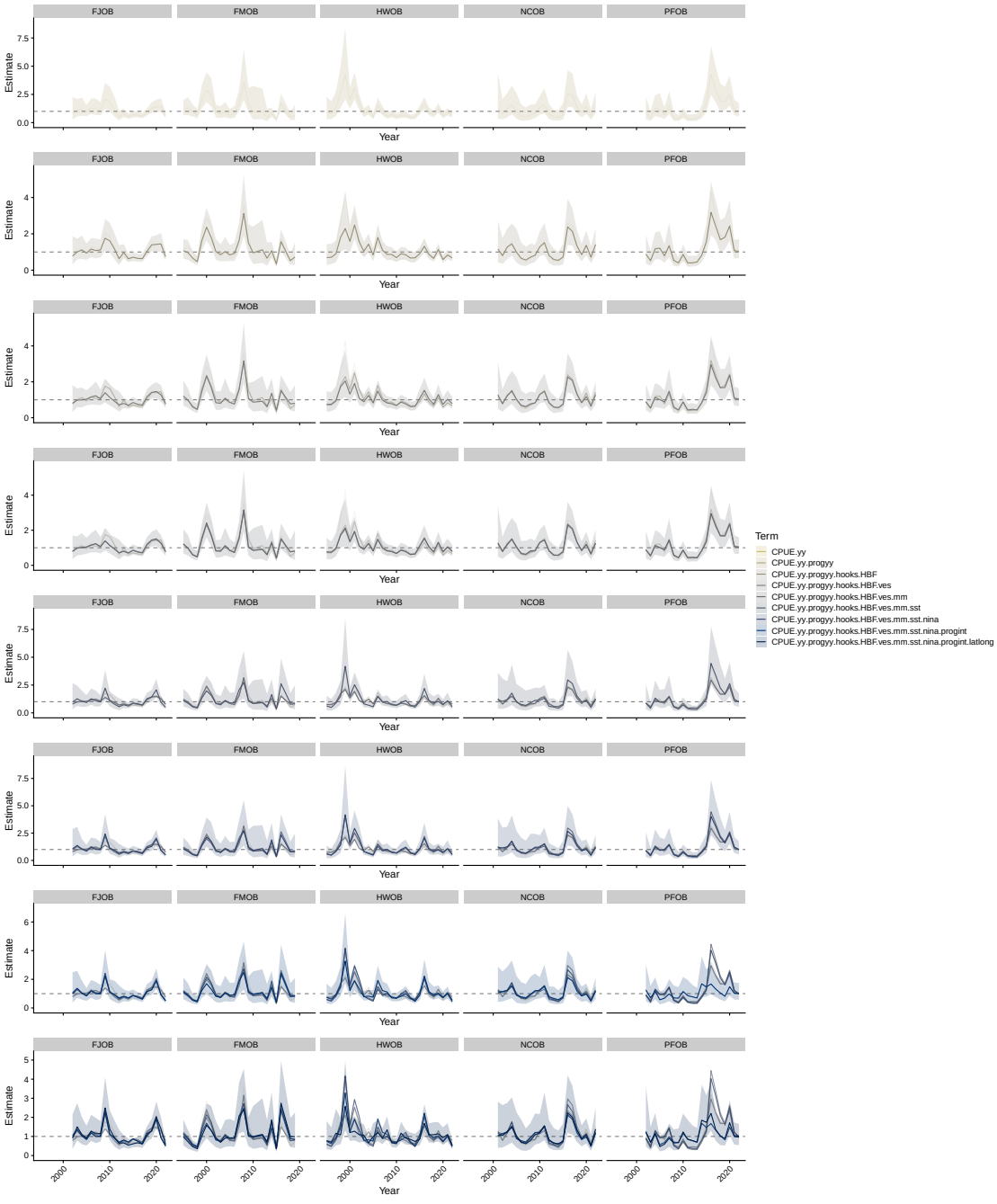

Figure C-37: CPUE standardisation effects for long-running observer program longline (Tremblay-Boyer & Neubauer 2019) by observer-program. Each row of plots corresponds to the addition of a variable, starting with a model that includes observer-program-year interactions. In each row, the posterior median and credible interval is shown for the updated model, posterior medians for the year effect from sub-models are shown for comparison.

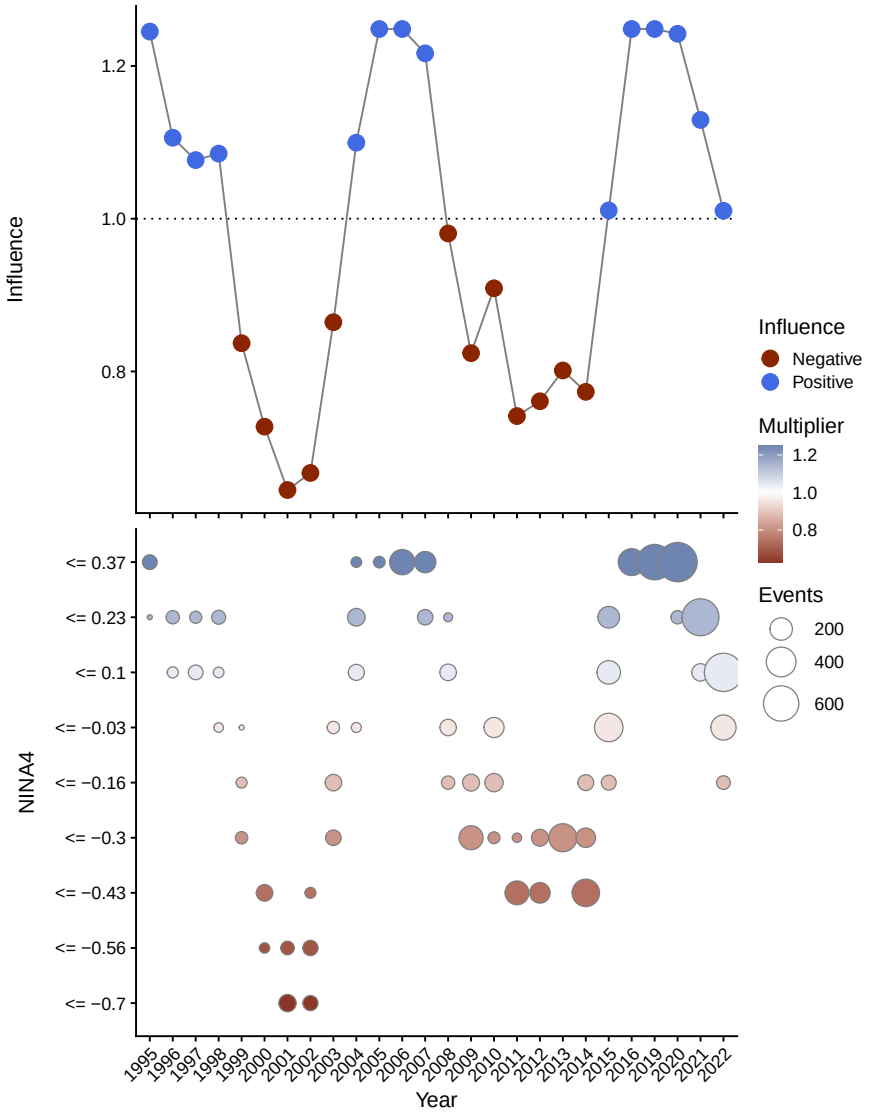

Figure C-38: Influence of the NINA4 index on catch-rates for long-running observer program longline (Tremblay-Boyer & Neubauer 2019) sets, with positive influence showing years where the over-all catch-rate in the model was standardised downward by the corresponding amount to account for influences the NINA4 index. Influence is shown in colour as a multiplier on average catch rates, with circle size corresponding to the amount of effort entering the model. Note that data for the 2022 year is preliminary.

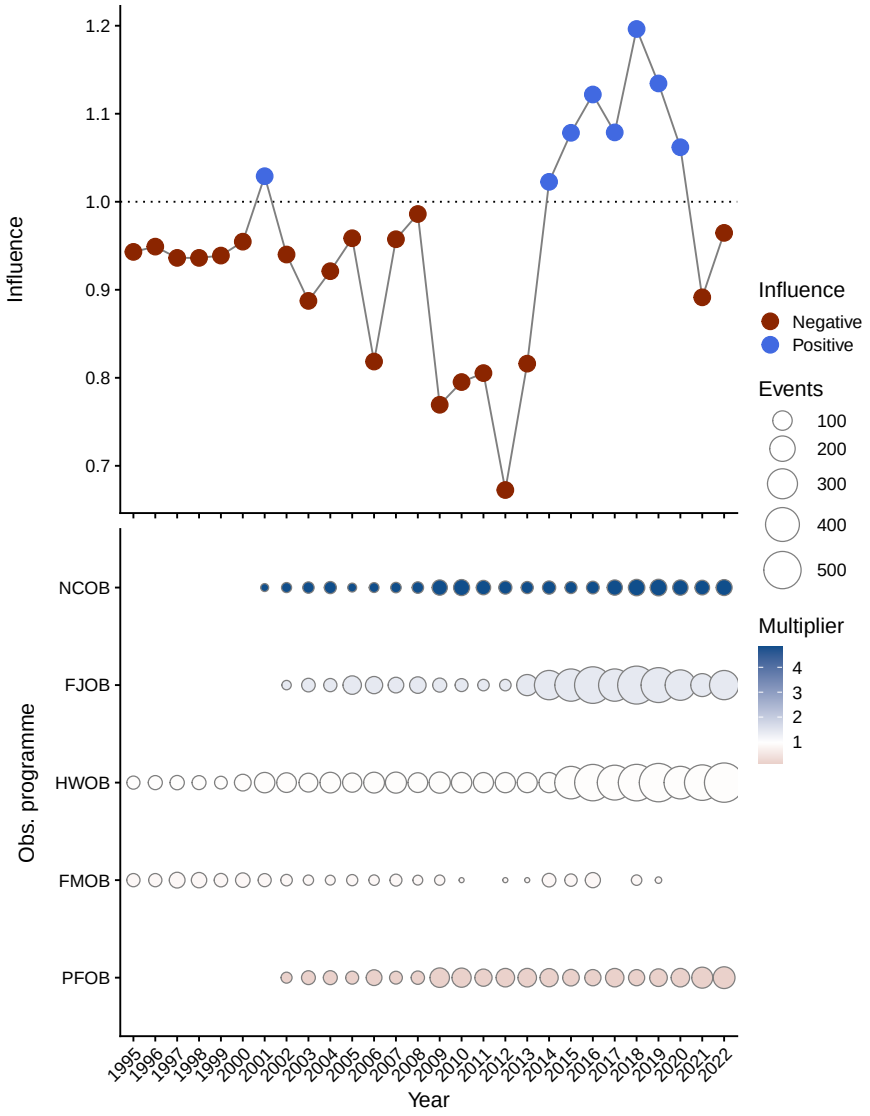

Figure C-39: Influence of observer program on catch-rates for long-running observer program longline (Tremblay-Boyer & Neubauer 2019) sets, with positive influence showing years where the over-all catch-rate in the model was standardised downward by the corresponding amount to account for influences of observer program. Influence is shown in colour as a multiplier on average catch rates, with circle size corresponding to the amount of effort entering the model. Note that data for the 2022 year is preliminary.

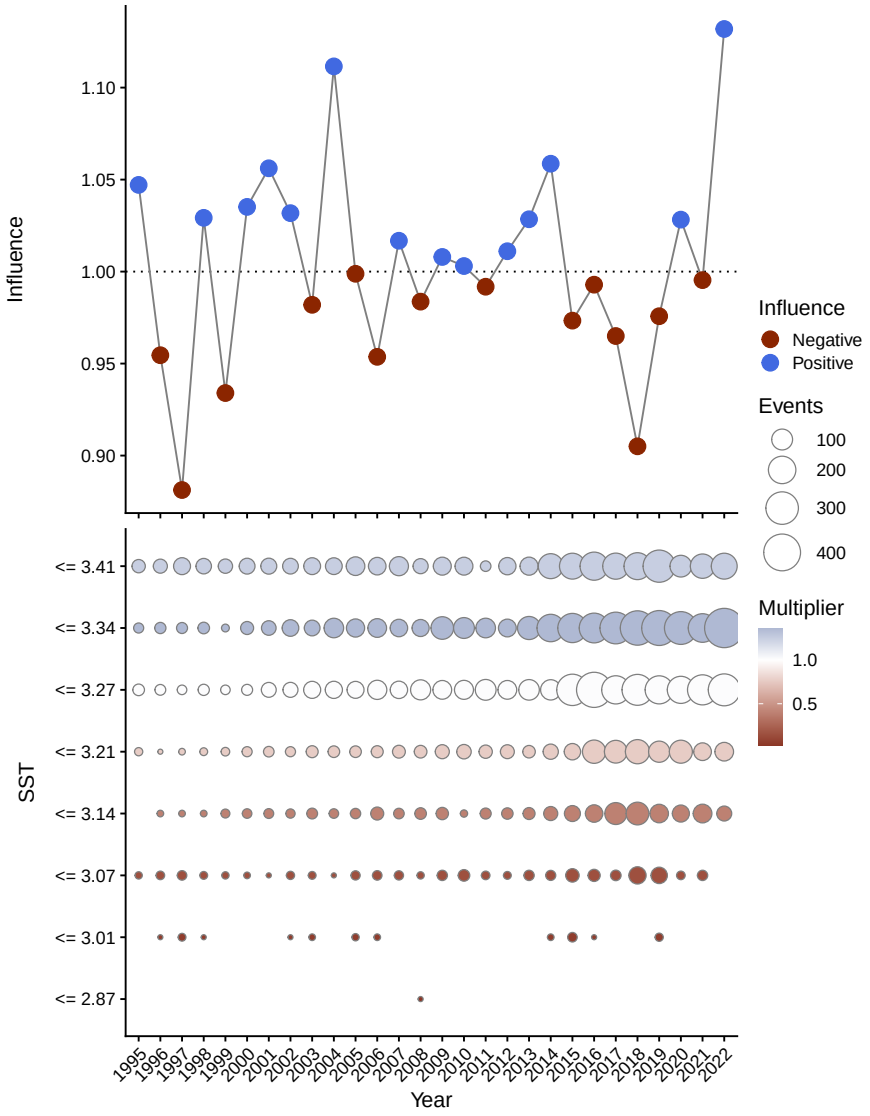

Figure C-40: Influence of sea-surface-temperature (SST) on catch-rates for long-running observer program longline (Tremblay-Boyer & Neubauer 2019) sets, with positive influence showing years where the over-all catch-rate in the model was standardised downward by the corresponding amount to account for influences of SST. Influence is shown in colour as a multiplier on average catch rates, with circle size corresponding to the amount of effort entering the model. Note that data for the 2022 year is preliminary.

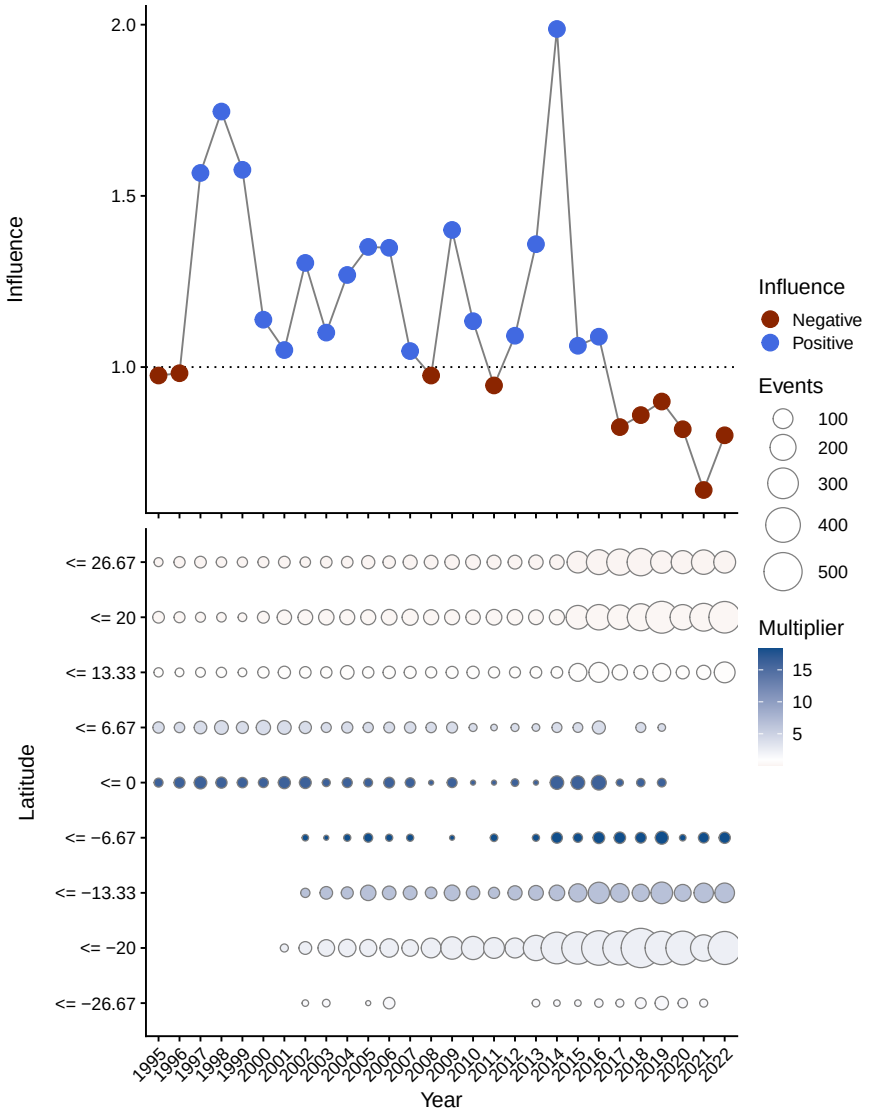

Figure C-41: Influence of latitude on catch-rates for long-running observer program longline (Tremblay-Boyer & Neubauer 2019) sets, with positive influence showing years where the over-all catch-rate in the model was standardised downward by the corresponding amount to account for influences of latitude. Influence is shown in colour as a multiplier on average catch rates, with circle size corresponding to the amount of effort entering the model. Note that data for the 2022 year is preliminary.

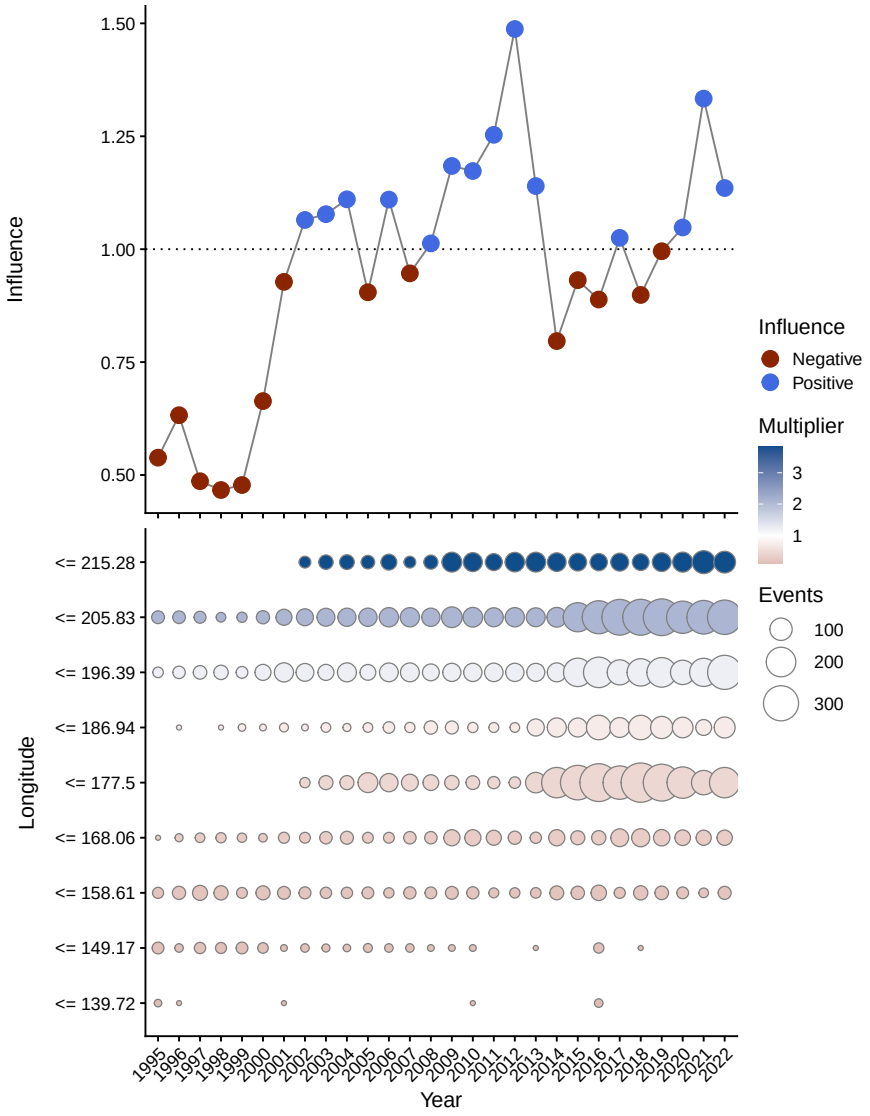

Figure C-42: Influence of longitude on catch-rates for long-running observer program longline (Tremblay-Boyer & Neubauer 2019) sets, with positive influence showing years where the over-all catch-rate in the model was standardised downward by the corresponding amount to account for influences of longitude. Influence is shown in colour as a multiplier on average catch rates, with circle size corresponding to the amount of effort entering the model. Note that data for the 2022 year is preliminary.

C.4 CPUE diagnostics for distant water fleet longline

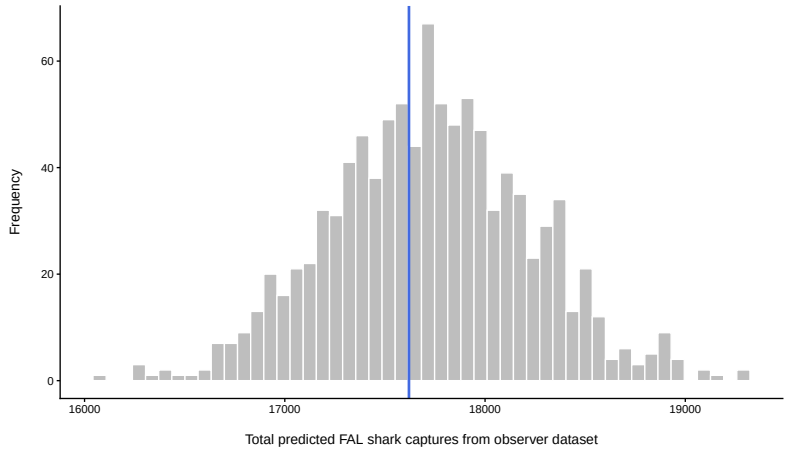

Figure C-43: Observed interactions (vertical line) and model predictions from the model used to derive CPUE from observed for distant water fleet longline sets.

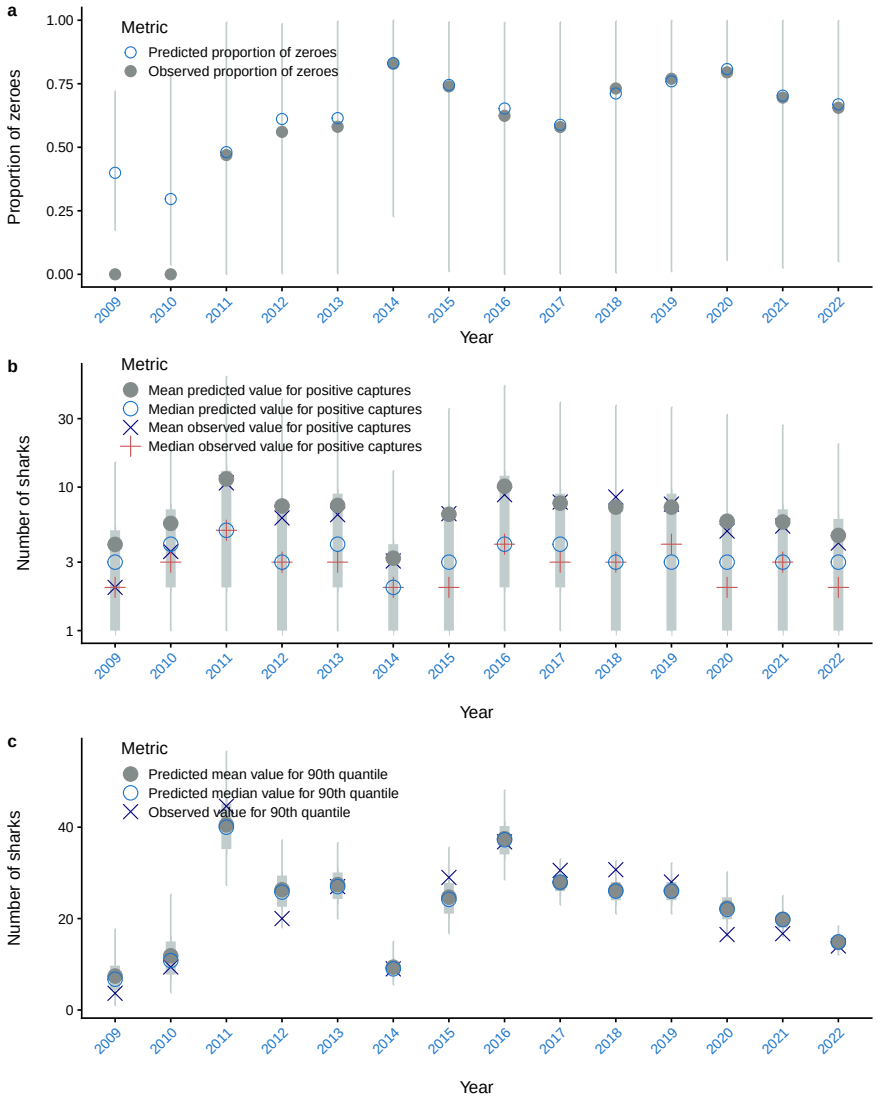

Figure C-44: Posterior predictive model diagnostics by model year for distant water fleet longline sets, with (a) observed and predicted proportion of zero captures, (b) observed and predicted positive captures and (c) dispersion statistics (90% percentile) of observed data and predictions.

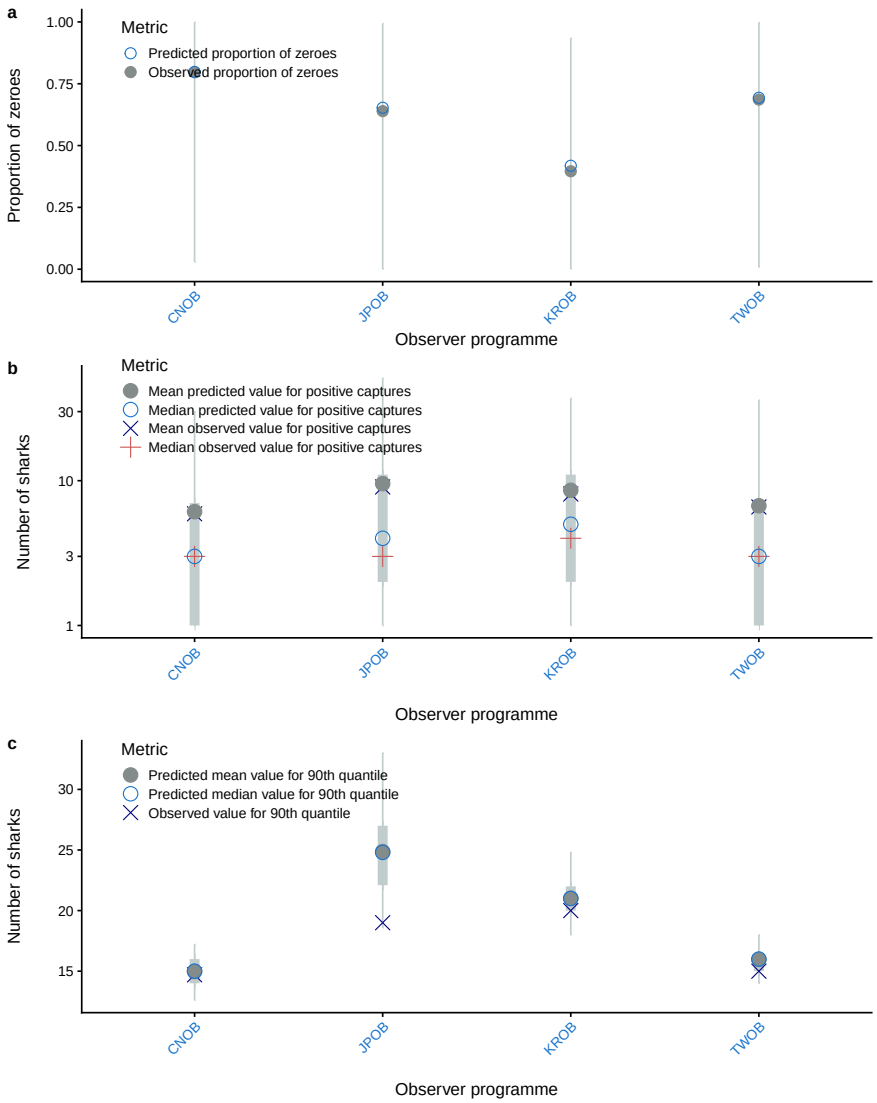

Figure C-45: Posterior predictive model diagnostics by observer program for distant water fleet longline sets, with (a) observed and predicted proportion of zero captures, (b) observed and predicted positive captures and (c) dispersion statistics (90% percentile) of observed data and predictions.

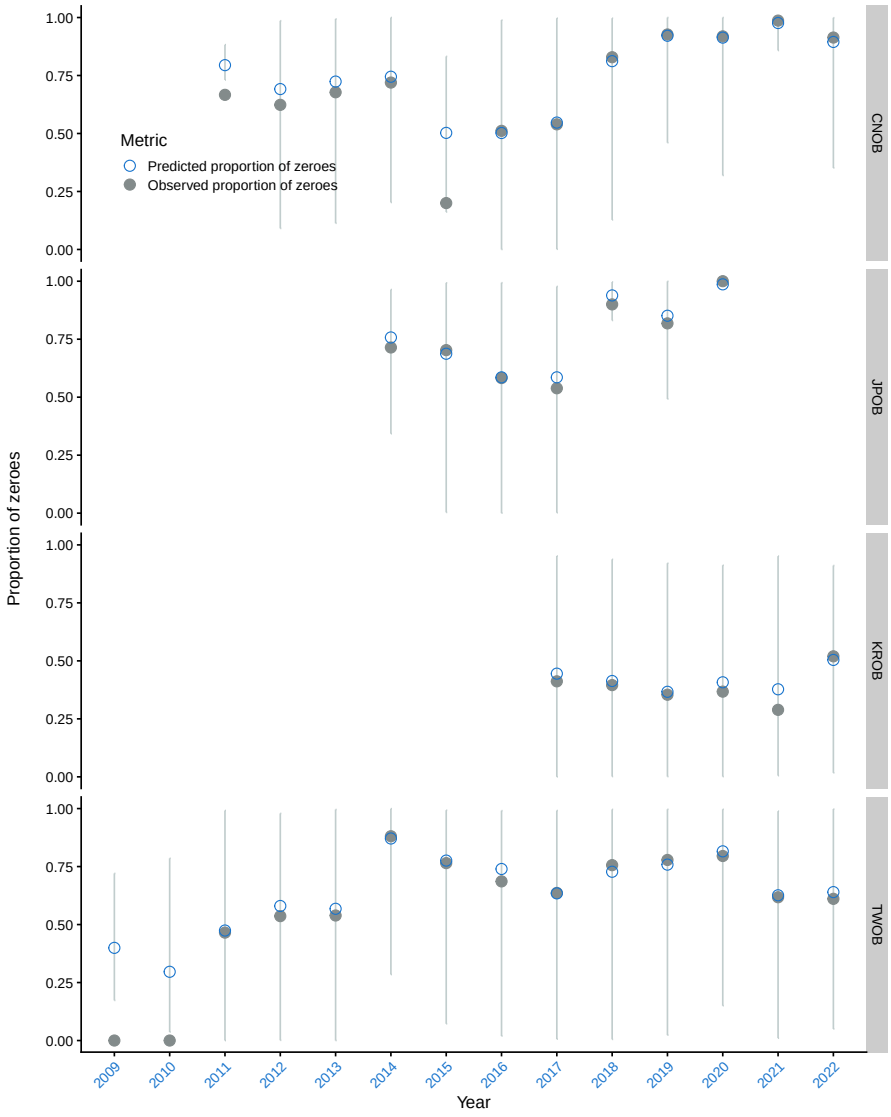

Figure C-46: Posterior predictive model diagnostics for observed and predicted proportion of zero captures by observer program and year for distant water fleet longline sets.

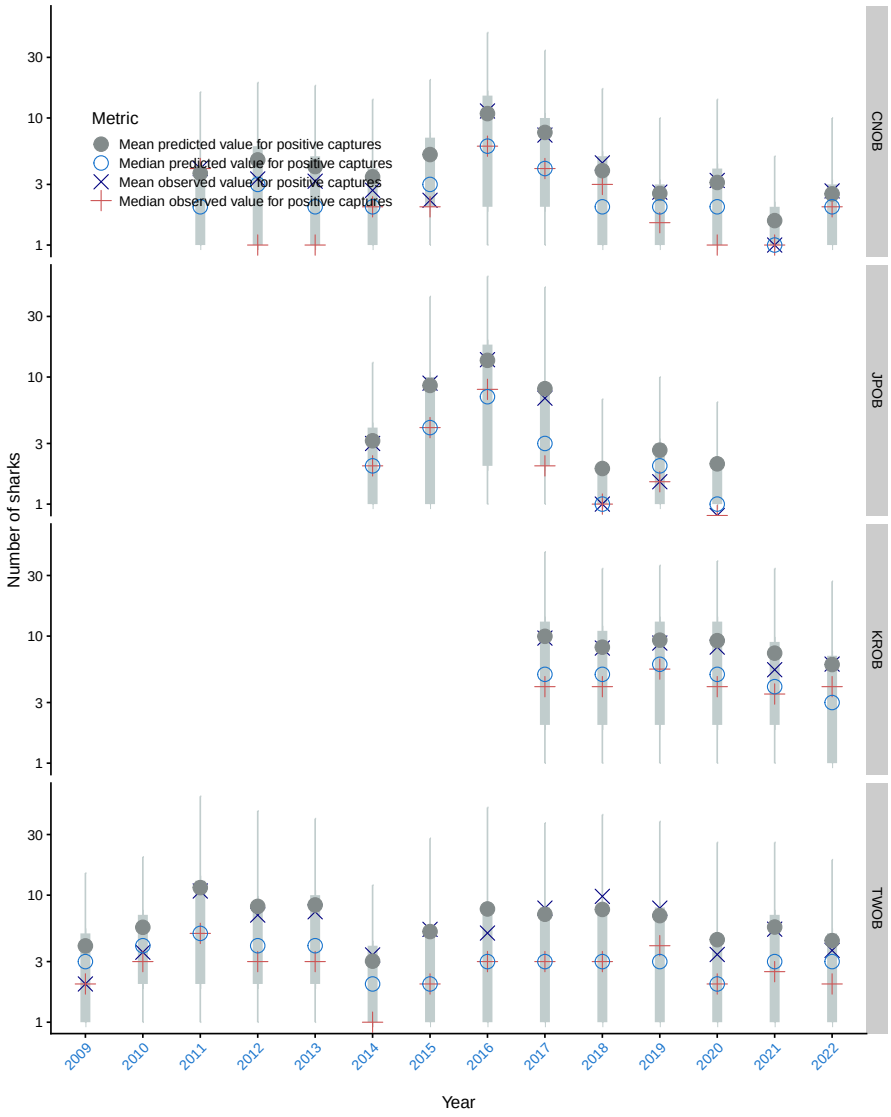

Figure C-47: Posterior predictive model diagnostics for bserved and predicted positive captures by observer program and year for distant water fleet longline sets.

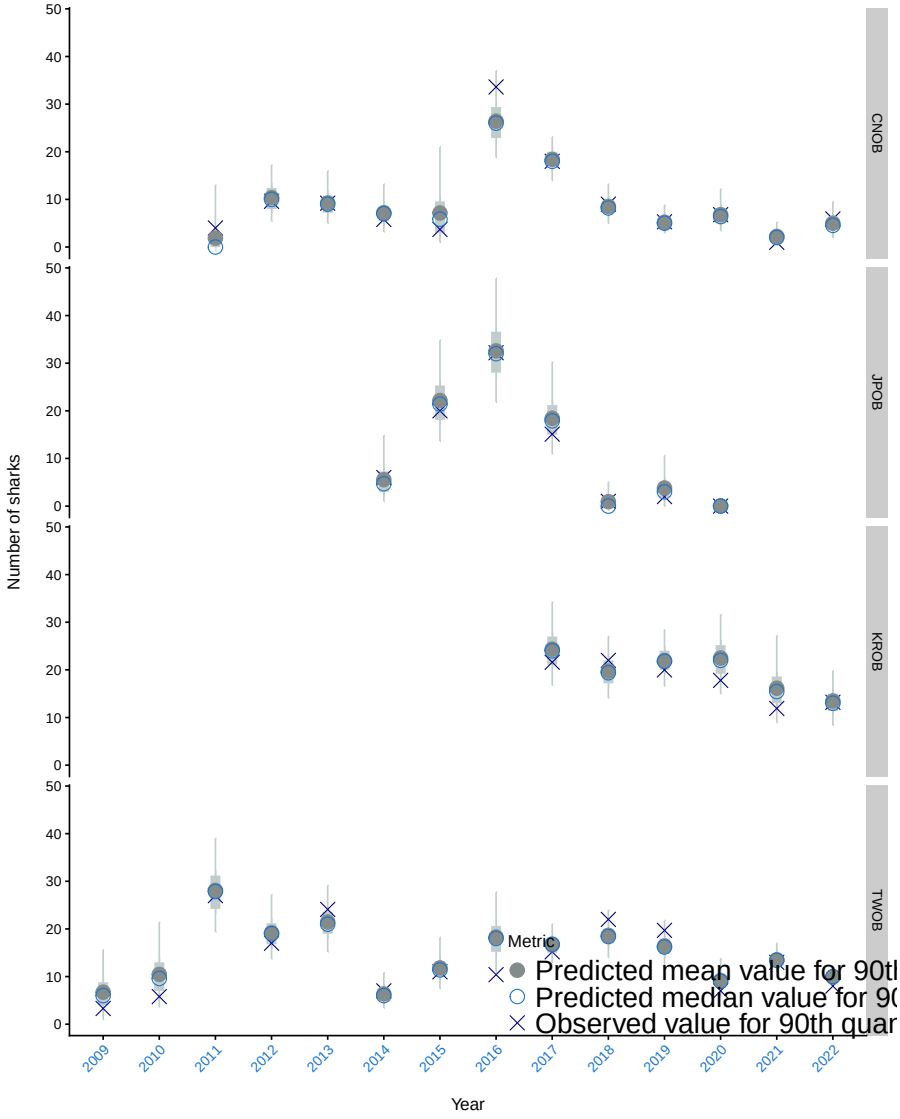

Figure C-48: Posterior predictive model diagnostics for dispersion statistics (90% percentile) of observed data and predictions by observer program and year for distant water fleet longline sets.

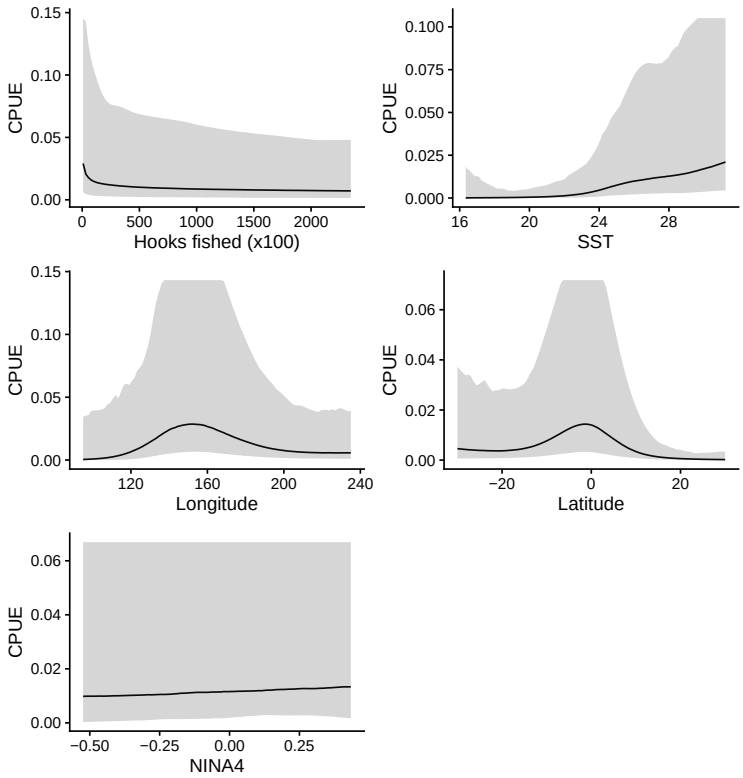

Figure C-49: Conditional effects estimated in the model used to derive CPUE from observed for distant water fleet longline sets.

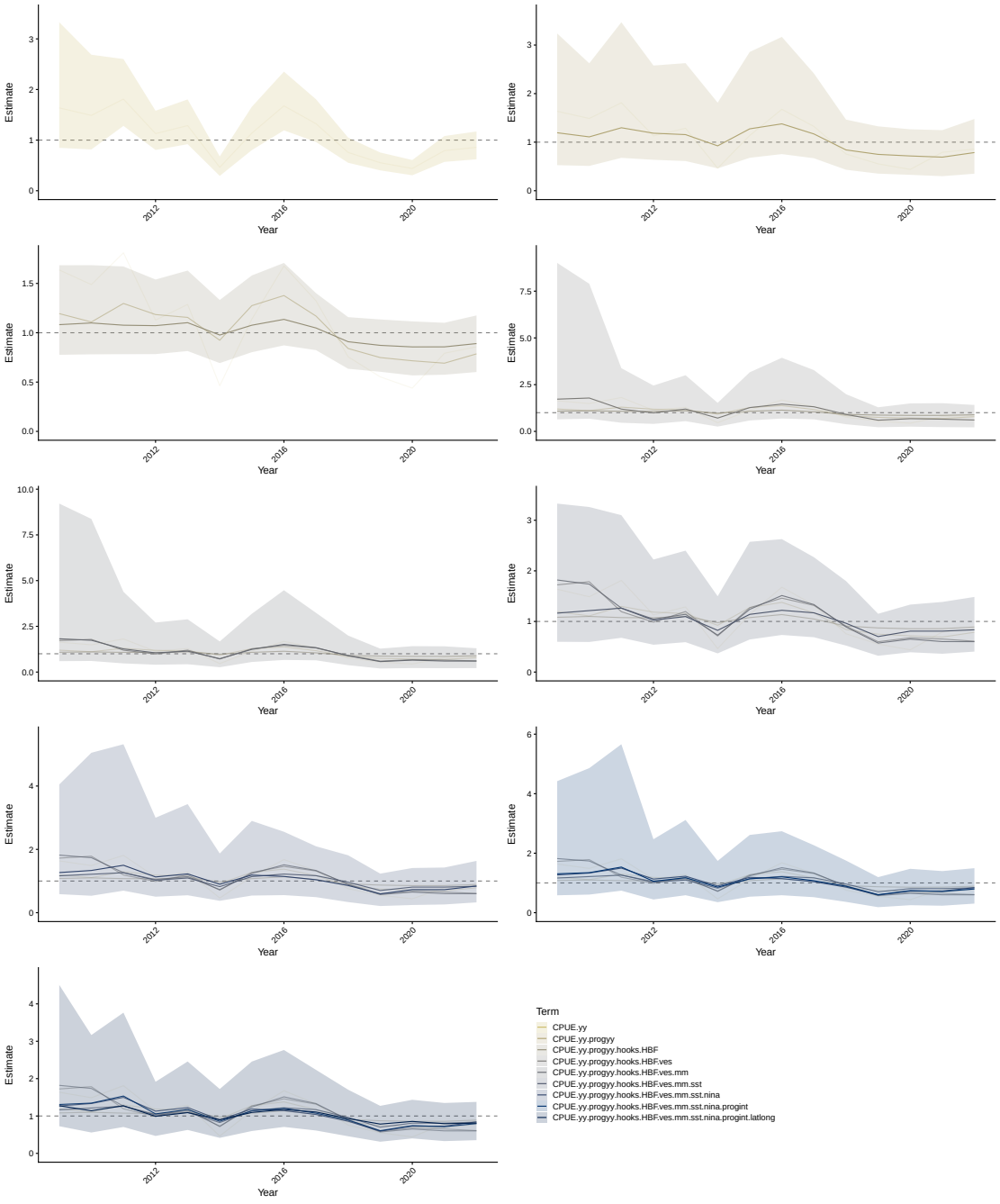

Figure C-50: CPUE standardisation effects for distant water fleet longline sets. Each row of plots corresponds to the addition of a variable, starting with a model that includes observer-program-year interactions. In each row, the posterior median and credible interval is shown for the updated model, posterior medians for the year effect from sub-models are shown for comparison.

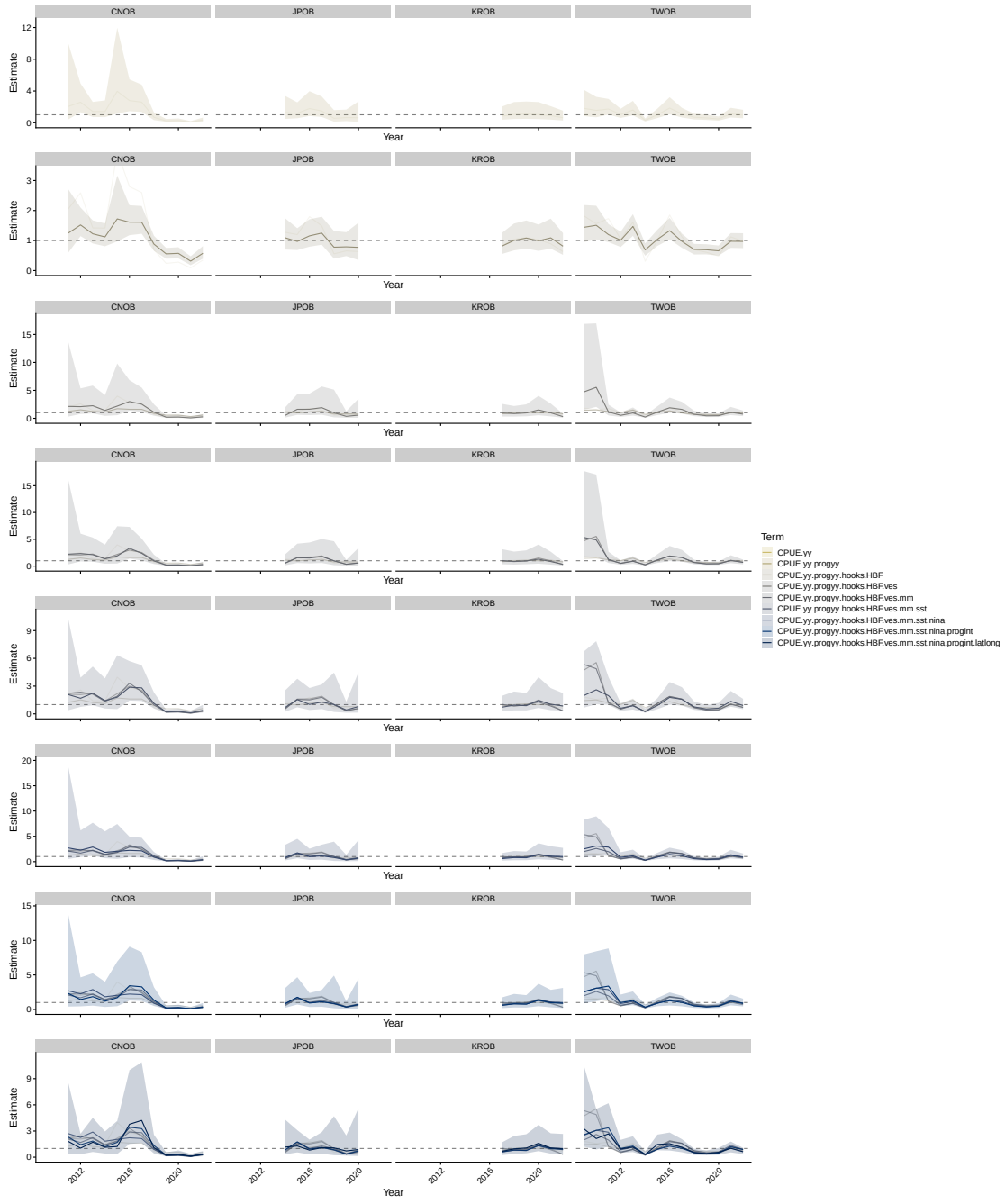

Figure C-51: CPUE standardisation effects for distant water fleet longline by observer-program. Each row of plots corresponds to the addition of a variable, starting with a model that includes observer-program-year interactions. In each row, the posterior median and credible interval is shown for the updated model, posterior medians for the year effect from sub-models are shown for comparison.

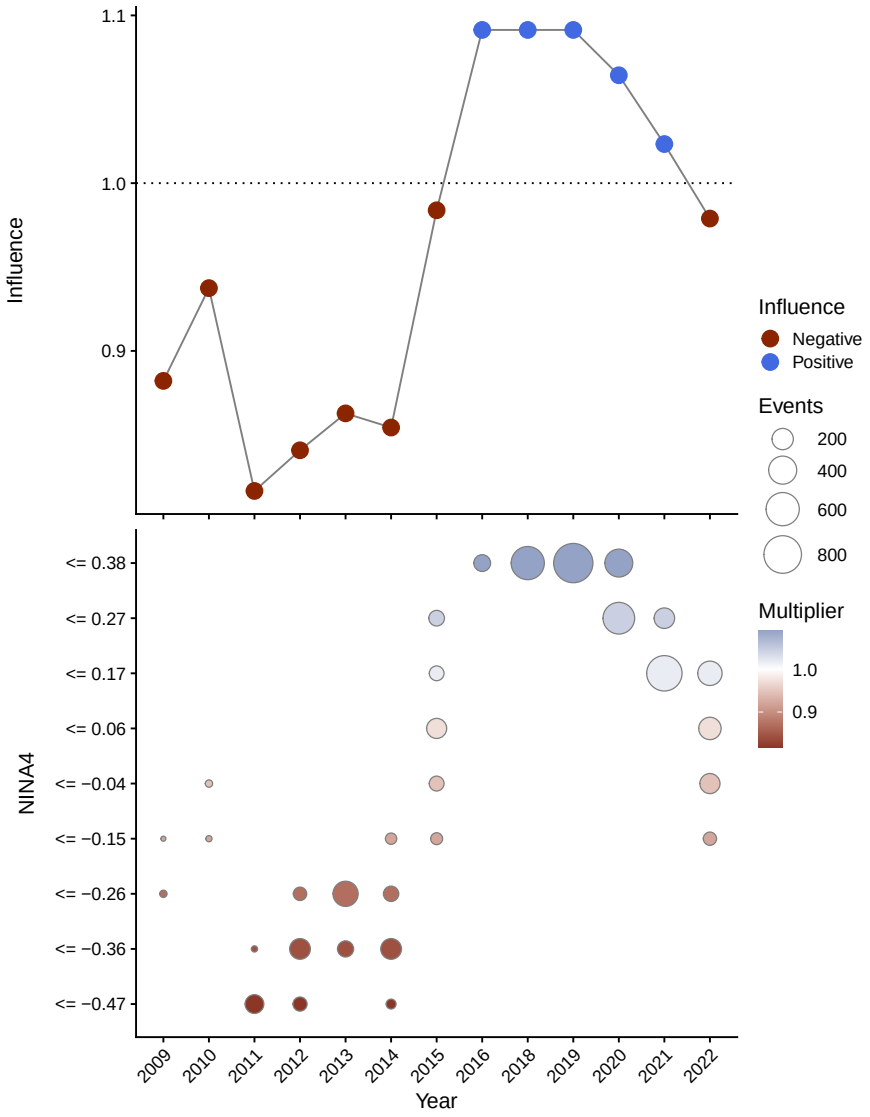

Figure C-52: Influence of the NINA4 index on catch-rates for distant water fleet longline sets, with positive influence showing years where the over-all catch-rate in the model was standardised downward by the corresponding amount to account for influences the NINA4 index. Influence is shown in colour as a multiplier on average catch rates, with circle size corresponding to the amount of effort entering the model. Note that data for the 2022 year is preliminary.

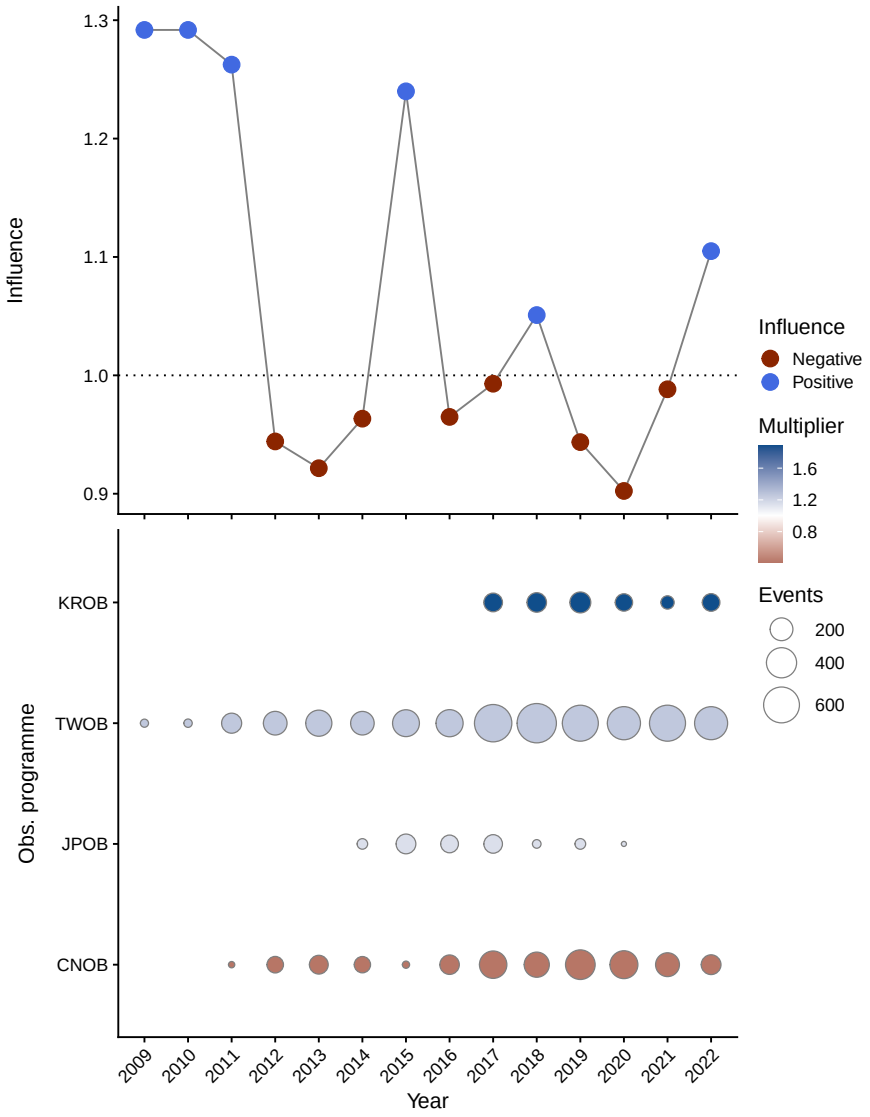

Figure C-53: Influence of observer program on catch-rates for distant water fleet longline sets, with positive influence showing years where the over-all catch-rate in the model was standardised downward by the corresponding amount to account for influences of observer program. Influence is shown in colour as a multiplier on average catch rates, with circle size corresponding to the amount of effort entering the model. Note that data for the 2022 year is preliminary.

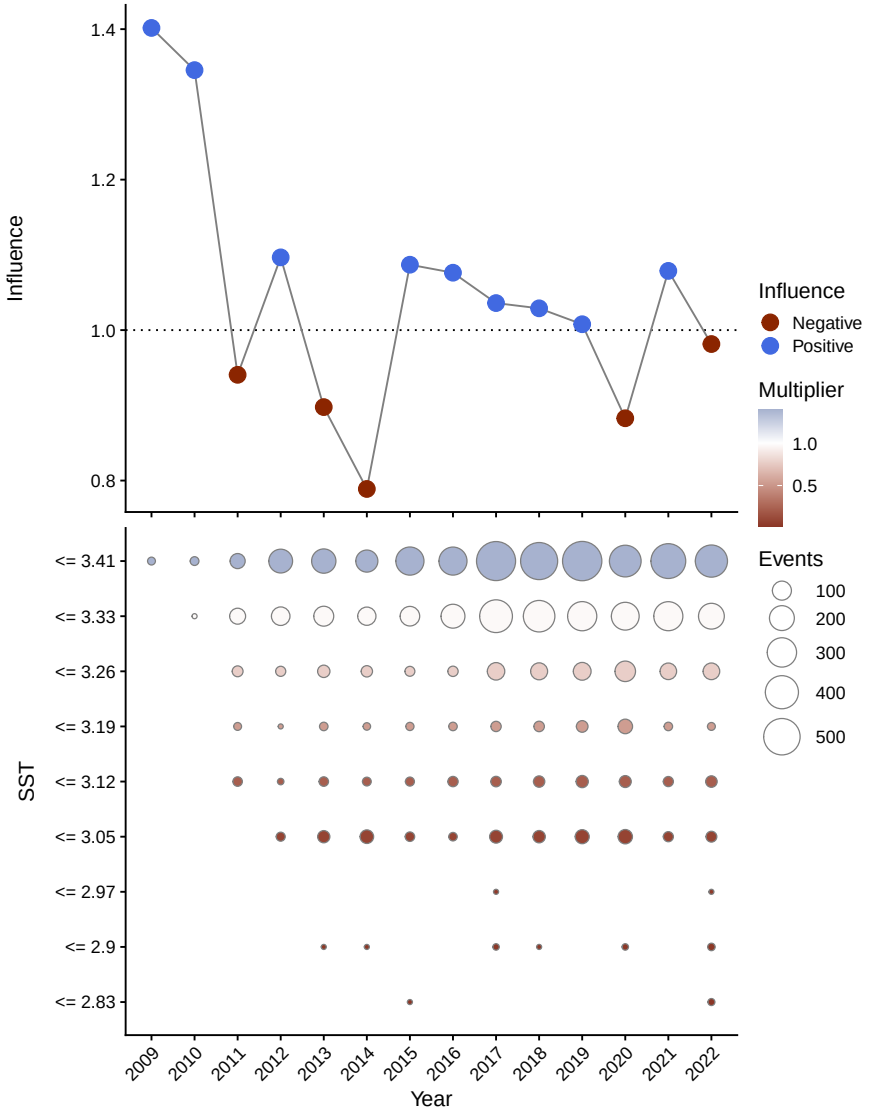

Figure C-54: Influence of sea-surface-temperature (SST) on catch-rates for distant water fleet longline sets, with positive influence showing years where the over-all catch-rate in the model was standardised downward by the corresponding amount to account for influences of SST. Influence is shown in colour as a multiplier on average catch rates, with circle size corresponding to the amount of effort entering the model. Note that data for the 2022 year is preliminary.

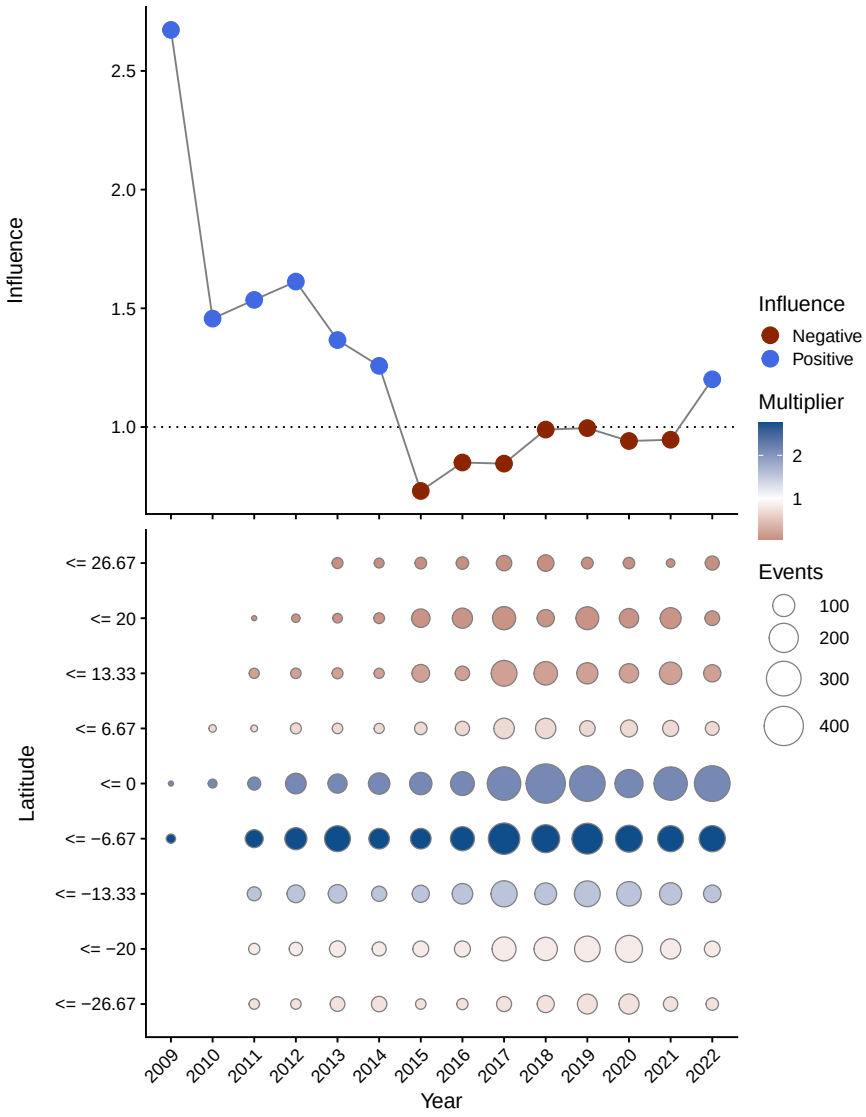

Figure C-55: Influence of latitude on catch-rates for distant water fleet longline sets, with positive influence showing years where the over-all catch-rate in the model was standardised downward by the corresponding amount to account for influences of latitude. Influence is shown in colour as a multiplier on average catch rates, with circle size corresponding to the amount of effort entering the model. Note that data for the 2022 year is preliminary.

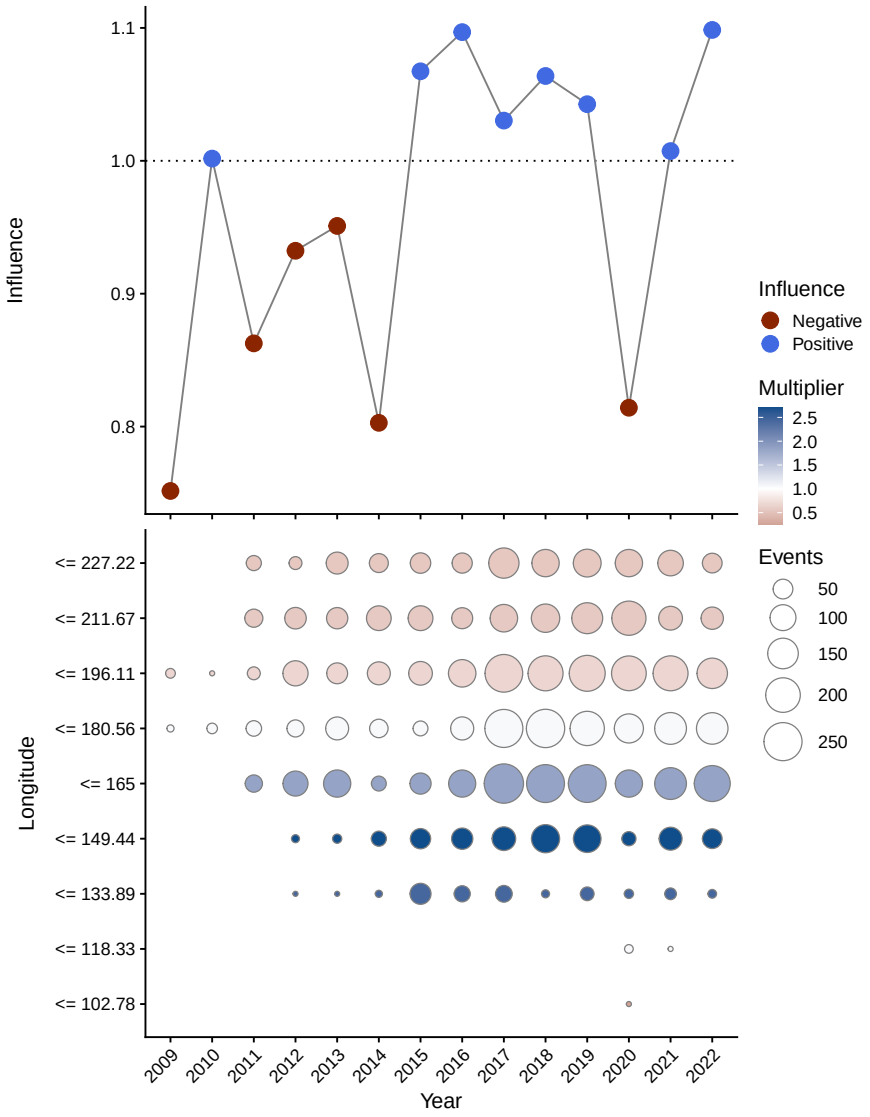

Figure C-56: Influence of longitude on catch-rates for distant water fleet longline sets, with positive influence showing years where the over-all catch-rate in the model was standardised downward by the corresponding amount to account for influences of longitude. Influence is shown in colour as a multiplier on average catch rates, with circle size corresponding to the amount of effort entering the model. Note that data for the 2022 year is preliminary.

C.5 CPUE diagnostics for free-school purse seine

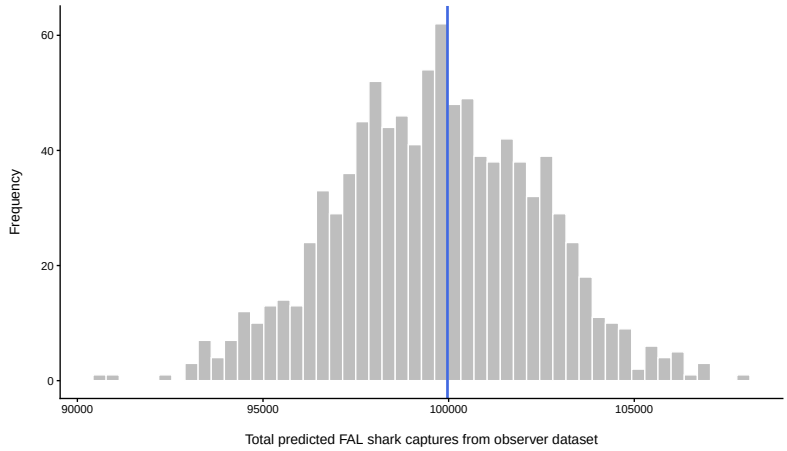

Figure C-57: Observed interactions (vertical line) and model predictions from the model used to derive CPUE from observed for free-school purse seine sets.

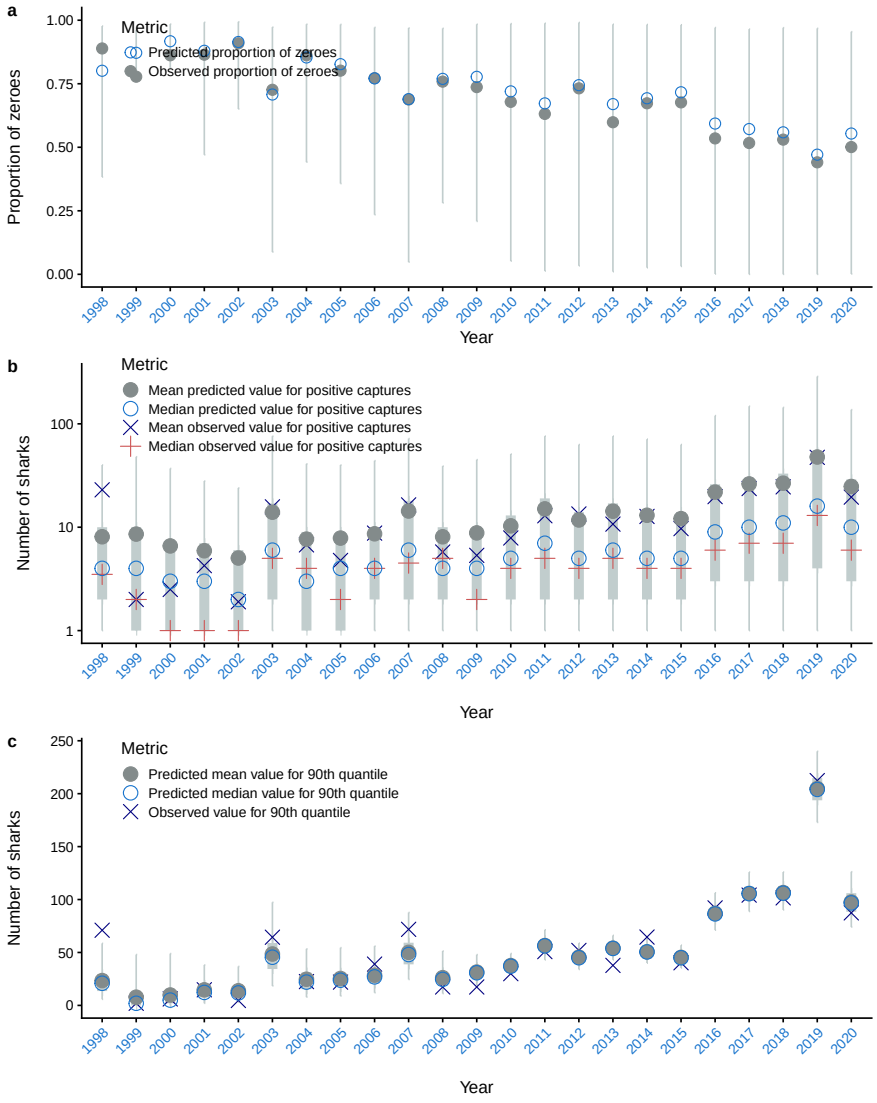

Figure C-58: Posterior predictive model diagnostics by model year for free-school purse seine sets, with (a) observed and predicted proportion of zero captures, (b) observed and predicted positive captures and (c) dispersion statistics (90% percentile) of observed data and predictions.

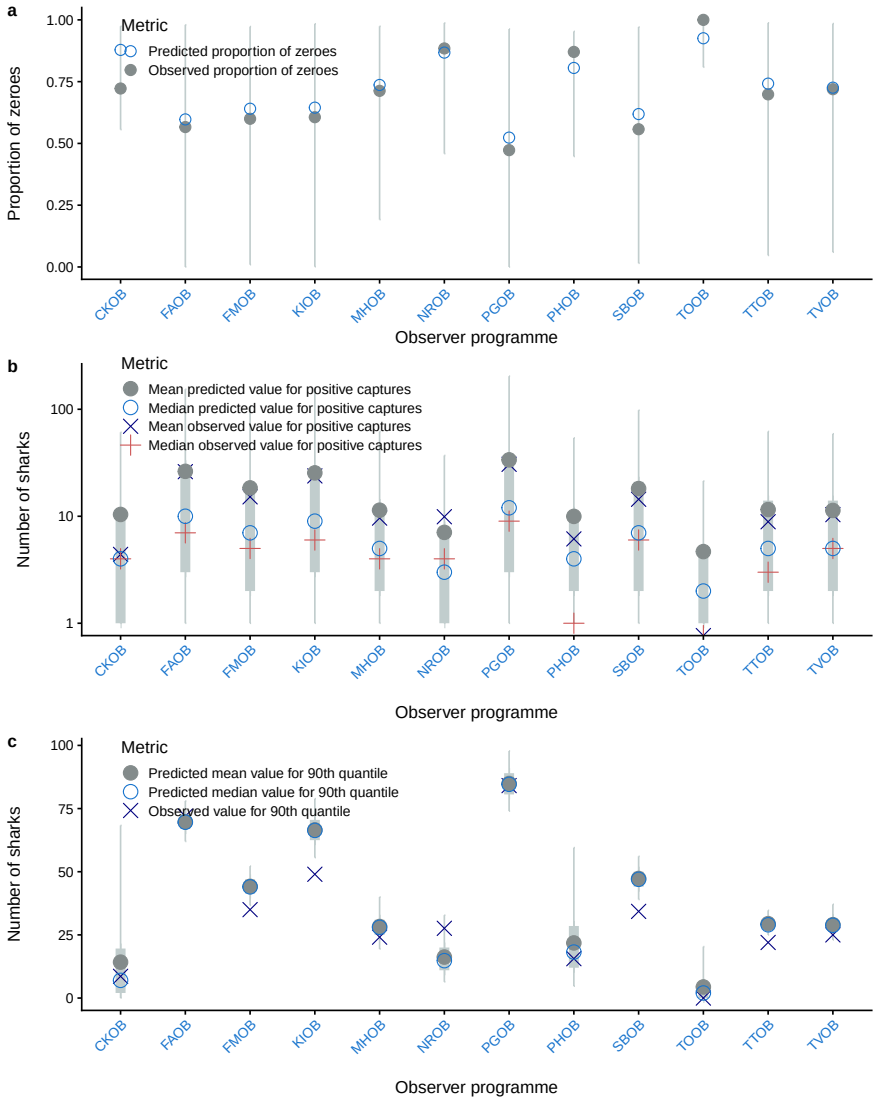

Figure C-59: Posterior predictive model diagnostics by observer program for free-school purse seine sets, with (a) observed and predicted proportion of zero captures, (b) observed and predicted positive captures and (c) dispersion statistics (90% percentile) of observed data and predictions.

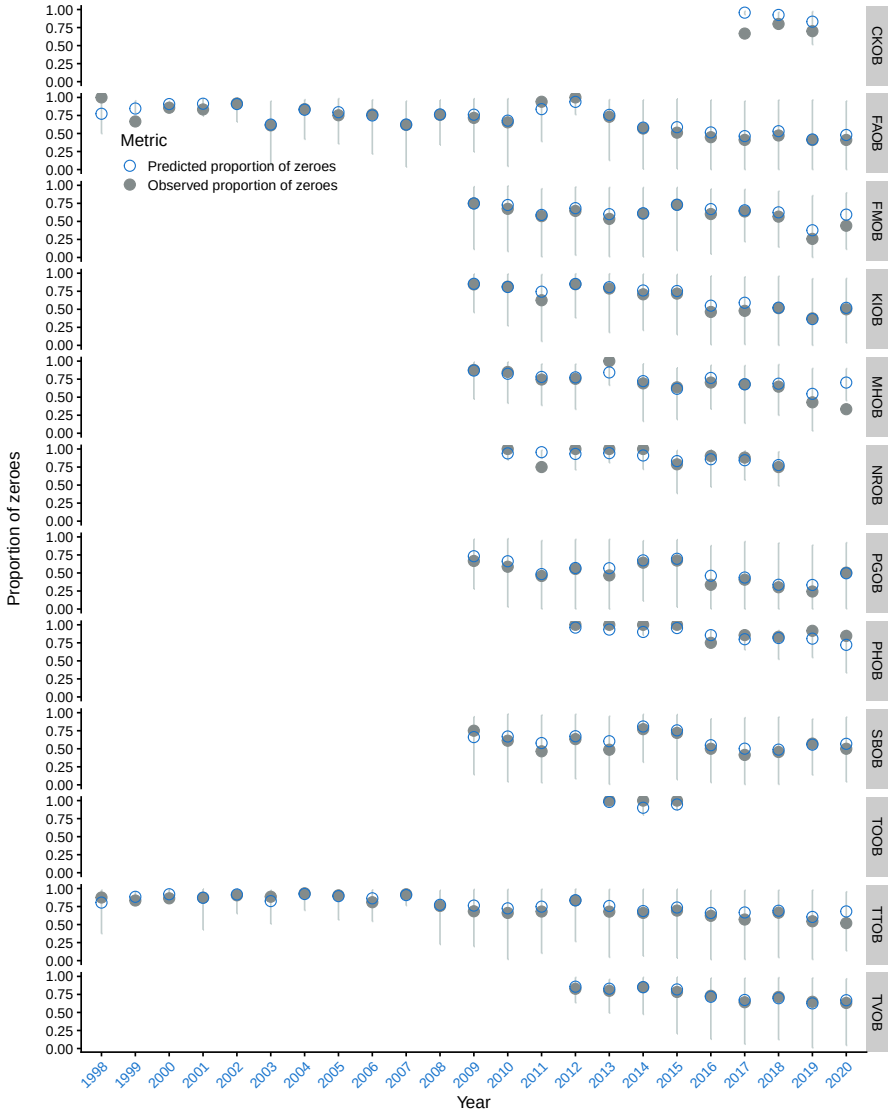

Figure C-60: Posterior predictive model diagnostics for observed and predicted proportion of zero captures by observer program and year for free-school purse seine sets.

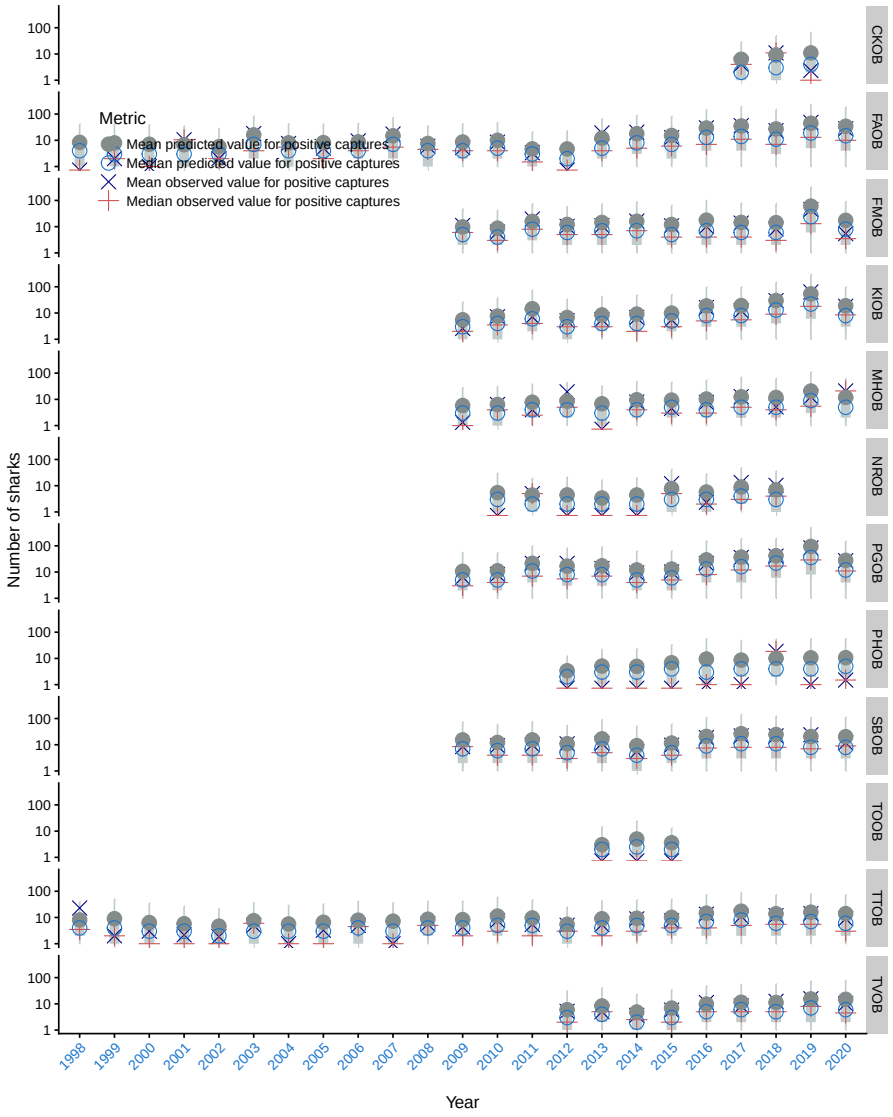

Figure C-61: Posterior predictive model diagnostics for bserved and predicted positive captures by observer program and year for free-school purse seine sets.

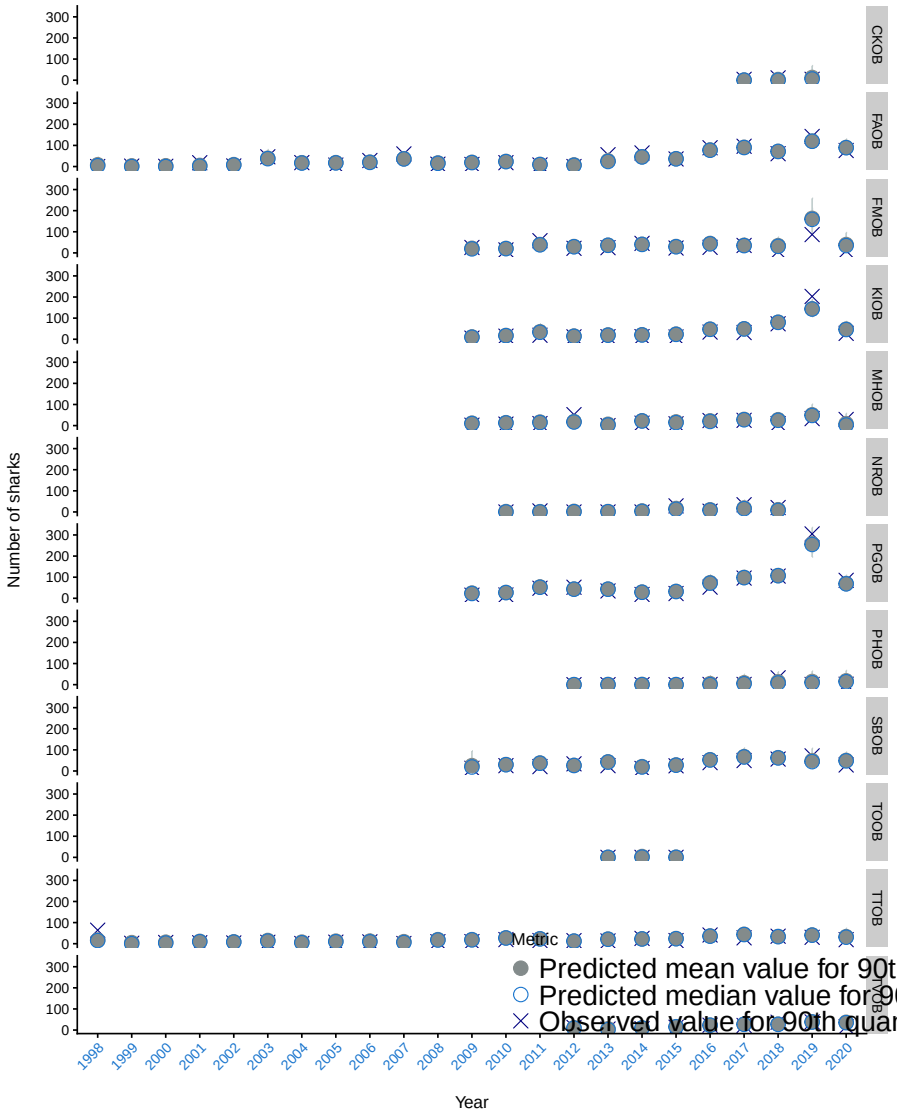

Figure C-62: Posterior predictive model diagnostics for dispersion statistics (90% percentile) of observed data and predictions by observer program and year for free-school purse seine sets.

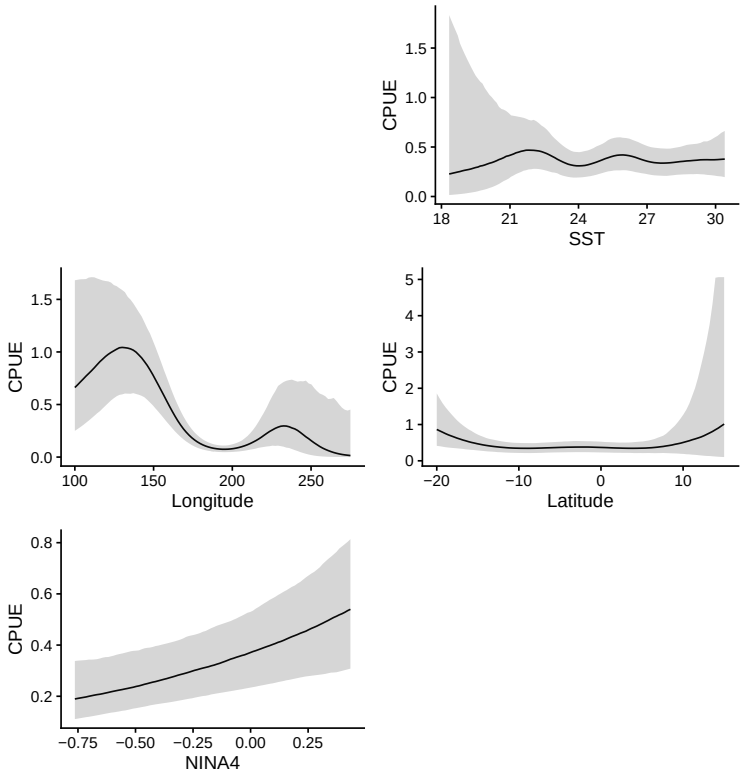

Figure C-63: Conditional effects estimated in the model used to derive CPUE from observed for free-school purse seine sets.

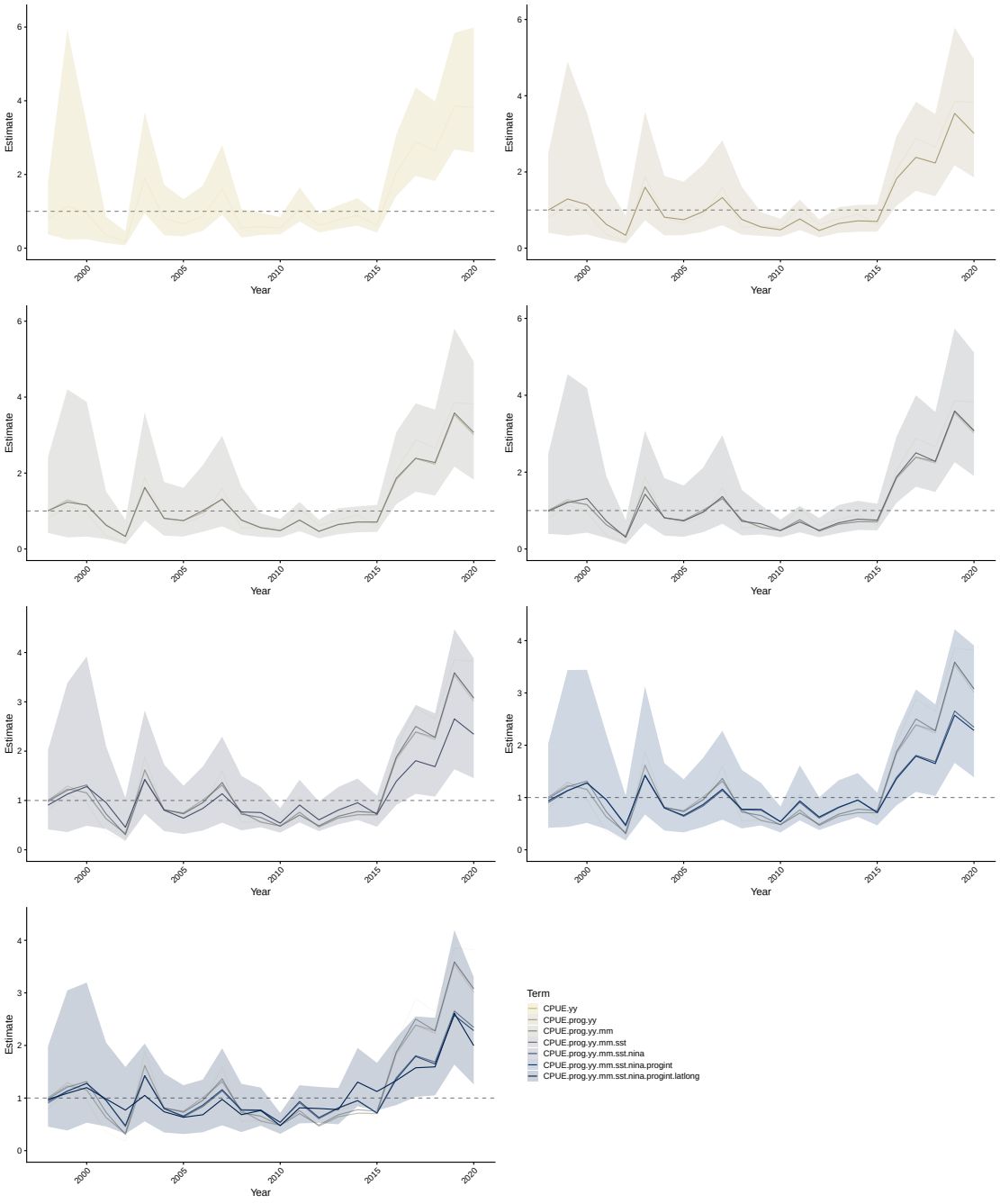

Figure C-64: CPUE standardisation effects for free-school purse seine sets. Each row of plots corresponds to the addition of a variable, starting with a model that includes observer-program-year interactions. In each row, the posterior median and credible interval is shown for the updated model, posterior medians for the year effect from sub-models are shown for comparison.

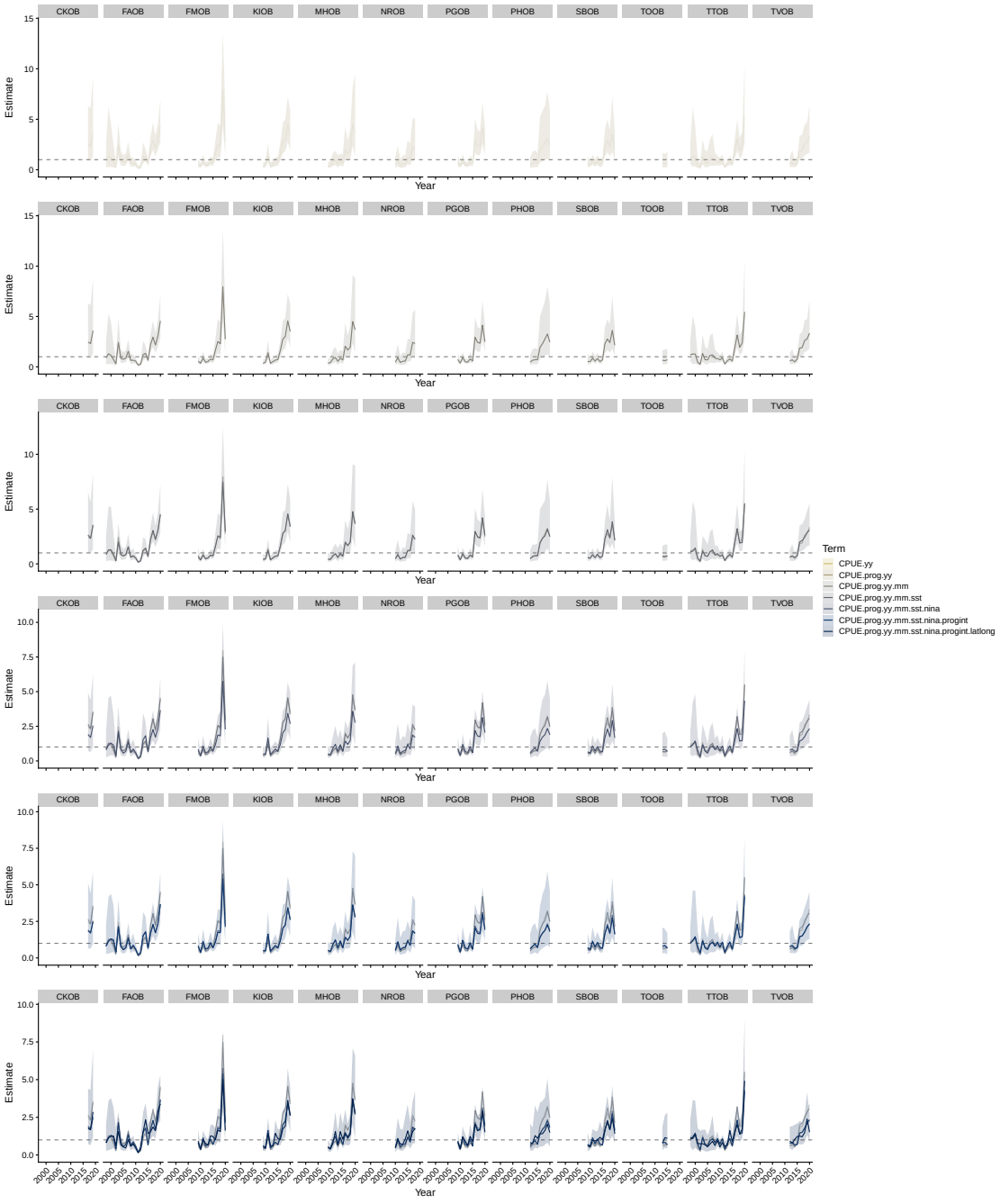

Figure C-65: CPUE standardisation effects for free-school purse seine by observer-program. Each row of plots corresponds to the addition of a variable, starting with a model that includes observer-program-year interactions. In each row, the posterior median and credible interval is shown for the updated model, posterior medians for the year effect from sub-models are shown for comparison.

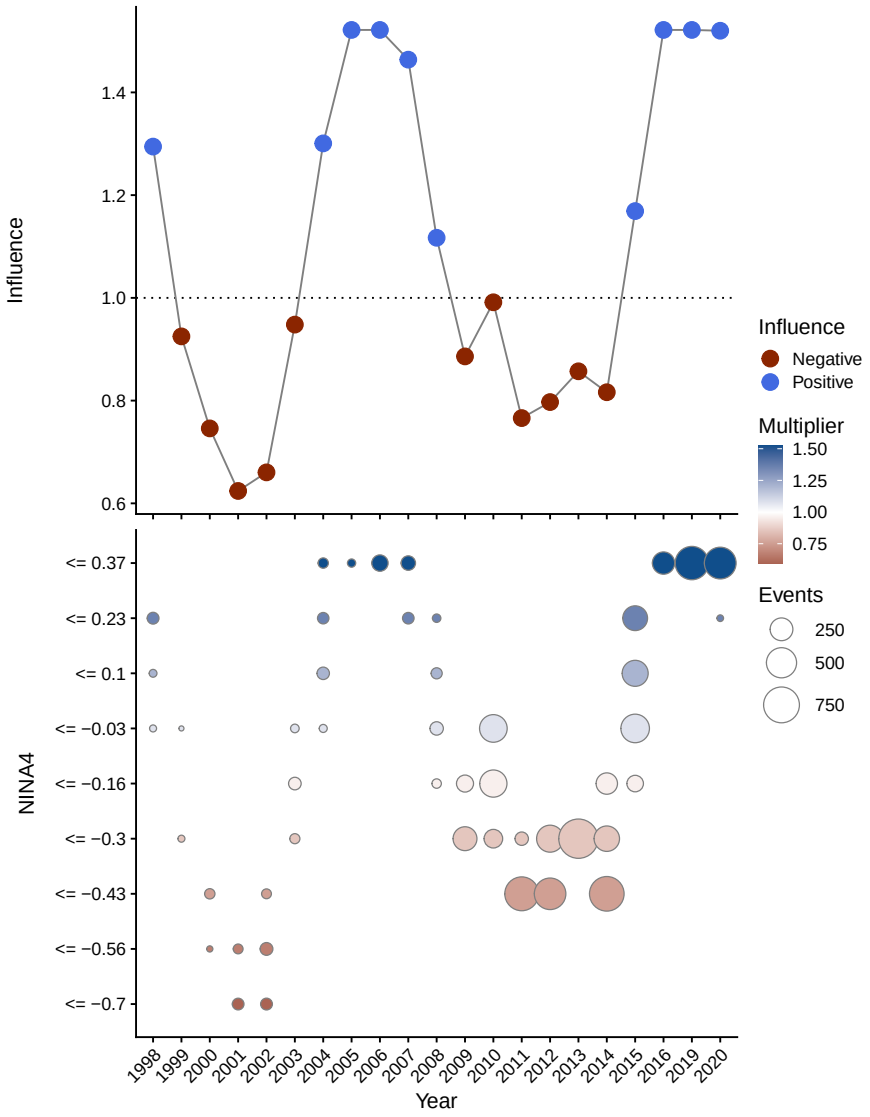

Figure C-66: Influence of the NINA4 index on catch-rates for free-school purse seine sets, with positive influence showing years where the over-all catch-rate in the model was standardised downward by the corresponding amount to account for influences the NINA4 index. Influence is shown in colour as a multiplier on average catch rates, with circle size corresponding to the amount of effort entering the model. Note that data for the 2022 year is preliminary.

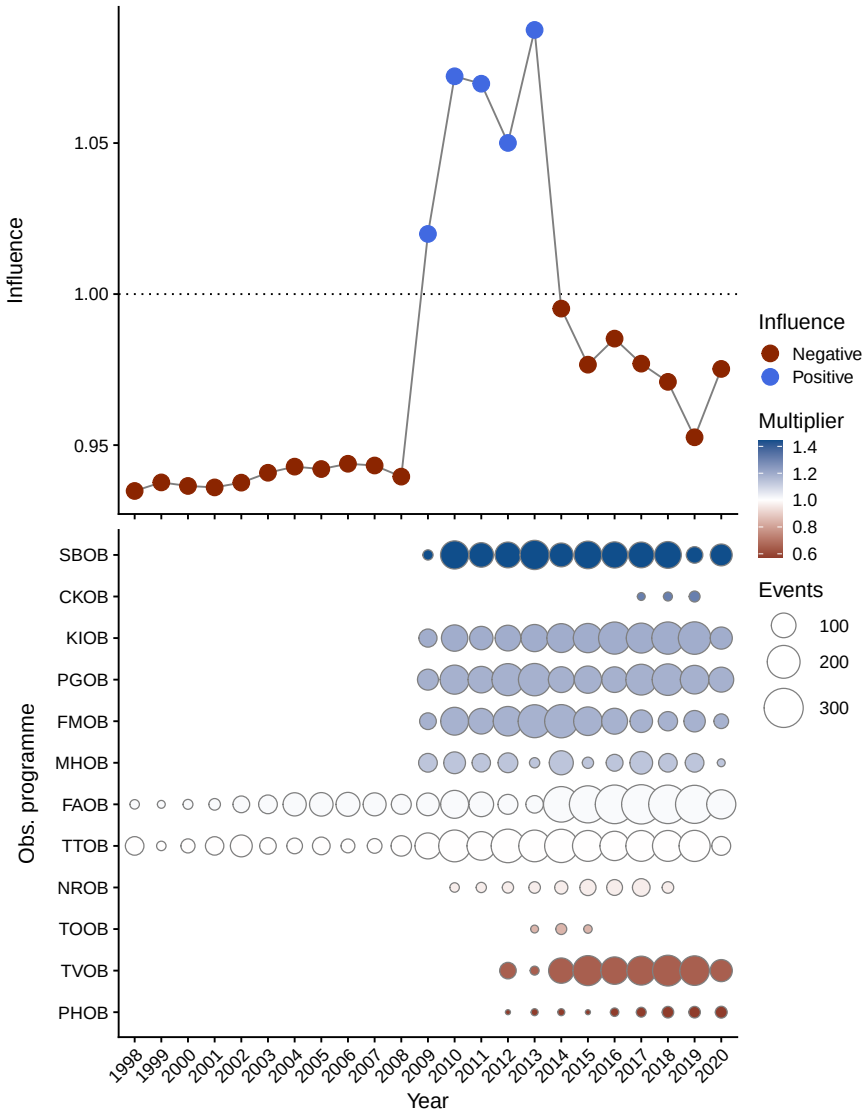

Figure C-67: Influence of observer program on catch-rates for free-school purse seine sets, with positive influence showing years where the over-all catch-rate in the model was standardised downward by the corresponding amount to account for influences of observer program. Influence is shown in colour as a multiplier on average catch rates, with circle size corresponding to the amount of effort entering the model. Note that data for the 2022 year is preliminary.

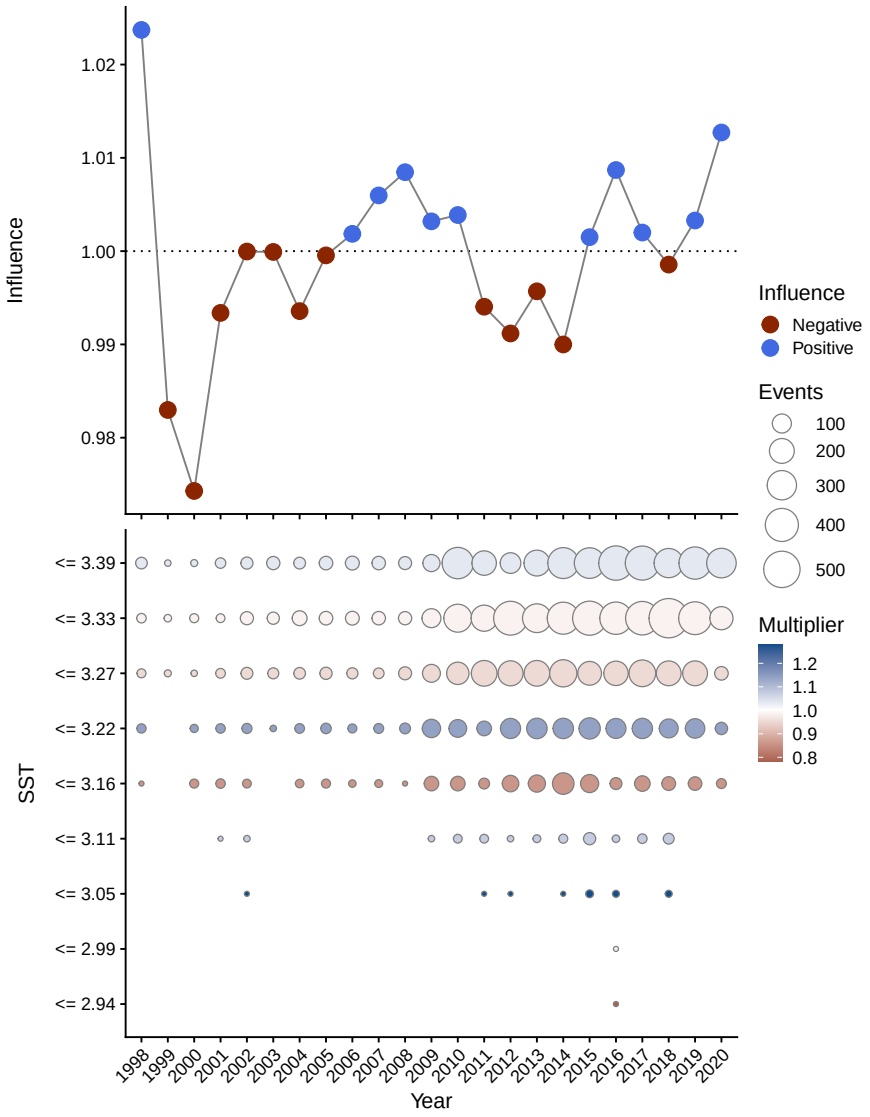

Figure C-68: Influence of sea-surface-temperature (SST) on catch-rates for free-school purse seine sets, with positive influence showing years where the over-all catch-rate in the model was standardised downward by the corresponding amount to account for influences of SST. Influence is shown in colour as a multiplier on average catch rates, with circle size corresponding to the amount of effort entering the model. Note that data for the 2022 year is preliminary.

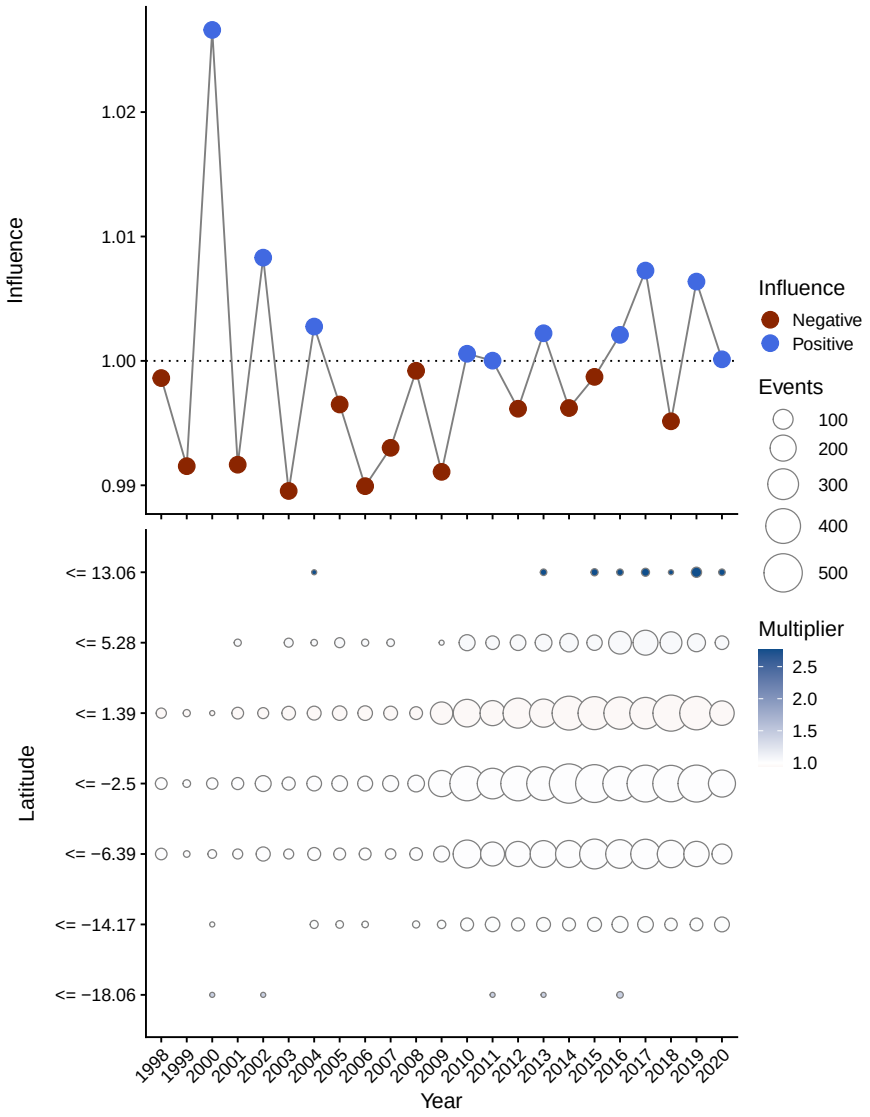

Figure C-69: Influence of latitude on catch-rates for free-school purse seine sets, with positive influence showing years where the over-all catch-rate in the model was standardised downward by the corresponding amount to account for influences of latitude. Influence is shown in colour as a multiplier on average catch rates, with circle size corresponding to the amount of effort entering the model. Note that data for the 2022 year is preliminary.

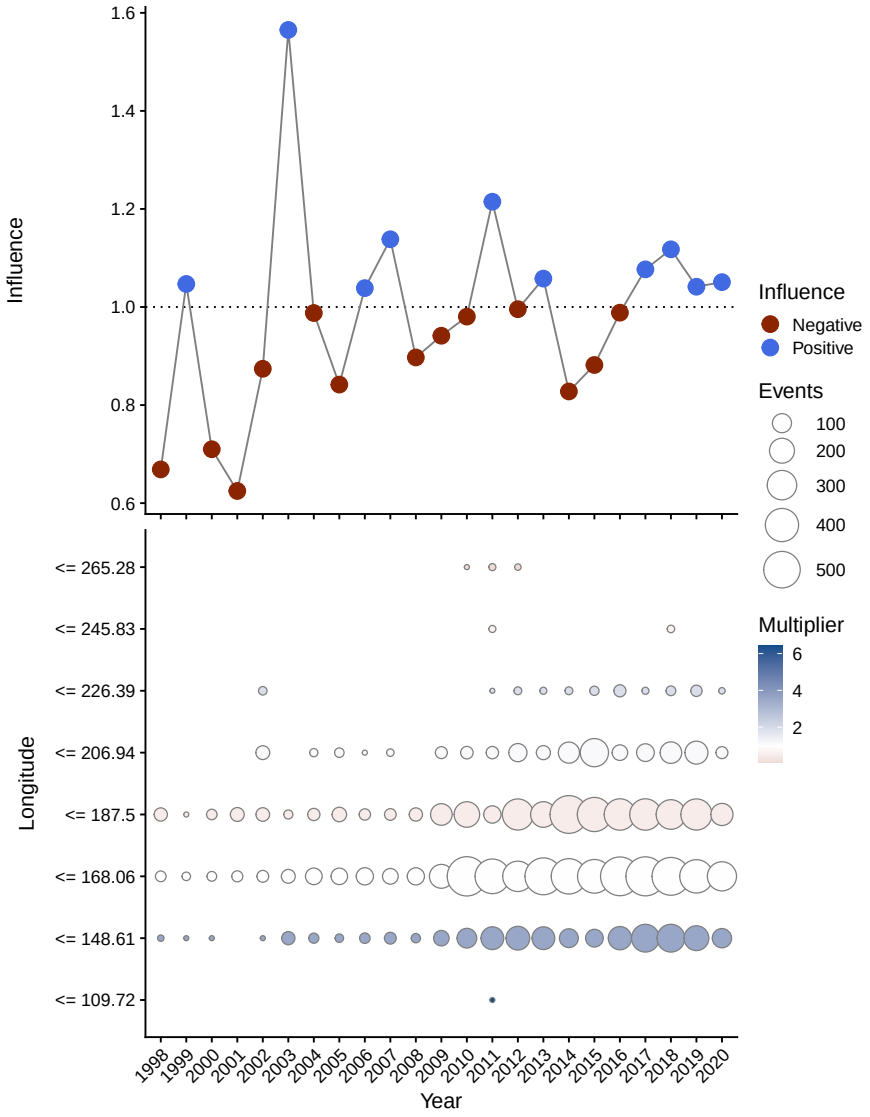

Figure C-70: Influence of longitude on catch-rates for free-school purse seine sets, with positive influence showing years where the over-all catch-rate in the model was standardised downward by the corresponding amount to account for influences of longitude. Influence is shown in colour as a multiplier on average catch rates, with circle size corresponding to the amount of effort entering the model. Note that data for the 2022 year is preliminary.

C.6 CPUE diagnostics for object-associated purse seine

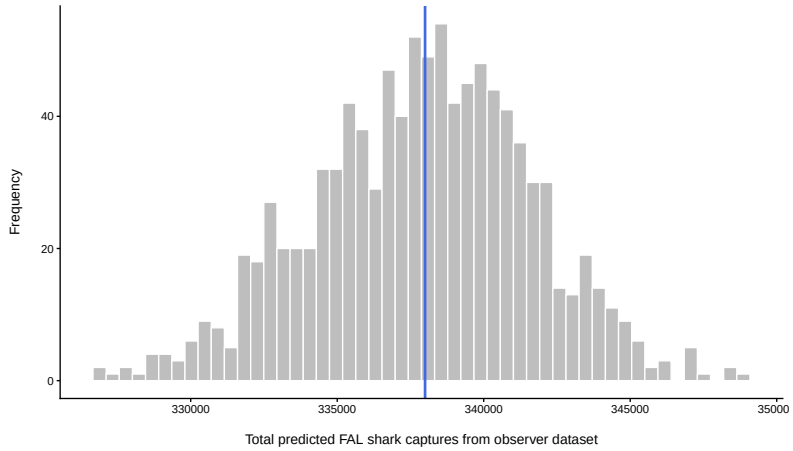

Figure C-71: Observed interactions (vertical line) and model predictions from the model used to derive CPUE from observed for object-associated purse seine sets.

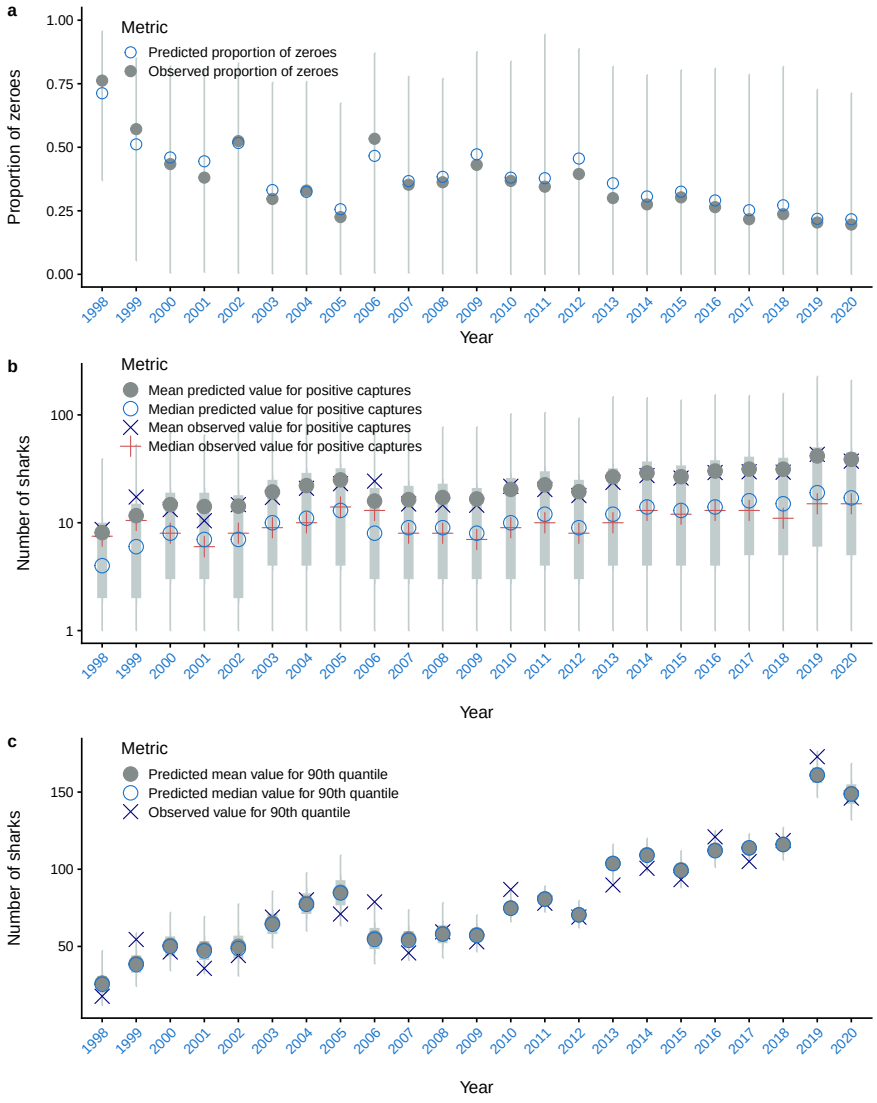

Figure C-72: Posterior predictive model diagnostics by model year for object-associated purse seine sets, with (a) observed and predicted proportion of zero captures, (b) observed and predicted positive captures and (c) dispersion statistics (90% percentile) of observed data and predictions.

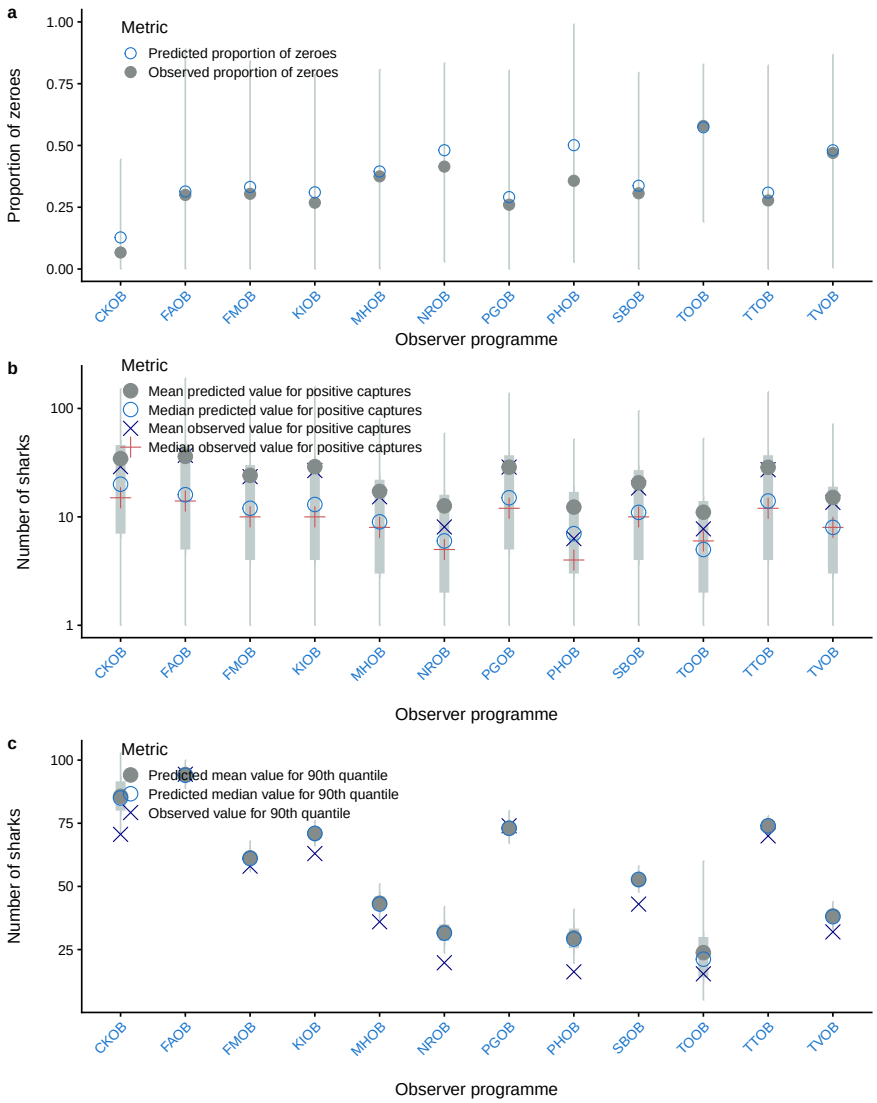

Figure C-73: Posterior predictive model diagnostics by observer program for object-associated purse seine sets, with (a) observed and predicted proportion of zero captures, (b) observed and predicted positive captures and (c) dispersion statistics (90% percentile) of observed data and predictions.

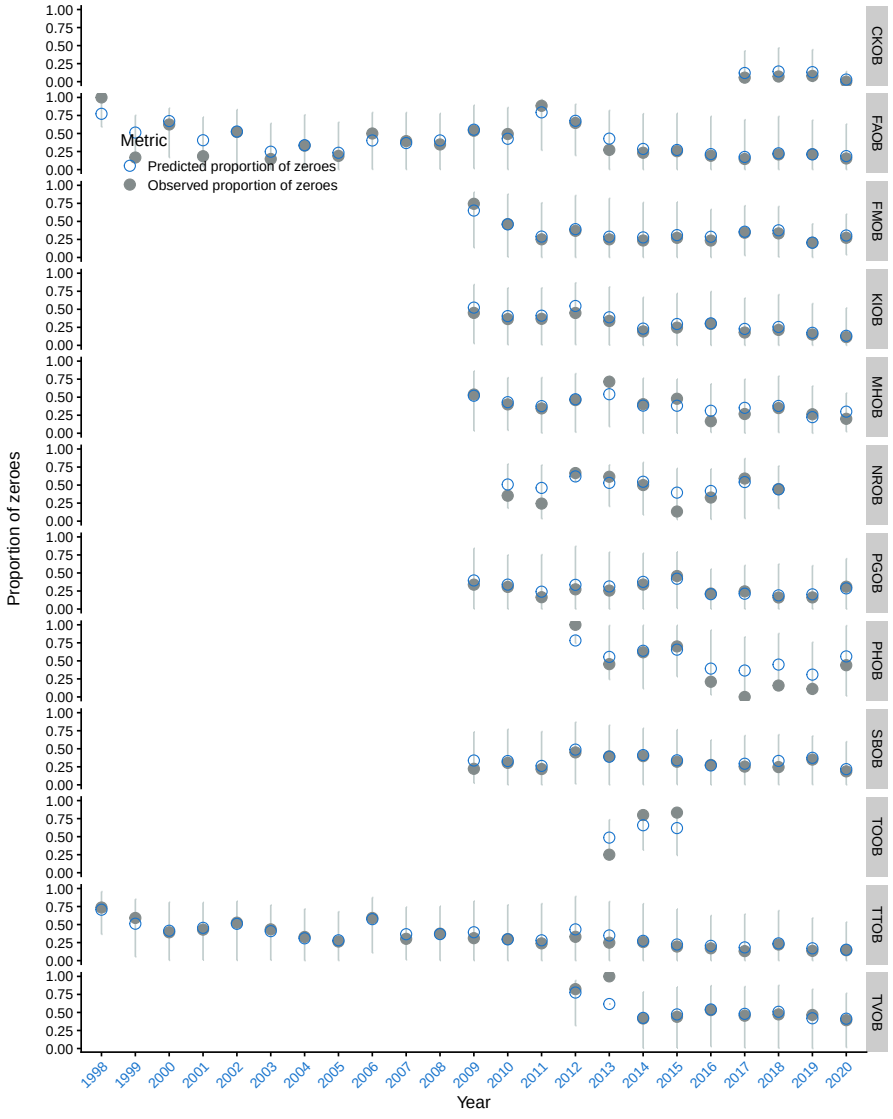

Figure C-74: Posterior predictive model diagnostics for observed and predicted proportion of zero captures by observer program and year for object-associated purse seine sets.

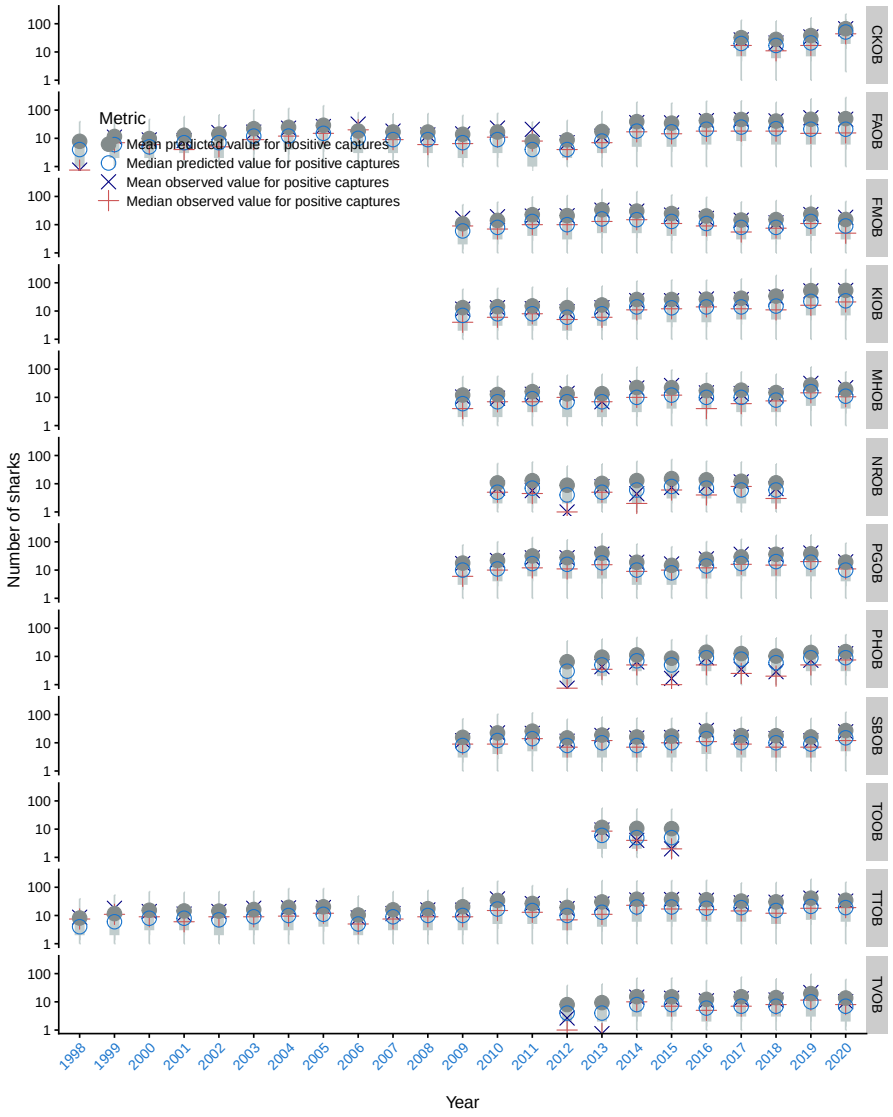

Figure C-75: Posterior predictive model diagnostics for bserved and predicted positive captures by observer program and year for object-associated purse seine sets.

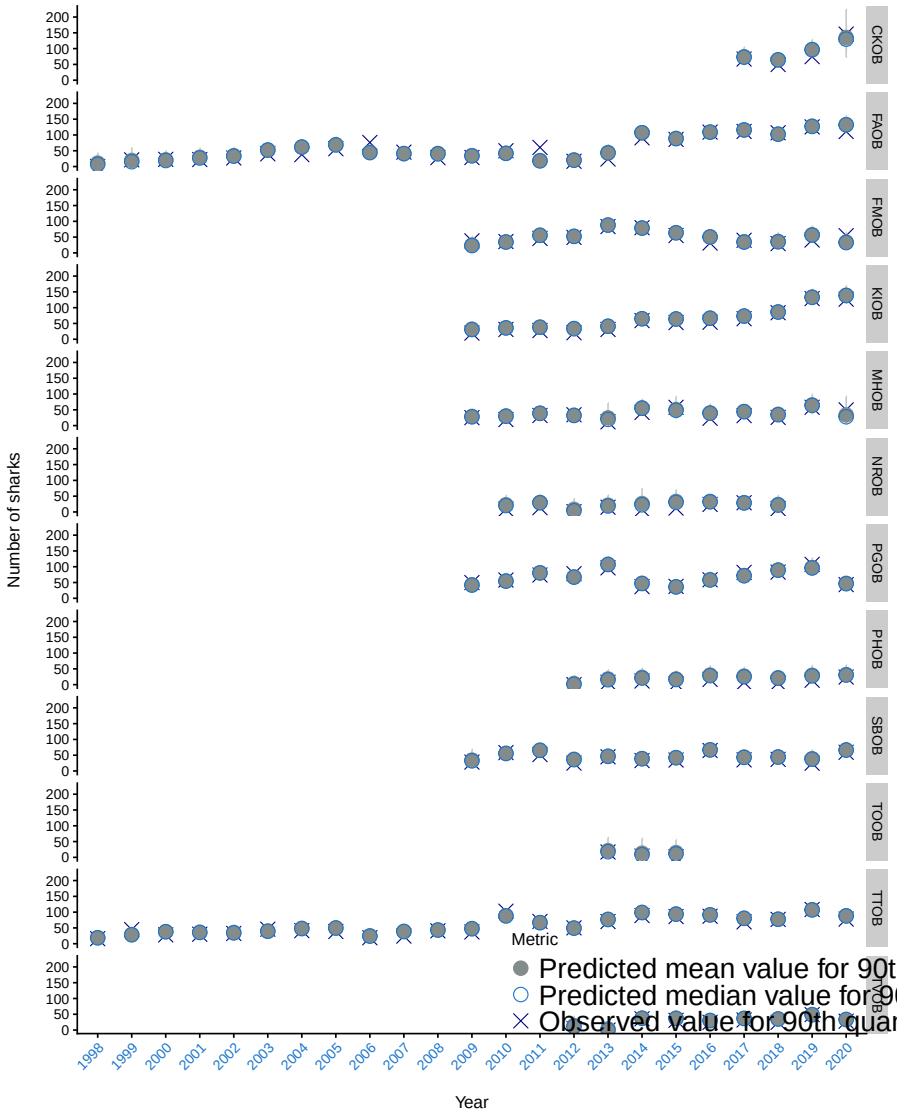

Figure C-76: Posterior predictive model diagnostics for dispersion statistics (90% percentile) of observed data and predictions by observer program and year for object-associated purse seine sets.

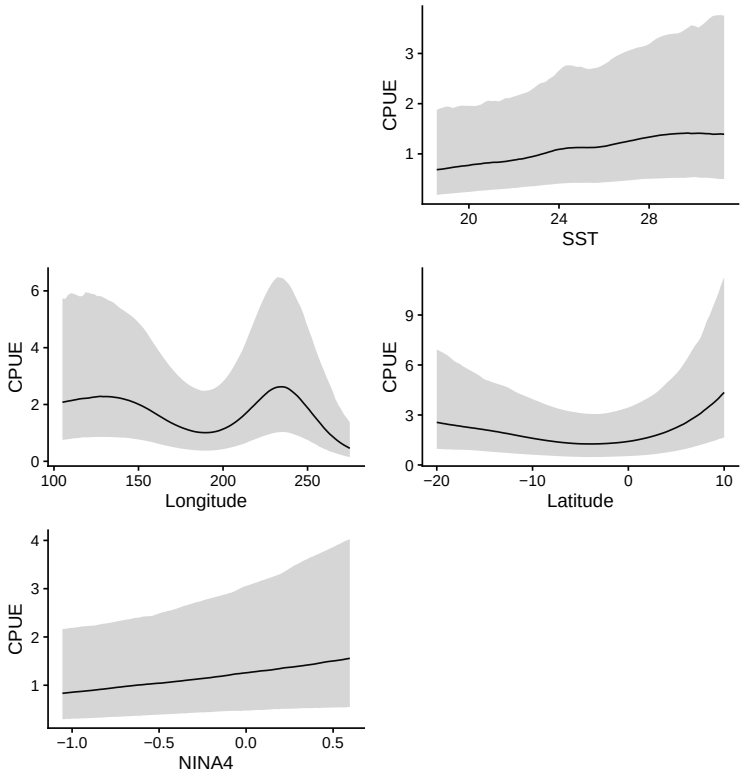

Figure C-77: Conditional effects estimated in the model used to derive CPUE from observed for object-associated purse seine sets.

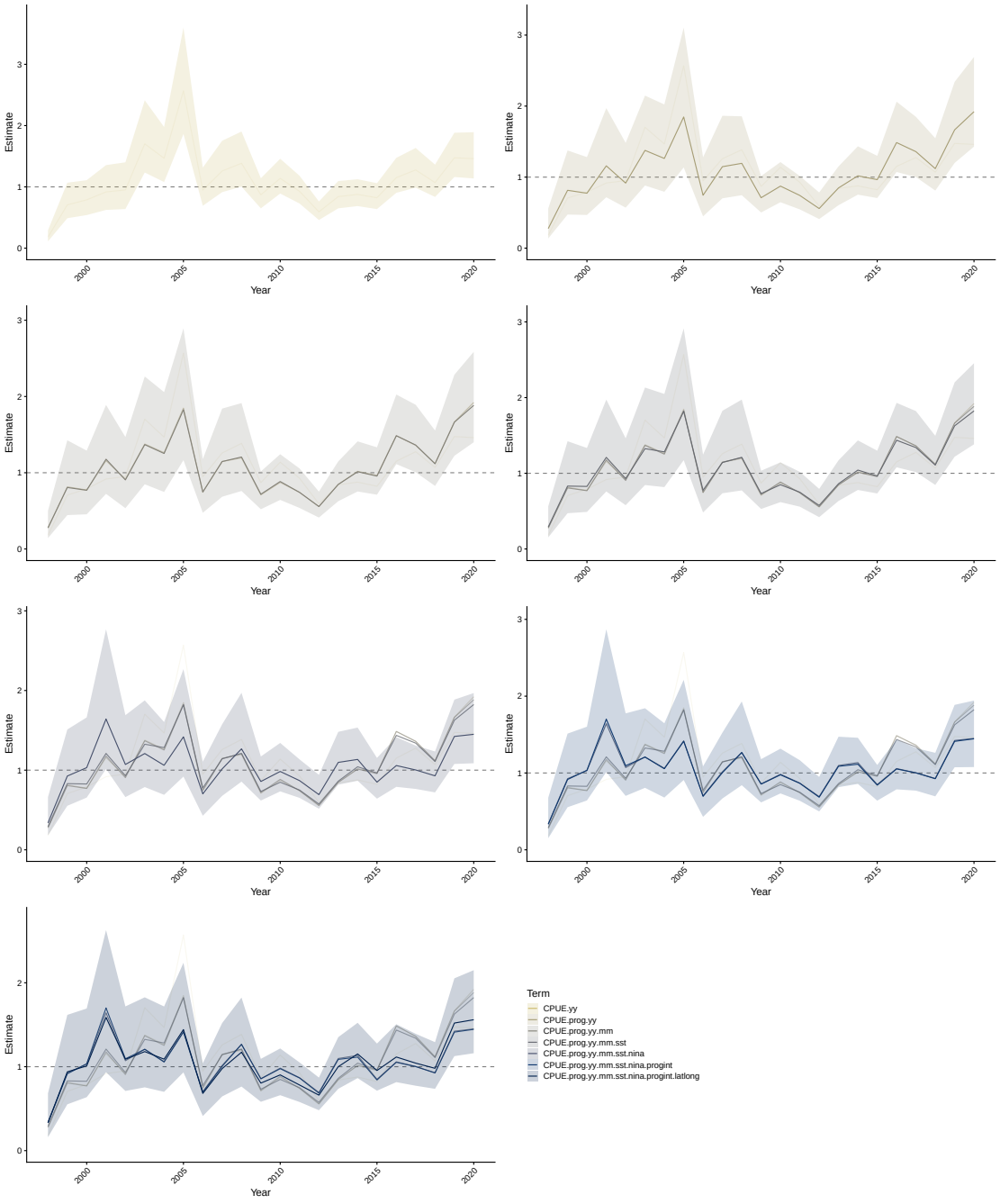

Figure C-78: CPUE standardisation effects for object-associated purse seine sets. Each row of plots corresponds to the addition of a variable, starting with a model that includes observer-program-year interactions. In each row, the posterior median and credible interval is shown for the updated model, posterior medians for the year effect from sub-models are shown for comparison.

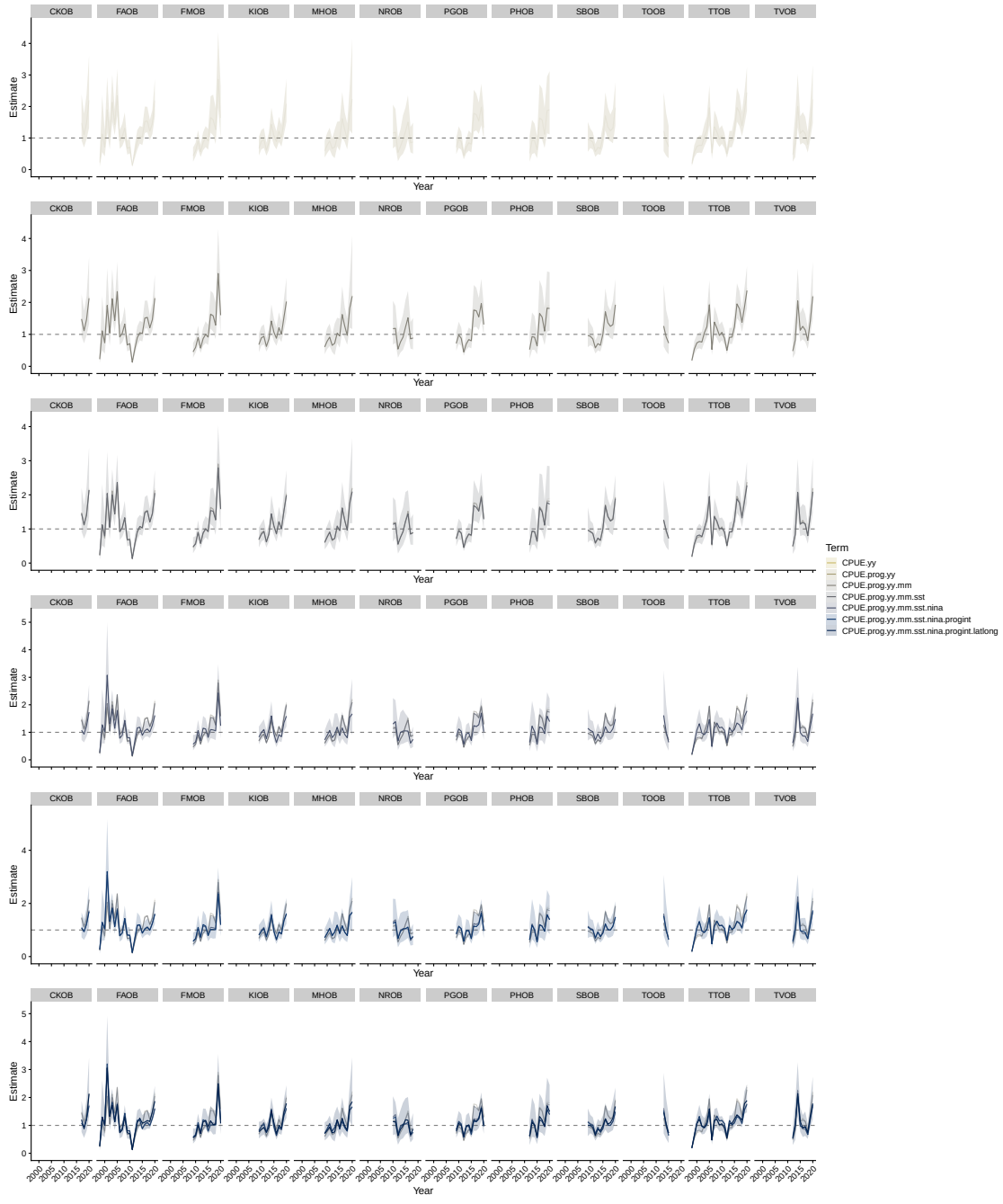

Figure C-79: CPUE standardisation effects for object-associated purse seine by observer-program. Each row of plots corresponds to the addition of a variable, starting with a model that includes observer-program-year interactions. In each row, the posterior median and credible interval is shown for the updated model, posterior medians for the year effect from sub-models are shown for comparison.

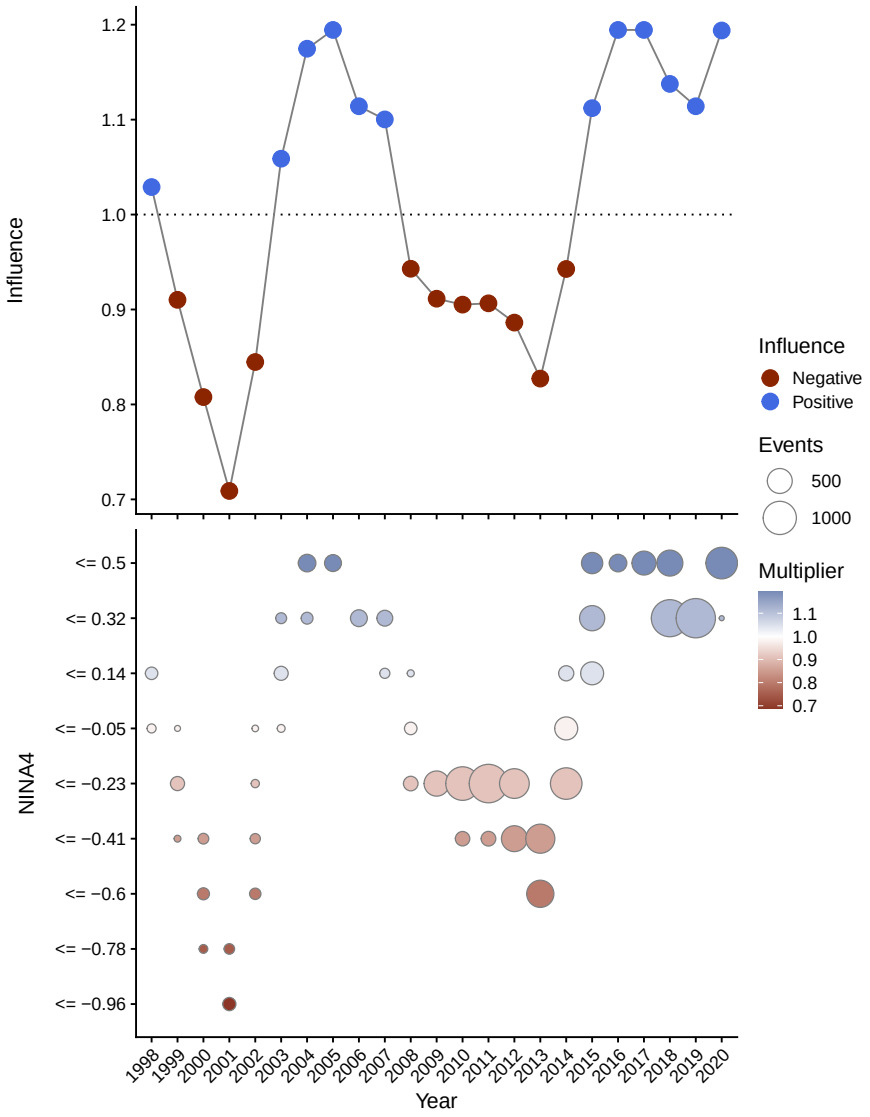

Figure C-80: Influence of the NINA4 index on catch-rates for object-associated purse seine sets, with positive influence showing years where the over-all catch-rate in the model was standardised downward by the corresponding amount to account for influences the NINA4 index. Influence is shown in colour as a multiplier on average catch rates, with circle size corresponding to the amount of effort entering the model. Note that data for the 2022 year is preliminary.

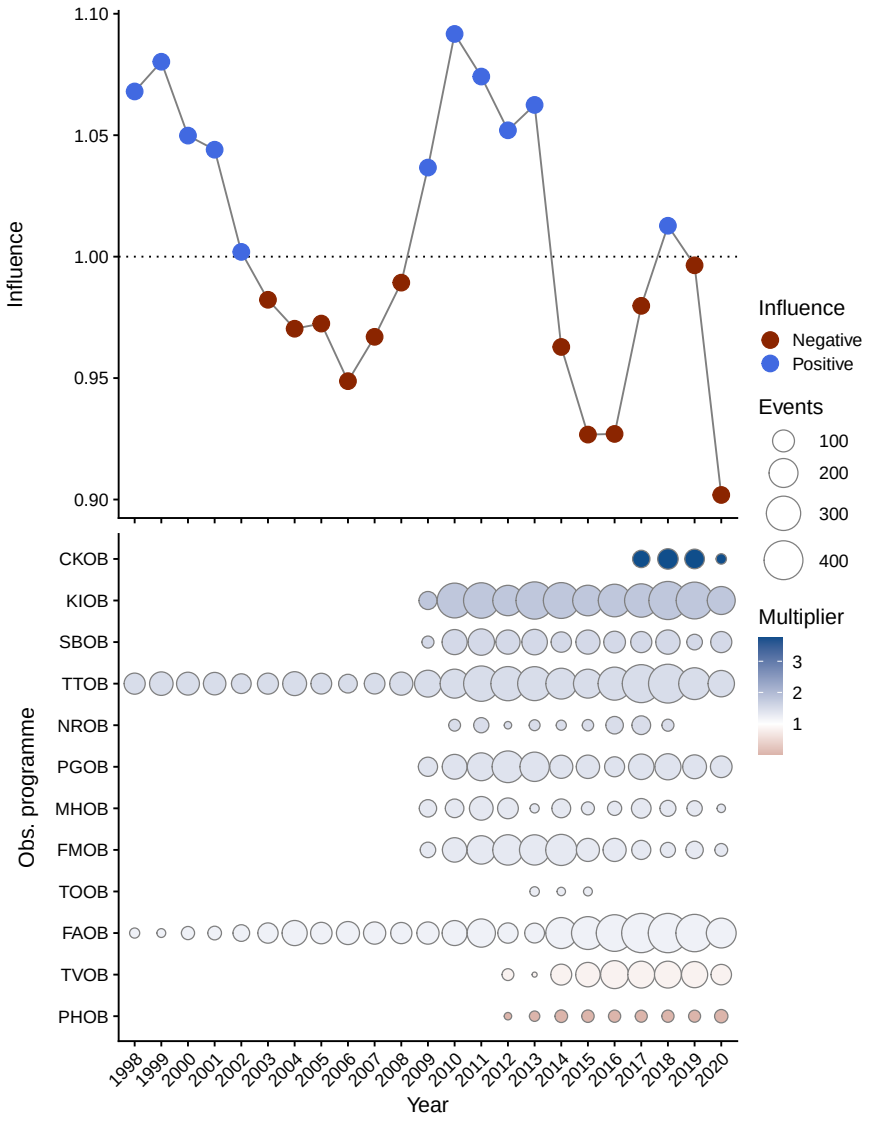

Figure C-81: Influence of observer program on catch-rates for object-associated purse seine sets, with positive influence showing years where the over-all catch-rate in the model was standardised downward by the corresponding amount to account for influences of observer program. Influence is shown in colour as a multiplier on average catch rates, with circle size corresponding to the amount of effort entering the model. Note that data for the 2022 year is preliminary.

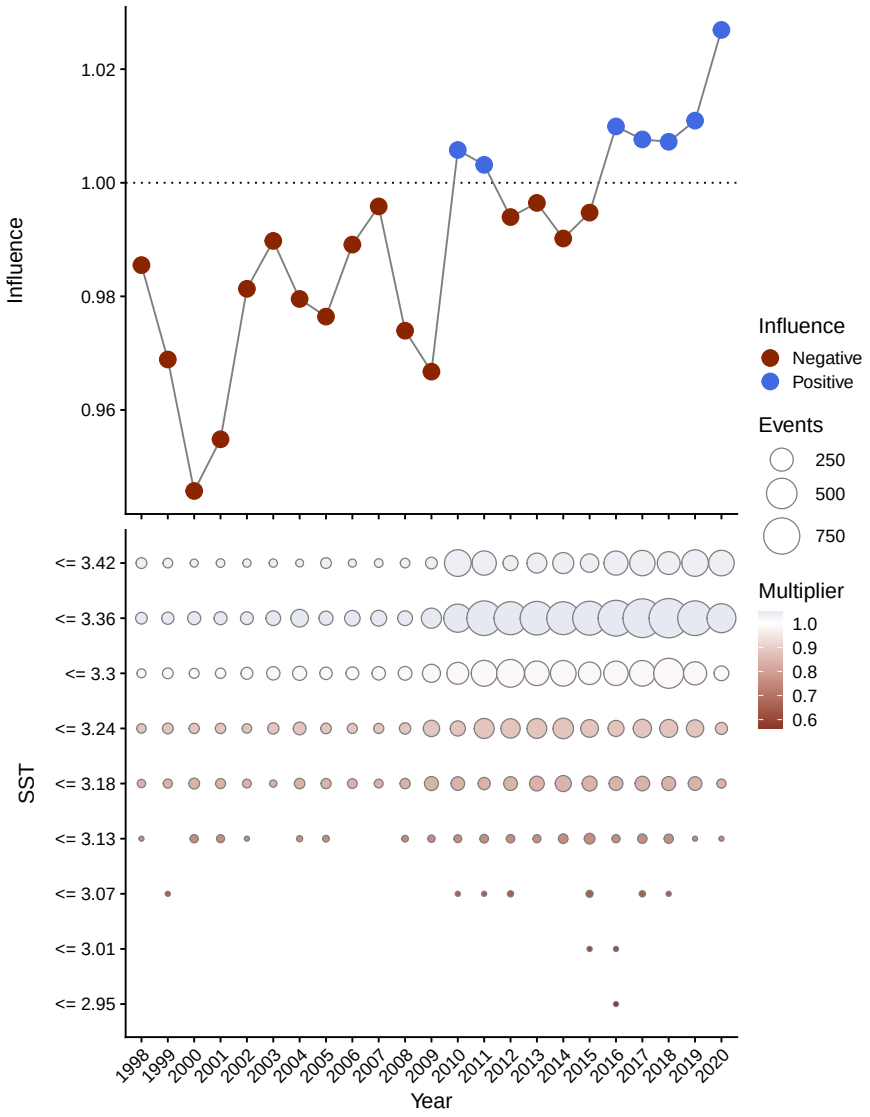

Figure C-82: Influence of sea-surface-temperature (SST) on catch-rates for object-associated purse seine sets, with positive influence showing years where the over-all catch-rate in the model was standardised downward by the corresponding amount to account for influences of SST. Influence is shown in colour as a multiplier on average catch rates, with circle size corresponding to the amount of effort entering the model. Note that data for the 2022 year is preliminary.

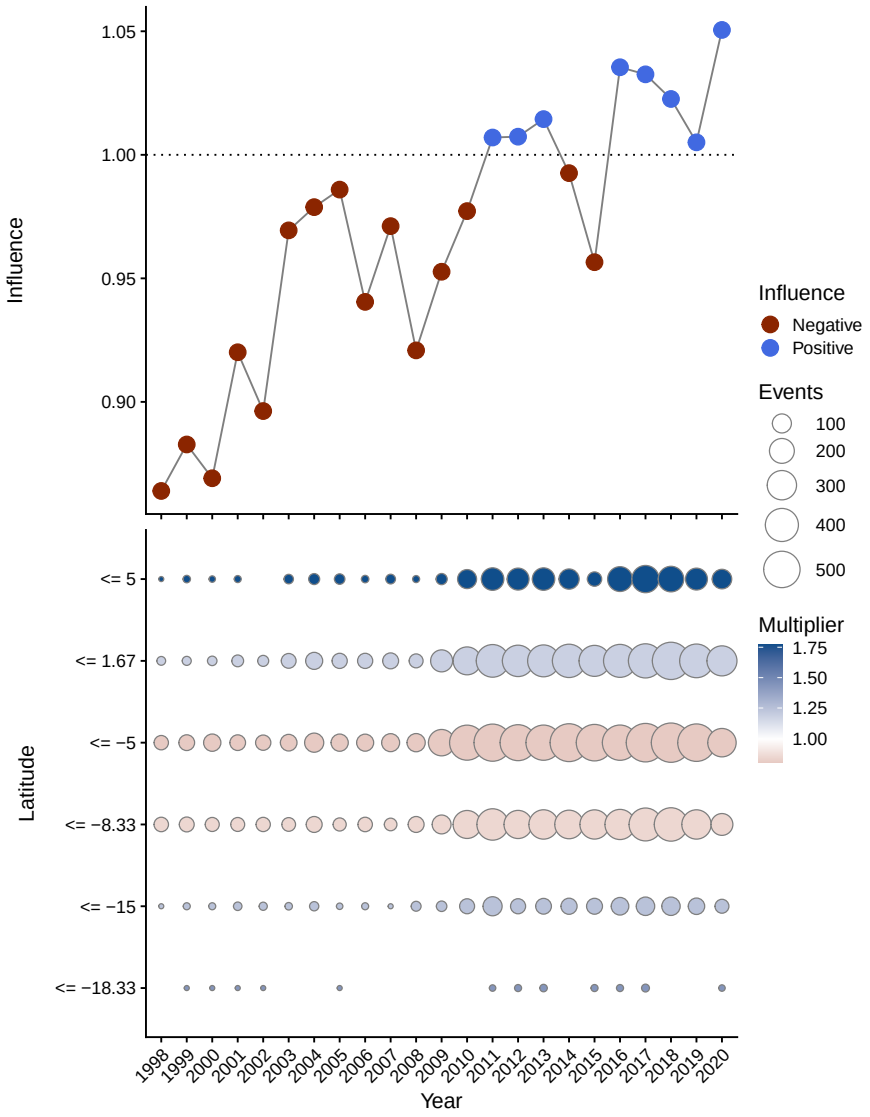

Figure C-83: Influence of latitude on catch-rates for object-associated purse seine sets, with positive influence showing years where the over-all catch-rate in the model was standardised downward by the corresponding amount to account for influences of latitude. Influence is shown in colour as a multiplier on average catch rates, with circle size corresponding to the amount of effort entering the model. Note that data for the 2022 year is preliminary.

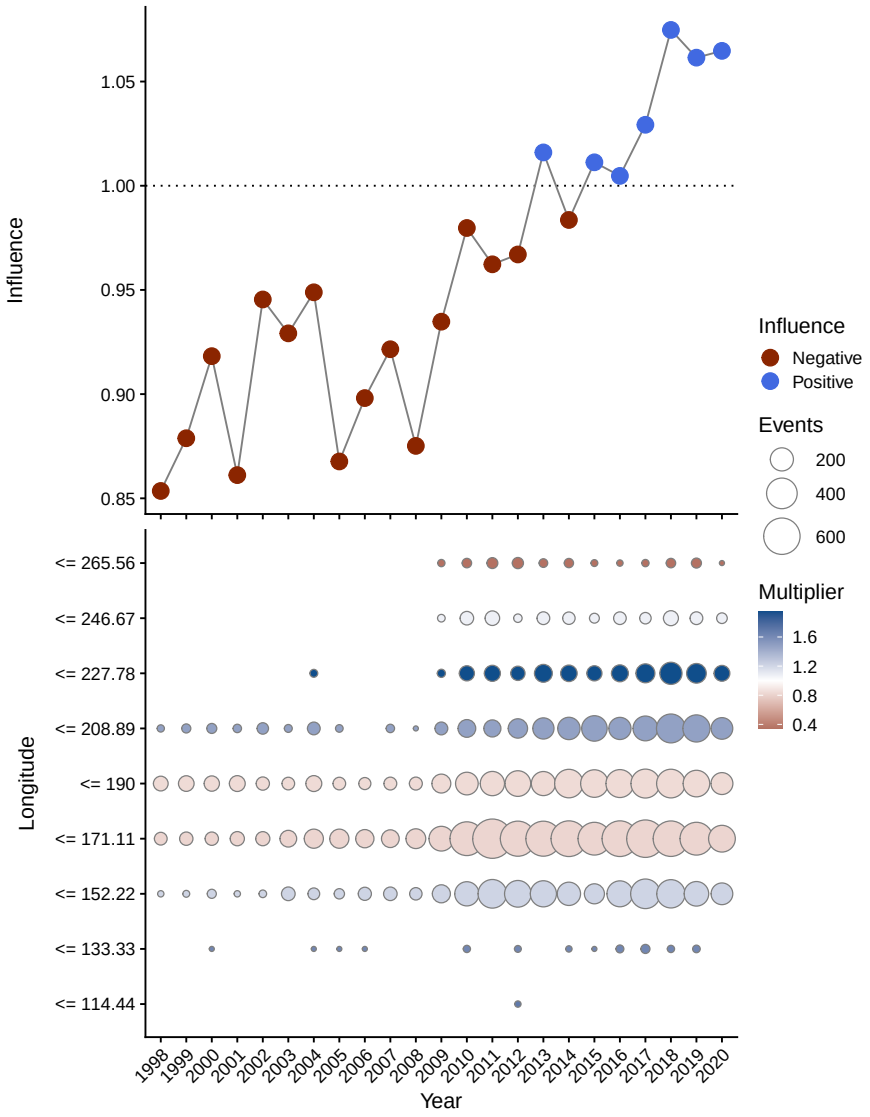

Figure C-84: Influence of longitude on catch-rates for object-associated purse seine sets, with positive influence showing years where the over-all catch-rate in the model was standardised downward by the corresponding amount to account for influences of longitude. Influence is shown in colour as a multiplier on average catch rates, with circle size corresponding to the amount of effort entering the model. Note that data for the 2022 year is preliminary.

APPENDIX D PREDICTING INTERACTIONS ACROSS THE WCPO - SUPPLEMENTARY FIGURES

D.1 Longline model fits

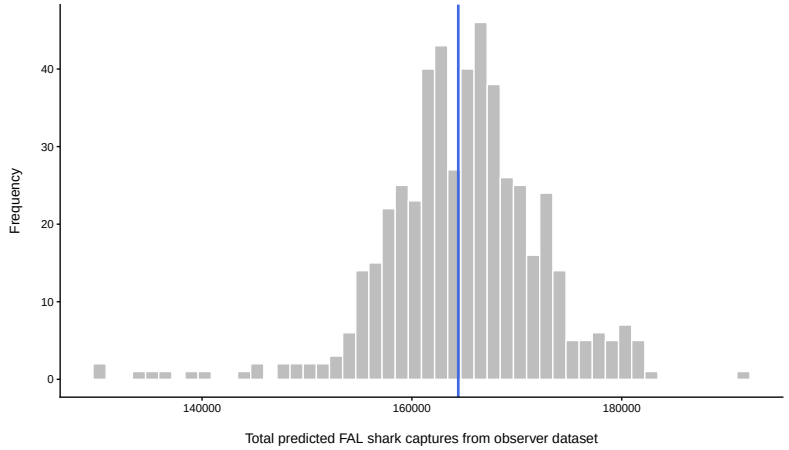

Figure D-85: Observed interactions (vertical line) and model predictions from the model used to derive CPUE from observed for longline sets.

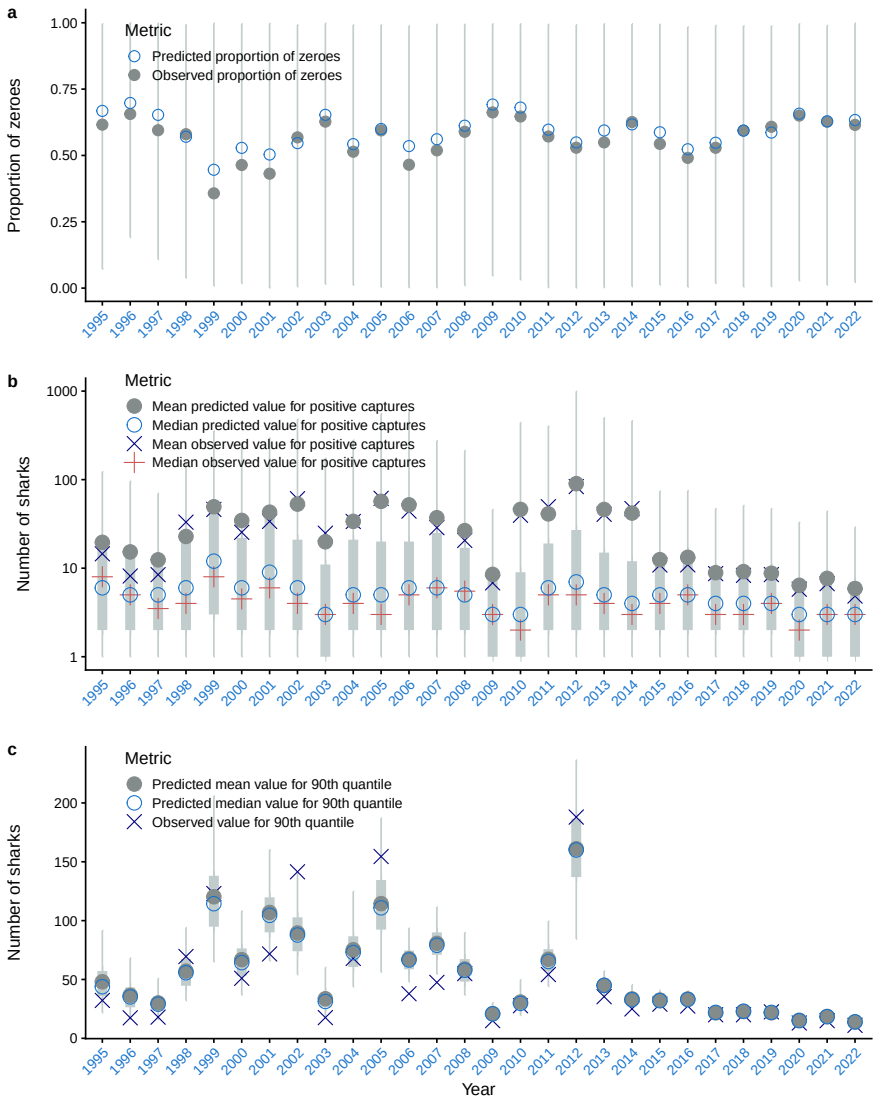

Figure D-86: Posterior predictive model diagnostics by model year for longline sets, with (a) observed and predicted proportion of zero captures, (b) observed and predicted positive captures and (c) dispersion statistics (90% percentile) of observed data and predictions.

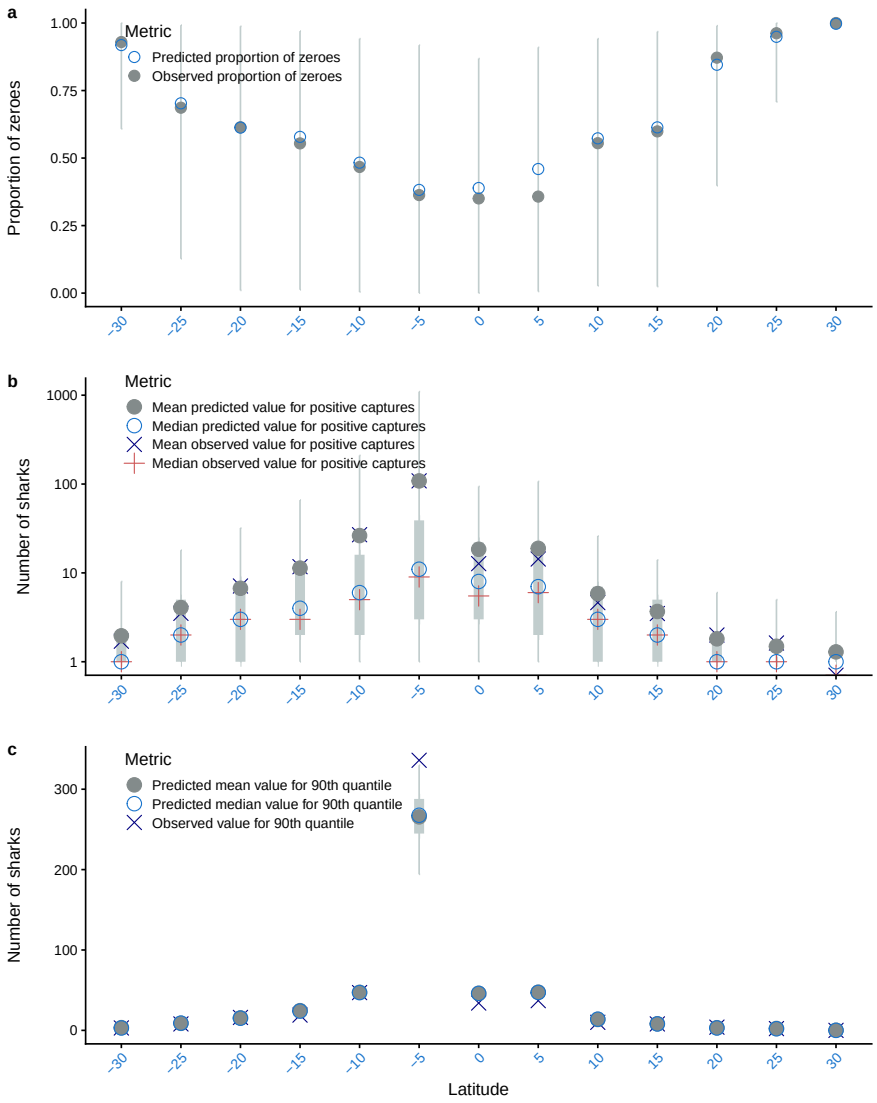

Figure D-87: Posterior predictive model diagnostics by latitude for longline sets, with (a) observed and predicted proportion of zero captures, (b) observed and predicted positive captures and (c) dispersion statistics (90% percentile) of observed data and predictions.

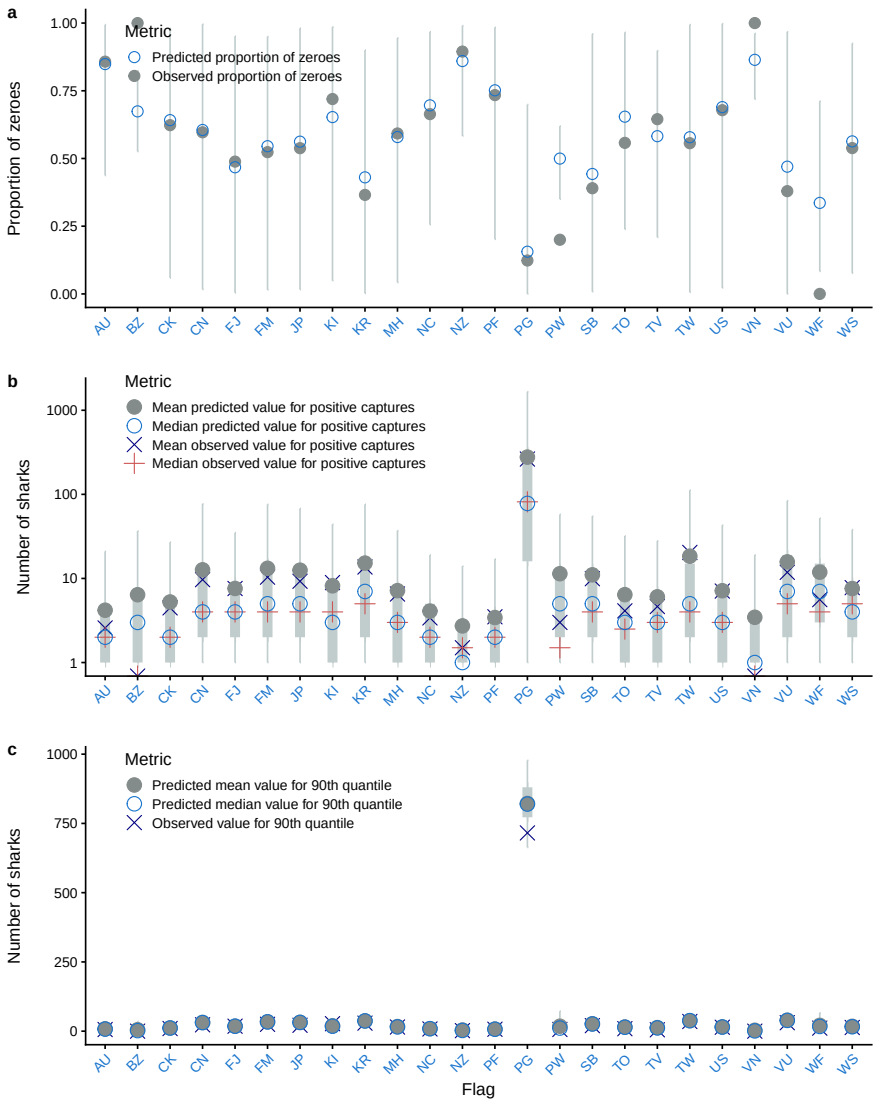

Figure D-88: Posterior predictive model diagnostics by observer program for longline sets, with (a) observed and predicted proportion of zero captures, (b) observed and predicted positive captures and (c) dispersion statistics (90% percentile) of observed data and predictions.

D.2 Purse-seine model fits

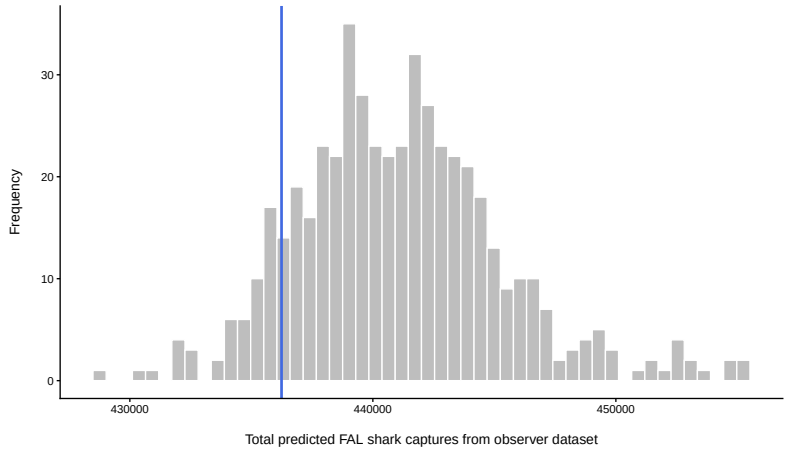

Figure D-89: Observed interactions (vertical line) and model predictions from the model used to derive CPUE from observed for purse-seine sets.

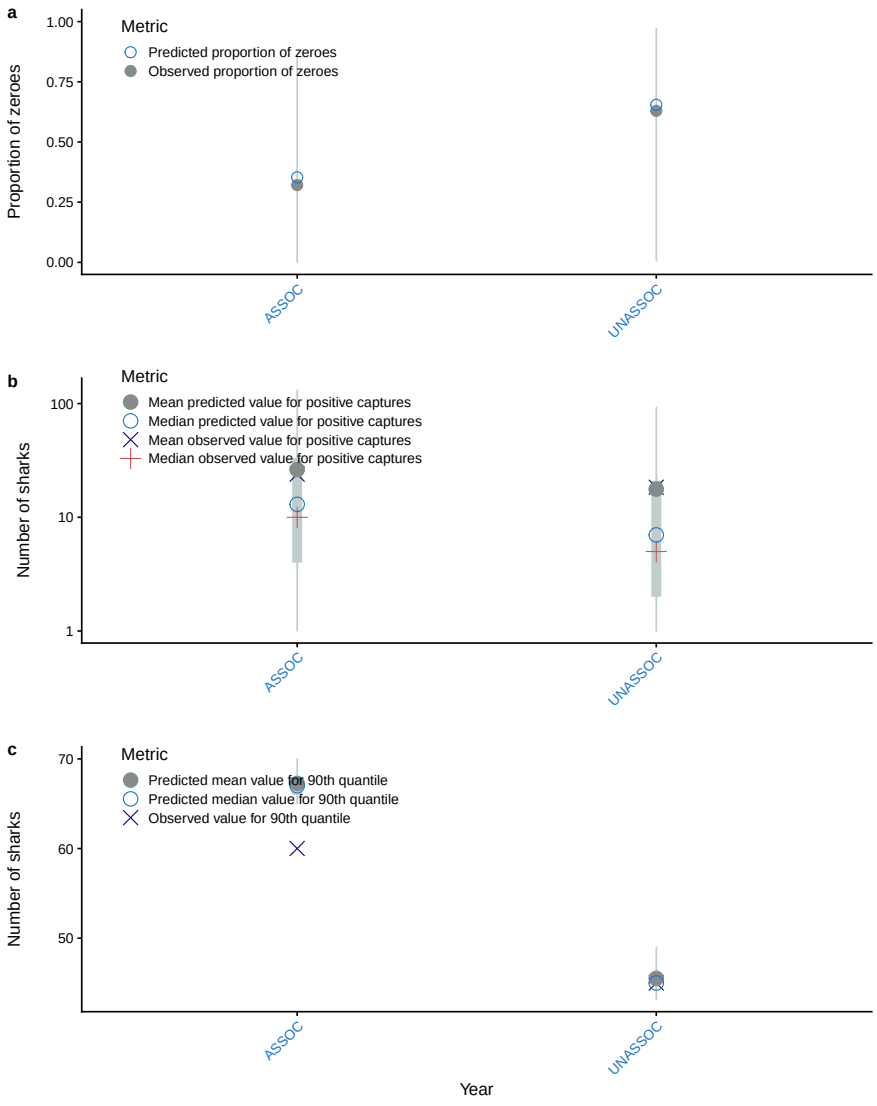

Figure D-90: Posterior predictive model diagnostics by set-type (ASSOC: object-associated sets; UNASSOC: free-school (un-associated) sets) for purse-seine sets, with (a) observed and predicted proportion of zero captures, (b) observed and predicted positive captures and (c) dispersion statistics (90% percentile) of observed data and predictions.

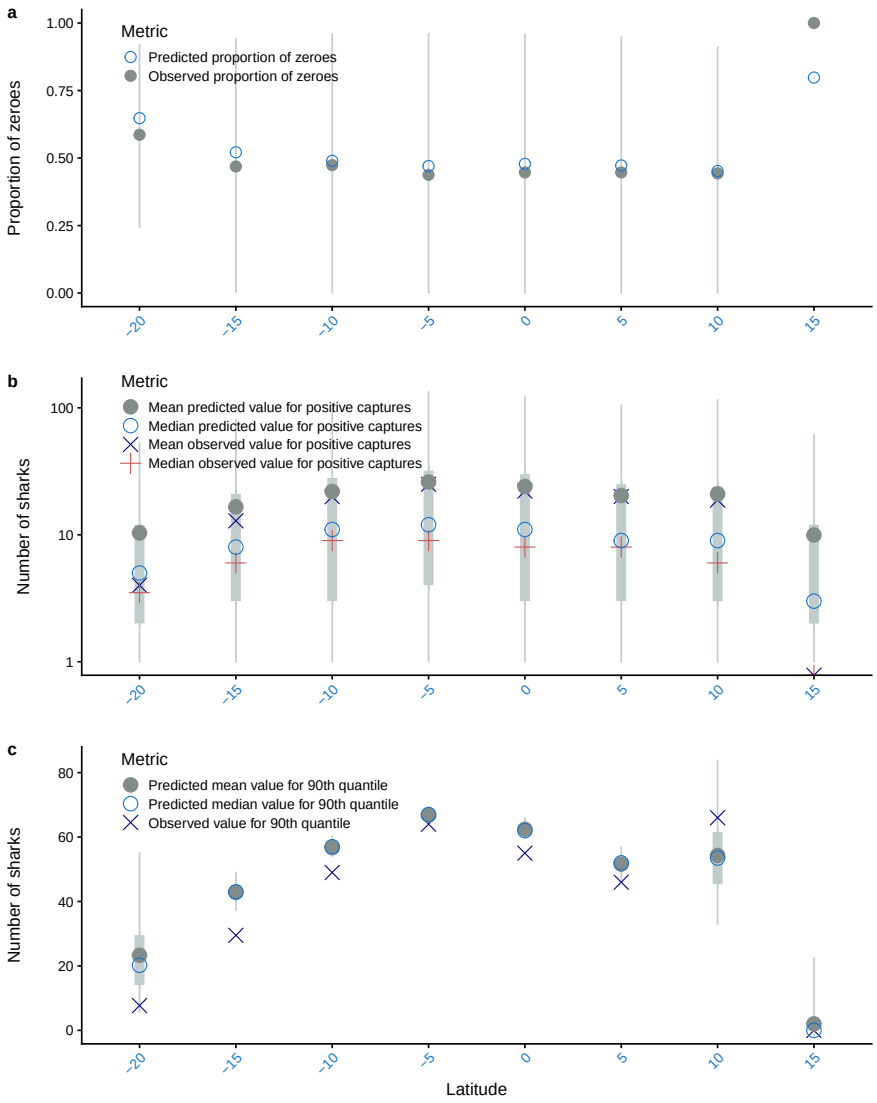

Figure D-91: Posterior predictive model diagnostics by latitude for purse-seine sets, with (a) observed and predicted proportion of zero captures, (b) observed and predicted positive captures and (c) dispersion statistics (90% percentile) of observed data and predictions.

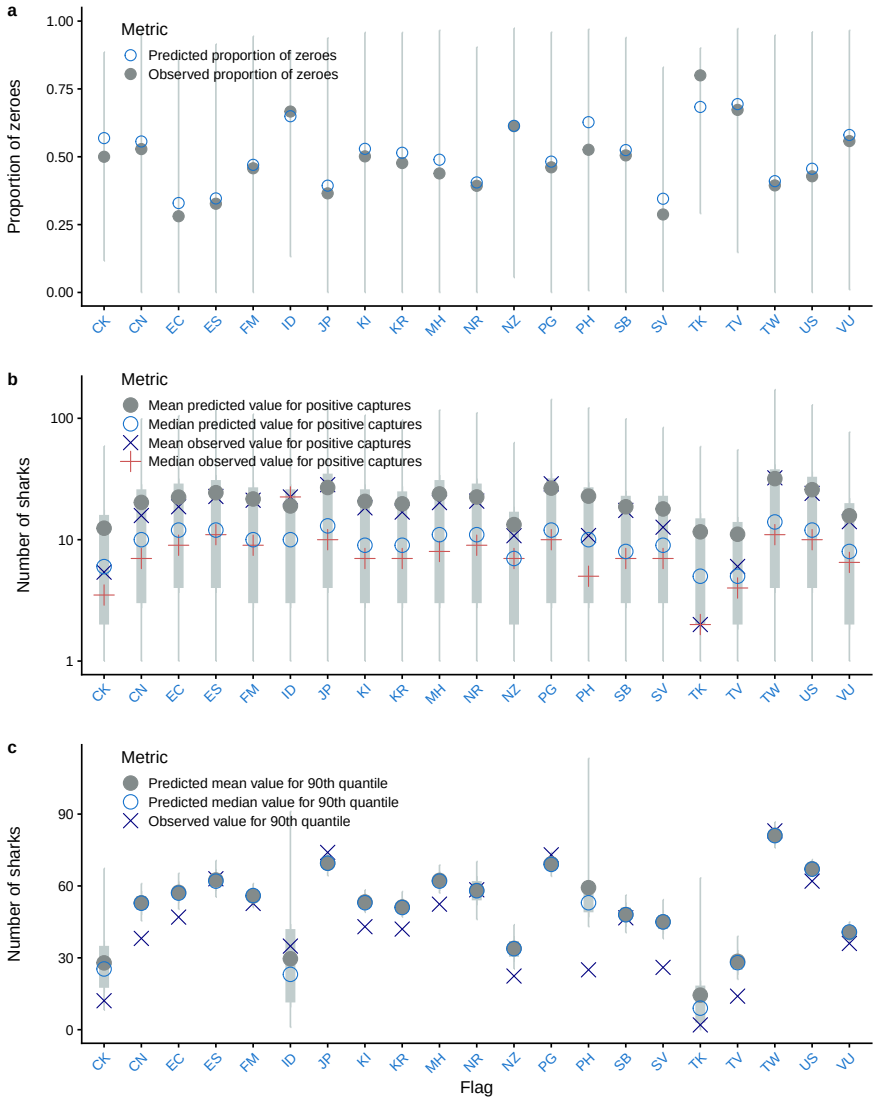

Figure D-92: Posterior predictive model diagnostics by observer program for purse-seine sets, with (a) observed and predicted proportion of zero captures, (b) observed and predicted positive captures and (c) dispersion statistics (90% percentile) of observed data and predictions.